

Aus der Abteilung für Strahlenzytogenetik  
Department of Radiation Sciences (DRS)  
Leitung: Prof. Dr. rer. nat. Horst Zitzelsberger  
Helmholtz Zentrum München

# **Phenotypic and functional characterization of primary murine endothelial cells after *in vivo* irradiation**

Dissertation  
zum Erwerb des Doktorgrades der Naturwissenschaften  
an der Medizinischen Fakultät der  
Ludwig-Maximilians-Universität zu München

vorgelegt von

Wolfgang Sievert

aus

Kiel

2016

Mit Genehmigung der Medizinischen Fakultät  
der Universität München

Betreuer:	Prof. Dr. rer. nat. Horst Zitzelsberger
Zweitgutachter:	Prof. Dr. Peter Nelson
Dekan:	Prof. Dr. med. dent. Reinhard Hickel
Tag der mündlichen Prüfung:	12.10.2016

**The human naivety  
is the worst enemy to any science.**

# TABLE OF CONTENTS

<b>ABBREVIATIONS</b>	<b>V</b>
<b>SUMMARY</b>	<b>VIII</b>
<b>ZUSAMMENFASSUNG</b>	<b>X</b>
<b>1. INTRODUCTION</b>	<b>1</b>
<b>1.1 Vasculature</b>	<b>1</b>
<b>1.1.1 Structure and function</b>	<b>1</b>
<b>1.1.2 Origin and neovascularisation</b>	<b>4</b>
<b>1.2 Endothelial cells</b>	<b>5</b>
<b>1.2.1 Isolation methods</b>	<b>5</b>
<b>1.2.2 Cell surface markers</b>	<b>10</b>
<b>1.3 Shear stress on heart endothelial cells</b>	<b>12</b>
<b>1.4 Tumor angiogenesis</b>	<b>16</b>
<b>1.5 Irradiation effects on endothelial cells</b>	<b>17</b>
<b>1.6 Aim of the study</b>	<b>19</b>
<b>2. MATERIALS AND METHODS</b>	<b>21</b>
<b>2.1 Materials</b>	<b>21</b>
<b>2.1.1 Devices and consumable materials</b>	<b>21</b>
<b>2.1.2 Chemicals</b>	<b>23</b>
<b>2.1.3 Buffers and solutions</b>	<b>24</b>
<b>2.1.4 Antibodies</b>	<b>26</b>
<b>2.1.5 BAC clones</b>	<b>27</b>
<b>2.1.6 Kits</b>	<b>27</b>
<b>2.1.7 Software</b>	<b>28</b>
<b>2.1.8 Cell lines and primary cells</b>	<b>28</b>
<b>2.1.9 Laboratory animals</b>	<b>29</b>
<b>2.2 Methods</b>	<b>30</b>
<b>2.2.1 Cell biological methods</b>	<b>30</b>
<b>2.2.1.1 Cell culture of cell lines and primary cells</b>	<b>30</b>
<b>2.2.1.2 Cell number and viability</b>	<b>30</b>
<b>2.2.1.3 Cryopreservation of cells</b>	<b>31</b>

2.2.1.4	Cell alignment assay	31
2.2.1.5	Cell migration assay	33
2.2.1.6	Tube formation assay	33
2.2.2	Molecular biological methods	33
2.2.2.1	Isolation of RNA	33
2.2.2.2	Quantification and qualification of RNA	34
2.2.2.3	Global mRNA expression analysis	34
2.2.3	Protein biochemical methods	35
2.2.3.1	Dialysis	35
2.2.3.2	Protein concentration	35
2.2.3.3	Biotinylation	36
2.2.4	Immunological methods	36
2.2.4.1	Immunofluorescence microscopy	36
2.2.4.2	Flow cytometry analysis	36
2.2.5	Histopathology and immunohistochemistry	37
2.2.5.1	Preparation of histological cryosection	37
2.2.5.2	Hematoxylin and eosin staining	37
2.2.6	Fluorescence in situ hybridization	37
2.2.6.1	BAC DNA isolation	38
2.2.6.2	Purification of plasmid-DNA	39
2.2.6.3	Concentration of plasmid-DNA	40
2.2.6.4	Labeling of probe-DNA via nick translation	40
2.2.6.5	Precipitation of probe-DNA	41
2.2.6.6	Fixation of cells	42
2.2.6.7	RNase and pepsin digestion	42
2.2.6.8	Denaturation, hybridization and detection	43
2.2.7	Animal model	43
2.2.7.1	Tumor implantation	43
2.2.7.2	Tumor growth measurements	44
2.2.7.3	Induction of repair blastema	44
2.2.7.4	Procedure of heart and thorax irradiation of mice	44
2.2.8	Statistics	45

<b>3. RESULTS</b>	<b>46</b>
3.1 Isolation of primary endothelial cells	46
3.1.1 Quality control experiment	49
3.2 Endothelial cells from different tissue	50
3.2.1 Distribution <i>in vivo</i> and yield after isolation	50
3.2.2 Size of isolated ECs and number of bound beads	52
3.2.3 Identification of primary endothelial cells	53
3.2.4 Surface markers of endothelial cells from normal and tumor tissue	55
3.2.5 Surface markers of heart endothelial cells in dependency of the age of mice	57
3.2.6 Surface markers of tumor endothelial cells with different growth rate	57
3.2.7 Morphology	58
3.2.8 Migration, flow alignment and tube formation	59
3.2.9 Ploidy level	62
3.3 mRNA expression of endothelial cells with high shear stress	64
3.3.1 Flow-dependent alignment	64
3.3.2 Flow-dependent gene expression	65
3.4 Irradiation effects of heart endothelial cells after local heart irradiation	72
3.4.1 Yield of endothelial cells after heart irradiation	72
3.4.2 Proportion and cell surface density of markers after heart irradiation	73
3.5 Irradiation effects of heart and lung endothelial cells after thorax irradiation	74
3.5.1 Surface markers of endothelial cells from non-irradiated hearts and lungs	74
3.5.2 Proportion of cell surface markers for heart and lung endothelial cells after irradiation	75
3.5.3 Irradiation-induced alterations in the cell surface density of markers involved in endothelial cell proliferation	77
3.5.4 Irradiation-induced alterations of endothelial progenitor cell surface markers	79
3.5.5 Irradiation-induced alterations of cell surface markers involved in inflammation	80

## Table of contents

---

<b>4. DISCUSSION</b>	<b>83</b>
4.1 Reproducible method for the isolation of viable endothelial cells from different tissue	83
4.2 Expression density of endothelial cell markers in benign and malignant tissue correlated with proliferation	84
4.3 Alteration of morphology and migration of tumor endothelial cells	86
4.4 Impairment of tube formation and flow alignment of tumor endothelial cells	87
4.5 Change of mRNA-expression of ECs under permanent high shear stress	89
4.6 Early and late radiation effects on heart endothelial cells	94
4.7 PERSPECTIVE	97
4.7.1 Effects of anti-angiogenic therapy	98
4.7.2 Effects of radiation therapy	99
<b>5. ACKNOWLEDGEMENTS</b>	<b>101</b>
<b>6. REFERENCES</b>	<b>102</b>
<b>7. APPENDIX</b>	<b>125</b>

## ABBREVIATIONS

ACE	angiotensin converting enzyme
AFN	atipamezol, flumazenil, naloxon
<i>Ankrd13</i>	ankyrin repeat domain 13
APC	allophycocyanin
BAC	bacterial artificial chromosome
<i>Bace2</i>	Beta-site amyloid precursor protein cleaving enzyme 2
<i>Basp1</i>	brain abundant, membrane attached signal protein 1
BSA	bovine serum albumin
<i>Cda</i>	Cytidine deaminase
dil-Ac-LDL	acetylated-low density lipoprotein labeled with 1,1'- dioctadecyl-3,3,3',3'-tetramethylindo-carbocyanine perchlorate
DMEM	Dulbecco's modified Eagle's medium
DMSO	dimethyl sulfoxide
DNA	deoxyribonucleic acid
ECs	endothelial cells
EDTA	ethylenediaminetetraacetic acid
EGM2	endothelial cell growth medium 2
ELISA	enzyme-linked immuno-sorbent assay
f	female
<i>Fgf2</i>	fibroblast growth factor 2
FSC	forward scatter
FISH	fluorescence in situ hybridization
FACS	fluorescence activated cell sorting
FCS	fetal calf serum
FITC	fluorescein isothiocyanate
g	green
<i>Galnt18</i>	Polypeptide N-acetylgalactosaminyltransferase 18
<i>Grcc10</i>	gene rich cluster, C10 gene
Gy	gray (unit of absorbed radiation)
H&E	hematoxylin and eosin
HCAM	homing cell adhesion molecule
HDMEC	human dermal microvascular endothelial cell

## Abbreviations

---

HCl	salt acid
HUVEC	human umbilical vein endothelial cell
ICAM-1	intercellular adhesion molecule-1
ICAM-2	intercellular adhesion molecule-2
IF	immunofluorescence
KCl	potassium chloride
m	male
MACS	magnetic activated cell sorting
mfi	mean fluorescence intensity
MMF	medetomidin, midazolam, fentanyl
mRNA	messenger ribonucleic acid
n.s.	not specified
NaCl	sodium chloride
NaOH	sodium hydroxide
NO	nitric oxide
<i>Nos3</i>	nitric oxide synthase 3
<i>Nus1</i>	nuclear undecaprenyl pyrophosphate synthase 1 homolog
o	orange
PARs	protease activated receptors
PBS	phosphate buffered saline
PE	phycoerythrin
PECAM-1	platelet endothelial adhesion molecule-1
PGLI2	prostacyclin
PI	propidium iodide
<i>Plxna4</i>	plexin A4
<i>Psmb9</i>	proteasome subunit, beta type, 9
r	red
<i>Rffl</i>	ring finger and FYVE-like domain containing protein
rpm	revolutions per minute
RNA	ribonucleic acid
RPMI	Roswell Park Memorial Institute
rRNA	ribosomal ribonucleic acid
s.c.	subcutaneous
Sca-1	stem cells antigen-1

## Abbreviations

---

SDS	sodium dodecylsulfate
<i>Sh2b3</i>	Sh2b adapter protein 3
SSC	saline sodium citrate
<i>Ssh3</i>	slingshot homolog 3
<i>Syt17</i>	synaptotagmin XVII
TF	tissue factors
<i>Tmem44</i>	transmembrane protein 44
TNF- $\alpha$	tumor necrosis factor alpha
t-PA	tissue plasminogen activator
tRNA	transfer ribonucleic acid
VCAM-1	vascular cell adhesion molecule-1
VE-cadherin	vascular endothelial cadherin
VEGFR	vascular endothelial growth factor receptor
vs.	versus
vWF	von Willebrand factor
<i>Zswim4</i>	zinc finger, SWIM domain containing 4

## SUMMARY

The inner cellular lining of all blood vessels consists of a monolayer of endothelial cells (ECs) that have a low proliferation rate in healthy tissue. Under pathological conditions such as wound healing, inflammation and in growing tumors, the proliferation rate of ECs is elevated. Radiotherapy is commonly used for the local control of solid tumors. During radiotherapy of patients with thoracic tumors, the surrounding healthy tissue including ECs of heart and lung may become damaged which in turn can change the proliferation rate of these resting ECs. This damage may increase the risk to develop cardiac diseases in patients after thoracic irradiation at later time-points. It is hypothesized that the protein profile of resting and growing primary ECs is different. To address this question, viable primary ECs are required. Established methods allow the isolation of ECs only from very young mice at low yields and purities. The analysis of late radiation-induced effects on primary ECs requires the availability of primary ECs from old mice.

I succeeded to establish a novel method for the isolation of viable primary ECs at high purity from non-proliferating (heart from young and old mice), proliferating benign (repair blastema) and malignant (tumor) tissues at high yields. These ECs were characterized phenotypically, functionally and with respect to their gene expression profiling under static and physiological flow conditions.

The expression density of proliferation markers such as endoglin and VE-cadherin is higher on isolated ECs of proliferating tissues from repair blastema and tumor compared to non-proliferating normal tissues from heart and lung. The expression density of the progenitor marker mucosialin is elevated on tumor-derived ECs, but not on those of repair blastemas. The inflammatory markers PECAM-1, ICAM-1 and ICAM-2 were found to be elevated on ECs of repair blastema and tumor compared to ECs from heart and lung. Further, I could show that tumor ECs are larger, have a significantly higher migration capacity and distribute in a more chaotic pattern in cell culture compared to ECs derived from normal tissues. Tube formation assays showed that tumor ECs have a smaller number of branching points and loops compared to that of normal ECs. In contrast to normal tissue ECs, tumor-derived ECs show no tendency to align under flow conditions. The results suggest that increased expression of surface molecules on ECs in

proliferating tissues contributes to a loss of EC function that might be responsible for a chaotic tumor vasculature.

In contrast to the short-term effects in tumors and repair blastemas induced by proliferation, irradiation can cause long-term effects in heart and lung ECs. Local thorax irradiation of mice resulted in a temporary and differential up-regulation of proliferation markers such as HCAM, integrin  $\beta$ 3, endoglin, VE-cadherin and VEGFR-2 on ECs after 8 Gy at later time-points. The progenitor marker mucosialin is increased on lung ECs 15 to 20 weeks after irradiation. Inflammatory markers such as PECAM-1, ICAM-1, ICAM-2 and VCAM-1 started to increase 10 weeks after thorax irradiation with 8 Gy. Interestingly, ICAM-1 and VCAM-1 remained up-regulated even 20 weeks after thorax irradiation on heart and lung ECs. The persistent increase of both markers ICAM-1 and VCAM-1 after irradiation may suggest a predisposition for the development of atherosclerotic plaques in heart and lung ECs at later time points.

Shear stress on ECs induced by blood flow is disturbed in heart capillaries with atherosclerotic plaques as well as in tumor vasculature. mRNA expression analysis of genes from heart ECs under normal flow conditions and pathological static conditions *in vitro* show significant changes related to extracellular organisation, cell membrane function, signaling, hemostasis, metabolism and smooth muscle contraction. Moreover, it was observed that mRNA expression of the inflammation markers *Pecam1*, *Icam1* and *Icam2* was higher on heart ECs under static conditions. The protein expression of these inflammatory markers was also elevated on ECs from pathologic conditions. These results provide the basis for subsequent investigations on the role of irradiation on gene expression profiles of ECs derived from normal and tumor tissues.

## Zusammenfassung

Die innere Oberfläche aller Blutgefäße besteht aus einer einschichtigen Lage aus Endothelzellen, die im gesunden Gewebe eine niedrige Vermehrungsrate aufweisen. Unter pathologischen Bedingungen wie Wundheilung, Entzündung und wachsenden Tumoren ist die Vermehrungsrate von Endothelzellen erhöht. Für die lokale Kontrolle von soliden Tumoren wird allgemein die Strahlentherapie verwendet. Während der Strahlentherapie von Patienten mit einem Tumor im Thorax-Bereich kann benachbartes gesundes Gewebe einschließlich Endothelzellen des Herzens und der Lunge beschädigt werden, wodurch sich die Vermehrungsrate dieser ruhenden Endothelzellen verändern kann. Diese Beschädigung kann das Risiko einer auftretenden Herzerkrankung nach Thorax-Bestrahlung zu späteren Zeitpunkten erhöhen. Es wird angenommen, dass das Proteinprofil von ruhenden und wachsenden primären Endothelzellen unterschiedlich ist. Für diese Fragestellung sind lebensfähige primäre Endothelzellen erforderlich. Etablierte Methoden erlauben die Isolierung von Endothelzellen nur von sehr jungen Mäusen mit geringer Ausbeute und Reinheit. Die Analyse von späten bestrahlungs-induzierten Effekten von primären Endothelzellen erfordert die Verfügbarkeit von primären Endothelzellen von alten Mäusen.

Mir ist es gelungen, eine neue Methode für die Isolierung von lebensfähigen primären Endothelzellen mit hoher Reinheit aus nicht wachsenden (Herz von jungen und alten Mäusen), wachsenden benignen (Reparatur-Blastem) und malignen (Tumor) Geweben mit hoher Ausbeute zu etablieren. Diese Endothelzellen wurden phänotypisch, funktionell und hinsichtlich ihrer Genexpressionsprofile unter statisch und physiologischen Flussbedingungen charakterisiert.

Die Expressionsdichte der Proliferations-Marker wie Endoglin und VE-Cadherin ist höher auf isolierten Endothelzellen von wachsenden Geweben aus Reparatur-Blastem und Tumor im Vergleich zu nicht wachsendem, normalem Gewebe aus Herz und Lunge. Die Expressionsdichte des Vorläufer-Markers Mucosialin ist erhöht auf Endothelzellen aus dem Tumor, aber nicht auf denen aus dem Reparatur-Blastem. Die Entzündungsmarker PECAM-1, ICAM-1 und ICAM-2 waren erhöht auf Endothelzellen aus dem Reparatur-Blastem und Tumor im

Vergleich zu Endothelzellen aus Herz und Lunge. Des Weiteren konnte ich zeigen, dass die Tumor-Endothelzellen größer sind, eine signifikant höhere Migrationskapazität und eine chaotische Verteilung in Zellkultur im Vergleich zu Endothelzellen aus normalem Gewebe aufweisen. Tube-Bildungs-Versuche zeigten, dass Tumor-Endothelzellen eine geringere Anzahl von Verzweigungspunkten und Schlaufen im Vergleich zu normalen Endothelzellen aufweisen. Im Gegensatz zu normalen Endothelzellen zeigen Tumor-Endothelzellen keine Ausrichtung unter Flussbedingungen. Diese Ergebnisse legen nahe, dass eine erhöhte Expression von Oberflächenmolekülen auf Endothelzellen in wachsenden Geweben an einem Verlust der Endothelzellen-Funktion mitwirkt, die für die chaotische Tumor-Vaskularisierung verantwortlich sein könnte.

Im Gegensatz zu den durch das Wachstum bedingten kurzfristigen Auswirkungen in Reparatur-Blastemen und Tumoren, kann Bestrahlung langfristige Auswirkungen in Endothelzellen des Herzens und der Lunge verursachen. Lokale Thorax-Bestrahlung von Mäusen mit 8 Gy führt zu einer vorübergehenden und unterschiedlichen Hochregulierung der Proliferations-Marker HCAM, Integrin  $\beta 3$ , Endoglin, VE-Cadherin und VEGFR-2 auf Endothelzellen zu späteren Zeitpunkten. Der Vorläufer-Marker Mucosialin ist auf Lungen-Endothelzellen 15-20 Wochen nach Bestrahlung erhöht. Entzündungs-Marker wie PECAM-1, ICAM-1, ICAM-2 und VCAM-1 waren ab 10 Wochen nach Thorax-Bestrahlung mit 8 Gy erhöht. Interessanterweise blieben 20 Wochen nach Thorax-Bestrahlung ICAM-1 und VCAM-1 auf Herz- und Lungen-Endothelzellen hochreguliert. Die anhaltende Erhöhung der beiden Marker ICAM-1 und VCAM-1 nach Bestrahlung legt eine Prädisposition für die Entwicklung von arteriosklerotischen Plaques in Herz- und Lungen-Endothelzellen zu späteren Zeitpunkten nahe.

Die durch Blutfluss verursachte Scherbelastung auf Endothelzellen ist in Herz-Kapillaren mit arteriosklerotischen Plaques sowie in Tumorgefäßen gestört. mRNA-Expressionsanalysen von Genen aus Herz-Endothelzellen unter normalen Fluss- und pathologisch statischen Bedingungen *in vitro* zeigen signifikante Veränderungen bezüglich extrazellulärer Organisation, Funktionen der Zellmembran, Signalgebung, Blutstillung, Stoffwechsel und Kontraktion der glatten Muskulatur. Zudem wurde festgestellt, dass die mRNA-Expression von Entzündungs-Markern *Pecam1*, *Icam1* und *Icam2* unter statischen Bedingungen

höher auf Herz-Endothelzellen war. Die Protein-Expression dieser Entzündungs-Marker war ebenfalls auf Endothelzellen aus pathologischen Bedingungen erhöht. Diese Ergebnisse liefern die Basis für weitere Untersuchungen über die Wirkung der Bestrahlung auf Genexpressionsprofile von Endothelzellen aus normalen und Tumorgeweben.

# 1. INTRODUCTION

The inner cellular lining of all blood vessels consists of a monolayer of endothelial cells (ECs). This monolayer (endothelium) has direct contact with the blood and the circulating cells (Feletou 2011). The diffusion limit of oxygen from the endothelium to non-vascular tissue in the body ranges from 100 to 200  $\mu\text{m}$  (Hoeben et al. 2004). Therefore, a dense network of blood vessels is necessary for an adequate supply of each cell with oxygen and nutrients in the whole body. In adult organisms, the vascular system is fully developed. The proliferation rate of these resting ECs is commonly low. In contrast, under pathological conditions such as wound healing, inflammation and tumors the proliferation rate is high. The induce formation of new blood vessel from existing vessels is one of the hallmarks for the development of tumors (Hanahan and Weinberg 2011).

Thoracic radiotherapy is commonly used for the treatment of Hodgkin's lymphoma and breast cancer patients (Gabriels et al. 2012). However, surrounding healthy tissue including the heart also may receive radiation doses. The pathological consequences of radiation-induced heart disease are myocardial fibrosis, cardiomyopathy, coronary artery disease, valvular disease and pericardial disease (Taunk et al. 2015). Experimental studies of radiation-induced heart diseases have shown major functional changes in the microvasculature of the myocardium, particularly to microvascular ECs (Schultz-Hector and Trott 2007). In a mouse model, it was shown that local heart irradiation with single doses of 2 and 8 Gy led to a significant temporary increase in microvascular density after 20 weeks (Seemann et al. 2012).

The high proliferation rate of ECs in tumors and hearts after irradiation represent pathological hallmarks. It has therefore been assumed that proteins expressed in ECs of resting and growing tissues may be different.

## 1.1 Vasculature

### 1.1.1 Structure and function

Although the endothelium shows organ specific variability, arteries and veins have a general structure consisting of three layers: the tunica interna (intima), the tunica

media (media) and the tunica externa (adventitia) (Figure 1) (Martinez-Lemus 2012)). The tunica interna consists mostly of ECs, the tunica media consists mainly of smooth muscle cells and the tunica externa is composed mostly of collagen fibers and extra-cellular matrix. In capillaries, the endothelial monolayer with the basal lamina is the only cell barrier between blood and intercellular space, stroma and parenchymal cells (Bolender 1974). In healthy tissue, ECs are surrounded with external pericytes in a ratio between 1:1 and 10:1 (Armulik et al. 2011). Pericytes play an important role in the regulation of capillary barriers, capillary diameter and endothelial proliferation. In healthy tissue, ECs are typically flat and align in the direction of blood flow as response to fluid shear stress (Resnick et al. 2003; Aird 2007). Shear stress is the force per unit area created when a tangential force of blood flow acts on the endothelium (Pan 2009).

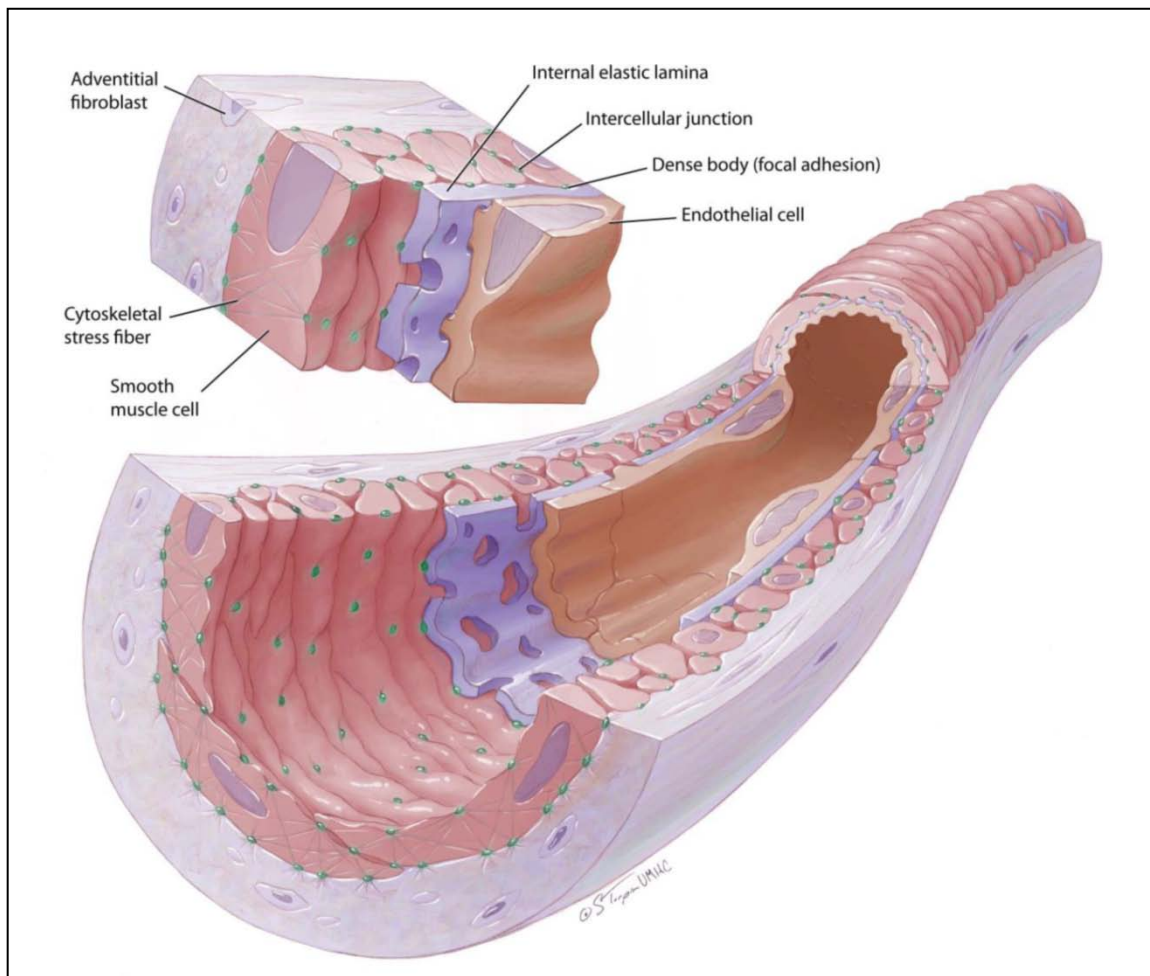


**Figure 1:** Schematic representation of the vascular wall (arteriole) (Martinez-Lemus 2012).

The endothelium plays an important role not only as a supply system or cell barrier but also in many physiological functions, including vascular permeability, leukocyte trafficking, hemostasis and the regulation of vasomotor tone (Aird 2007). The endothelium is semipermeable and allows the transport of fluids and solutes into and out of the blood. Tight junctions and adherens junctions are recognized as intercellular junctions in the endothelium. Tight junctions are located in the most apical position toward the vessel lumen and strictly control permeability. Adherent junctions are ubiquitously distributed. The transfer of solutes and fluids between blood and underlying tissue occurs by different mechanisms and depends on the organ. In continuous non-fenestrated endothelium (heart, lung, skin, brain), water and solutes (<3 nm) are able to pass between ECs, whereas larger solutes pass through ECs via channels or caveolae. Caveolae are particularly present in heart capillaries and rare in brain capillaries due to the blood-brain barrier. Continuous fenestrated endothelium is characterized by greater permeability (70 nm) to water and solutes via diaphragms and is observed in tissue with increased filtration (exocrine and endocrine glands, gastric and intestinal mucosa). Discontinuous endothelium has larger fenestrations (100-200 nm) without diaphragms and is found predominantly in the liver, but also in the spleen and bone marrow (Aird 2007; Feletou 2011). The passage of leukocytes from blood to underlying tissue is performed by an adhesion cascade that includes attachment, rolling and transmigration with the help of different endothelial adhesion molecules. The accumulation of lymphocytes, monocytes, macrophages and neutrophils is an important step in the inflammatory response of the immune system. ECs are also involved in hemostasis. On the pro-coagulant side, ECs synthesize tissue factors (TF), plasminogen activator inhibitor, von Willebrand factor (vWF) and protease activated receptors (PARs). The synthesis of endothelial vWF and PARs induces the adhesion of thrombocytes to the endothelium (Sadler 1998; Alberelli and De Candia 2014). TP is involved in the blood clotting due to the formation of fibrin (Mackman 2009). On the anti-coagulant side, ECs express tissue factor inhibitor, heparin, thrombomodulin, endothelial protein C receptor, tissue plasminogen activator (t-PA), ecto-ADPase, prostacyclin, and nitric oxide (NO) (Aird 2007). Endothelial heparin acts as a cofactor for antithrombin, which inhibits pro-coagulant enzymes (Olson and Chuang 2002). Prostacyclin (PGLI<sub>2</sub>) inhibits the adhesion of thrombocytes (Weiss and Turitto 1979). The synthesis of t-PA

activates fibrinolysis. Thrombomodulin is expressed on the surface of ECs and inactivates thrombin. Maintenance of the physiologic laminar shear stress is known to be crucial for normal vascular function (Cunningham and Gotlieb 2005). Steady laminar shear stress promotes the release of factors from ECs (NO, PGL<sub>2</sub>, t-PA, thrombomodulin) that inhibit coagulation, migration of leucocytes and smooth muscle proliferation. Low or disturbed shear stress shift the profile of factors in a situation that leads to the opposite effects (Traub and Berk 1998).

### **1.1.2 Origin and neovascularisation**

Vessel density results from the metabolic needs of oxygen and nutrients (Bergers and Benjamin 2003). The development of new blood vessels can occur by vasculogenesis and angiogenesis (Buschmann and Schaper 1999). During embryonic vasculogenesis, blood vessels are formed from endothelial progenitor cells (angioblasts) that assemble into a primitive network. The extension in a complex vascular system occurs by angiogenesis (Bergers and Benjamin 2003). In this way new blood vessels are formed from preexisting ECs which are stimulated by a variety of factors. A less established formation is the arteriogenesis, which describes the proliferation of collateral arteries from preexisting ECs and which is stimulated by shear stress even in the absence of hypoxia (Heil et al. 2006). In adults, the vasculature is usually quiescent and the turnover rate of ECs is generally low.

The neovascularisation is the formation of new blood vessels in adult organism. In healthy tissue, the formation occurs only in wound healing, in the female reproductive cycle and during pregnancy (Reynolds and Redmer 2001; Hoeben et al. 2004). During vasculogenesis, endothelial progenitor cells can be mobilized from the bone marrow and transported through the blood-flow to incorporate in growing vessels. The angiogenesis starts with vasodilation and an increased vascular permeability, followed by extravasation of plasma proteins and loosening of pericytes (Figure 2). After degradation of the vascular basement membrane, ECs proliferate and migrate towards chemotactic angiogenic stimuli and form a column in the perivascular space. The association of a new basal lamina and pericytes leads to an intact blood vessel (Bergers and Benjamin 2003).

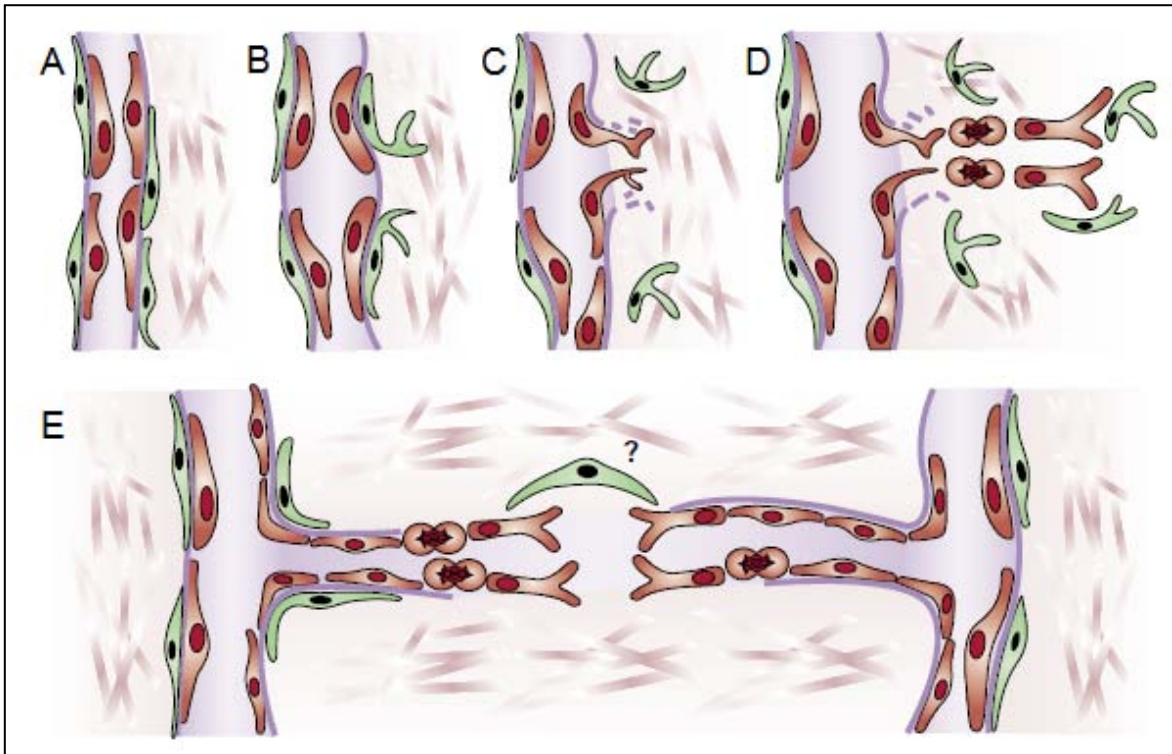


**Figure 2:** New blood vessel formation **(A)** Blood vessels arise from pre-existing capillaries. **(B)** First, pericytes (green) detach and blood vessels dilate before **(C)** the basement membrane and extracellular matrix is degraded. **(D)** After degradation, ECs (red) proliferate and migrate towards chemotactic stimuli and form a column in the perivascular space. **(E)** ECs from two growing columns adhere to each other and create a lumen. Little is known about this fusion mechanism (Bergers and Benjamin 2003).

## 1.2 Endothelial cells

### 1.2.1 Isolation methods

All EC isolation methods generally consist of the generation of a single cell suspension from the corresponding tissue and the separation of ECs from all other cells. Tissue digestion was performed often with collagenase and trypsin, occasionally with pronase, dispase and hyaluronidase. The first isolation methods that are still commonly used were derived from the human umbilical vein (Jaffe et al. 1973; Gimbrone et al. 1974). This endothelium is large and can easily be obtained. In this case, high purities of macrovascular ECs can be obtained by clamping the vein and performing short enzymatic digestion. Alternatively, large arteries were also useful. Here, macrovascular ECs can be obtained by gentle scraping of the intimal surface (Ryan et al. 1980; Gajdusek and Schwartz 1983).

Unfortunately, these simple methods are not suitable for the isolation of microvascular ECs from a complex organ. In this case, ECs must be separated from all other cells.

Early methods relied on the morphology of ECs after seeding. The cells become adherent and proliferate in the following days. Initially, the development of capillaries or the removal of the endothelium from the vessels was the basis for successful EC isolation (White and Parshley 1951; Maruyama 1963). This was replaced by the observation that ECs show a typical cobblestone morphology at confluence *in vitro* (Ryan 1984; Marks et al. 1985; Davies et al. 1987; Launder et al. 1987). Contaminated cells show often spindle-shaped morphology and also become strongly adherent and must be separated early in culture from ECs to ensure that ECs are not overgrown. In addition, ECs and contaminated cells tend to change their morphology and behavior depending on the growth medium, with the result that it is not possible to distinguish between them. Some manual techniques include removal of contaminating colonies using a needle or cell scraper (Marks et al. 1985; King et al. 2004). Other procedures perform the removal of ECs from their contaminants. Once identified, the ECs are encapsulated and detached from their environment with the help of cloning rings/discs or glass beads (King et al. 2004; Teng et al. 2006). Although this procedure is still used, magnetic beads are generally used for successful separation. In this case, beads are coated with a specific molecule or antibody, which recognizes ECs. After incubation, the cells with bound beads are separated with the help of a magnet. The method of MACS (Magnetic Activated Cell Sorting) separates cells with bound beads in a column placed in a magnet (Bussolati et al. 2003; Hida et al. 2004). Cells without bound beads are in the flow-through whereas cells with bound beads stick to the column and can be eluted when the column is removed from the magnet. A refinement of this method is the use of magnetic beads without a column. Thereby, a blockage of the column can be prevented. The cells with bound beads are collected inside a tube in a magnetic field. Unbound material is simply removed by aspiration. After washing steps, the tube is removed from the magnetic field and the bead-bound cells can be used (DeCarlo et al. 2008; Sobczak et al. 2010; Jin et al. 2012; Mackay et al. 2013). A further method is the use of FACS (Fluorescence Activated Cell Sorting) after labelling ECs with a specific antibody conjugated with a fluorescent dye (Kevil and

Bullard 2001; Huang et al. 2003; Okaji et al. 2004; Fehrenbach et al. 2009; Pratumvinit et al. 2013). Generally, the separation of cells via FACS is only successful if target cells comprise more than 30 % of the cell population (Scott and Bicknell 1993). Culturing ECs for a longer period of time with subsequent changing of medium can enrich the EC proportion due to the removal of blood and dead cells. Another possibility is the use of percoll or dextran gradient centrifugation (Grimwood et al. 1995; Kallmann et al. 2002; Wu et al. 2003; Cha et al. 2005). In this case, the EC fraction appears in a distinct layer within the gradient and can be collected without the majority of contaminated cells.

During the last 40 years, many investigators have used different methods for EC isolation. The isolation of ECs from heart, lung or tumors is a particular challenge. Not only a high level of purity but also a gentle isolation procedure is necessary to obtain viable ECs. Very often purification steps were repeated or performed after time-consuming culture *in vitro* to obtain high purity of ECs (Table 1). Whatever the method might be, most important is the full characterization of the isolated cells as ECs. This can prevent the possibility to come under criticism for studies on ECs, which may consist more probably of mesothelial cells (Scott and Bicknell 1993).

**Table 1:** Isolation, purification and identification of murine ECs isolated from heart, lung or tumor.

Reference	Tissue	Method of isolation and purification	Identification	Purity	Age
(Modzelewski et al. 1994)	fibrosarcoma	collagenase/Dnase digestion, FACS using ACE	FACS: uptake of LDL, IF: factor VIII	>95%	14-16 days
(Dong et al. 1997)	lung	collagenase, beads coated with PECAM-1, trypsin to remove beads, repeated separation, limiting-dilution method	FACS, ELISA: PECAM-1, mucosialin, VCAM-1, ICAM-1, VE-cadherin, ELISA: P-selectin, (E-selektin - $\alpha$ ), in vitro: cobblestone morphology, tube formation after TNF	>98%	8-11 weeks
(Marelli-Berg et al. 2000)	heart, lung	collagenase, trypsin, incubation with CD31, CD105, biotinylated Isolectin and streptavidin-conjugated microbeads, separation in column on magnet	FACS: Isolectin, endoglin, VCAM-1 (low expression of PECAM-1, ICAM-1, ICAM-2)	pure	6-8 weeks
(Li et al. 2001)	heart	collagenase, trypsin/DNase	in vitro IF: uptake of dil-Ac-LDL, eNOS, PECAM-1, VE-cadherin, FACS: PECAM-1	>98%	n. s.
(Hannum et al. 2001)	adenocarcinoma	collagenase/DNase, FACS using three different PECAM-1 antibodies	FACS: PECAM-1, PCR: PECAM-1	pure	n. s.
(Allport and Weissleder 2003)	heart, lung, lung carcinoma	collagenase, beads coated with PECAM-1, after days: beads coated with ICAM-2	FACS: PECAM-1, ICAM-2, VE-Cadherin, Sca-1; (E-selektin - $\uparrow$ and VCAM-1 after TNF - $\alpha$ )	80-95%	6-16 weeks
(Lim et al. 2003)	heart, lung	collagenase, beads coated with PECAM-1, after few days: beads coated with ICAM-2	in vitro: cobblestone morphology, FACS: PECAM-1, ICAM-1, ICAM-2, VE-cadherin, VCAM-1 (heart ECs)	85-99%	8-10 weeks
(Ewing et al. 2003)	lung	collagenase/dispase, after 3 days: FACS using dil-Ac-LDL	in vitro IF: uptake of dil-Ac-LDL, FACS: PECAM-1, MECA32, isolectin, VCAM-1 after TNF- $\alpha$	pure	n. s.
(Langley et al. 2003)	heart, lung	collagenase, incubation at 33°C (temperature-sensitive SV40 large T antigen), after 10-20 days: FACS using E-selectin and VCAM-1 (2x)	in vitro: cobblestone morphology, tube formation, in vitro IF: ICAM-1, VCAM-1, uptake of dil-Ac-LDL	pure	n. s.
(Hida et al. 2004)	melanoma liposarcoma	collagenase, MACS using PECAM-1, after 14 days: MACS using lectin	FACS: Lectin, in vitro IF: PECAM-1, VEGFR2	ca. 98%	8-10 weeks

**Table 1 continued:** Isolation, purification and identification of murine ECs isolated from heart, lung or tumor.

Reference	Tissue	Method of isolation and purification	Identification	Purity	Age
(Kuhlencordt et al. 2004)	lung	collagenase, after 2-4 days: beads coated with ICAM-2 (2x)	in vitro: cobblestone morphology, FACS: PECAM-1, ICAM-1, in vitro IF: uptake of dil-Ac-LDL	>95%	12-16 weeks
(Okaji et al. 2004)	colorectal tumor	trypsin/collagenase/hyaluronidase/DNAse, FACS using dil-Ac-LDL	FACS: Dil-Ac-LDL, in vitro: tube formation, in vitro IF: MECA-32	>97%	8 weeks
(Lim and Lusinskas 2006)	heart, lung	collagenase, beads coated with PECAM-1, after 7-9 days: beads coated with ICAM-2	in vitro: cobblestone morphology, FACS: PECAM-1, ICAM-2	85-99%	7-9 days
(Teng et al. 2006)	heart	perfusion of heart with collagenase solution, after several days: in vitro isolation of ECs with the help of cloning disks	in vitro: cobblestone morphology, in vitro IF: uptake of dil-Ac-LDL	pure	6-12 weeks
(Fehrenbach et al. 2009)	lung	collagenase, after 2-3 days: FACS using ICAM-2	in vitro: cobblestone morphology, tube formation, FACS: PECAM-1, ICAM-2, in vitro IF: VE-cadherin	pure	7-14 days
(Sobczak et al. 2010)	lung	collagenase/dispase, beads coated with PECAM-1, after 3-4 days: beads coated with ICAM-2	in vitro IF: VE-cadherin, VEGFR2	pure	6-8 days
(Jelonek et al. 2011)	heart	collagenase, beads coated with PECAM-1	in vitro IF: PECAM-1	pure	vital ECs up to 28 weeks
(Jin et al. 2012)	heart, lung	collagenase, beads coated with PECAM-1, after 5-9 days: beads coated with ICAM-2	FACS: PECAM-1, VE-cadherin	>85%	1-8 weeks
(Pratumvinit et al. 2013)	heart	collagenase/dispase, FACS using PECAM-1 and Sca-1	FACS: Sca-1, PECAM-1, mucosialin	pure	3-24 weeks

### 1.2.2 Cell surface markers

It is necessary not only to prove the purity of isolated cells, but also to prove that these cells are indeed ECs. An identification of ECs directly after isolation would be the best to avoid long-term culture effects which can influence the behavior of ECs. ECs express specific markers that can be used for identification *in vivo* and *in vitro*. In many cases, these molecules have been discovered by monoclonal antibodies directed against ECs (Garlanda and Dejana 1997). Some of the EC markers are constitutively expressed and are presented in the endothelium of all tissues. Other molecules are expressed only after stimulation by inflammatory cytokines or growth factors. Unfortunately, markers will not only be expressed by ECs, but also by different other cell types. Table 2 shows a (not definitive) summary of constitutively expressed EC markers. Traditional constitutive markers are the von Willebrand factor (vWF/factor VIII-related antigen) and the angiotensin converting enzyme (ACE). The vWF has been shown to be highly expressed on ECs from large vessels, but is not or marginally expressed in some capillary ECs (Kuzu et al. 1992). Another problem is that mesothelial cells can also express ACE and vWF (Chung-Welch et al. 1989). Mesothelial cells form a monolayer that line the body's serous cavities and internal organs (pleura, pericardium, peritoneum and male/female reproductive organs) (Mutsaers 2002). Further markers include the staining with lectin (*Griffonia simplicifolia* for mouse ECs) and the uptake of dil-Ac-LDL. Lectin can also be bound by epithelial cells and fibroblasts (Marelli-Berg et al. 2000; Fehrenbach et al. 2009), and mesothelial cells and fibroblasts are also able to uptake dil-Ac-LDL (Lou et al. 1998; Fehrenbach et al. 2009). Mucosialin is mainly expressed by hematopoietic progenitor cells and by ECs. Endoglin is expressed on ECs and several different normal and tumor cell types (Postiglione et al. 2005). VE-cadherin is mainly located at junctions between ECs, but also expressed by lymph node sinus macrophages (Lampugnani et al. 1992; Vestweber 2008). Thrombomodulin is expressed on ECs and mesothelial cells (Verhagen et al. 1996). Endothelial adhesion molecules which are involved in the attachment of leukocytes on the endothelium during leukocytes recruitment or inflammation are more suitable for the identification of ECs. Endothelial adhesion molecule-1 (PECAM-1), intercellular adhesion molecule-1 (ICAM-1), intercellular adhesion molecule-2 (ICAM-2), vascular cell adhesion molecule-1 (VCAM-1) and

E-selectin are involved in the passage of leukocytes from blood to underlying tissue. Whereas PECAM-1 and ICAM-2 are constitutively expressed on all ECs, ICAM-1 and VCAM-1 are less distributed and E-selectin is absent on the EC surface and must be induced. However, ICAM-1 and VCAM-1 may also be induced by contaminating mesothelial cells. PECAM-1 and ICAM-2 are also expressed by lymphocytes, platelets and monocytes. The EC identification can also be conducted by their cobblestone morphology and functional assays including tube formation in matrigel and the alignment in flow direction. Neither the cobblestone nor the tube formation is absolutely specific for ECs. Mesothelial cells can also display cobblestone morphology (Dong et al. 1997). It is also reported that ECs isolated from heart or tumor did not exhibit the typically tight cobblestone formation at confluence (Modzelewski et al. 1994; McDouall et al. 1996).

In conclusion, the clear identification of ECs remains a critical factor. These data indicate that the identification of ECs requires the staining of cells with more than just one or two antibodies. The best means for EC identification could be using as many markers as possible or examining a series of unique markers to make an assessment leading to the unambiguous identification of ECs.

**Table 2:** Endothelial cell markers.

Marker	Cell type	Reference
Angiotensin-converting enzyme	ECs, epithelial cells, fibroblasts, macrophages, T-lymphocytes	(Smallridge et al. 1986; Chung-Welch et al. 1989; Belloni and Tressler 1990)
Uptake of acetylated LDL	ECs, epithelial cells, fibroblasts, macrophages, smooth muscle cells, pericytes	(Voyta et al. 1984; Lou et al. 1998; Fehrenbach et al. 2009)
Lectin ( <i>Griffonia simplicifolia</i> )	ECs, epithelial cells, fibroblasts	(Laitinen 1987; Marelli-Berg et al. 2000; Fehrenbach et al. 2009)
Factor VIII-related antigen/ von Willebrand factor (Weibel-Palade bodies)	ECs, epithelial cells, platelets, megakaryocytes	(Chung-Welch et al. 1989; Belloni and Tressler 1990; Kuzu et al. 1992)
PECAM-1	ECs, platelets, megakaryocytes, B and T lymphocyte subsets, monocytes, neutrophils, tumor cells	(Tang et al. 1993; DeLisser et al. 1994; Vecchi et al. 1994; Scholz and Schaper 1997)
Mucosialin	ECs, hematopoietic progenitor cells, tumor cells	(Lin et al. 1995; Krause et al. 1996; Natkunam et al. 2000)

**Table 2 continued:** Endothelial cell markers.

ICAM-1 (up-regulated by cytokine)	ECs, leukocytes, epithelial cells, fibroblasts	(Dustin et al. 1986; Springer 1990; de Fougerolles et al. 1991)
ICAM-2	ECs, lymphocytes, monocytes, platelets	(Springer 1990; de Fougerolles et al. 1991)
Endoglin	ECs, macrophages, B lymphocytes, syncytiotrophoblasts, tumor cells	(Gougos and Letarte 1988; Duff et al. 2003; Postiglione et al. 2005; Fonsatti et al. 2010)
VE-cadherin	ECs, trophoblasts, lymph node sinus macrophages	(Lampugnani et al. 1992; Bulla et al. 2005; Vestweber 2008)
Thrombomodulin	ECs, smooth muscle cells, mesothelial cells	(Esmon 1995; Verhagen et al. 1996; Rabausch et al. 2005)
VCAM-1 (up-regulated by cytokine)	ECs, macrophages, mesothelial cells	(Springer 1990; Mutsaers 2002)

Further markers such as CD36, MUC18 (CD146), Tie-2, Sca-1, VEGFR-2, endothelial cell specific adhesion molecule (ESAM) and P-selectin (inducible) are rare described for primary mouse ECs and their use as marker is still not clear (Kobayashi et al. 2005; Lim and Lusinskas 2006; Kajimoto et al. 2010; Sobczak et al. 2010; Pratumvinit et al. 2013).

### 1.3 Shear stress on heart endothelial cells

The cultivation of primary heart and tumor ECs under shear stress due to liquid flow (medium) allows the physiological conditions in blood vessels to be simulated. The response of ECs to shear stress is closely linked to the regulation of vascular tone, blood coagulation and fibrinolysis, angiogenesis and vascular remodeling and plays an important role in maintaining the homeostasis of the circulatory system (Ando and Yamamoto 2013). Impairment of the EC response to shear stress leads to the development of vascular diseases such as hypertension, thrombosis, aneurysms and atherosclerosis. The intensity of shear stress mainly depends on the diameter of blood vessels. Under physiological conditions, shear stress ranges from 2-12 dyn/cm<sup>2</sup> for aorta and veins, whereas shear stress ranges from 20-40 dyn/cm<sup>2</sup> for arterioles and capillaries (Kamiya et al. 1984; Papaioannou

and Stefanadis 2005). A variety of shear-induced molecular responses in ECs was identified as candidates for shear stress sensors: Ion channels, receptors, adhesion molecules and glycocalyx (which are expressed in the cell membrane), primary cilia and caveolae (which constitute membrane microdomains), and actin-containing stress fibers, other cytoskeletal components and the lipid bilayer membrane (which support cell structures) (Figure 3) (Yamamoto and Ando 2011; Ando and Yamamoto 2013).

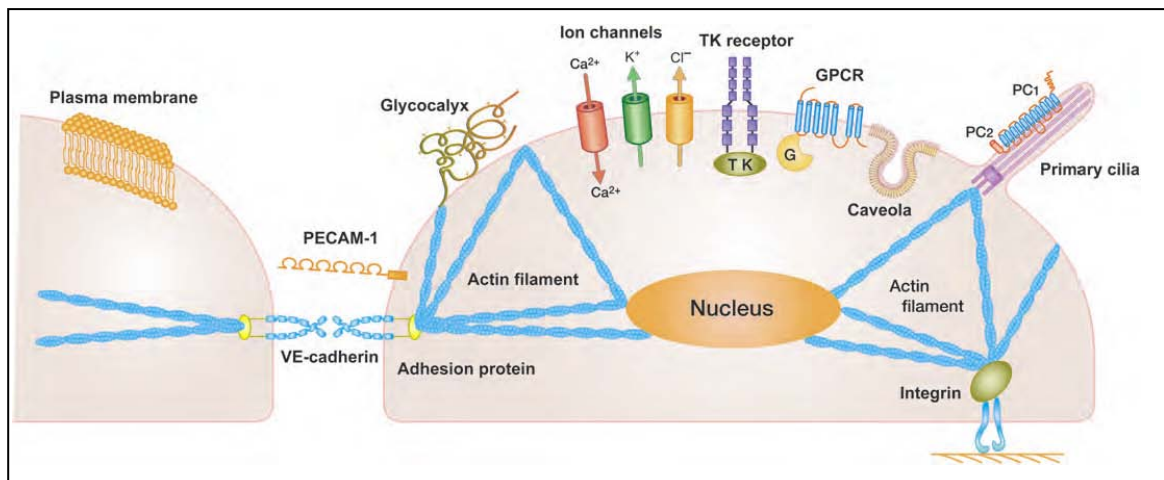


**Figure 3:** Candidates for shear stress sensors (Ando and Yamamoto 2013).

Shear stress is known to activate a variety of ion channels on ECs. Studies have demonstrated that flow activates Ca<sup>2+</sup>-channels and K<sup>+</sup>-channels, which leads to the hyperpolarization of ECs (Olesen et al. 1988; Hutcherson and Griffith 1994; Helmlinger et al. 1996; Yamamoto et al. 2000). The depolarization of ECs is executed by activation of Cl<sup>-</sup>-channels (Barakat et al. 1999; Nilius and Droogmans 2001). Shear stress also activates receptor tyrosin kinases and GTP binding protein-coupled receptors (GPCRs). As a result, receptor-tyrosin kinases VEGFR and Tie-2 or the membrane-bound G-protein can be activated even in the absence of their ligands VEGF and angiopoietin (Gudi et al. 1998; Shay-Salit et al. 2002; Lee and Koh 2003). Protein kinases, including extracellular signal-regulated kinase (ERK) are activated through the small G-protein Ras, which leads to the activation of NO synthase and inhibition of apoptosis (Jin et al. 2003). Shear stress due to liquid flow also leads to tyrosin phosphorylation of PECAM-1 in ECs, which positively regulates the Ras signalling pathways, leading to ERK activation (Osawa et al. 1997; Fujiwara et al. 2001; Ando and Yamamoto 2013). It was

shown that VE-cadherin forms a complex with PECAM-1 and VEGFR2 in which PECAM-1 transfers mechanical force (Tzima et al. 2005). These results indicate that PECAM-1 and VE-cadherin may play important roles in sensing shear stress generated by liquid flow. The surface of ECs is lined with a layer of membrane-bound glycocalyx, which contains proteoglycan and glycosaminoglycan including heparan sulfate, chondroitin sulfate and hyaluronic acid (van den Berg et al. 2003; Fu and Tarbell 2013; Alphonsus and Rodseth 2014). Shear stress affects the conformation of the glycocalyx, which influences the signal transduction by changing the local concentration of ions, enzymes, growth factors and cytokines (Siegel et al. 1996; Tarbell and Pahakis 2006). Enzymatic degradation of heparan sulfate with heparinase inhibits NO production in bovine aortic ECs in response to shear stress, suggesting a role of the glycocalyx plays in the intervention of shear stress-induced NO production (Florian et al. 2003). The presence of primary cilia was shown in embryonic ECs, HUVECs and human aortic ECs (Iomini et al. 2004). The bending of primary cilia by shear stress induces cytoskeleton deformation and activates the  $Ca^{2+}$ -channels polycystin-1 (PC1) and polycystin-2 (PC2) (Nauli et al. 2008; AbouAlaiwi et al. 2009). Caveolae are small (50–100 nm) membrane invaginations below the surface of ECs that are rich in caveolins, cholesterol and sphingolipids (Shaul and Anderson 1998). They are involved in shear stress signal transduction using various receptors, ion channels and protein kinases (Anderson 1993; Rizzo et al. 1998; Rizzo et al. 2003). Treatment of ECs with caveolin-1 antibody has been shown to suppress the ERK activation in response to shear stress (Park et al. 2000). Living cells stabilize their structure and shape by the use of an interconnected network of cytoskeleton components that includes microfilaments, microtubules and intermediate filaments. The endothelial cytoskeleton changes in response to shear stress and is able to bind directly or indirectly shear stress receptors (Helmke and Davies 2002). This leads to a reorientation of actin microfilaments to form stress fibers (Noria et al. 2004). Shear stress also changes the physical components of the endothelial lipid bilayer membrane (Lenaz 1987). It was shown that shear stress increased the membrane fluidity in HUVECs and bovine aortic ECs (Haidekker et al. 2000; Butler et al. 2001). The lipid bilayer membrane itself may act as sensor for shear stress. Additionally, it was shown that blood flow may determine the vessel size. A reduction of blood flow leads to a decrease in the vessel diameter (Langille and

O'Donnell 1986), which confirmed the physiological significance of blood flow detection by ECs.

In order to explore differences of the molecular phenotype of ECs under static and shear stress conditions at the transcriptome level microarray analysis is the tool of choice. In the living cardiovascular system, shear stress may present the normal situation. The absence of shear stress may present the pathological situation (Chen et al. 2001). The information of cardiovascular gene expression between both situations can be used to direct the attention to previously unknown or ignored genes/pathways. However, differences between the origin of ECs (e.g. different organism and tissue) and experimental conditions (e.g. different flow rate and duration) make the comparison between data sets difficult and limit their interpretation. Although limited, studies suggest three patterns of gene expression (Resnick et al. 2003). First, the immediate induction of gene expressions within seconds or minutes followed by a decrease to static levels; second, the immediate induction or suppression with sustained expression levels last for several hours; and third, the delayed induction or suppression of genes several hours after the onset of shear stress with sustained expression levels during flow condition. It seems that the first two conditions play a role in the activation of ECs and may be found in regions of inflammation or atherosclerosis, whereas the third condition plays a role in inhibition of proliferation, adhesion, thrombogenesis and inflammation (Resnick et al. 2003). Most data regarding flow transduction have been obtained during the first hours of flow exposure (Ando and Yamamoto 2013). Several pathways may be involved at later points in time, but later data for shear stress-regulated molecules and mechanisms are missing. Not only the change of gene expression from static to flow conditions is important, but also the gene expression under continuous flow, which is more representative for the functional status of normal ECs *in vivo*. This will lead to a better understanding of blood flow-dependent events, including angiogenesis, vascular remodeling and atherosclerosis, which may contribute to the development of new therapies for patients with vascular diseases.

## 1.4 Tumor angiogenesis

The origin of a tumor, i.e. the transformation of a normal cell into a tumor cell, can be explained by oncogene activation, tumor-suppressor mutation, high levels of telomerase or the induction of aneuploidy (Duesberg et al. 1999; Hahn and Weinberg 2002; Shay and Wright 2011). Normal and tumor tissue are dependent on an adequate supply of oxygen and nutrients. When the growing tissue reaches a certain size, in which the supply is no longer sufficient via diffusion, the tumor needs the connection to the existing normal vascular system. The induction of tumor vasculature is called angiogenic switch. The angiogenic balance is tightly regulated by pro- and anti-angiogenic signals. In normal physiological angiogenesis, new vessels rapidly mature and become stable. Pro- and anti-angiogenic factors are in balance. During tumor angiogenesis, the balance tips to the direction of pro-angiogenic factors. In adult organs, *in vivo* experiments showed that the normal EC turnover rate was very long. With a doubling time of years, normal ECs are among the longest-lived cells in the body outside the central nervous system. Only 1 in every 10,000 ECs (0.01 %) is in the cell division cycle at any given time. In contrast, about 14 % of normal intestinal epithelial cells are in the cell division cycle (Hanahan and Folkman 1996). The ECs doubling time in tumors is very short and is measured in days and may even be the limiting factor for tumor growth. Beside the low turnover rate, tumor blood vessels are also different in their architecture compared to normal blood vessels (Figure 4). Tumor blood vessels are not organized into definitive arterioles, venules and capillaries. Instead, tumor vessels show a chaotic vasculature (Denekamp and Hill 1991; McDonald and Choyke 2003; Jain 2005). Tumor ECs are irregularly shaped and tortuous, show variable diameters and have fewer branches. The tumor vasculature is often leaky and perivascular cells, usually in close contact to ECs, are often loosely associated or less common than in normal tissue. All this leads to dysfunctional capillaries with slower and sometimes oscillating blood flow.

In conclusion, in normal tissue, the vessel density is dynamically controlled by the metabolic needs of nutrients and oxygen. The vasculature is quiescent. In tumor tissue, as soon as the increased tissue mass outgrows the ability of existing vasculature to provide sufficient nutrients, the angiogenic switch is induced. The vasculature is able to produce capillaries. Obviously the excessive production of

tumor ECs leads to dysfunction of tumor vessels. The structural and functional abnormalities in tumor vessels reflect the pathological nature of their induction.

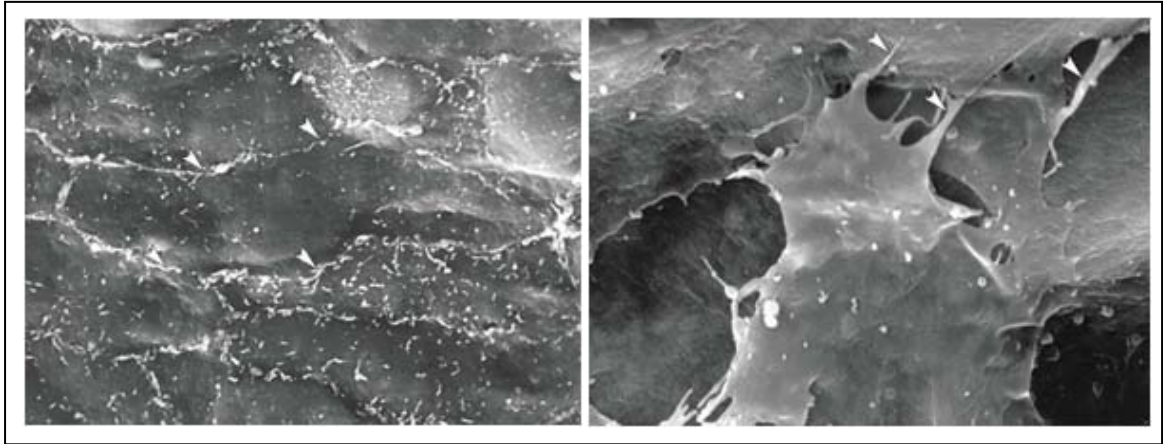


**Figure 4:** Luminal surface of a normal blood vessel (left, mouse mammary gland) and a tumor blood vessel (right, mouse mammary carcinoma) by scanning electron microscopy. In contrast to normal ECs tumor ECs are irregularly shaped and tortuous, show variable diameters and have fewer branches (arrows) (McDonald and Choyke 2003).

## 1.5 Irradiation effects on endothelial cells

Radiotherapy is commonly used for the local treatment of solid tumors residing in the thorax. However, radiotherapy may also induce delayed damage in surrounding healthy tissue, including the heart and lung. Although the volume exposure is kept as low as possible in adjustment of radiotherapy for breast cancer patients, parts of the heart still may receive radiation doses between 10-40 Gy, with a mean dose of few Gy (Andratschke et al. 2011; Darby et al. 2013). Experimental studies on the pathogenesis of radiation-induced heart diseases have demonstrated major functional changes in the microvasculature of the myocardium, particularly in microvascular ECs (Schultz-Hector and Trott 2007). Radiation exposure of a large lung volume may induce lung fibrosis leading to pulmonary hypertension, which can also participate to cardiac dysfunction (Marcus et al. 2008; Ghobadi et al. 2012). The risk for radiation-induced heart diseases increases significantly 10 years after radiation therapy (Darby et al. 2010). Radiation effects on ECs have been analyzed by commercially available cell lines such as human umbilical vein endothelial cells (HUVECs), human dermal microvascular endothelial cells (HDMECs), human pulmonary microvascular endothelial cells and by *in vitro* experiments (Gaugler et al. 1997; Heckmann et al.

1998; Quarmby et al. 1999; Quarmby et al. 2000; Gaugler et al. 2004). However, results may not be important to the pathogenesis of late radiation damage due to the high proliferation rate of these ECs *in vitro* (Sievert et al. 2015). In contrast, primary ECs in healthy tissue show a very low proliferation rate (Hobson and Denekamp 1984). Recently, the mechanisms of radiation induced heart dysfunction in mice after low and high doses were investigated by the European Cardiovascular Radiation Risk Research Project CARDIORISK. The development of vascular damage after irradiation was found to be dose- and time-dependent (Seemann et al. 2012; Azimzadeh et al. 2013). After 20 weeks, local heart irradiation with single doses of 2 and 8 Gy led to a significant increase in microvascular density, co-occurring with an increased epicardial thickness after 8 Gy. After 40 weeks, microvascular density returned to normal and decreased at 60 weeks (Seemann et al. 2012). These temporary changes were presumably based on stimulated proliferation of ECs in response to radiation-induced damage. It was shown that total body irradiation resulted in depletion and reduced vasculogenesis of endothelial progenitor cells (Lee et al. 2012). Injection of bone marrow-derived endothelial progenitor cells in mice 16 and 28 weeks after heart irradiation with 16 Gy revealed no repair of microvascular damage at 40 weeks (Seemann et al. 2014). However, studies which investigate the role of endothelial progenitor cells after local heart irradiation are rare.

While it is widely recognized that adhesion molecules of ECs are involved in inflammation and atherosclerotic lesions (Davies et al. 1993), their contribution to radiation-induced microvascular heart diseases remains unclear. Immunohistochemistry showed that ICAM-1 in the endothelium of mouse carotid arteries was decreased 1 and 4 weeks after local irradiation with 14 Gy (Hoving et al. 2012). Immunofluorescence staining of the Arteria saphena demonstrated an increased expression of PECAM-1, ICAM-1 and VCAM-1 3–6 months after local irradiation with 2–10 Gy (Patties et al. 2014). However, immunofluorescence staining of heart tissue indicated no alteration in PECAM-1 and VCAM-1 expression 20 weeks after local irradiation with 2 and 8 Gy (Patties et al. 2015). Recently, a proteomic study on isolated cardiac microvascular ECs showed significantly increased expression levels of ICAM-1 and ICAM-2 16 weeks after local heart irradiation with 8 Gy (Azimzadeh et al. 2015). However, a causal relationship between an increased expression of inflammatory proteins and late

radiation-induced diseases in heart and lung has not been proven and thus remains speculative (Sievert et al. 2015).

## 1.6 Aim of the study

Previous isolation methods of primary ECs from the heart and tumor of mice were based on collagenase digestion followed by purification techniques, such as magnetic bead separation or FACS-sorting using an antibody, such as PECAM-1, which is directed against ECs. In both cases, very often the purification step needed to be repeated to remove contaminating cells (Table 1). This resulted in low yields of primary ECs. Furthermore, magnetic beads which remain bound to isolated ECs represent a steric hindrance and prevents the attachment of freshly isolated primary ECs in cell culture (Gargett et al. 2000; Cha et al. 2005). Additionally, the use of hearts from mice which are older than 28 weeks resulted in ECs, that did not become adherent. These cells could not be maintained or expanded in cell culture, and underwent apoptotic cell death within a few days. ECs isolated from young mice, which are not fully grown yet, have the capacity to proliferate and therefore have the ability to get rid of the attached beads with sustained cell division. However, the results obtained by this analysis using *in vitro* cultured ECs may not be representative for the functional status of ECs of adult animals *in vivo*. The doubling time of ECs *in vitro* (days) does not reflect the very low proliferation rate (years) of ECs in healthy tissues of adult mice.

Based on the problems which appeared with the previously described isolation methods for ECs, the goal of my work was the analysis and characterization of isolated primary ECs from normal non-proliferating and proliferating benign and malignant tissue. For that a new method is necessary that provides high yields of vital ECs not only from young mice (proliferating tissue) but also from old mice (quiescent tissue). Importantly, the isolated ECs should be free of contaminating cells and free of magnetic beads which are bound to the cells. The absence of contaminating cells avoids a further purification step and thus results in higher yields. The isolation of bead-free ECs allows not only that these cells get adherent *in vitro* but also provide the possibility to analyze them directly after isolation by flow cytometry. This immediate analysis reflects much better the *in vivo* status of

primary ECs compared to those cells which were cultured *in vitro*. Furthermore, the identification of primary ECs should be demonstrated with more than two or three markers.

Based on the newly established method, a specific aim was to explore the difference between normal quiescent ECs and malignant proliferating ECs. In this context it was intended to analyse the expression of different cell surface markers, morphology and functions like migration, tube formation and alignment under liquid flow. The results should provide a clarification of organ-specific immunological interactions and functional changes in the interplay of existing and evolving ECs from benign and malignant tissue.

An additional aim was to examine the cardiovascular gene expression of ECs under physiological shear stress compared to pathological static conditions. This should improve the understanding of blood flow-dependent events, including angiogenesis, vascular remodeling and atherosclerosis, which may contribute to the development of new therapies for patients with vascular diseases.

Furthermore, it was an important aim of this thesis to investigate the development of late radiation damage in the microvasculature using this novel method. The analysis of primary heart ECs after local irradiation *in vivo* should provide evidences to clarify the long clinical development and progression of radiation heart damage *in situ*.

## 2. MATERIALS AND METHODS

All materials and methods used in this study are described below. Commonly used methods, materials and devices are not listed separately.

### 2.1 Materials

#### 2.1.1 Devices and consumable materials

**Table 3:** Used devices and their producer

device	producer
4 °C refrigerator profi line	Liebherr, Biberach an der Riß, Germany
-20 °C Comfort	Liebherr, Biberach an der Riß, Germany
-80 °C Herafreeze Basic	Thermo Fisher Scientific, Waltham, USA
Agilent Bioanalyzer 2100	Agilent Technologies, Waldbronn, Germany
autoclav Systec VX-150	Systec, Linden, Germany
cryogenic storage system Biosafe®	Cryotherm, Kirchen/Sieg, Germany
cryostat Leica CM 1950	Leica, Wetzlar, Germany
direct-Q3 ultrapure water system	Merck Millipore, Billerica, USA
DNA-microarray scanner	Agilent Technologies, Waldbronn, Germany
dry bottle with silicate	ibidi, Martinsried, Germany
external humidifier column	ibidi, Martinsried, Germany
FACS Calibur instrument	BD Bioscience, Heidelberg, Germany
Fluidic Unit	ibidi, Martinsried, Germany
Fresco 21 centrifuge	Thermo Fisher Scientific, Waltham, USA
Gulmay RS225A	xstrahl, Camberley, United Kingdom
heated lid and heated plate	ibidi, Martinsried, Germany
heating block	Haep Labor Consult, Bovenden, Germany
ibidi air pressure pump	ibidi, Martinsried, Germany
ice machine MF22	Scotsman, Milan, Italy
incubator BBD 6220	Thermo Fisher Scientific, Waltham, USA
incubator Heracell 240i	Thermo Fisher Scientific, Waltham, USA
intelli-mixer RM-2L	Elmi, Riga, Latvia
laminar flow safe 2020	Thermo Fisher Scientific, Waltham, USA
lead plate with 9x13 and 15x18 mm <sup>2</sup> windows	own fabrication
Magnetic Particle Concentrator DynaMag	Thermo Fisher Scientific, Waltham, USA
magnetic stirrer RCT basic	IKA, Staufen, Germany
megafuge 16R centrifuge	Thermo Fisher Scientific, Waltham, USA
Mikro-Dismembrator S	Sartorius Stedim Biotech, Göttingen, Germany
microscope 40C	Zeiss, München, Germany
microscope observer.Z1	Zeiss, München, Germany

## Materials and Methods

**Table 3 continued:** Used devices and their producer

microscope Primo Vert	Zeiss, München, Germany
mouse jig	own fabrication
Mr. Frosty™ Freezing Container	Thermo Fisher Scientific, Waltham, USA
NanoDrop spectrophotometer	Thermo Fisher Scientific, Waltham, USA
PCR-unit (GeneAmp®PCR System 9700)	Thermo Fisher Scientific, Waltham, USA
plate reader EL808	BioTek, Bad Friedrichshall, Germany
RNase	Thermo Fisher Scientific, Waltham, USA
scale Kern ew 420	Kern, Balingen, Germany
sonograph	GE Healthcare, Fairfield, USA
temperature controller HT200	ibidi, Martinsried, Germany
The BRICK, active gas mixer	ibidi, Martinsried, Germany

**Table 4:** Use consumable materials and their producer

<b>consumable material</b>	<b>producer</b>
cell culture flask 12.5 mm <sup>2</sup>	BD Bioscience, Heidelberg, Germany
cell culture flask 25, 75, 162 mm <sup>2</sup>	Corning B.V. Life Sciences, Amsterdam, the Netherlands
cell culture plate 6, 12 well	Corning B.V. Life Sciences, Amsterdam, the Netherlands
cell strainer 70 µm	BD Bioscience, Heidelberg, Germany
chamber slide (2, 4, 8 well)	Thermo Fisher Scientific, Waltham, USA
cover slip (round, 15x15 mm, 24x50 mm)	Gerhard Menzel, Braunschweig, Germany
cryo tube 20	TPP Techno Plastic Products, Trasadingen, Switzerland
needle 18Gx2, 20Gx1½, 27Gx¾, 30Gx½	B.Braun, Melsungen, Germany
perfusion set, 50 cm, ID 0.8 mm	ibidi, Martinsried, Germany
phase lock gel tube	Eppendorf, Hamburg, Germany
pipette tips 10, 100, 1000 µl	Sarstedt, Nümbrecht, Germany
quadriperm® cell culture vessel	Sigma-Aldrich, Steinheim, Germany
reaction tubes 1.5 ml	Sarstedt, Nümbrecht, Germany
reservoir set, 10 ml	ibidi, Martinsried, Germany
safe-lock tubes 0.5 ml	Eppendorf, Hamburg, Germany
single-use pipettes 1, 2, 5, 10, 25, 50 ml	Greiner Bio-One, Frickenhausen, Germany
slide-A-Lyzer G2 Dialysis Cassette	Thermo Fisher Scientific, Waltham, USA
syringes 1, 2, 3, 10 ml	B.Braun, Melsungen, Germany
syringe filter 0.22 µm	TPP Techno Plastic Products, Trasadingen, Switzerland
tissue culture dishes 22.1 cm <sup>2</sup>	TPP Techno Plastic Products, Trasadingen, Switzerland
tissue culture test plates 96U	TPP Techno Plastic Products, Trasadingen, Switzerland
tubes 15, 50 ml	Greiner Bio-One, Frickenhausen, Germany
tubes 5 ml for flow cytometry	Sarstedt, Nümbrecht, Germany

**Table 4 continued:** consumable materials and their producer

μ-Dish 35mm, low Culture-Insert, ibiTreat	ibidi, Martinsried, Germany
μ-Slide Angiogenesis	ibidi, Martinsried, Germany
μ-slide <sup>0.2</sup> Luer, μ-slide <sup>0.4</sup> Luer	ibidi, Martinsried, Germany
μ-Slide VI <sup>0.4</sup> Luer, ibiTreat	ibidi, Martinsried, Germany

## 2.1.2 Chemicals

**Table 5:** Used chemicals and their sources

chemical	source
pure acetic acid	Merck, Darmstadt, Germany
acetone	Sigma-Aldrich, Steinheim, Germany
Aqueous Mount	Zytomed Systems, Berlin, Germany
Biotin-Nick Translation Mix	Sigma-Aldrich, Steinheim, Germany
bovine serum albumin (BSA)	Sigma-Aldrich, Steinheim, Germany
chloroform	Merck, Darmstadt, Germany
collagenase A	Roche Diagnostics, Mannheim, Germany
dextran sulfate	Serva, Heidelberg, Germany
Dig-Nick Translation Mix	Sigma-Aldrich, Steinheim, Germany
dimethyl sulfoxide (DMSO)	Sigma-Aldrich, Steinheim, Germany
di-sodium hydrogen phosphate dihydrate	Merck, Darmstadt, Germany
Dulbecco's modified Eagle's medium (DMEM)	Sigma-Aldrich, Steinheim, Germany
phosphate buffered saline (PBS)	Sigma-Aldrich, Steinheim, Germany
ethylenediaminetetraacetic acid (EDTA)	Merck, Darmstadt, Germany
Endothelial Cell Growth Medium 2 (EGM2)	PromoCell, Heidelberg, Germany
eosin y-solution	Merck, Darmstadt, Germany
ethanol	Merck, Darmstadt, Germany
ethidium Bromide	Sigma-Aldrich, Steinheim, Germany
fixogum	Marabu, Tamm, Germany
FACS Clean	BD Bioscience, Heidelberg, Germany
FACS Rinse	BD Bioscience, Heidelberg, Germany
FACS Flow	BD Bioscience, Heidelberg, Germany
fetal bovine serum (FSC)	Sigma-Aldrich, Steinheim, Germany
forene 100%	Abbott, Wiesbaden, Germany
formamide	Sigma-Aldrich, Steinheim, Germany
Freund's adjuvant, incomplete	Sigma-Aldrich, Steinheim, Germany
gelatine	Merck, Darmstadt, Germany
glucose	Sigma-Aldrich, Steinheim, Germany
isoamyl alcohol	Sigma-Aldrich, Steinheim, Germany
Hanks' Balanced Salt Solution (HBSS)	Thermo Fisher Scientific, Waltham, USA
hematoxylin	Merck, Darmstadt, Germany
herring sperm DNA	Sigma-Aldrich, Steinheim, Germany
LB Broth	USB, High Wycombe, United Kingdom
L-glutamine 200 mM	Sigma-Aldrich, Steinheim, Germany
lysozyme-solution (5 mg/ml)	Sigma-Aldrich, Steinheim, Germany
β-mercaptoethanol 50 mM	Thermo Fisher Scientific, Waltham, USA
marker 1kb	Thermo Fisher Scientific, Waltham, USA

**Table 5 continued:** Used chemicals and their sources

matrigel	BD Bioscience, Heidelberg, Germany
methanol	Merck, Darmstadt, Germany
mouse Cot-1 DNA	Thermo Fisher Scientific, Waltham, USA
non-essential amino acid solution	Sigma-Aldrich, Steinheim, Germany
Nonidet P 40	Sigma-Aldrich, Steinheim, Germany
penicillin-streptomycin	Sigma-Aldrich, Steinheim, Germany
pepsin	Thermo Fisher Scientific, Waltham, USA
phenol	Sigma-Aldrich, Steinheim, Germany
potassium chloride (KCl)	Merck Millipore, Billerica, USA
primary antibody diluent	AbD Serotec, Puchheim, Germany
propidium iodide (PI)	Merck, Darmstadt, Germany
Roswell Park Memorial Institute (RPMI) 1640 medium	Sigma-Aldrich, Steinheim, Germany
salt acid (1N) (HCl)	Merck, Darmstadt, Germany
skimmed milk powder	BioRad Laboratories, München, Germany
sodium azide	Merck, Darmstadt, Germany
sodium bicarbonate	Sigma-Aldrich, Steinheim, Germany
sodium chloride (NaCl)	Merck, Darmstadt, Germany
sodium dodecylsulfate (SDS)	Merck, Darmstadt, Germany
sodium hydrogen phosphate monohydrate	Merck, Darmstadt, Germany
sodium hydroxide (NaOH)	Merck, Darmstadt, Germany
Tissue-Tek	Sakura Finetek, Alphen aan den Rijn, the Netherlands
tris	Merck, Darmstadt, Germany
tri-sodium citrate	Merck, Darmstadt, Germany
trypan Blue solution	Sigma-Aldrich, Steinheim, Germany
trypsin-EDTA solution	Sigma-Aldrich, Steinheim, Germany
ultrasound gel	Dahlhausen, Köln, Germany
Vectashield mounting medium with DAPI	Vector Laboratories, Burlingame, USA

### 2.1.3 Buffers and solutions

- carnoy's Fixative  
pure acetic acid (1 part)  
methanol (3 parts)
- glucose-buffer  
6 g glucose (50 mM)  
3.73 g EDTA (10 mM)  
3.03 g tris (25 mM)  
ad 1 liter with double distilled water
- LB-medium  
20 g LB Broth  
ad 1liter with double distilled water  
autoclave

## Materials and Methods

---

- phosphate buffer with Nonidet P 40, 0.1% (PN-buffer)  
142.39 g di-sodium hydrogen phosphate dihydrate in 8 liter distilled water  
set pH 8 with 6.9 g sodium hydrogen phosphate monohydrate in 500 ml distilled water  
add 0.1 % Nonidet P 40
- phosphate-Nonidet P 40-skimmed milk (PNM-buffer)  
5 g skimmed milk powder  
0.02 g sodium azide  
ad 100 ml with PN-buffer, incubation at 37 °C for several hours  
next day centrifugation (3000 g, 10 minutes), sterile filtration of supernatant  
storage at -20 °C
- NaOH/SDS-solution  
200 µl NaOH (1 M)  
40 µl sodium dodecylsulfate  
ad 1 liter with double distilled water
- mastermix  
5 ml formamide deionized  
1 g dextran sulfate  
1 ml 20x SSC pH 7  
mix, heating at 70 °C to solve dextran sulfate, set pH 7  
ad 7 ml with double distilled water
- sodium acetate (3 M)  
246 g sodium acetate  
ad 1 liter with double distilled water, set pH 4.8  
autoclave
- saline sodium citrate buffer (20x) (SSC)  
175.3 g/l (3M) NaCl  
88.2 g/l (0.3 M) tri-sodium citrate  
set pH 7, ad 1 liter with double distilled water
- tris-EDTA-buffer (TE-buffer)  
1.2 g Tris (10 mM)  
0.37 g EDTA (1 mM)  
ad 1 liter with double distilled water, set pH 7.5  
autoclave
- tris-EDTA-Saline-buffer (TES-buffer)  
1.21 g tris (10 mM)  
0.58 g NaCl (10 mM)  
0.37 g EDTA (1 mM)  
ad 1 liter with double distilled water, set pH 7.6  
autoclave
- sodium dodecylsulfate  
250 g sodium dodecylsulfate in 600 ml double distilled water, heating at 60–100 °C  
cool down and ad 1 liter with double distilled water

## 2.1.4 Antibodies

**Table 6:** Used antibodies (clon, host, isotype, conjugation) and their sources for FACS

antigen	clon	host and isotype	conjugation	source
Isotype	HybIgG2a	mouse IgG2a	FITC	abcam, Cambridge, United Kingdom
Isotype	R35-95	rat IgG2a, $\kappa$	FITC	BD Bioscience, Heidelberg, Germany
Isotype	A19-3	hamster IgG1, $\kappa$	FITC	BD Bioscience, Heidelberg, Germany
Isotype	A110-1	rat IgG1, $\lambda$	FITC	BD Bioscience, Heidelberg, Germany
Isotype	R35-95	rat IgG2a, $\kappa$	PE	BD Bioscience, Heidelberg, Germany
Isotype	R35-38	rat IgG2b, $\kappa$	PE	BD Bioscience, Heidelberg, Germany
Isotype	R3-34	rat IgG1, $\kappa$	PE	BD Bioscience, Heidelberg, Germany
Isotype	A95-1	rat IgG2b, $\kappa$	APC	BD Bioscience, Heidelberg, Germany
PECAM-1/ CD31	MEC 13.3	rat IgG2a, $\kappa$	PE	BD Bioscience, Heidelberg, Germany
PECAM-1/ CD31	MEC 13.3	rat IgG2a, $\kappa$	unconjugated	BD Bioscience, Heidelberg, Germany
Mucosialin/ CD34	RAM34	rat IgG2a, $\kappa$	FITC	eBioscience, Frankfurt am Main, Germany
HCAM/ CD44	IM7	rat IgG2b, $\kappa$	PE	BD Bioscience, Heidelberg, Germany
CD45	30-F11	rat IgG2b, $\kappa$	APC	BD Bioscience, Heidelberg, Germany
ICAM-1/ CD54	3E2	hamster IgG1, $\kappa$	FITC	BD Bioscience, Heidelberg, Germany
ICAM-2/ CD102	3C4	rat IgG2a, $\kappa$	FITC	BD Bioscience, Heidelberg, Germany
Integrin $\beta$ 3/ CD61	2C9.G2	hamster IgG1, $\kappa$	FITC	BD Bioscience, Heidelberg, Germany
E-selectin/ CD62E	10E9.6	rat IgG2a, $\kappa$	PE	BD Bioscience, Heidelberg, Germany
Endoglin/ CD105	MJ7/18	rat IgG2a, $\kappa$	PE	eBioscience, Frankfurt am Main, Germany
VCAM-1/ CD106	M/K-2	rat IgG1, $\kappa$	PE	life technologies, Darmstadt, Germany
Prominin-1/ CD133	13A4	rat IgG1, $\kappa$	FITC	eBioscience, Frankfurt am Main, Germany
VE-cadherin/ CD144	11D4.1	rat IgG2a, $\kappa$	PE	BD Bioscience, Heidelberg, Germany
VEGFR-2/ CD309	Avas 12alpha1	rat IgG2a, $\kappa$	PE	BD Bioscience, Heidelberg, Germany

## Materials and Methods

**Table 7:** Used antibodies (clon, host, isotype, conjugation) and their sources for immunofluorescence microscopy

antigen	host and isotype	conjugation	source
anti-rat	Goat, IgG	Alexa Fluor 594	Thermo Fisher Scientific, Waltham, USA
Isolectin B4	Griffonia Simplicifolia	FITC	Vector Laboratories, Burlingame, USA

**Table 8:** Used antibodies, sources and dilutions for FISH

antibody	source	antibody solution [ $\mu$ l]	PNM-buffer [ $\mu$ l]
Streptavidin-Avidin	Jackson ImmunoResearch, Newmarket, United Kingdom	10	240
anti-Digoxigenin-Cy3	Jackson ImmunoResearch, Newmarket, United Kingdom	4	496
Biot-anti-Streptavidin	Vector Laboratories, Burlingame, USA	10	240
Rat-anti-mouse-Cy3	Jackson ImmunoResearch, Newmarket, United Kingdom	10	240
Mouse-anti-rat-Cy3	Jackson ImmunoResearch, Newmarket, United Kingdom	10	240

### 2.1.5 BAC clones

**Table 9:** Used murine BAC clones for FISH

Name BAC	reference	reference sources	labeling
RP23-28913	Chromosome 1	www.ensembl.org	Digoxigenin
RP23-257F12	Chromosome 4	www.ensembl.org	Biotin
RP23-154G18	Chromosome 14	www.ensembl.org	Digoxigenin
RP23-154G18	Chromosome 14	www.ensembl.org	Biotin

### 2.1.6 Kits

**Table 10:** Used kits and their sources

kits	source
DSB-X™ Biotin protein labeling kit	Thermo Fisher Scientific, Waltham, USA
Dynabeads FlowComp™ Flexi, part A	Thermo Fisher Scientific, Waltham, USA
MycoAlert™ mycoplasma detection kit	Lonza, Basel Switzerland
Pierce™ BCA Protein Assay kit	Thermo Fisher Scientific, Waltham, USA
DNA Clean and Concentrator kit	Zymo Research, Irvine, USA

**Table 10 continued:** Used kits and their sources

RNA 6000 Nano Assay kit	Agilent Technologies, Waldbronn, Germany
RNeasy Micro kit	Qiagen, Hilden, Germany
two-color microarray-based gene expression analysis kit	Agilent Technologies, Waldbronn, Germany

## 2.1.7 Software

**Table 11:** Used software and their sources

software	source
Adobe Photoshop CS4 Version 11	Adobe Systems Incorporated, USA
AxioVision	Zeiss, München, Germany
Cell Quest Pro	BD Bioscience, Heidelberg, Germany
Feature Extraction software	Agilent Technologies, Waldbronn, Germany
Gen5	BioTek, Bad Friedrichshall, Germany
ibidi CamControl 0.1	ibidi, Martinsried, Germany
ibidi PumpControl 1.5	ibidi, Martinsried, Germany
ImageJ 1.48v	Wayne Rasband National Institutes of Health, USA
Isis	MetaSystems, Altussheim, Germany
Microsoft Office	Microsoft Corporation, Redmond, USA
SigmaPlot 11	Systat Software, wpcubed, Germany
TMPGEnc Video Mastering Works 5	Pegasys Inc., Tokyo, Japan
WimTaxis	Wimasis, München, Germany
WimTube	Wimasis, München, Germany

## 2.1.8 Cell lines and primary cells

**Table 12:** Used cell lines and their sources (incl. reference)

cells line	source	reference
H5V	Immortalized heart ECs from C57Bl/6-mice (Dr. Chrisou Kanthou, University of Sheffield)	(Garlanda et al. 1994)
CT26	Colon adenocarcinoma cells from BALB/c-mice (CT26.WT; ATCC CRL-2638)	(Brattain et al. 1980; Wang et al. 1995)
B16-F0	Melanoma cells from C57Bl/6-mice (B16-F0; ATCC CRL-6322)	(Fidler 1973; Fidler 1975)

**Table 13:** Used primary cells and their sources (incl. reference)

primary cells	source	reference
heart endothelial cells	this laboratory from mouse heart	(Sievvert et al. 2014)
lung endothelial cells	this laboratory from mouse lung	(Sievvert et al. 2014)
repair blastema endothelial cells	this laboratory from mouse repair blastema	(Sievvert et al. 2014)
CT26 endothelial cells	this laboratory from mouse tumor (CT26)	(Sievvert et al. 2014)
B16-F0 endothelial cells	this laboratory from mouse tumor (B16-F0)	(Sievvert et al. 2014)

### 2.1.9 Laboratory animals

Female/male BALB/c and C57Bl/6 mice (Charles River) within an age range of 4 to 100 weeks were used for the experiments. Mice were housed in single, ventilated cages under pathogen-free conditions. Experiments were in agreement with German law on animal experiments and welfare.

**Table 14:** Used pharmaceuticals and their sources

pharmaceutical	source
Medetomidine	Pfizer, Berlin, Germany
Midazolam	Ratiopharm, Ulm, Germany
Fentanyl	Jansen-Cilag, Neuss, Germany
Atipamezole	Pfizer, Berlin, Germany
Flumazenil	Insera Arzneimittel, Freiburg, Germany
Naloxone	Insera Arzneimittel, Freiburg, Germany

The anesthesia was performed by MMF (Medetomidin (0,50 mg/kg) + Midazolam (5,0 mg/kg) + Fentanyl (0,05 mg/kg)). The antagonist consists of AFN (Atipamezol (2,5 mg/kg) + Flumazenil (0,5 mg/kg) + Naloxon (1,2 mg/kg)).

## **2.2 Methods**

### **2.2.1 Cell biological methods**

#### **2.2.1.1 Cell culture of cell lines and primary cells**

Cells were regularly cultivated under sterile conditions in cell culture flasks at 37 °C, 95 % relative humidity and 5 % CO<sub>2</sub> in an incubator. Cell culture was performed under a laminar flow. Briefly, the adherent cells were washed twice with PBS and treated with trypsin-EDTA solution at 37 °C for detachment from the flask. The cells were seeded in adequate dilution with medium in new flask. All cell lines were passaged twice weekly to maintain them under exponential growth conditions. Cell lines were regularly screened and confirmed to be free from mycoplasma contaminations. CT26 cells were cultured in RPMI 1640 medium containing 5 % (v/v) heat-inactivated fetal calf serum, 2 mM L-glutamine, antibiotics (100 IU/ml penicillin and 100 µg/ml streptomycin), 50 µM β-mercaptoethanol and non-essential amino acids (1x). B16-F0 cells and the heart endothelial cell line H5V were cultured in DMEM containing 10 % (v/v) heat-inactivated fetal calf serum and antibiotics (100 IU/ml penicillin and 100 µg/ml streptomycin).

Freshly isolated primary microvascular PECAM-1 positive ECs from different tissue were counted and viable cells were seeded in gelatin coated (2 %) culture flasks with EGM2 (supplemented with 10 % FCS, streptomycin (100 µg/ml) and penicillin (100 U/ml)). The medium was exchanged every third day and cells were passaged when 90 % confluence were reached. For further functional assays, primary ECs in the first or second passage were used.

#### **2.2.1.2 Cell number and viability**

Viable cells were determined by the trypan blue exclusion test. Only non-viable cells absorbed trypan blue and appeared blue. Briefly, a dilution (1:2) of cell suspension and trypan blue was loaded in a Neubauer chamber and viable unstained cells were counted under the microscope. The dilution of the cell suspension was regulated with the result that approximately 100 cells could be

counted (statistical significance). The total number of cells was calculated as follows:

$$total\ cells = \frac{counted\ cells \times 10^4}{number\ quadrants} \times dilution$$

### 2.2.1.3 Cryopreservation of cells

For permanent storage the cells were cryopreserved in liquid nitrogen. After centrifugation (500 g, 5 minutes) at 4 °C, the cell pellet ( $2 \times 10^6$ ) was solved in cold medium/FCS/DMSO (50/40/10 %). DMSO prevents crystallization in the cells. The cell suspension was aliquoted into cryo tubes (1.8 ml) and continuously frozen in freezer container (to -80 °C). After 24 hours the cells were transferred into liquid nitrogen. For new cultivation, the cells were defrosted, centrifuged (400 g, 5 minutes) at 4 °C and seeded in culture flask. After 24 hours the medium was exchanged to remove dead cells.

### 2.2.1.4 Cell alignment assay

For the analysis of heart and tumor ECs with permanent shear stress, ECs were used directly after their isolation.  $4 \times 10^5$  cells in 50  $\mu$ l medium were seeded into a channel of a  $\mu$ -slideVI<sup>0.4</sup> (area per channel: 0.6 cm<sup>2</sup>). For the mRNA expression analysis, more heart ECs were necessary. Therefore  $1.8 \times 10^6$  heart ECs in 50  $\mu$ l or 100  $\mu$ l medium were seeded into a channel of a  $\mu$ -slideI<sup>0.2</sup> or  $\mu$ -slideI<sup>0.4</sup> (area per channel 2.5 cm<sup>2</sup>). The  $\mu$ -slideI<sup>0.2</sup> Luer (height of the channel: 200  $\mu$ m) allows the use of high shear stress, but is not recommended for static culture longer than 6 hours. For static condition, the  $\mu$ -slideI<sup>0.4</sup> Luer (height of the channel: 400  $\mu$ m) was used. After filling both ends of the channel with medium and incubation under static conditions at 37 °C, cells were exposed to flow conditions. A pump system, Fluidic Unit, gas mixer, temperature controller and heating system guaranteed constant conditions. In this way, simultaneous culture and observation of cells under perfusion were possible. First, the slide was connected with the perfusion set, which contains both syringe reservoirs and the branching tubes (Figure 5). All

tubes were filled with preheated medium. Then, reservoirs and tubes were connected with the Fluidic Unit. The pump generates a constant pressure and pumps the medium from one reservoir to the other and back. The flow rate of the medium is dependent by the pressure applied, viscosity of the medium and the flow resistance of the slide. The calibrated flow rate (ml/min) causes a wall shear stress ( $\text{dyn}/\text{cm}^2$ ) to which the cells are exposed. A PumpControl software controlled the pump and the Fluidic Unit. The Fluidic Unit switched synchronously two four way valves. In this way, a continuous flow through the slide with minimal consumption of medium was possible. A gas mixer was connected to the incubator to provide the medium with 5 %  $\text{CO}_2$ . The temperature controller and the heating system guaranteed a temperature of  $37\text{ }^\circ\text{C}$  inside the slide. Representative microscopy pictures of ECs were taken using an Axiovert 40C microscope.

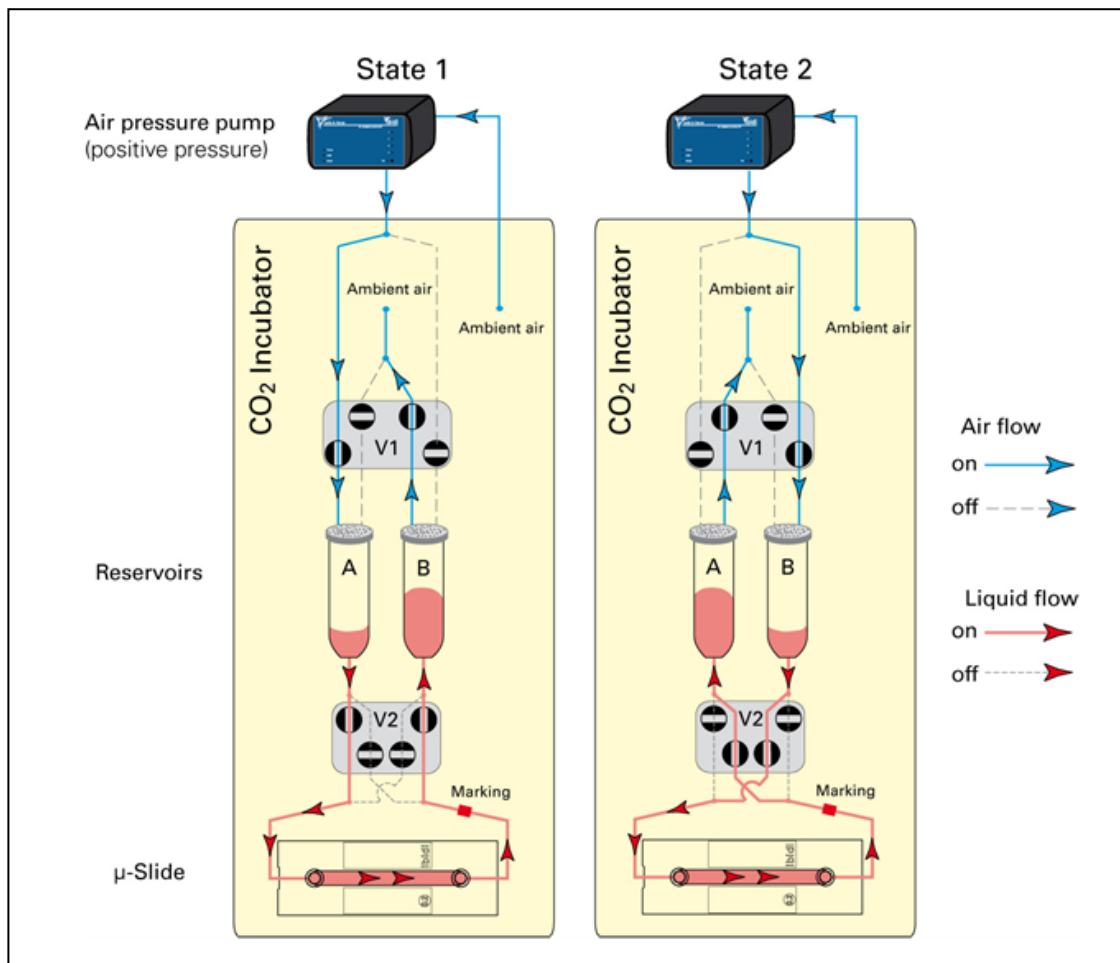


Figure 5: Principle of the ibidi pump ([www.ibidi.com](http://www.ibidi.com))

### **2.2.1.5 Cell migration assay**

10,000 ECs were seeded into m-dishes 35 mm, low with culture-insert in a volume of 70  $\mu$ l EGM2 medium supplemented with 10 % FCS, Streptomycin (100  $\mu$ g/ml) and Penicillin (100 U/ml). Cells were allowed to become adherent. The migration of heart and tumor ECs was captured on a video and analyzed. Films were analyzed with WimTaxis for quantitative evaluation of cell tracking.

### **2.2.1.6 Tube formation assay**

For tube formation, each well of a  $\mu$ -slide Angiogenesis was filled with 10  $\mu$ l chilled matrigel. After incubation for 30 minutes at 37 °C, H5V cells (10,000 cells/well), primary heart ECs (80,000 cells/well) or tumor ECs (20,000 cells/well) in passage 1 were added in 50  $\mu$ l medium. After 6 hours, pictures were recorded with an Axiovert 40C microscope. For quantitative evaluation, representative images were analyzed with WimTube. The total number of branching points and loops per image was determined.

## **2.2.2 Molecular biological methods**

### **2.2.2.1 Isolation of RNA**

The isolation of endothelial RNA was performed by RNeasy Micro kit, which is based on the selective binding properties of a silica-based membrane followed by centrifugation. Cells in the  $\mu$ -slide1 were lysed and homogenized with 350  $\mu$ l guanidine-thiocyanate-containing RLT-buffer. After adding of 350  $\mu$ l ethanol (70%), the mixture was transferred on a spin column, centrifuged and washed with 350  $\mu$ l RW1-buffer (8000 g for 15 seconds). DNA was removed by DNase treatment (10  $\mu$ l DNase + 70  $\mu$ l RDD-buffer) for 15 minutes on the spin column. After washing and drying steps, the RNA was eluted with 10  $\mu$ l RNase-free water and stored at -80°C. This procedure allows the purifications of RNA molecules longer than 200 nucleotides, leading to mRNA enrichment due to exclusion of RNA molecules smaller than 200 nucleotides (5S-rRNA, 5.8S-rRNA, tRNA).

### 2.2.2.2 Quantification and qualification of RNA

The quantification and qualification of endothelial RNA was performed by Agilent Bioanalyzer 2100 and RNA 6000 Nano Assay Kit. Briefly, a chip was loaded with gel-dye mix, RNA marker, denatured RNA ladder (70°C for 2 minutes) and denatured samples to be tested. The dye molecules intercalate into RNA and were electrophoretically separated. The Bioanalyzer detects the fluorescence of RNA fragments and generates an electropherogram (Figure 6). The results provide information about the length distribution of the RNA fragments reflecting the integrity of the RNA sample. Beside the control peak, two distinct ribosomal peaks (18S-rRNA and 28S-rRNA) are detectable. A proprietary algorithm (Agilent) analyses the electropherogram and calculates the so-called RNA Integrity Number (RIN) which ranges from 1 (RNA completely degraded) to 10 (RNA not degraded at all). Samples with RINs higher than 7 are generally accepted to be used in microarray analysis.

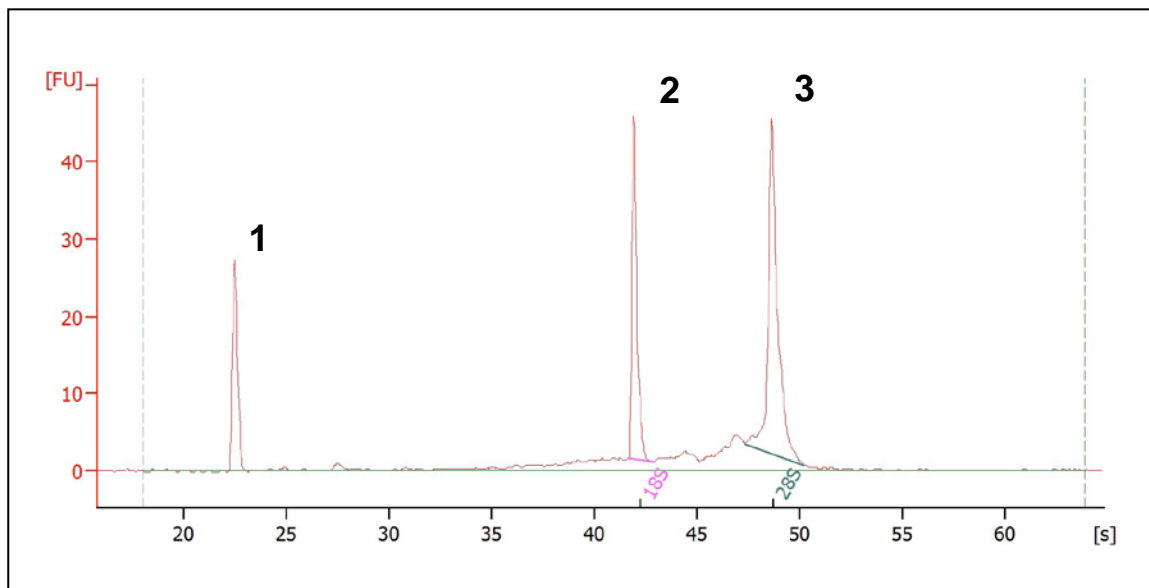


**Figure 6:** Representative electropherogram for quality control of RNA isolated from ECs 7 days under static conditions. The concentration of RNA was 52 ng/ $\mu$ l and the RNA Integrity Number was 9.1 (1: RNA marker, 2: 18S-RNA peak, 3: 28S-RNA peak).

### 2.2.2.3 Global mRNA expression analysis

The analysis of global gene expression was performed using the mouse one-color microarray-based gene expression analysis kit (Agilent Whole Genome Mouse

8x60k, AMADID: 28005). Briefly, 25 ng heart endothelial RNA was amplified, labelled and purified and subjected to hybridization on the array. After washing, slides were scanned using the Agilent DNA Microarray Scanner (G2505C). Fluorescence intensities of hybridised microarray spots were extracted from scanned images using the Agilent Feature Extraction software and the output was written to text files. Subsequent bioinformatics analysis was performed within the Integrative Biology Group (Research Unit Radiation Cytogenetics, Helmholtz Zentrum München) together with Dr. Kristian Unger. Briefly, text files were imported into the R statistical platform (R Core Team, 2015 (<https://www.r-project.org/>)) using the Bioconductor package `Agi4x44PreProcess` (<http://www.bioconductor.org/packages//2.10/bioc/html/Agi4x44PreProcess.html>), quality filtered and normalised using the RMA algorithm. Differential expression was calculated using functions of the Bioconductor package `limma` (<https://bioconductor.org/packages/release/bioc/html/limma.html>).

## **2.2.3 Protein biochemical methods**

### **2.2.3.1 Dialysis**

A dialysis cassette was used to remove sodium azide from the antibody PECAM-1. For the purification, 300 µl of the antibody was loaded in the cassette via 20Gx1½ needle and dialyzed first twice for 2 hours and then over night in PBS.

### **2.2.3.2 Protein concentration**

The protein determination was performed by Pierce BCA protein assay. Colorimetric detection of proteins is based on the biuret reaction, linked to the sensitive reagent bicinchoninacid. For quantification of proteins, different concentrations of BSA (25–2000 µg/ml) act as standard. Samples and standards were incubated in a 96-well plate at 37 °C for at least 30 minutes. The absorbance was measured at 550 nm via plate reader EL808.

### **2.2.3.3 Biotinylation**

The biotinylation of PECAM-1 was performed by DSB-X™ Biotin protein labeling kit. Briefly 200 µl of the antibody were mixed with 20 µl sodium bicarbonate and 2 µl DSB-X biotin for 1½ hours at room temperature. DSB-X-conjugated antibody and free DSB-X biotin were separated using a spin column.

## **2.2.4 Immunological methods**

### **2.2.4.1 Immunofluorescence microscopy**

For the PECAM-1 staining, primary ECs were seeded into chamber slides. After washing with PBS and fixation with cold acetone (4 °C), dried cells were incubated with PECAM-1 (1:100 in primary antibody diluent) for 1 hour at 23 °C. After repeating washing and drying step, cells were stained with Alexa Fluor 594-labeled secondary antibody (1:200 in PBS) for 1 hour at 37 °C. For the isolectin staining, cells were blocked with PBS/BSA (0.2 %) and incubated with isolectin-FITC-labeled antibody (1:50 in PBS/BSA 0.2 %) for 30 minutes at 4 °C. For both stainings, cell nuclei were co-stained via Mounting medium with Dapi. Samples were analyzed using a fluorescence microscope equipped with 10x, 20x and 100x objective and standard filters. Image procession was performed with Axiovision and Photoshop.

### **2.2.4.2 Flow cytometry analysis**

The fluorescence activated cell sorting (FACS) is a method for the quantitative identification of cell surface markers. The antigens were detected by specific fluorescence-labeled antibodies. Appropriately labeled isotype-matched immunoglobulins in the same concentration were used as negative controls. Briefly, after a washing step in PBS/FCS (10 %)  $0.1 \times 10^6$  viable cells were incubated on ice with antibodies for 30 minutes in the dark. Following a further washing step in PBS/FCS (10 %), cells were analyzed on the FACS Calibur instrument and evaluated with Cell Quest Pro. Dead cells were excluded from the analysis by a propidium iodide co-staining and gating strategy. The percentage of positive stained cells was calculated as the number of specific-stained cells minus

the number of unspecific-stained cells. The mean fluorescence intensity (mfi) was calculated by subtraction the mean for unspecific fluorescence intensity from the mean for specific fluorescence intensity.

## **2.2.5 Histopathology and immunohistochemistry**

### **2.2.5.1 Preparation of histological cryosection**

The isolated mouse tissue was frozen in Tissue-Tek with the help of dry ice and stored at -80 °C. For cryo slices, the blocks were pre-cooled at -20 °C and consecutive slices (5–8 µm thickness) were cut and collected on glass slides. After drying, the slides were stored at -20 °C.

### **2.2.5.2 Hematoxylin and eosin staining**

For the HE staining, the slides were dried at room temperature and covered with cold acetone for 10 minutes at 4 °C for fixation. After drying and washing in PBS for 10 minutes, the slides were stained in hematoxylin for 1 minute. Then the slides were washed with warm flowing tap water for 10 minutes and stained in 200 µl eosin added with two drops acetic acid (100 %) for 2 minutes. After washing with flowing tap water for 5 minutes, the slides were embedded with Aqueous Mount and cover slips freed from air bubbles.

## **2.2.6 Fluorescence in situ hybridization**

The method of fluorescence in situ hybridization (FISH) is based on complementary base pairing of single-strand fluorescence labeled probe DNA with single-stranded target DNA in metaphases and interphases. In this study, the signals were detected by indirect markers with biotin and digoxigenin. These haptens were coupled on nucleotides and would integrate into the DNA. The detection was performed by fluorescence labeled antibodies against biotin and digoxigenin. In this study, FISH was used for the analysis of the ploidy level of primary heart and tumor ECs. It was considered that only interphases can be analyzed because of the low proliferation rate of primary ECs *in vitro*. The labeling

of all mouse chromosomes (2x19, X, Y) cannot be evaluated due to the multiplicity of signals. Therefore only three chromosomes were labeled (Figure 7).

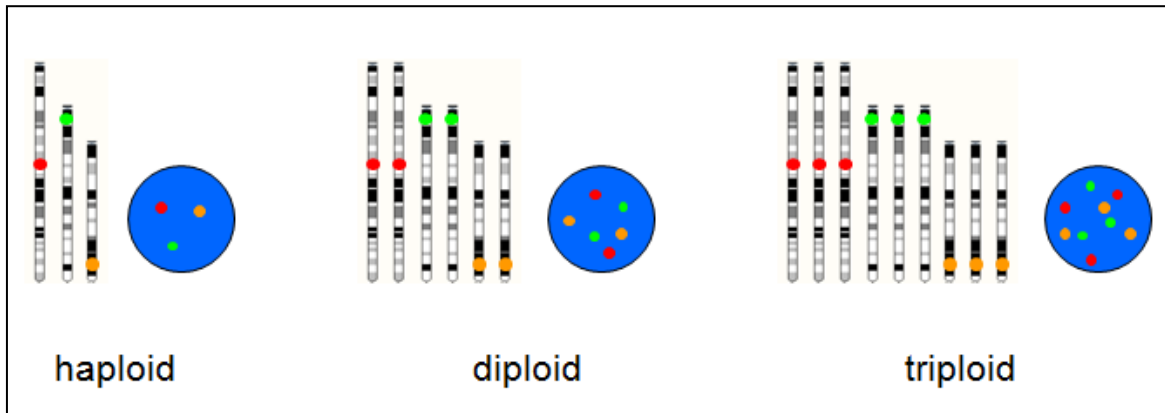


**Figure 7:** Schematic figure of the FISH principle with three different probes for chromosome 1 (red), chromosome 4 (green) and chromosome 14 (orange). The haploid, diploid and triploid ploidy levels are illustrated in metaphases and interphases.

Chromosome 1 was labeled with digoxigenin (red signal), chromosome 4 was labeled with biotin (green signal) and chromosome 14 was labeled with digoxigenin and biotin (orange signal). The results of these three chromosomes have been used to determine the ploidy level of the cells.

### 2.2.6.1 BAC DNA isolation

Bacterial Artificial Chromosome (BAC) is an artificial chromosome from bacteria, based on components of F-plasmid from *E. coli*. This cloning vector can contain foreign DNA up to a size of 300 kb. A BAC-vector contains regulatory genes for unidirectional replication (*oriS* and *repE*) and genes (*parA* and *parB*), which limit the copying rate per cell around one or two. Further, the BAC-vector contains an antibiotic resistance marker and a cloning segment, into which the foreign DNA can be inserted.

Based on the transformation of such vectors in bacterium cells and their culturing, a larger quantity of foreign DNA can be harvested. The BACs used in this study are listed in table 9.

For the proliferation of bacteria, 10 ml LB-medium were mixed with chloramphenicol (20 µg/ml) and the corresponding bacteria. The bacteria were

transferred from glycerin stock in LB-medium with the help of an inoculation loop. If the medium was cloudy after 16 hours at 37 °C in an incubator shaker, the cell suspension was centrifuged (6000 rpm) at 4 °C for 30 minutes. The supernatant was discarded and the cell pellet was washed with 5 ml TES-buffer (6000 rpm, 10 minutes, 4 °C) and resuspended in 2 ml glucose-buffer and 2 ml lysozyme-solution. After incubation at room temperature for 5 minutes, 4 ml NaOH/SDS and immediately 3 ml sodium acetate (ice cold) were added. The compound was mixed and incubated on ice for 15 minutes. After centrifugation (6000 rpm, 10 minutes, 4 °C), the supernatant was filtered and mixed with the double volume of ethanol (100 %). The mixture was incubated at room temperature for 10 minutes and centrifuged (13.000 rpm) at 4 °C for 30 minutes. The supernatant was discarded and the pellet was dried and solved in 1 ml TE-buffer at 4 °C over night. On the next day, the RNA-digestion was processed. The sample was separated in 2 tubes (500 µl), 5 µl RNase A solution were added and incubated at 37 °C for 1 hour in a heating block. Afterwards the sample was transferred in phase lock gel tube, which was previously centrifuged (13.000 rpm) at room temperature for 3 minutes. A mixture of 500 µl phenol/chloroform/isoamyl alcohol (25+24+1) was added, mixed and centrifuged (13.000 rpm) at room temperature for 5 minutes. This last step was repeated. After centrifugation, the upper phase was transferred in new phase lock gel tube. A mixture of 500 µl chloroform/isoamyl alcohol (24+1) was added, mixed and centrifuged (13.000 rpm) at 4 °C for 5 minutes. The upper phase was transferred in a new tube. The plasmid-DNA was precipitated by adding the double volume of ethanol (100 %, ice cold) at -20 °C over night. On the next day, the tube was centrifuged (13.000 rpm) at 4 °C for 30 minutes. The supernatant was discarded and the DNA-pellet was washed with 500 µl ethanol (70 %, 4 °C). After centrifugation (13.000 rpm, 20 minutes, 4 °C), the pellet was dried and solved in 100 µl double distilled water at 4 °C over night.

### **2.2.6.2 Purification of plasmid-DNA**

The purification was performed by DNA Clean and Concentrator kit. Briefly, the plasmid-DNA was mixed with the double volume of binding buffer and transferred on the column. After centrifugation (16.000 g, 30 seconds), the flow rate was discarded and the column was washed twice with 200 µl wash buffer. For the

elution, 35 µl double distilled water were added on the column, incubated at room temperature for 5–10 minutes and centrifuged (16.000 g) for 30 seconds.

#### **2.2.6.3 Concentration of plasmid-DNA**

The isolated plasmid-DNA concentration was measured by NanoDrop spectrophotometer according to manufacturer's instructions. Briefly, 1 µl of the DNA-solution to be measured was placed on the sample position of the spectrophotometer. At a wavelength of 260 nm, the optical density of the solution was measured. The ratio of absorbance at 260 and 280 nm was used to assess the DNA purity. A ratio between 1.8 and 2 is generally accepted for high level of purity.

#### **2.2.6.4 Labeling of probe-DNA via nick translation**

The probe-DNA was labeled with Biotin-16-dUTP and Digoxigenin-dUTP. The enzyme DNase I generated randomly single-strand breaks (nicks) in double-strand DNA at low enzyme concentration in the presence of MgCl<sub>2</sub>. The resulting 3' ends were elongated by DNA-polymerase I and the template was reduced via 5'->3' exonuclease activity. For the reconstruction of the DNA-strand, new nucleotides were used. One of them was conjugated with Biotin-dUTP or Digoxigenin-dUTP, which are detected by antibodies.

For the nick translation 1 µg of the probe-DNA, 4 µl of the translation-mix and double distilled water were mixed on ice in a total volume of 20 µl and incubated at 15 °C for 45 minutes in the PCR-unit. The adequate size of the fragments were controlled by agarose gel electrophoresis (Figure 8). For that, 3 µl of the sample were mixed with 7 µl loading buffer and filled in 1.5 % agarose gel (50 ml TAE-buffer and 2.5 µl ethidium bromide). When the fragment size between 500 and 1000 bp was reached, the enzymes were inactivated by incubation at 65 °C for 10 minutes.

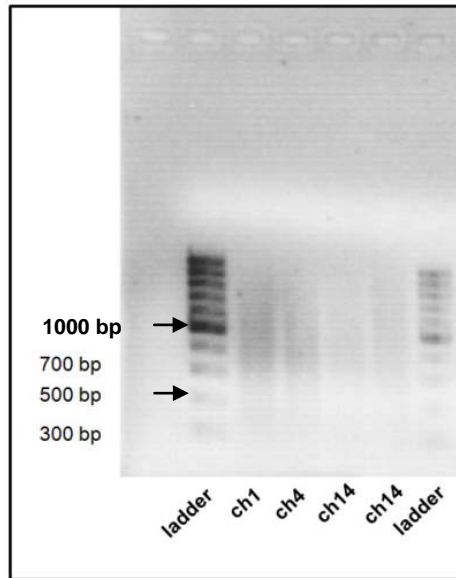


**Figure 8:** Presentation of agarose gel electrophoresis after nick translation. The adequate size of fragments between 500 and 1000 bp was reached for chromosome 1 (ch1), chromosome 4 (ch4) and chromosome 14 (ch14).

#### 2.2.6.5 Precipitation of probe-DNA

After labeling, the probe-DNA was precipitated in the presence of herring sperm DNA and mouse Cot-1 DNA. The excess of Cot-1 DNA I blocked non-specific hybridisation and resulted in saturation of high repetitive sequences. In this way, false positive signals were avoided.

For the precipitation, biotin and digoxigenin labeled probe DNA (10 µl RP23-289I3-Dig, 10 µl RP23-257F12-Bio, 5 µl RP23-154G18-Dig, 5 µl RP23-154G18-Bio), 53 µl Cot-1 DNA, 8.8 µl herring sperm DNA and sodium acetate (1/10 volume) were mixed. Then, ethanol (2.5 x volume, 100 %, -20 °C) was added and incubated at -20 °C over night.

Afterwards, the sample was centrifuged (13.000 UpM) at 4 °C for 30 minutes. The supernatant was removed and 500 µl ethanol (70 %, ice cold) were added. After repeated centrifugation (13.000 UpM) at 4 °C for 20 minutes and removal of supernatant, the DNA-pellet was dried. The pellet was resolved in 12 µl double distilled water and 28 µl mastermix 1.0 at 37 °C for at least 3 hours with the help of a shaker (550 rpm). The probe DNA was stored at -20 °C. The binding specificity was checked by hybridisation on metaphases from normal spleen cells. The

isolation of spleen cells was kindly performed by Katrin-Janine Goldmann and metaphase preparations were provided for the experiments.

#### **2.2.6.6 Fixation of cells**

The cells were seeded in adequate dilution with medium on a glass slide and incubated in quadriperm cell culture dish in an incubator. When 20–30 % confluence was reached, the medium was removed and replaced by hypotonic solution KCl. After incubation at 37 °C for 15 minutes, carnoy's fixative (methanol/acetic acid, (4:1) -20 °C) was added and incubated on ice for 20 minutes. The removing and adding of new carnoy's fixative for 20 minutes was repeated twice. After drying, the glass slide was stored at room temperature at least for 1 week before starting with denaturation and hybridization.

#### **2.2.6.7 RNase and pepsin digestion**

For the RNase digestion, the sample was incubated in 2xSSC at room temperature for 5 minutes. The glass slide was covered with 200 µl RNase (50 µg/ml), followed by a plastic film and incubated in a metal box with high humidity at 37 °C. B16-F0 and heart ECs were incubated for 5 minutes. Tumor ECs were incubated for 7 minutes. Afterward, the slides were washed three times in 2xSSC for 2 minutes.

For the pepsin digestion, the sample was incubated in PBS at room temperature. The glass slide was incubated in pepsin solution (10 µg/ml) at 37 °C. B16-F0 and heart ECs were incubated for 1 minute. Tumor ECs were incubated for 2 minutes. Afterward, the glass slides were washed at room temperature twice in PBS for 5 minutes, incubated in MgCl<sub>2</sub> solution for 5 minutes, rinsed in PBS, incubated in formaldehyde (1 %) for 4 minutes, rinsed in PBS and washed twice in PBS for 5 minutes.

### **2.2.6.8 Denaturation, hybridization and detection**

The FISH probe (3–5  $\mu$ l) was denatured at 76 °C for 7 minutes and incubated at 37 °C for at least 30 minutes. The target glass slide was incubated at 72 °C in 70 % formamide/2xSSC for 2 minutes and incubated in an ethanol series (70, 90 and 100 %) each time for 2 minutes. After drying on a heating plate at 37 °C for 5 minutes, the sample was covered with the FISH probe (3  $\mu$ l or 10  $\mu$ l) followed by a cover slip (round or 15x15 mm). This area was marked and sealed with fixogum. After drying on the heating plate at 37 °C for at least 15 minutes, the glass slide was incubated at 37 °C in a metal box for 48 hours. After hybridization, the fixogum and the cover slip were removed. The glass slide was washed at 42 °C in 2xSSC for 10 minutes, three times in 50 % formamide/2xSSC for 15 minutes, shortly in 2xSSC, in 2xSSC for 15 minutes and in PN-buffer for 15 minutes. After this, the glass slide was washed in PN-buffer at room temperature for 15 minutes. The sample was covered with PNM-buffer and plastic film and incubated in a metal box with high humidity at 37 °C for 20 minutes. After blocking, the sample was treated in series with 100  $\mu$ l Streptavidin-Avidin/anti-Digoxigenin-Cy3 (1:2), 100  $\mu$ l Biot-anti-Streptavidin/rat-anti-mouse-Cy3 (1:2) and 100  $\mu$ l Streptavidin-Avidin/mouse-anti-rat-Cy3 (1:2) in a metal box with high humidity at 37 °C for 20 minutes. After each incubation, the sample was washed twice in PN-buffer for 5 minutes to remove excess antibodies. Afterward, the slide was washed shortly three times in double distilled water and dried. The glass slide was covered with Vectashield Mounting Medium (with Dapi), followed by a cover slip (24x50 mm) and stored at 4 °C.

## **2.2.7 Animal model**

### **2.2.7.1 Tumor implantation**

In order to establish tumors *in vivo*,  $1 \times 10^5$  viable CT26 or B16-F0 cells in 50  $\mu$ l medium were injected s.c. into the shaven backs of anesthetized 10 weeks old BALB/c or C57Bl/6 mice. For the intraperitoneal injection ( $27 \text{G} \times \frac{3}{4}$ ) of the anesthetic MMF, the mice were weighted and immobilized in the hand. The anesthesia was finished with AFN 30 minutes after tumor injection.

### 2.2.7.2 Tumor growth measurements

One week after tumor injection, tumor diameters were measured without anesthetic at least three times per week by ultrasonography. Therefore the subcutaneously tumor was covered with ultrasound gel and the diameters of the tumor was determined (height, width, depth). Tumor volumes were determined by using the formula for an ellipsoid ( $\pi/6abc$ , where a, b and c are the measured diameters of the tumors). Mice were sacrificed when the tumor had reached a volume ranging between 0.3 and 0.4 cm<sup>3</sup> (Figure 9).

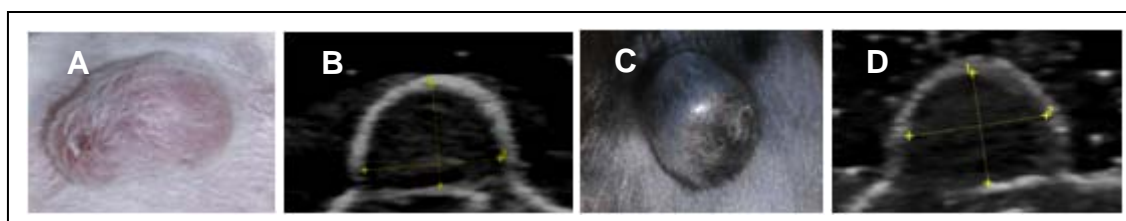


**Figure 9:** Representative macroscopic and ultrasound pictures of a subcutaneous murine tumor CT26 (A, B) and B16-F0 (C, D).

### 2.2.7.3 Induction of repair blastema

PBS and sterile incomplete Freund's adjuvant (1:1) were mixed via Mikro-dismembrator with the help of a chromium steel ball in a shaking tube at 3000 rpm twice for two minutes. The resulting emulsion was transferred in a 3 ml syringe. To induce a repair blastema, 0.5 ml sterile air and 0.5 ml sterile incomplete Freund's adjuvant/PBS-emulsion were injected ( $27G \times \frac{3}{4}$ ) s.c. into the shaven backs of anesthetized 10 weeks old C57Bl/6 mice. For the intraperitoneal injection ( $27G \times \frac{3}{4}$ ) of the anesthetic MMF, the mice were weighted and immobilized in the hand. The anesthesia was finished with AFN 10 minutes after emulsion injection. Three weeks after injection the repair blastema was dissected.

### 2.2.7.4 Procedure of heart and thorax irradiation of mice

Each mouse was immobilized without anesthetic in a specially designed jig. Preceding the exposure, the position of the heart and thorax inside the jig was localized by digital radiographs (Figure 10).

10 weeks old male C57Bl/6 mice received local heart irradiation with a single X-ray dose of 8 or 16 Gy (200 kV, 10 mA); age-related control mice received sham irradiation. The heart irradiation field consisted of a 9 x 13 mm<sup>2</sup> window in a 2 mm thick lead plate. The mice were sacrificed by cervical dislocation 16 weeks after heart irradiation.

10 weeks old female C57Bl/6 mice received local thorax irradiation with a single X-ray dose of 2 or 8 Gy (200 kV, 10 mA); age-related control mice received sham irradiation. The thorax irradiation field consisted of a 15 x 18 mm<sup>2</sup> window in the lead plate. The mice were sacrificed by cervical dislocation 5, 10, 15 and 20 weeks after thorax irradiation.

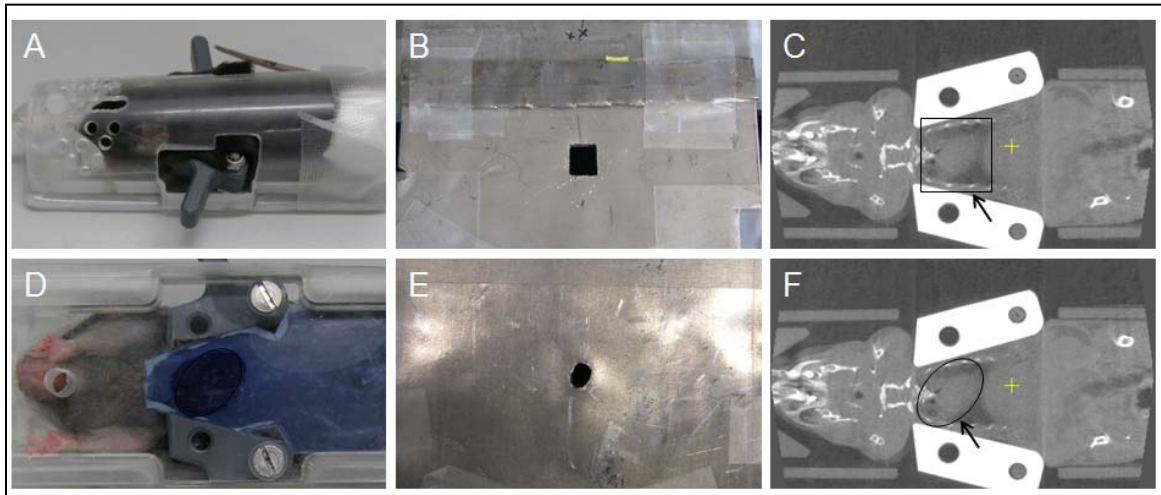


**Figure 10:** Representative pictures of mouse heart and thorax irradiation. **(A)** Fixed mouse in the jig (top view), **(B)** lead for thorax irradiation with 15 x 18 mm<sup>2</sup> window, **(C)** radiograph shows the position of the thorax (arrow), **(D)** fixed mouse in the jig (bottom view) after heart irradiation; a gafchromic film below the mouse presents the irradiation field due to the colour change from light blue to dark blue, **(E)** lead for heart irradiation with 9 x 13 mm<sup>2</sup> window, **(F)** radiograph show the position of the heart (arrow).

### 2.2.8 Statistics

Analysis of the number of positively stained cells (proportion of cells) and the mean fluorescence intensity (mfi) (expression density of protein per cell) were performed by CellQuest software. Comparative analysis of the data was carried out using the Student's t-test (two paired and unpaired). The significance levels were  $p^* < 0.05$  (5 %);  $p^{**} < 0.01$  (1 %) and  $p^{***} < 0.001$  (0.1 %). Data were presented as means of the number (n) of indicated experiments.

### 3. RESULTS

It has been assumed that surface markers on ECs from normal resting and growing tissues may be different. The establishment of my new EC-isolation method allows the analysis of primary ECs directly after their isolation. Thereby the physiological status of EC surface markers in resting and growing tissue can be determined without previous long-term *in vitro* cell culture. For isolation of ECs from non-proliferating tissue, heart and lung of the mice were used. For the isolation of ECs from proliferating benign and malignant tissue, repair blastema and tumors (B16-F0 melanoma and CT26 colon carcinoma) were used.

Heart irradiation is known to lead to a change in the microvascular density. After a temporary increase, the microvascular density was found to be decreased. This effect results in late radiation-induced heart diseases.

Based on the newly established method, the differences between non-proliferating and proliferating ECs could be investigated. Selected surface markers which differ in ECs derived from non-proliferating (normal tissues) and proliferating tissues (tumors) may provide possible targets in the future that could be used for therapeutic intervention for patients with tumors or for patients that have to undergo a thoracic irradiation therapy.

#### 3.1 Isolation of primary endothelial cells

A new method for the isolation of primary ECs was established (Sievert et al. 2014). For each isolation procedure, one to four mice were sacrificed by craniocervical dislocation. Heart, lung, repair blastema and tumors were collected under aseptic conditions. The left and right atria were surgically removed from the heart to reduce contaminations with macrovascular ECs. After washing in ice-cold PBS and mechanical mincing with a sterile scalpel blade, tissue fragments with a size of 1 mm<sup>3</sup> were transferred into 10 ml of pre-warmed (37 °C) digestion solution consisting of collagenase A (0.5 units/ml) diluted in HBSS/10 % FCS. The tissues were incubated for 45 minutes at 37 °C under gentle rotation (2 rpm). Afterwards the suspension was dispersed by forcing it through a sterile 18 G injection needle 10 times. The single cell suspension was filtered through a 70 µm cell strainer and

washed twice in 50 ml HBSS/10 % FCS solution at 4 °C (400xg for 10 minutes). The cell pellet was resuspended in 600 µl ice-cold isolation buffer and DSB-X biotin-labeled anti-mouse PECAM-1-antibody (25 µl; 0.5 mg/ml) was added. After incubation for 10 minutes at 4 °C under gentle rotation (3 rpm) and washing in ice-cold isolation buffer (2 ml), the cell pellet was resuspended in 1 ml cold isolation buffer. Magnetic dynabeads coated with streptavidin (75 µl) were added and incubated for 15 minutes at 4 °C under gentle rotation (3 rpm). Afterwards the tube was placed in the magnetic separator. After 2 minutes, the bead-free, unbound PECAM-1-negative cells were removed from the cell suspension by pipetting. PECAM-1-positive cells immobilized in the DSB-X-streptavidin-bead-complex, remained on the wall of the tube due to the magnetic field. After at least 5 washing steps with isolation buffer (1 ml), cells attached to beads were resuspended in 1 ml release buffer and incubated for 2 minutes at 21 °C. By pipetting the cell suspension 10 times, the cells were detached from the beads by biotin-streptavidin competition. Then the tube was placed in the magnetic separator. After 1 minute, bead-free PECAM-1-positive ECs could be isolated, whereas the magnetic beads remained on the wall of the tube (Figure 11) (Sievert et al. 2014).

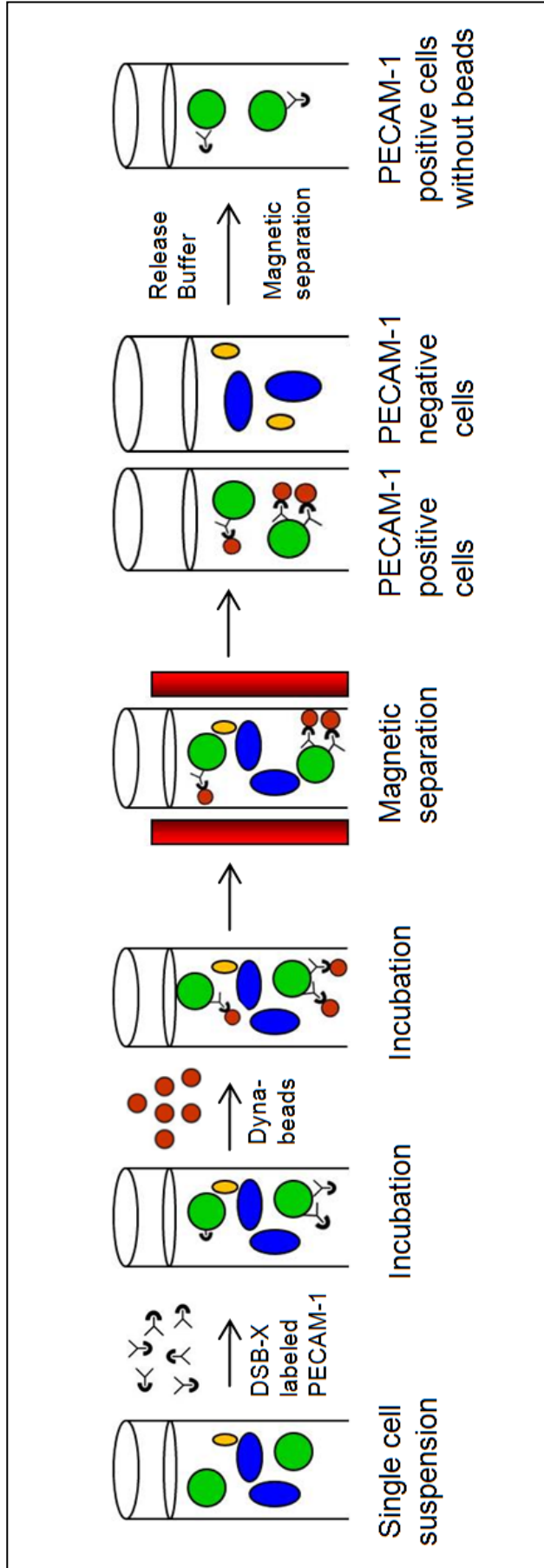


**Figure 11:** Schematic representation of the isolation procedure of primary, bead-free ECs. After mechanical (scalpel) and enzymatic (collagenase A digestion for 45 minutes and pass through an injection needle) disintegration of the tissue, viable ECs were isolated using DSB-X biotin labeled anti-PECAM-1 antibody and streptavidin coated micro-beads via biotin-streptavidin competition. DSB-X biotin-labeled PECAM-1 antibody was added to the single cell suspension and after incubation ECs (green) are bound to DSB-X labeled PECAM-1. FlowComp dynabeads (red) coated with streptavidin were added and after incubation, ECs bound to the DSB-X-streptavidin-bead-complex were separated from PECAM-1-negative cells (blue and yellow) in a magnetic field. Unbound PECAM-1-negative cells were removed from the cell suspension by pipetting. PECAM-1-positive cells remained on the wall of the tube due to the magnetic field. After washing steps the tube was removed from the magnet. Cells attached to beads were resuspended in FlowComp release buffer and after a second magnetic separation, PECAM-1-positive cells without magnetic beads could be isolated, whereas the beads remained in the tube.

### 3.1.1 Quality control experiment

To test the efficiency of the new method, a PECAM-1-positive mouse EC line (H5V) and a PECAM-1-negative mouse colon cancer cell line (CT26) were mixed at a ratio of 1:20. After a simulated digestion with collagenase (Figure 12A, second column) and magnetic bead separation (Figure 12A, third column) according to the method described in Figure 11, the percentage of PECAM-1 positively stained H5V cells remained unchanged compared to that of untreated H5V cells. The mean surface expression density of PECAM-1 (which remained high after collagenase digestion (Figure 12B, second column)) decreased to 17 % (mfi:  $31 \pm 4$ ) following PECAM-1-biotin-streptavidin competition (Figure 12B, third column). Despite the low expression density of free PECAM-1 molecules on the cell surface of H5V cells after PECAM-1-biotin-streptavidin competition, the recovery rate of H5V cells was more than 70 % after the separation procedure (Figure 12C). It is assumed that the recovery rate of primary ECs is higher because the mean cell surface density of PECAM-1 on heart, repair blastema and tumor ECs (mfi:  $85 \pm 8$ ,  $479 \pm 14$ ,  $211 \pm 67$ ) is higher compared to that of H5V cells (mfi:  $31 \pm 4$ ). Analysis by flow cytometry revealed that no contaminating PECAM-1-negative tumor (CT26) cells were present in the PECAM-1-positive EC fraction. This result demonstrates that it is possible to recover PECAM-1-positive ECs from a mixture of different cells with high efficiency and purity (Sievert et al. 2014).

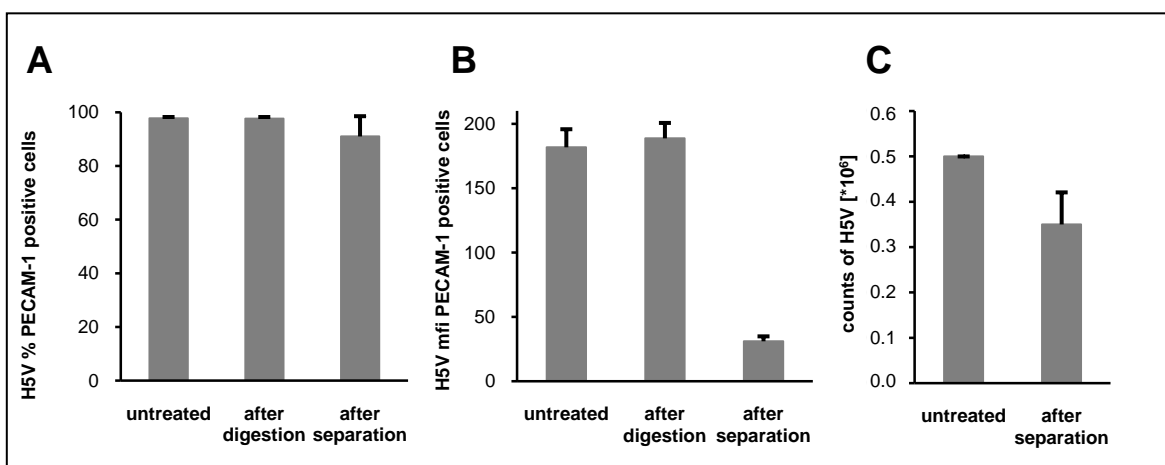


**Figure 12:** Control experiment for the new isolation method of ECs: Separation of PECAM-1-positive H5V cells mixed with PECAM-1-negative CT26 tumor cells at a ratio of 20:1. **(A)** The percentage of PECAM-1-positive H5V cells remained unchanged after a simulated digestion and after separation. **(B)** The fluorescence intensity (mfi) remained stable after digestion (second column), but decreased to 17 % (mfi: 31) after separation (third column). **(C)** The recovery rate of H5V cells after separation was higher than 70 %.

## 3.2 Endothelial cells from different tissue

### 3.2.1 Distribution *in vivo* and yield after isolation

To determine the distribution and density of capillaries and the fraction of necrotic and apoptotic areas, sections of hearts and tumors of mice were analyzed by PECAM-1 immunofluorescence and H&E staining (Sievert et al. 2014). Viable tumor tissue is characterized by compact tissue with high cell densities, whereas necrosis is characterized by increased eosin staining and a bulky extracellular matrix. In heart sections, capillaries and myocardial tissues were homogeneously distributed. PECAM-1-positive vessels were localized in close proximity to cardiomyocytes (Figure 13A, B). In contrast, the capillary densities in tumor sections were lower and vessels were predominantly localized in the viable outer borders, but not in the necrotic center of the tumor (Figure 13C, D). In line with these findings, the yield of ECs originated from heart and lung tissues was much higher compared to that of tumors and repair blastemas (Figure 14).

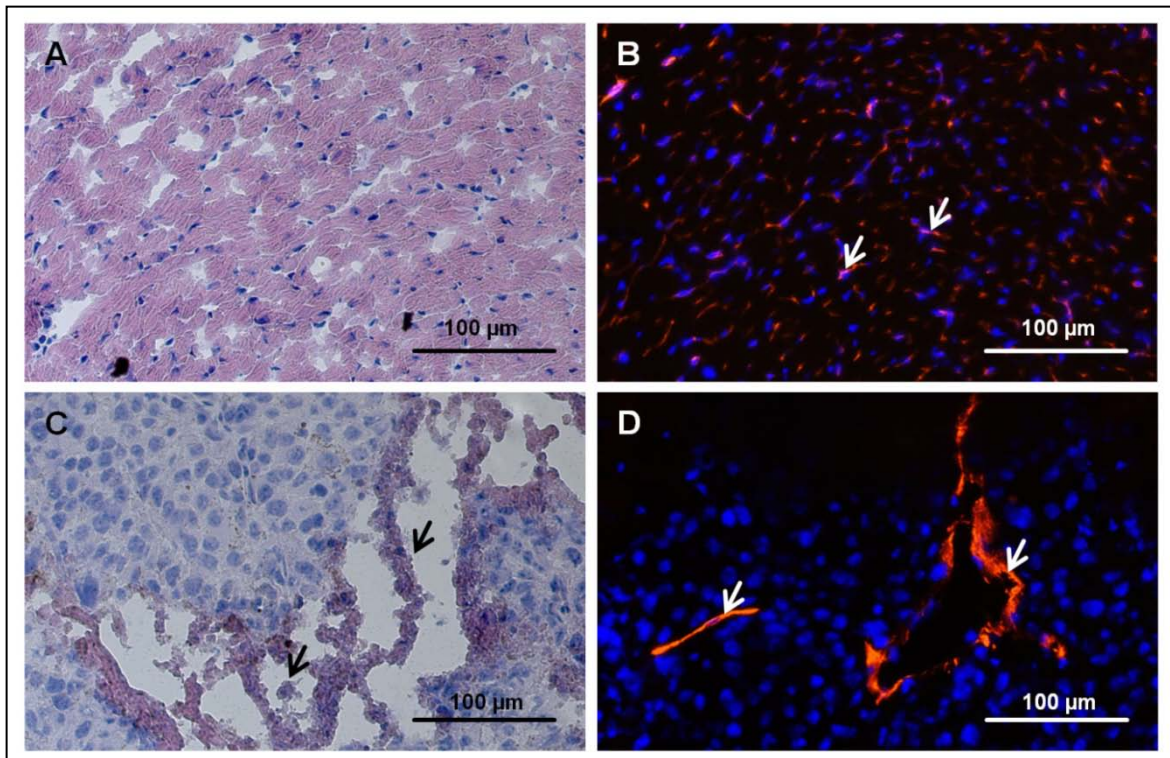


**Figure 13:** Localization of necrosis/apoptosis fraction and capillaries in heart and tumor (B16-F0, size between 0.3–0.4 cm<sup>3</sup>). (A, C) H&E staining of heart and tumor, respectively. Arrows indicate the fraction of necrotic/apoptotic areas. (B, D) PECAM-1 immunostaining of heart and tumor, respectively. Arrows indicate PECAM-1-positive ECs (red).

## Results

An important feature of the newly established method is that similar amounts of viable, primary microvascular ECs that became adherent to plastic could be isolated from tumor and normal tissues of young (5 weeks old) and old mice (100 weeks old) (Table 15) (Sievert et al. 2014).

**Table 15:** Heart weight, number of viable heart ECs and EC adherence after two days as a function of mice age (n=2).

age of mouse [weeks]	sex	weight of heart [g]	ECs counts directly after isolation	total adherent ECs after 2 days
5	f	0.07	350,000	60,000
20	f	0.11	400,000	40,000
50	f	0.12	490,000	40,000
100	m	0.14	550,000	50,000

It was possible to isolate approximately  $0.45 \times 10^6$  PECAM-1-positive ECs from one heart, approximately  $3 \times 10^6$  PECAM-1-positive ECs from one lung, approximately  $0.025 \times 10^6$  PECAM-1-positive ECs from one repair blastema and approximately  $0.1 \times 10^6$  PECAM-1-positive ECs from one tumor (Figure 14) (Sievert et al. 2014).

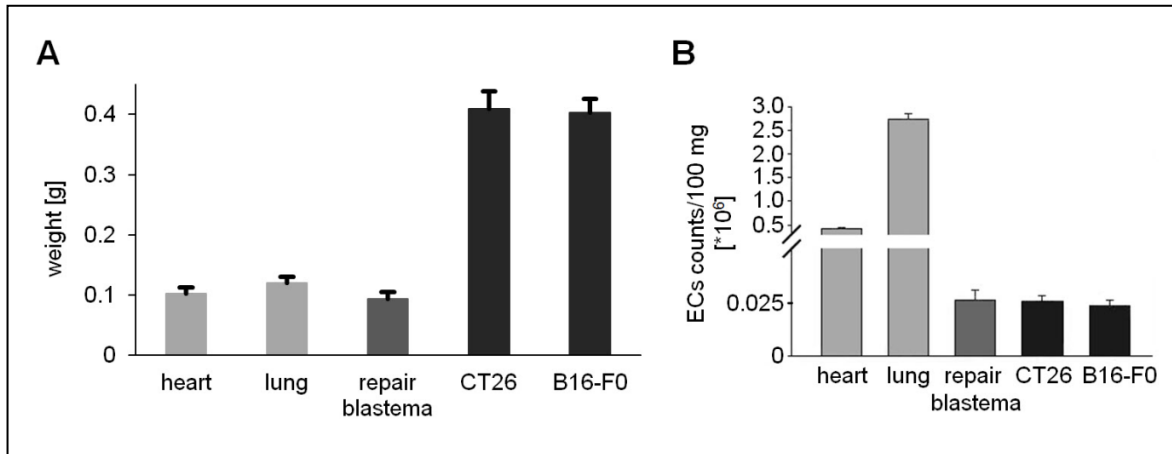


**Figure 14:** Weight of various tissues and counts of isolated ECs. **(A)** Summary of the total weight of separate tissues; weight of heart (n=10) and lung (n=3) taken from 13–15 weeks old female mice; weight of repair blastemas (n=10) taken from a balloon which was induced by using Freund's adjuvant/PBS-emulsion; weight of CT26 (n=10) and B16-F0 (n=10) tumors which were taken when their size was ranging between 0.3 and 0.4 cm<sup>3</sup>. **(B)** Corresponding isolated EC counts were calculated per 100 mg tissue.

### 3.2.2 Size of isolated ECs and number of bound beads

After digestion and magnetic bead separation of PECAM-1-positive and PECAM-1-negative cells, primary ECs were inspected under the microscope (Sievert et al. 2014). In most cases, ECs isolated from the heart and lung bound 2–5 microbeads (Figure 15A), whereas ECs originated from repair blastema and tumors (CT26, B16-F0) bound more than 20 beads (Figure 15B, C). After biotin-streptavidin competition, almost all ECs were completely separated from the magnetic beads (Figure 15D–F). The size of ECs from repair blastema and both tumors were twice the size of ECs derived from normal heart and lung tissues. The diameter of heart and lung ECs ranged between 1.5 and 2  $\mu\text{m}$ , whereas that of repair blastema and tumor ECs ranged from 3 to 4  $\mu\text{m}$ . Determination of the height of the forward scatter (FSC-height) by flow cytometry (Figure 16) confirmed that the mean FSC-height of ECs from repair blastema ( $350\pm 7$ ) and tumors (CT26:  $400\pm 40$ , B16-F0:  $437\pm 17$ ) was about twice the size of ECs derived from heart ( $225\pm 6$ ) and lung ( $189\pm 6$ ) tissues. The purity of ECs isolated from heart, lung and tumors was almost 100 %.

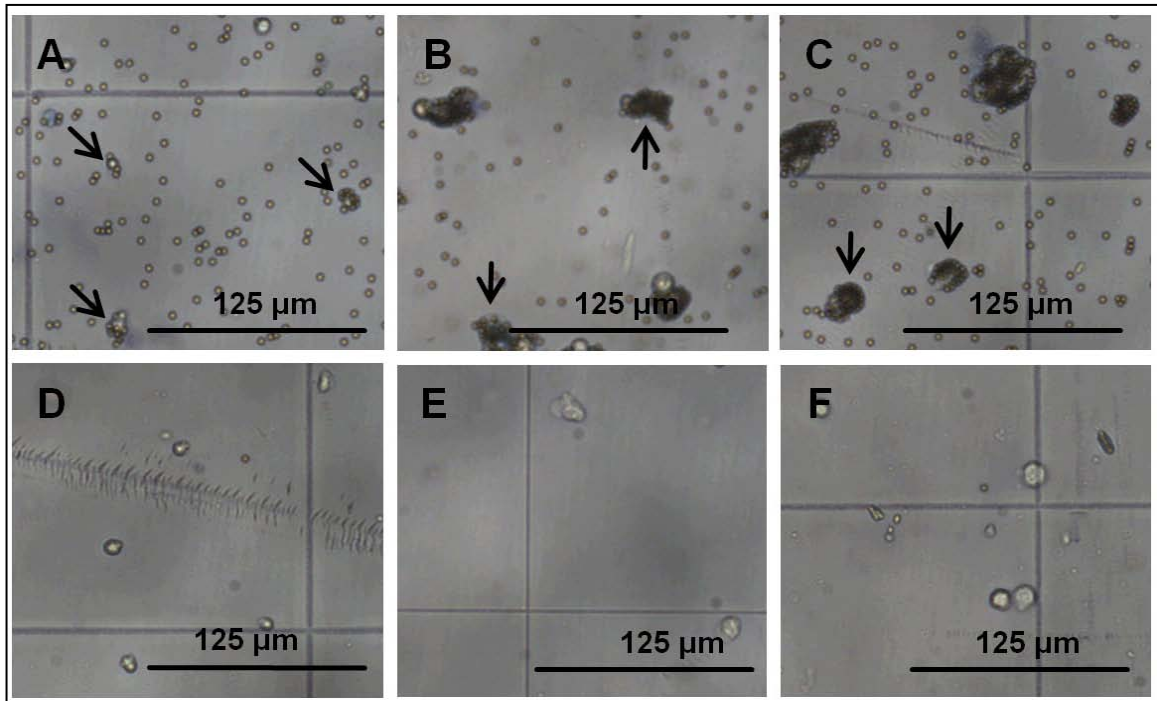


**Figure 15:** Primary ECs isolated from different tissue. **(A-C)** Isolated ECs from heart, repair blastema and B16-F0 with bound dynabeads. Arrows indicate specific binding of corresponding PECAM-1-positive ECs to dynabeads. **(D-F)** Isolated ECs from heart, repair blastema and B16-F0 after biotin-streptavidin competition without any bound dynabeads.

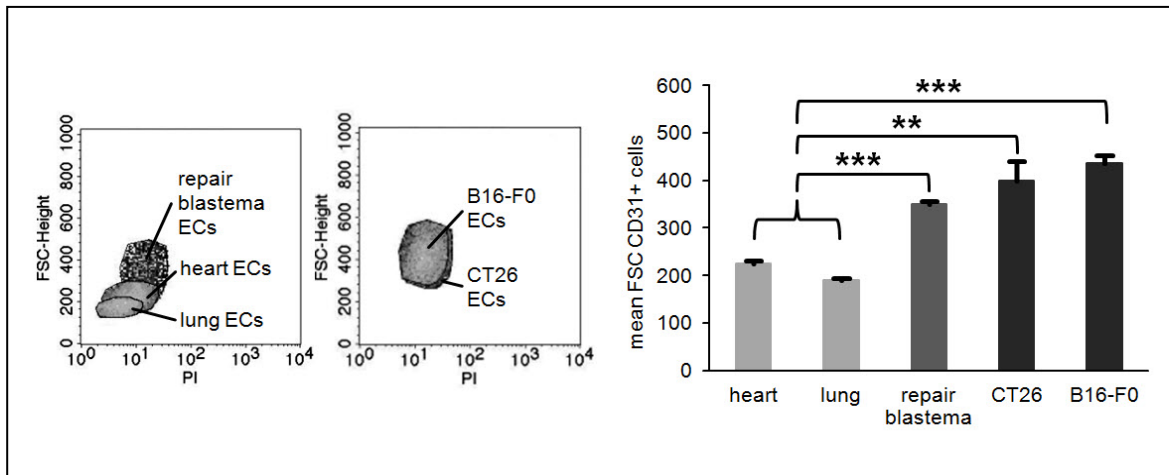


**Figure 16:** Size of primary ECs isolated from different tissue. Mean of the forward scatter (FSC) from PECAM-1 positive ECs isolated from heart (n=4), lung (n=3), repair blastema (n=2), CT26 (n=4) and B16-F0 (n=4) measured using flow cytometry. Asterisk represent significantly different values ( $p^{**} < 0.01$ ;  $p^{***} < 0.001$ ).

### 3.2.3 Identification of primary endothelial cells

Primary ECs isolated from heart, lung, repair blastema and tumors were characterized by flow cytometry using EC-specific antibodies directed against PECAM-1, endoglin, VE-cadherin, mucosialin, ICAM-1 and ICAM-2 (Sievert et al. 2014). The leukocyte marker CD45, which was used as control, was not detectable on the population of separated ECs. A representative histogram of each antibody staining pattern is illustrated in Figure 17. The summary of the proportion of positively stained cells and the mean fluorescence intensity values are depicted in Figure 19A, B. The proportion of positive stained cells for PECAM-1, endoglin, VE-cadherin, mucosialin, ICAM-1 and ICAM-2 is nearly 100 % ( $94 \pm 4$  %), independent of the origin of the tissue from which the ECs were generated.

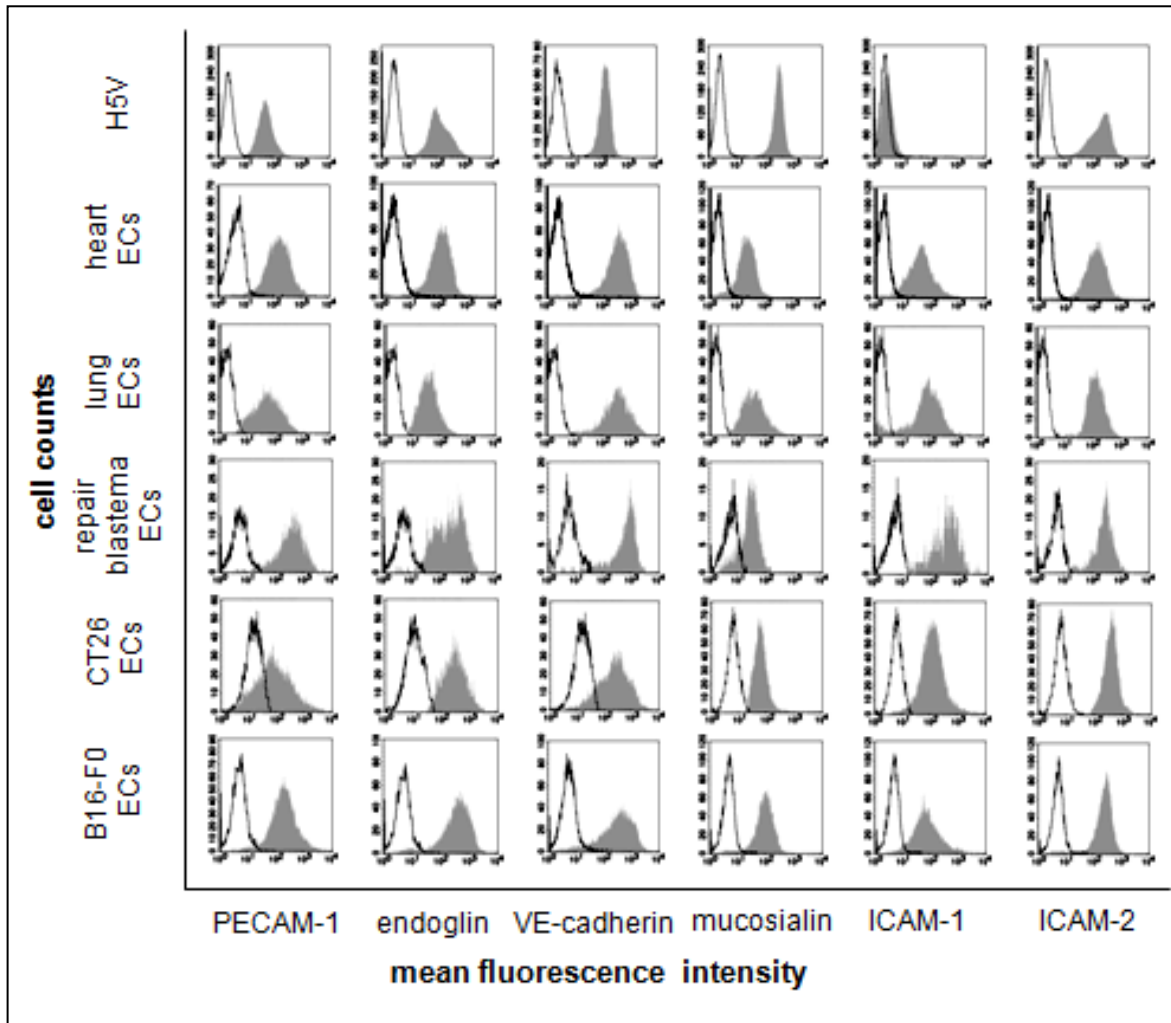


**Figure 17:** Identification of ECs derived from different tissue using flow cytometry. Control EC line H5V and primary ECs isolated from heart, lung, repair blastema, CT26 and B16-F0 can be identified with EC-specific antibodies directed against PECAM-1, endoglin, VE-cadherin, mucosialin, ICAM-1 and ICAM-2.

Comparative *in vitro* immunofluorescence studies showed that the fluorescence intensity of PECAM-1 and isolectin B4 was different between heart (Figure 18B, E) and tumor ECs (Figure 18C, F). Both markers were also used to stain the control murine endothelial cell line H5V (Figure 18A, D) (Sievert et al. 2014).

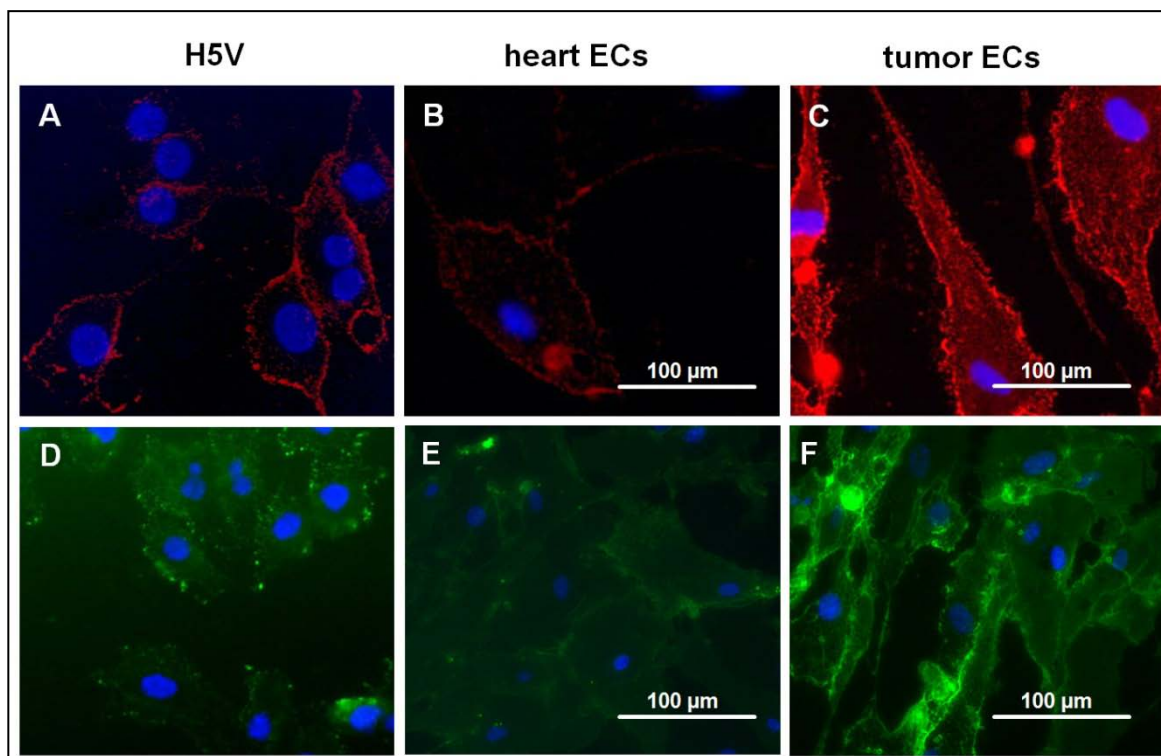


**Figure 18:** Identification of ECs derived from different tissue using immunofluorescence. (A-C) PECAM-1 staining (red) of H5V, primary heart and tumor (B16-F0) ECs. (D-F) Isolectin B4 staining (green) of H5V, primary heart and tumor (B16-F0) ECs.

### 3.2.4 Surface markers of endothelial cells from normal and tumor tissue

The proportion of positive stained cells for PECAM-1, endoglin, VE-cadherin, mucosialin, ICAM-1 and ICAM-2 is nearly 100 % ( $94 \pm 4$  %) independent of the origin of the tissue from which the ECs were generated. In contrast, the proportion of the proliferation marker integrin  $\beta 3$  was low on heart ECs ( $30 \pm 7$  %) and high on tumor ECs ( $96 \pm 4$  %). For the analysis of ECs isolated from the repair blastema, all PECAM-1 negative cells were removed using a special gating strategy. Only PECAM-1 positive cells were illustrated in the histograms. In general, the cell surface expression density of typical EC markers is higher on ECs derived from tumors than that of normal heart and lung tissues, except for VE-cadherin. The marker densities of PECAM-1 ( $p=0.006$ ), endoglin ( $p=0.0004$ ), mucosialin ( $p=0.0005$ ), ICAM-1 ( $p=0.03$ ) and ICAM-2 ( $p=0.001$ ) were all significantly increased (two to four-fold) in tumors as compared to ECs derived from normal tissue (Figure 19B). The expression density of PECAM-1 ( $p=0.007$ ) on ECs

derived from repair blastema was six-fold higher and that of endoglin ( $p < 0.001$ ) twice as high as that found on normal heart and lung tissues. The expression density of mucosialin on ECs from repair blastema was similar to that found on heart or lung ECs, whereas the expression density of ICAM-2 was more similar to that seen in tumor ECs. Furthermore, ECs from the repair blastema show a two-fold higher expression of VE-cadherin ( $p = 0.01$ ) and a five-fold higher expression density of ICAM-1 ( $p = 0.1$ ) compared to that of ECs from normal heart and lung tissues (Sievert et al. 2014).

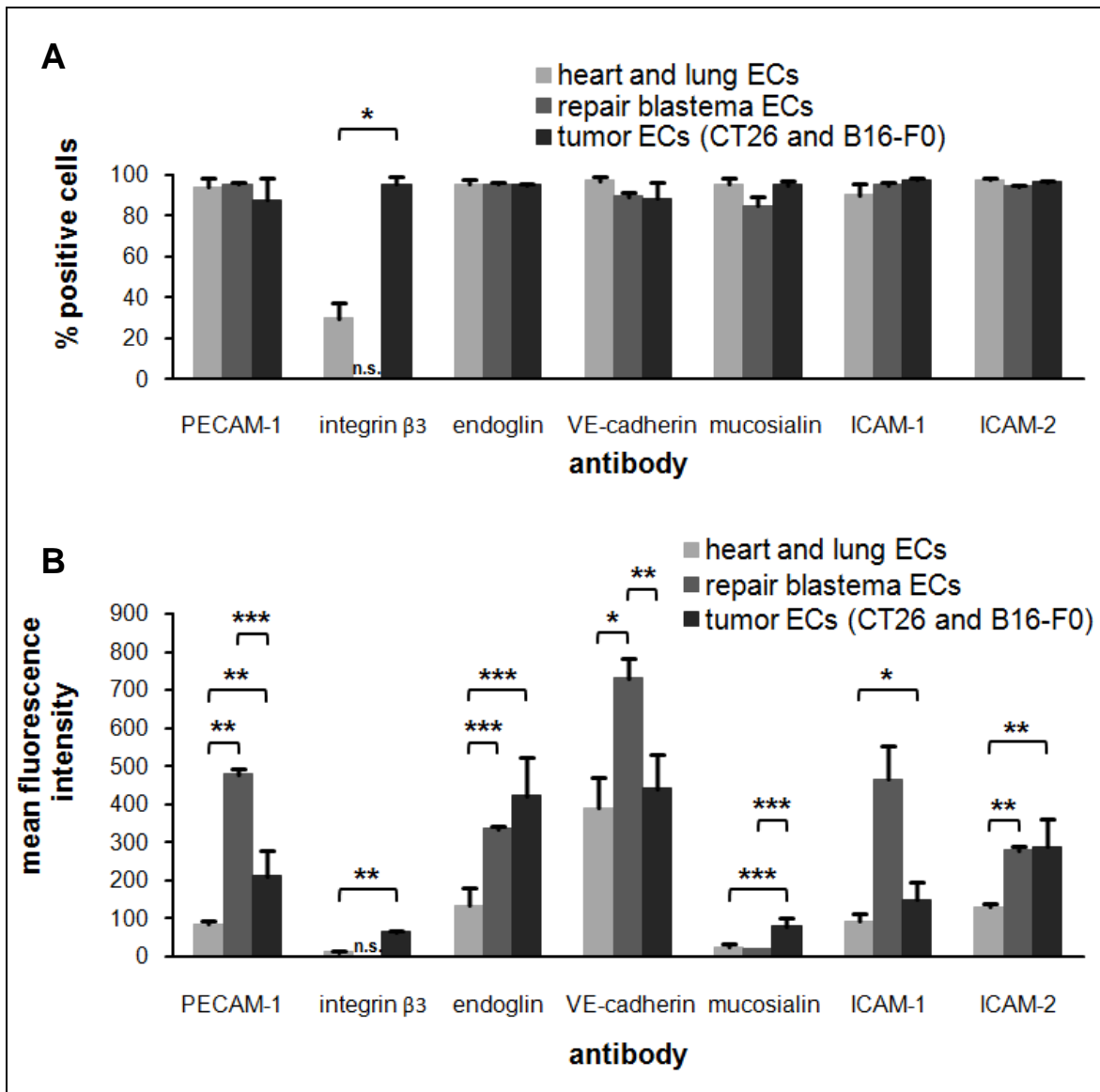


**Figure 19:** Identification and characterization of ECs derived from different tissue. **(A)** Percentage of positively stained cells and **(B)** mean fluorescence intensity (PECAM-1, integrin  $\beta 3$ , endoglin, VE-cadherin, mucosialin, ICAM-1 and ICAM-2) of ECs isolated from heart ( $n=5$ ), lung ( $n=3$ ), repair blastema ( $n=2$ ), CT26 ( $n=3$ ) and B16-F0 ( $n=3$ ). Asterisk represent significantly different values ( $p^* < 0.05$ ;  $p^{**} < 0.01$ ;  $p^{***} < 0.001$ ).

### 3.2.5 Surface markers of heart endothelial cells in dependency of the age of mice

Comparative flow cytometric analysis revealed that— except for the case of VE-cadherin (mean fluorescence intensity (mfi):  $360 \pm 83$  vs  $244 \pm 6$ ) – the densities of typical cell surface markers of ECs such as PECAM-1 (mfi:  $86 \pm 6$  vs  $87 \pm 2$ ), endoglin (mfi:  $153 \pm 11$  vs  $155 \pm 17$ ), mucosialin (mfi:  $22 \pm 1$  vs  $22 \pm 1$ ), ICAM-1 (mfi:  $73 \pm 20$  vs  $84 \pm 11$ ), ICAM-2 (mfi:  $128 \pm 14$  vs  $137 \pm 18$ ) were expressed at similar densities on heart ECs of young (5 weeks) and old (85 weeks) mice (Table 16). This suggests that expression patterns remain stable on ECs of young and old mice. The density of the EC marker VE-cadherin which enables tight junctions is substantially higher in ECs of young mice compared to that of old mice (Sievert et al. 2014).

**Table 16:** Mean fluorescence intensity (mfi) of PECAM-1, endoglin, VE-cadherin, mucosialin, ICAM-1 and ICAM-2 of heart ECs in dependency of the age of mice (n=2).

age of mice [weeks]	mfi PECAM-1	mfi endoglin	mfi VE-cadherin	mfi mucosialin	mfi ICAM-1	mfi ICAM-2
5	$86 \pm 6$	$153 \pm 11$	$360 \pm 83$	$22 \pm 1$	$73 \pm 20$	$128 \pm 14$
85	$87 \pm 2$	$155 \pm 17$	$244 \pm 6$	$22 \pm 1$	$84 \pm 11$	$137 \pm 18$

### 3.2.6 Surface markers of tumor endothelial cells with different growth rate

The B16-F0 tumors grow faster compared to CT26 tumors *in vivo* (Figure 20A). The mean doubling times for B16-F0 and CT26 tumors were 1.9 and 3.6 days ( $p < 0.001$ ) (Figure 20B). The expression densities of the EC markers PECAM-1 ( $p = 0.002$ ), endoglin ( $p = 0.002$ ) and mucosialin ( $p = 0.01$ ) were higher on ECs derived from fast-growing B16-F0 tumors, whereas the expression densities of the cellular adhesion molecule ICAM-1 ( $p < 0.05$ ) and ICAM-2 ( $p = 0.008$ ) were found to be elevated in the slow-growing CT26 tumor (Figure 20C) (Sievert et al. 2014).

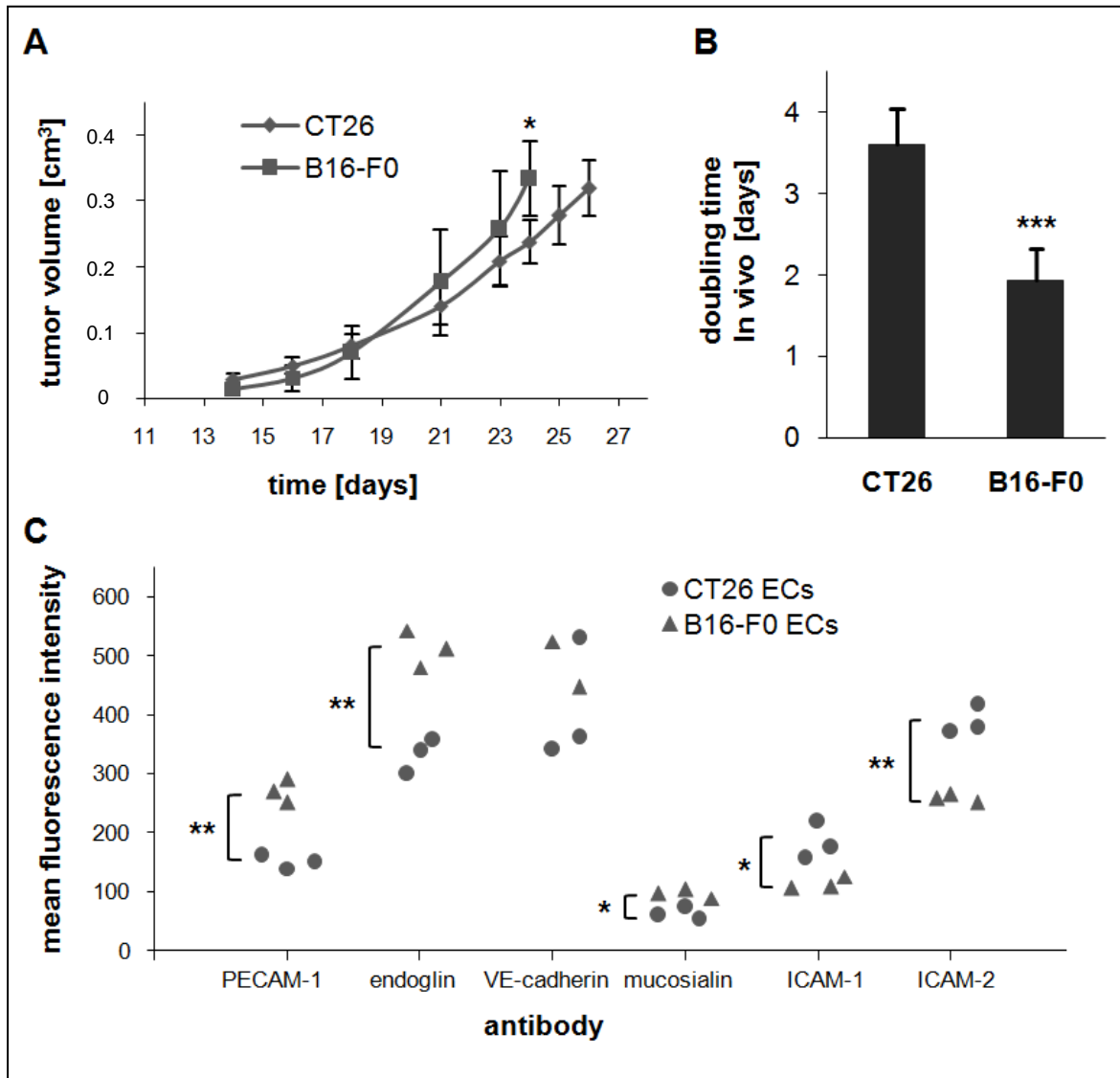


**Figure 20:** Differences in expression of EC markers derived from slow- and fast-growing tumors (CT26 and B16-F0). **(A, B)** Growth curves and doubling times of CT26 (n=15) and B16-F0 (n=15) *in vivo*. **(C)** Mean fluorescence intensity values (PECAM-1, endoglin, VE-cadherin, mucosalin, ICAM-1 and ICAM-2) from slow-growing tumor ECs (CT26 (n=3)) and fast-growing tumor ECs (B16-F0 (n=3)). Asterisk represent significantly different values ( $p^* < 0.05$ ;  $p^{**} < 0.01$ ;  $p^{***} < 0.001$ ).

### 3.2.7 Morphology

Primary ECs derived from normal (heart) and tumor (B16-F0) tissues became adherent 1–2 days after seeding (Figure 21A, B). The diameter of ECs increased over the following 5–7 days until the cells reached 100 % confluence (Figure 21C, D). Adherent tumor ECs were found to be larger, to spread faster and to distribute in a more chaotic pattern compared to ECs from normal tissues (Sievert et al. 2014).

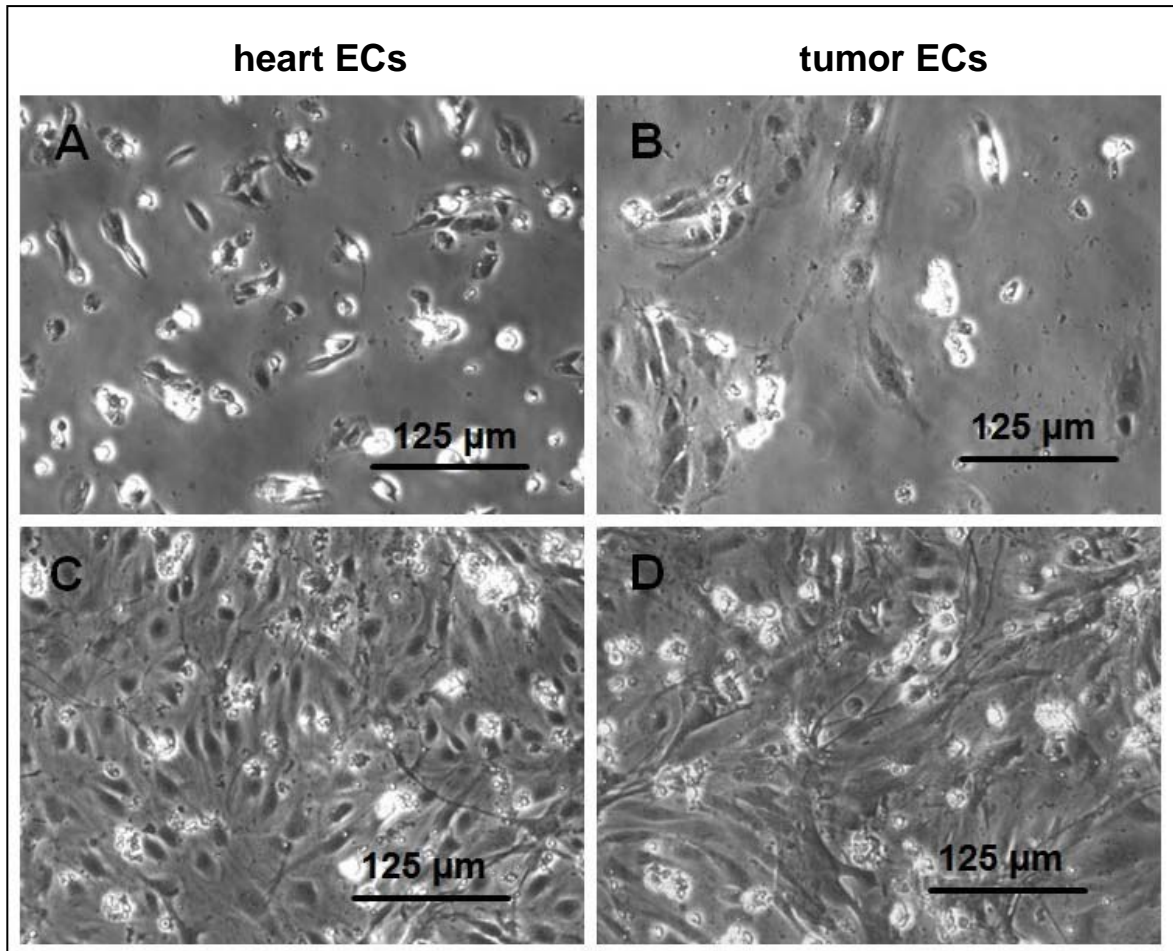


**Figure 21:** Phenotypic characteristics of heart and tumor (B16-F0) ECs. **(A, B)** Adherent heart and tumor ECs after 2 days. **(C, D)** Adherent heart and tumor ECs after 7 days.

### 3.2.8 Migration, flow alignment and tube formation

Although heart and tumor ECs became confluent, cell divisions were not detectable within 33 hours, as expected (Figure 22). The migratory capacity of heart ECs ( $134 \pm 68 \mu\text{m}$ ,  $p < 0.002$ ) is significantly lower compared to that of tumor ECs ( $199 \pm 108 \mu\text{m}$ ) (Figure 24A) (Sievert et al. 2014).

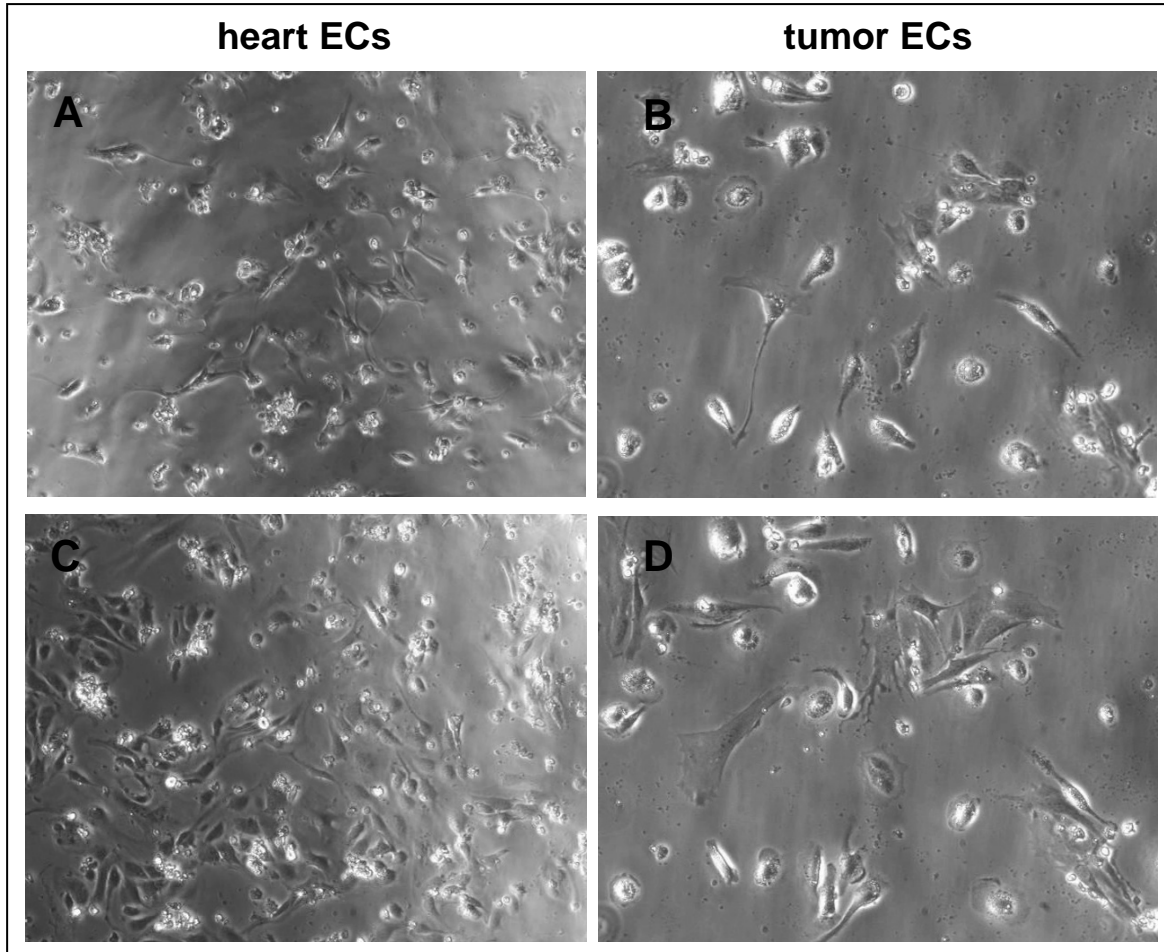


**Figure 22:** Migration of heart and tumor (B16-F0) ECs. After heart and tumor cells become adherent, the monitoring of the same place was started (**A**, **B**). Every minute a picture was taken. Although the confluence seems to be increased 33 hours later, cell divisions were not detectable (**C**, **D**).

The cultivation of primary heart and tumor ECs under permanent shear stress allows the physiological conditions in blood vessels to be simulated. Therefore, 2 days after allowing the cells to attach, ECs were cultured under constant flow conditions using the IBIDI system. To avoid detachment of cells, the flow was started at a rate of 2 ml/min ( $3.5 \text{ dyn/cm}^2$ ) for the first day. After that, the flow was increased to 4 ml/min ( $7 \text{ dyn/cm}^2$ ). After two days, heart ECs started to elongate in the direction of the flow. Four days later, most heart ECs showed an alignment in the direction of the flow (Figure 23A). In contrast, ECs derived from tumors did not align in the direction of the flow (Figure 23B) (Sievert et al. 2014).

Due to the larger size of tumor ECs compared to normal tissue ECs (Figure 16), a higher number of heart (80,000 cells/well) than tumor (20,000 cells/well) ECs was

seeded into the matrigel. The numbers used mirror the minimum number of cells that are required to allow a tube formation within a defined area (Figure 23C, D). Tubes formed by tumor ECs show a significantly smaller number of branching points ( $n: 58 \pm 16$ ,  $p < 0.04$ ) and loops ( $n: 15 \pm 6$ ,  $p = 0.02$ ) per image compared to that of ECs derived from heart tissues (number of branching points:  $176 \pm 6$ , number of loops:  $68 \pm 8$ ) (Figure 24B, C) (Sievert et al. 2014).

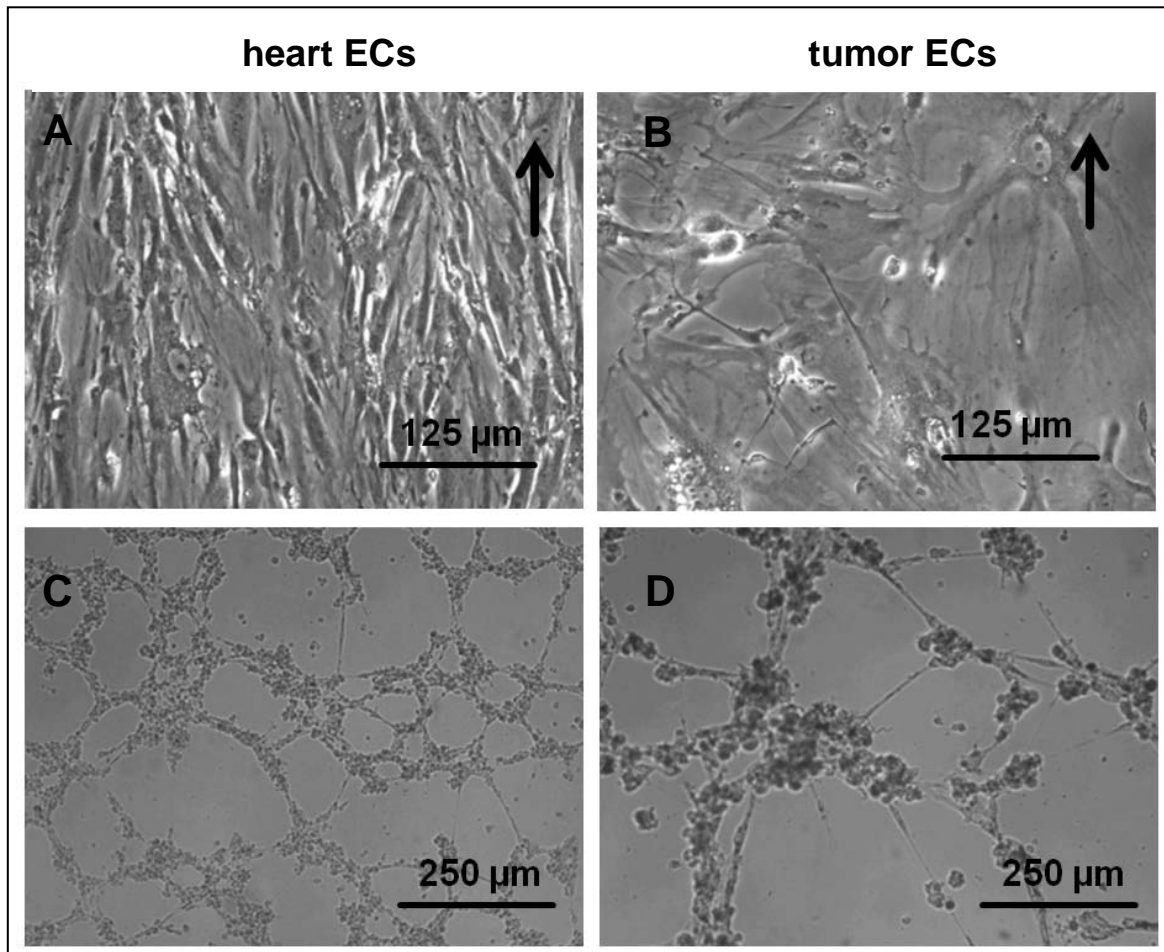


**Figure 23:** Functional characteristics of heart and tumor (B16-F0) ECs. **(A, B)** Heart and tumor ECs under flow conditions (4 ml/min) after 4 days. Before starting the flow, cells were incubated for 2 days under static conditions and 1 day under low flow conditions (2 ml/min). Arrows indicate flow direction. **(C, D)** Tube formation of heart and tumor ECs in matrigel.

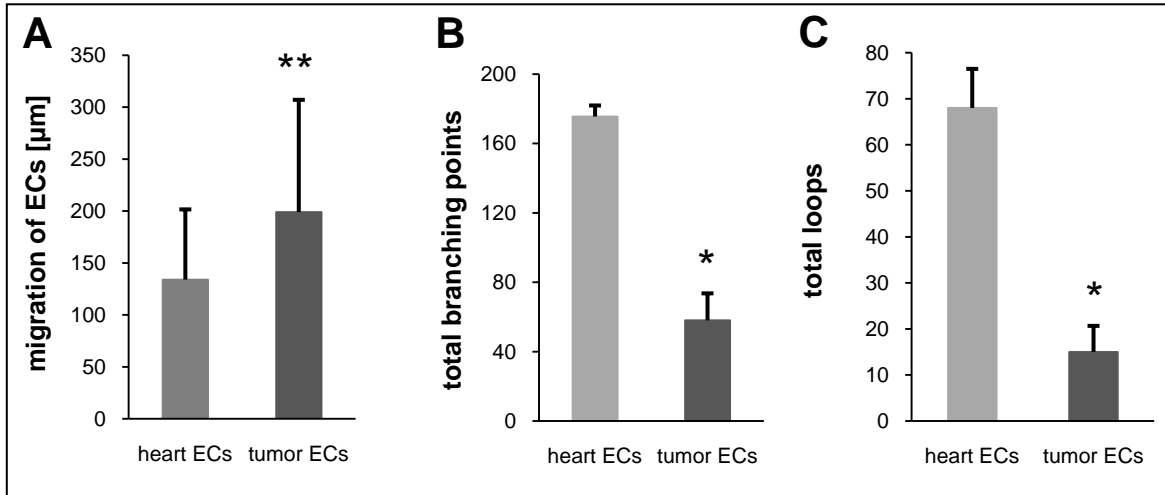


**Figure 24:** Migration and functional characteristics of heart and tumor (B16-F0) ECs. **(A)** Migration of heart and tumor ECs. **(B, C)** Number of total branching points and total loops of heart and tumor ECs in matrigel. Asterisk represent significantly different values ( $p^* < 0.05$ ;  $p^{**} < 0.01$ ).

### 3.2.9 Ploidy level

In this thesis, FISH was used for the determination of the ploidy level of primary heart and tumor ECs. It can be assumed that only interphases can be analyzed, because of the low proliferation rate of heart and tumor ECs *in vitro*. Therefore, three probes with different fluorescence dyes were used (Figure 7). The probe RP23-289I3 was labeled with digoxigenin and hybridized specific to chromosome 1 (red signal), the probe RP23-257F12 was labeled with biotin and hybridized specific to chromosome 4 (green signal), the probe RP23-154G18 was labeled with digoxigenin and biotin and hybridized specific to chromosome 14 (orange signal). The frequency of these three signals have been used to detect the ploidy level of the cells (Figure 7). The specificity was controlled by metaphases from mouse spleen cells (Figure 25, upper line). As expected for normal cells, each chromosome exists twice. Additionally, B16-F0 tumor cells, from which the tumor ECs were isolated, were also investigated. Very often the metaphases from B16-F0 showed a triploid ploidy level (Figure 25, bottom line). This underlines the need for an isolation method of primary ECs without contamination by tumor cells.

In contrast to B16-F0 tumor cells, heart and tumor (B16-F0) ECs showed a normal diploid ploidy level (Figure 26, Table 17).

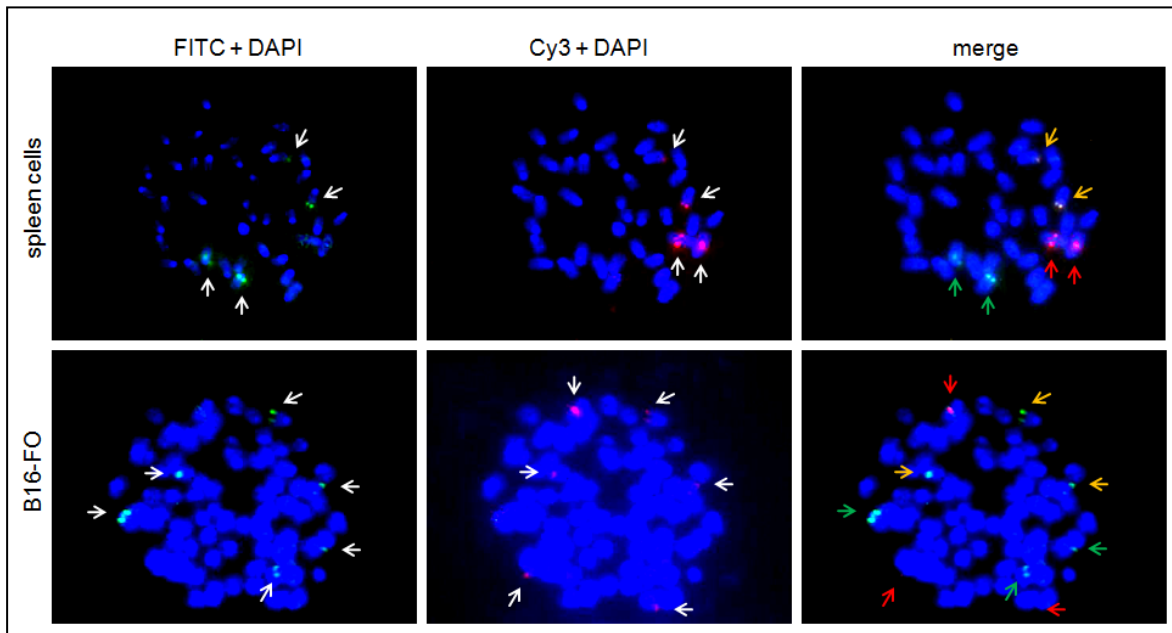


**Figure 25:** FISH-analysis for mouse spleen (upper line) and B16-F0 tumor (bottom line) cells with the probes for chromosome 1 (RP23-289I3, red signal), chromosome 4 (RP23-257F12, green signal) and chromosome 14 (RP23-154G18, orange signal). Arrows indicate the signals in metaphases.

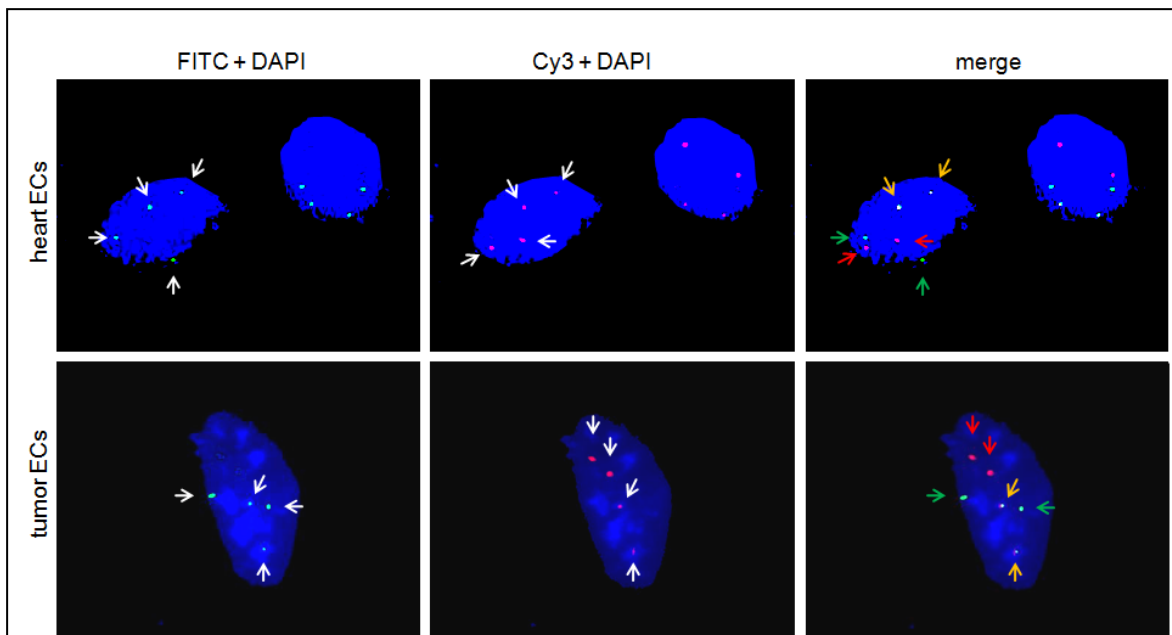


**Figure 26:** FISH-analysis for heart (upper line) and tumor (B16-F0) (bottom line) ECs with the probes for chromosome 1 (RP23-289I3, red signal), chromosome 4 (RP23-257F12, green signal) and chromosome 14 (RP23-154G18, orange signal). Arrows indicate the signals in interphases.

**Table 17:** Result of FISH-analysis for heart and tumor (B16-F0) ECs with the probes RP23-289I3 (red signal), RP23-257F12 (green signal) and RP23-154G18 (orange signal).

sample	number of counted cell nucleus with associated signals				result
	loss	diploid	loss and gain	gain	
heart ECs	1x2r1g2o	<b>46x2r2g2o</b>	1x2r3g1o 1x3r1g1o	1x5r5g5o	<b>diploid</b>
tumor ECs	1x2r1g2o	<b>45x2r2g2o</b>	2x2r3g1o	2x2r3g2o	<b>diploid</b>

g: green, o: orange, r: red

### 3.3 mRNA expression of endothelial cells with high shear stress

#### 3.3.1 Flow-dependent alignment

The cultivation of primary heart ECs under high permanent shear stress allows physiological conditions in capillaries to be simulated. Therefore, 2 days after allowing the cells to attach, ECs were cultured under constant flow conditions. To avoid detachment of cells, the flow was started at a rate of 0.68 ml/min (3.5 dyn/cm<sup>2</sup>) for 2 hours, followed by 0.97 ml/min (5 dyn/cm<sup>2</sup>) for 20 h and 1,95 ml/min (10 dyn/cm<sup>2</sup>) for 2 hours. One day after starting flow, cells were exposed to a flow rate of 3.9 ml/min (20 dyn/cm<sup>2</sup>). Four days later, most heart ECs showed an alignment in the direction of the flow (Figure 27B), contrary to ECs under static conditions (Figure 27A). ECs from this model were used for RNA isolation.

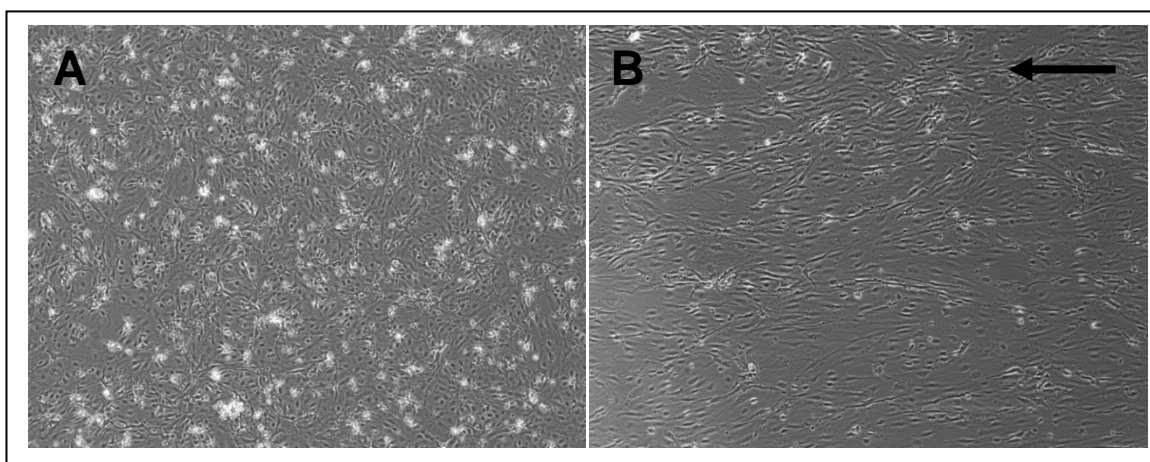


**Figure 27:** Heart ECs under static (**A**) and flow conditions (**B**) ( $20 \text{ dyn/cm}^2$ ) after 4 days. Before being exposed to high flow ( $20 \text{ dyn/cm}^2$ ), cells were incubated for 2 days under static conditions and 1 day under increasing flow conditions ( $3.5 \text{ dyn/cm}^2$  for 2 hours,  $5 \text{ dyn/cm}^2$  for 20 hours,  $10 \text{ dyn/cm}^2$  for 2 hours). Arrows indicate flow direction.

### 3.3.2 Flow-dependent gene expression

The results of the mRNA microarray analysis showed 4,248 differently expressed genes (corrected p-value  $< 0.1$ /absolute  $\log_2$  fold-change  $> 0.5$ ) of heart ECs under flow conditions compared to static conditions. A heatmap of the top 50 differentially expressed genes are shown in Figure 28. A clear separation of gene expression between static (A) and flow (B) conditions can be identified. Pathway enrichment analysis testing specific enrichment of all differentially genes identified in pathways of the Reactome interactome database (<http://www.reactome.org/>) resulted in 24 pathways (corrected p-value  $< 0.1$ , Table 18). The pathways can be assigned to different specific cell components and functions: Extracellular organisation, cell membrane, signal molecules, hemostasis, metabolism, developmental biology and smooth muscle contraction. The extracellular organisation includes the pathways "extracellular matrix organisation", "collagen formation", "assembly of collagen fibrils and other multimeric structures", "elastic fibre formation", "molecules associated with elastic fibres", "integrin cell surface interactions", "non-integrin membran-ECM interactions", "chondroitin sulfate/dermatan sulfate metabolism" and "laminin interactions". The pathway "cholesterol biosynthesis" suggests specific involvement of the cell membrane. With regard to signaling, the pathways "signaling by Rho GTPase", "signaling by VEGF", "NRAGE signals death through JNK", "nitric oxide stimulates guanylate cyclase"

## Results

and signaling in angiogenesis such as "axon guidance", "signaling by NGF", "Netrin-1 signaling" and "semaphorin interactions" were shown to be specifically deregulated. The hemostasis includes the pathways "hemostasis", "platelet activation, signaling and aggregation" and "platelet homeostasis". The pathways "metabolism", "developmental biology" and "smooth muscle contraction" present specific own categories.

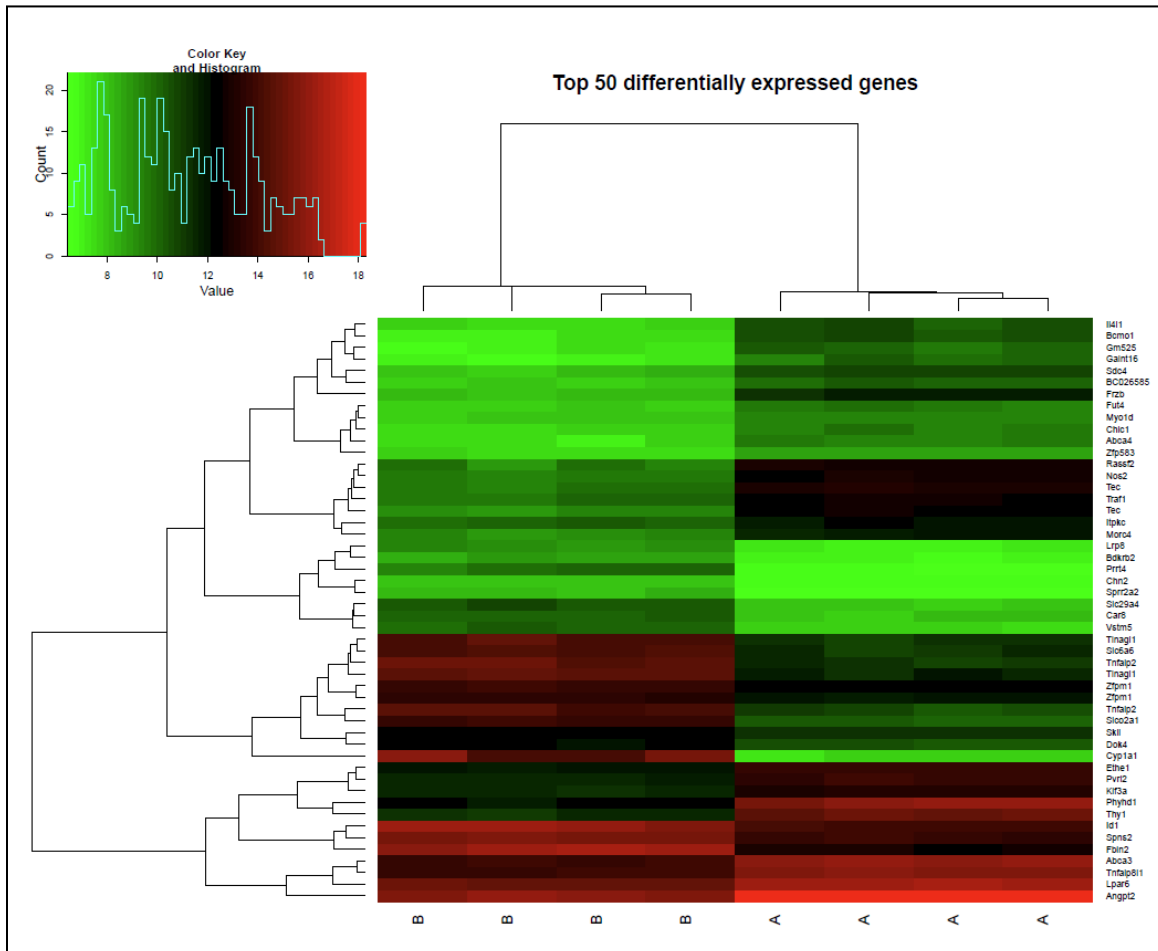


**Figure 28:** Heatmap of top 50 differentially expressed gene-probes of heart ECs under static (A) and flow (B) conditions (20 dyn/cm<sup>2</sup> for 4 days). Log<sub>2</sub> transformed expression is reflected by the colour key as indicated on the top-left including the frequencies of each intensity (turquoise histogram line).

## Results

**Table 18:** Involved pathways based on differential gene expression in response to 4 days high shear stress (20 dyn/cm<sup>2</sup>). The pathways can be assigned to different specific cell components and functions (category (cat)): Extracellular organisation (A), cell membrane (B), signal molecules (C), hemostasis (D), metabolism (E), developmental biology (F) and smooth muscle contraction (G). Matches and %-match indicate the number and percentage of genes which are included in the corresponding pathway. Furthermore the corrected p-value (p-val < 0.1) and the false discovery rate (FDR < 0.1) are shown.

pathway name	cat	genes in pathway	matches	%-match	p-val	FDR
Extracellular matrix organization	A	263	91	34.6	9.6698E-10	1.4998E-06
Assembly of collagen fibrils and other multimeric structures	A	54	26	48.15	1.1018E-06	0.00056962
Hemostasis	D	475	132	27.79	7.5225E-07	0.00056962
Cholesterol biosynthesis	B	22	14	63.64	5.2106E-06	0.00161634
Molecules associated with elastic fibres	A	30	17	56.67	4.8617E-06	0.00161634
Axon guidance	C	318	91	28.62	1.2728E-05	0.00259808
Elastic fibre formation	A	41	20	48.78	1.4876E-05	0.00259808
Signaling by Rho GTPases	C	122	43	35.25	1.5076E-05	0.00259808
Collagen formation	A	86	33	38.37	2.0306E-05	0.00314947
Developmental Biology	F	498	128	25.7	6.1882E-05	0.00872533
Signalling by NGF	C	281	79	28.11	9.028E-05	0.01166875
Metabolism	E	1569	340	21.67	0.00011066	0.01320248
Integrin cell surface interactions	A	66	24	36.36	0.00066401	0.0650533
NRAGE signals death through JNK	C	45	18	40	0.00085215	0.0650533
Netrin-1 signaling	C	42	17	40.48	0.00100663	0.0650533
Nitric oxide stimulates guanylate cyclase	C	25	12	48	0.00093547	0.0650533
Non-integrin membrane-ECM interactions	A	42	17	40.48	0.00100663	0.0650533
Platelet homeostasis	D	79	27	34.18	0.00095549	0.0650533
Semaphorin interactions	C	67	24	35.82	0.00085041	0.0650533
Smooth Muscle Contraction	G	22	11	50	0.00099631	0.0650533
Platelet activation, signaling and aggregation	D	205	57	27.8	0.00111354	0.06908398
Chondroitin sulfate/dermatan sulfate metabolism	A	50	19	38	0.00128611	0.0767217
Laminin interactions	A	23	11	47.83	0.0015837	0.09097492
Signaling by VEGF	C	106	33	31.13	0.00172045	0.09530074

In order to study the putative functional role of genes that are known to be involved in endothelial adhesion and migration of leukocytes, *Pecam1*, *Vcam1*, *Icam1* and *Icam2* were investigated. mRNA expression analysis showed that *Pecam1*, *Icam1*

and *Icam2* were higher expressed on heart ECs under static conditions compared to flow conditions (Table 19). Further *Pecam1*, *Vcam1*, *Icam1* and *Icam2* were investigated for correlation with all other genes of the gene expression microarray dataset. Positive correlations suggests an activating relationship and negative correlation an inhibitory relationship. From the whole correlation network the top 5 positively and top 5 negatively correlating genes were identified (Figure 29) according to the level of significance (e.g. their corrected p-values and correlation coefficients). Next these genes were compared for significant differential expression between static (A) and flow (B) conditions. The level of significance is fulfilled, when  $\log_{2}FC > 0.5$  or  $< -0.5$ , P.value  $< 0.05$  and adj.p.value  $< 0.1$ . In contrast to *Pecam1* and *Vcam1* (table 20, 21), *Icam1* fulfills the level of significance for all activated and inactivated genes relating to differential gene expression between static and flow condition (table 22). The functions of the genes include membrane-trafficking (*Syt17*), internalization of ligand-activated EGFR (*Ankrd13b*), proliferation (*Fgf2*), loss of stress fibers (*Basp1*), migration (*Plxna4*), proteolysis (*Grcc10*, *Psmb9*, *Bace2*), morphogenesis (*Nus1*) and cytoskeletal reorganization (*Ssh3*).

All gene probes from the *Icam2* correlation network suggesting an activating relationship reached the level of significance, whereas only two gene probes from the *Icam2* correlation network suggesting an inhibitory relationship reached the level of significance (table 23). The functions of the activated gene-probes include pyrimidine metabolism (*Cda*), atheroprotective effects (*Nos3*), protein glycosylation (*Galnt18*), cell adhesion (*Sh2b3*) and maybe sensory receptor (*Tmem44*). The functions of the significant inactivated gene-probes include proteolysis (*Rffl*) and regulation of transcription (*Zswim4*).

**Table 19:** Significant mRNA expression of *Pecam1*, *Icam1* and *Icam2* between flow (B) and static (A) conditions. The level of significance is fulfilled when  $\log_{2}FC > 0.5$  or  $< -0.5$ , P.value  $< 0.05$  and adj.p.value  $< 0.1$ .

gene	logFC	P.Value	adj.P.Val	comp. B-A
<i>Pecam1</i>	0.51	0.016	0.049	up
<i>Icam1</i>	1.61	0.013	0.042	up
<i>Icam2</i>	0.85	0.005	0.02	up



**Figure 29:** Functional correlation for *Pecam1*, *Vcam1*, *Icam1* and *Icam2*. For each gene the top 5 activated and inactivated gene-probes are shown.

**Table 20:** Functional correlation of gene-probes with *Pecam1*. Five gene-probes with an activating and five gene-probes with an inactivating correlation are listed. In each group, gene-probes with the highest significance (p-val and coef) were selected. These gene-probes were compared for significant differential expression between static (A) and flow (B) conditions. When the level of significance ( $\log_{2}FC > 0.5$  or  $< -0.5$ , P.value  $< 0.05$  and adj.p.value  $< 0.1$ ) is fulfilled, the gene is marked in green, otherwise the gene is marked in red.

gene	p-val	coef	logFC	P. Value	adj. P.Val	function	comp. A-B
<i>Inpp5e</i>	3.6E-05	0.98	-0.31	0.02	0.05	phosphatase (Humbert et al. 2012)	up
<i>Iffo1</i>	6.7E-05	0.97	-0.47	0.01	0.03	component of cytoskeleton (Herrmann et al. 2007)	up
<i>Stom</i>	0.00013	0.96	-0.27	0.02	0.05	regulation of ion channels and transporters (Rungaldier et al. 2013)	up
<i>Bora</i>	0.00014	0.96	-0.25	0.03	0.08	cell division (Hutterer et al. 2006)	up

## Results

**Table 20 continued:** Functional correlation of gene-probes with *Pecam1*.

<i>Zfp92</i>	0.00018	0.96	-0.21	0.03	0.08	regulation of transcription (Papworth et al. 2006)	up
<i>Rplp1</i>	0.00019	-0.96	0.08	0.30	0.44	structural component of ribosome (Ishii et al. 2006)	down
<i>Timm17b</i>	0.00015	-0.96	0.26	0.04	0.09	transport of proteins in mitochondrion (Shames et al. 2011)	down
<i>Bcl7a</i>	0.00011	-0.96	0.25	0.04	0.11	B cell malignancy (Ramos-Medina et al. 2013)	down
<i>Ctbs</i>	7.1E-05	-0.97	0.12	0.19	0.32	glycosidase (Liu et al. 1999)	down
<i>Tctex1d2</i>	4.5E-05	-0.97	0.27	0.02	0.06	ciliogenesis (Gholkar et al. 2015)	down

**Table 21:** Functional correlation of gene-probes with *Vcam1*. Five gene-probes with an activating and five gene-probes with an inactivating correlation are listed. In each group, gene-probes with the highest significance (p-val and coef) were selected. These gene-probes were compared for significant differential expression between static (A) and flow (B) conditions. When the level of significance (logFC >0.5 or <-0.5, P.value <0.05 and adj.p.value <0.1) is fulfilled, the gene is marked in green, otherwise the gene is marked in red.

gene	p-val	coef	logFC	P. Value	adj. P.Val	function	comp. A-B
<i>Slc16a8</i>	2.1E-06	0.99	0.02	0.83	0.89	monocarboxylate membrane transporter (Pineiro et al. 2012)	up
<i>Sh3pxd2a</i>	6.5E-05	0.97	0.04	0.77	0.84	extracellular matrix degradation (Stylli et al. 2009)	up
<i>Mgat2</i>	0.00011	0.96	0.00	0.99	1.00	protein glycosylation (Tan et al. 1995)	up
<i>Hmgxb3</i>	0.00022	0.96	0.03	0.77	0.84	regulation of transcription (Stros et al. 2007)	up
<i>Acbd5</i>	0.00027	0.95	-0.45	0.02	0.06	cell metabolism (Fan et al. 2010)	up
<i>Mrgprb1</i>	7.8E-05	-0.97	0.00	0.97	0.98	G-protein-coppled sensory receptor (Liu et al. 2008)	down
<i>Sfrs18</i>	0.00014	-0.96	-0.07	0.73	0.82	processing of mRNA (Zimowska et al. 2003)	down
<i>Cpne1</i>	0.00016	-0.96	0.22	0.30	0.44	membrane-trafficking (Creutz et al. 1998)	down
<i>Hsf4</i>	0.00018	-0.96	0.00	1.00	1.00	heat shock proteins (Merath et al. 2013)	down
<i>Txnip</i>	0.00019	-0.96	0.13	0.54	0.66	redox homeostasis (Zhou and Chng 2013)	down

## Results

**Table 22:** Functional correlation of gene-probes with *Icam1*. Five gene-probes with an activating and five gene-probes with an inactivating correlation are listed. In each group, gene-probes with the highest significance (p-val and coef) were selected. These gene-probes were compared for significant differential expression between static (A) and flow (B) conditions. When the level of significance (logFC >0.5 or <-0.5, P.value <0.05 and adj.p.value <0.1) is fulfilled, the gene is marked in green, otherwise the gene is marked in red.

gene	p-val	coef	logFC	P. Value	adj. P.Val	function	comp. A-B
<i>Syt17</i>	3.6E-07	0.99	-0.60	0.01	0.03	membrane-trafficking (Schwarz 2004)	up
<i>Ankrd13b</i>	5.8E-07	0.99	-1.34	0.00	0.00	internalization of ligand-activated EGFR (Tanno et al. 2012)	up
<i>Fgf2</i>	1.9E-06	0.99	-0.50	0.02	0.06	proliferation (Wang et al. 2008a)	up
<i>Basp1/ Cap-23</i>	4.5E-06	0.99	-1.14	0.01	0.04	loss of stress fibers (Wiederkehr et al. 1997)	up
<i>Plxna4</i>	5.9E-06	0.99	-1.62	0.00	0.00	migration (Waimey et al. 2008)	up
<i>Grcc10</i>	8.3E-07	-0.99	0.70	0.01	0.02	proteolysis (Lee et al. 2009)	down
<i>Psmb9/ Lmp2</i>	3.6E-06	-0.99	0.96	0.00	0.02	proteolysis (Powell 2006)	down
<i>Nus1/ Ngbr</i>	4.6E-06	-0.99	1.05	0.00	0.00	morphogenesis (Miao et al. 2006)	down
<i>Ssh3</i>	5E-06	-0.99	0.61	0.02	0.05	cytoskeletal reorganization (Ohta et al. 2003)	down
<i>Bace2</i>	7.4E-06	-0.99	1.85	0.00	0.02	proteolysis (Bennett et al. 2000)	down

**Table 23:** Functional correlation of gene-probes with *Icam2*. Five gene-probes with an activating and five gene-probes with an inactivating correlation are listed. In each group, gene-probes with the highest significance (p-val and coef) were selected. These gene-probes were compared for significant differential expression between static (A) and flow (B) conditions. When the level of significance (logFC >0.5 or <-0.5, P.value <0.05 and adj.p.value <0.1) is fulfilled, the gene is marked in green, otherwise the gene is marked in red.

gene	p-val	coef	logFC	P. Value	adj. P.Val	function	comp. A-B
<i>Cda</i>	1.3E-06	0.99	-1.89	0.00	0.02	pyrimidine metabolism (Demontis et al. 1998)	up
<i>Nos3</i>	5.9E-06	0.99	-1.77	0.00	0.00	atheroprotective effects (Fish and Marsden 2006)	up
<i>Galnt18/ GalNac-T15</i>	7E-06	0.99	-0.93	0.01	0.03	protein glycosylation (Cheng et al. 2004)	up
<i>Sh2b3/ Lnk</i>	8.2E-06	0.99	-0.70	0.01	0.03	cell adhesion and migration (Devalliere et al. 2012)	up
<i>Tmem44</i>	1.1E-05	0.98	-1.03	0.00	0.00	maybe sensory receptor (Moyer et al. 2009)	up
<i>Snupn</i>	1.4E-06	-0.99	0.29	0.02	0.05	nuclear protein transporter (Strasser et al. 2005)	down
<i>Sowahb</i>	1.8E-06	-0.99	0.09	0.19	0.31	cell-cell signaling (Mosavi et al. 2004)	down

**Table 23 continued:** Functional correlation of gene-probes with *Icam2*.

<i>Rffl</i>	5E-06	-0.99	0.97	0.00	0.01	proteolysis, endocytic recycling (Ciechanover et al. 2000; Coumailleau et al. 2004)	down
<i>Zswim4</i>	7.5E-06	-0.99	0.59	0.01	0.04	regulation of transcription (Makarova et al. 2002)	down
<i>Clip1/Clip-170</i>	8.6E-06	-0.98	0.43	0.01	0.04	microtubule binding (Fukata et al. 2002)	down

### 3.4 Irradiation effects of heart endothelial cells after local heart irradiation

#### 3.4.1 Yield of endothelial cells after heart irradiation

The number of isolated ECs was counted directly after isolation. The counts of ECs irradiated with 16 Gy were significantly reduced by 15 % compared with age-matched control hearts (Figure 30).

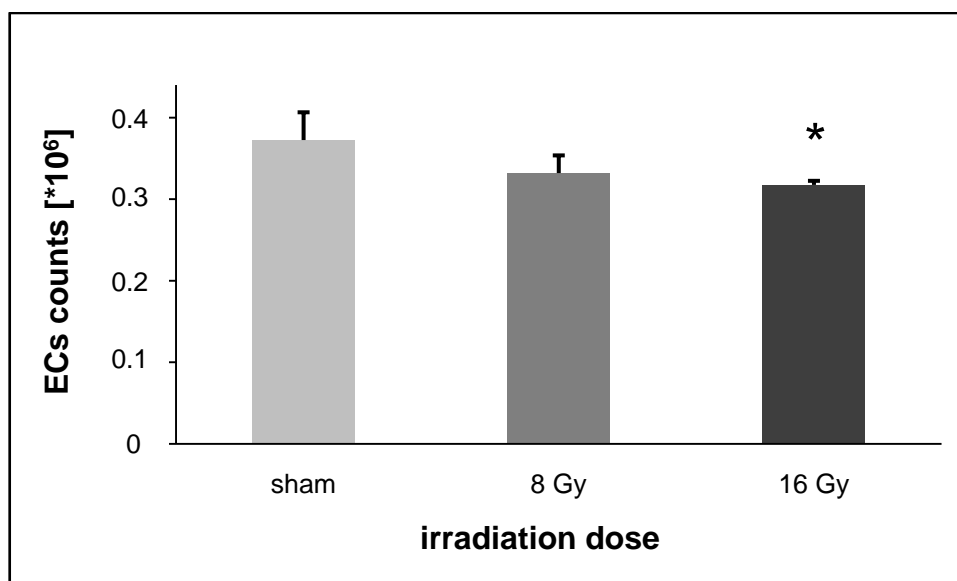


**Figure 30:** Number of isolated mouse heart ECs 16 weeks after local heart irradiation with 0 (sham), 8 or 16 Gy. The amount of ECs from 16 Gy irradiated hearts was significantly lower than the amount of ECs from sham-irradiated hearts. Four biological replicates in each group were used for the statistical analysis. Asterisk represent significantly different values ( $p^* < 0.05$ ).

### 3.4.2 Proportion and cell surface density of markers after heart irradiation

Primary ECs directly after isolation from un-irradiated and irradiated hearts were characterized by flow cytometric analysis using EC-specific antibodies directed against PECAM-1, endoglin, VE-cadherin, ICAM-1, ICAM-2 and mucosialin. The

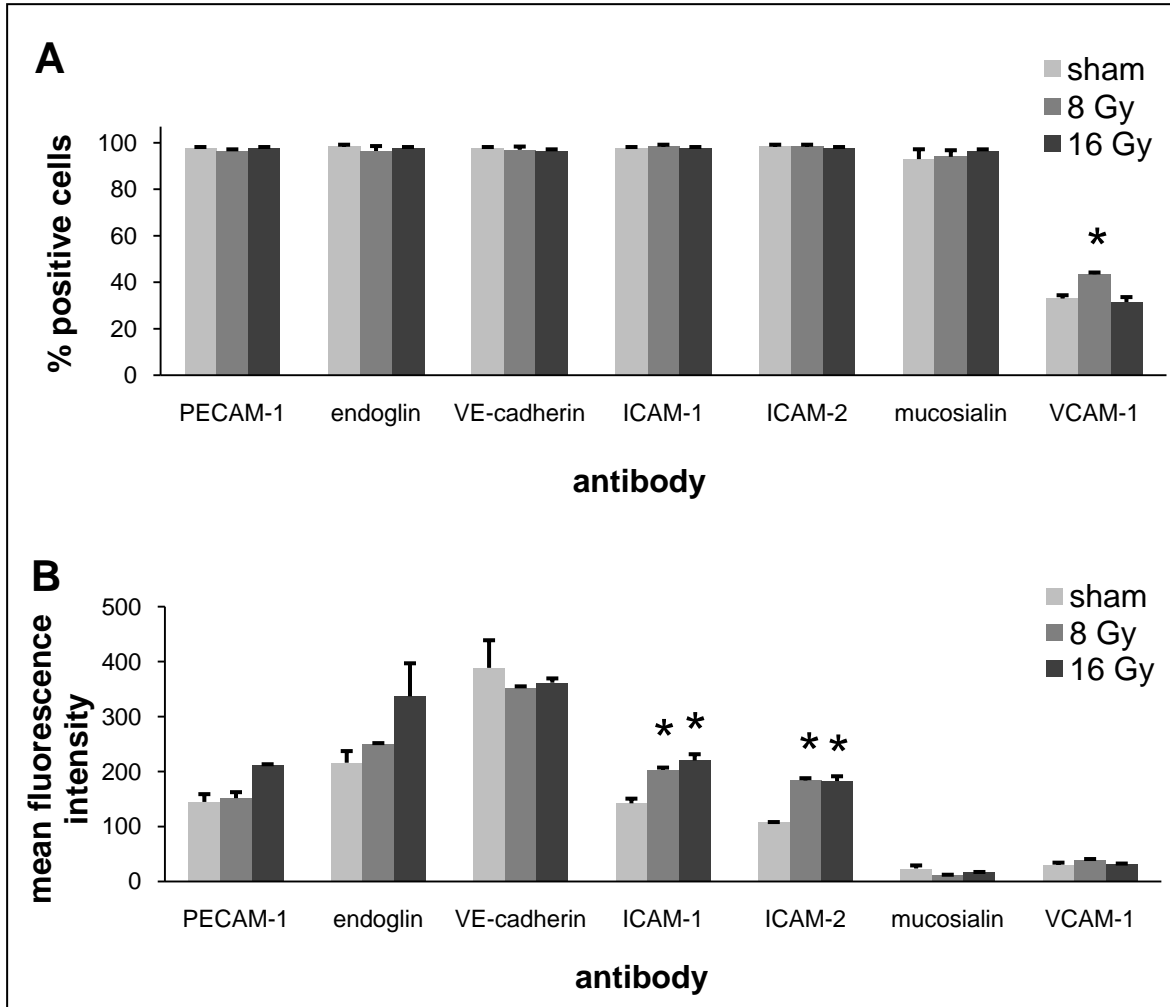


**Figure 31:** Characterization of ECs isolated from mouse hearts 16 weeks after local heart irradiation with 0 (sham), 8 or 16 Gy. **(A)** The proportion of cells that stained positively for ECs-specific markers (PECAM-1, endoglin, VE-cadherin, ICAM-1, ICAM-2 and mucosialin) was nearly 100% ( $97 \pm 2\%$ ), independent of the radiation dose. The amount of ECs that stained positively for VCAM-1 was significantly increased after 8 Gy (44%) compared to sham-irradiated ECs (33%). **(B)** Mean fluorescence intensity values are shown for ECs-specific markers (PECAM-1, endoglin, VE-cadherin, ICAM-1, ICAM-2, mucosialin and VCAM-1). Cell surface densities were significantly increased for ICAM-1 (mfi: 204 and 220) and ICAM-2 (mfi: 184 and 183) after irradiation with 8 and 16 Gy compared to sham-irradiated ECs (mfi: 142 and 108). Three biological replicates in each group were used for the statistical analysis. Asterisk represent significantly different values ( $p^* < 0.05$ ).

leukocyte marker was not detectable on the population of separated ECs. The proportion of cells stained positively for PECAM-1, endoglin, VE-cadherin, ICAM-1, ICAM-2 and mucosialin is nearly 100 % ( $97\pm 2$  %) independent of the dose of irradiation (Figure 31A). In contrast, the proportion of ECs stained positively for VCAM-1 was significantly increased after 8 Gy (44 % vs. 33 %;  $p=0.03$ ) compared to sham ECs. Analysis of the cell surface densities (Figure 31B) showed significant increase of ICAM-1 (mfi: 204 and 220 vs. 142;  $p=0.035$  and  $0.02$ ) and ICAM-2 (mfi: 184 and 183 vs. 108;  $p=0.02$  and  $p<0.05$ ) 16 weeks after irradiation with 8 and 16 Gy compared to sham-irradiated ECs.

### **3.5 Irradiation effects of heart and lung endothelial cells after thorax irradiation**

#### **3.5.1 Surface markers of endothelial cells from non-irradiated hearts and lungs**

Primary ECs derived from non-irradiated hearts and lungs were examined directly after isolation by flow cytometric analysis using EC-specific antibodies directed against endoglin, VE-cadherin, mucosialin, PECAM-1, ICAM-1 and ICAM-2. The leukocyte marker CD45 was not detectable on the isolated EC population. Almost all lung and heart cells ( $97\pm 2$  %) stained positively for endoglin, VE-cadherin, mucosialin, PECAM-1, ICAM-1 and ICAM-2 (Figure 32A). In contrast, the proportion of ECs that stained positively for prominin-1 (13 % vs. 4 %;  $p=0.02$ ) and VCAM-1 (28 % vs 13 %;  $p<0.05$ ) was significantly higher on heart ECs compared to lung ECs. Significantly more ECs from lung stained positively for HCAM (53 % vs. 16 %;  $p=0.002$ ) compared to heart ECs (Figure 32B). The percentage of ECs that stained positively for integrin  $\beta 3$  and VEGFR-2 showed no significant differences between lung and heart. Analysis of the cell surface densities of the markers showed that endoglin (mfi: 159 vs. 72;  $p=0.01$ ), VEGFR-2 (mfi: 14 vs. 6;  $p=0.02$ ), ICAM-2 (mfi: 135 vs. 91;  $p=0.006$ ) and VCAM-1 (mfi: 29 vs. 10;  $p=0.002$ ) were significantly higher expressed on heart ECs compared to lung ECs, whereas ICAM-1 (mfi: 240 vs. 110;  $p=0.007$ ) was higher expressed on lung ECs compared to heart ECs (Figure 32C, D).

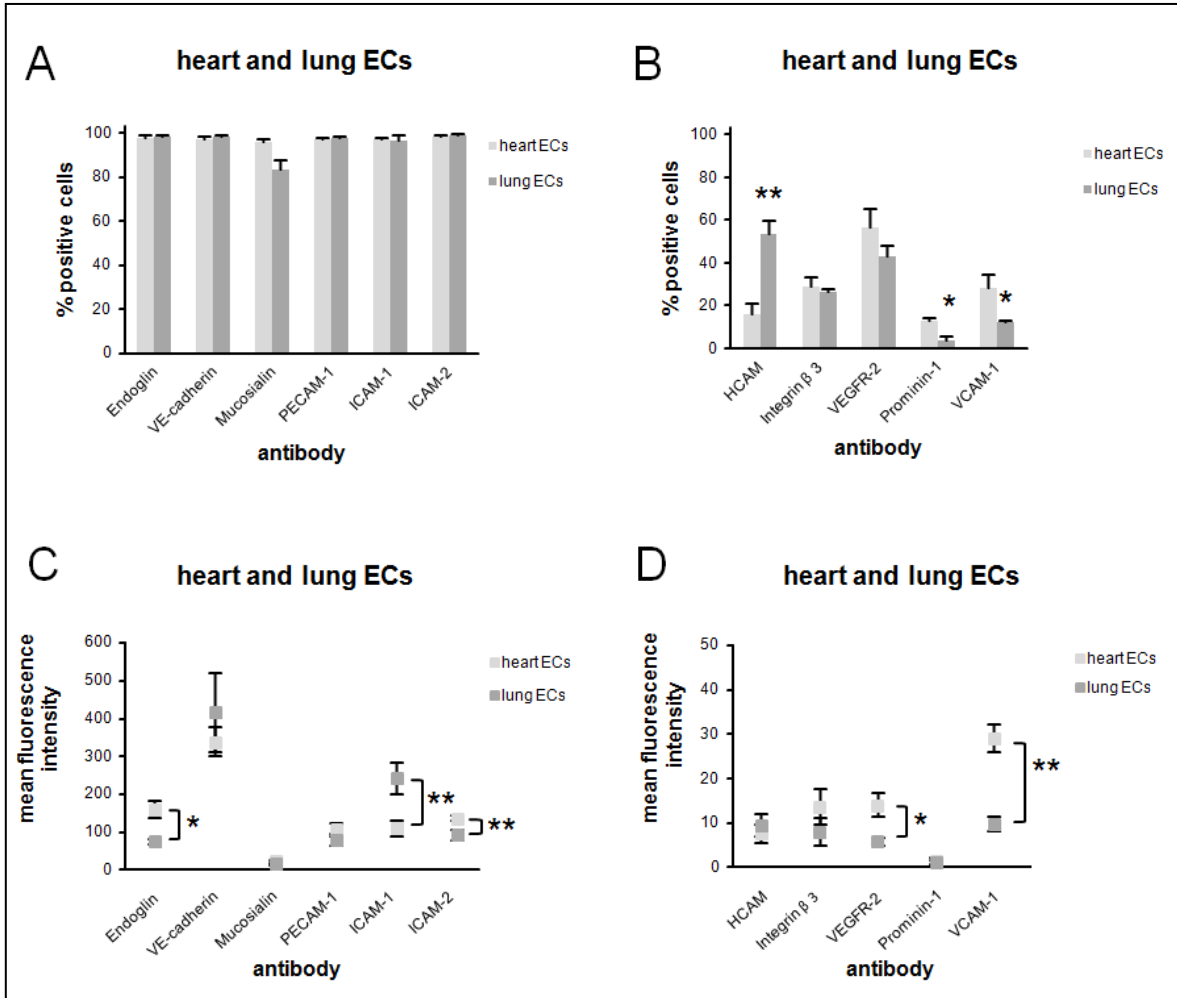


**Figure 32:** Characterization of ECs isolated from non-irradiated heart and lung. **(A)** Purity of ECs isolated from heart and lung indicated by EC-specific antibodies against endoglin, VE-cadherin, mucosalin, PECAM-1, ICAM-1 and ICAM-2. **(B)** Proportion of positively stained heart and lung ECs (HCAM, integrin β3, VEGFR-2, prominin-1 and VCAM-1). The amount of ECs that stained positively for prominin-1 and VCAM-1 was significantly higher on heart ECs (13 % and 28 %) compared to lung ECs (4 % and 13 %). HCAM was higher expressed on lung ECs (53 %) compared to heart ECs (16 %). **(C, D)** Mean fluorescence intensity values are shown for endoglin, VE-cadherin, mucosalin, PECAM-1, ICAM-1, ICAM-2, HCAM, integrin β3, VEGFR-2, prominin-1 and VCAM-1. Cell surface densities were significantly increased for endoglin, VEGFR-2 and VCAM-1 on heart ECs compared to lung ECs, whereas ICAM-1 was significantly increased on lung ECs compared to heart ECs. Three biological replicates in each group were used for the statistical analysis. Asterisk represent significantly different values ( $p^* < 0.05$ ;  $p^{**} < 0.01$ ).

### 3.5.2 Proportion of cell surface markers for heart and lung endothelial cells after irradiation

The proportion of positively stained heart and lung ECs did not change significantly at any time after irradiation with 2 Gy. The proportion of ECs that stained positively for HCAM was increased (61 % and 41 % vs. 16 %;  $p=0.0008$

## Results

and  $p=0.04$ ) 10 and 15 weeks after 8 Gy for heart ECs (Figure 33). 10 weeks after irradiation with 8 Gy, the percentage of integrin  $\beta 3$ -positive cells increased (40 % vs. 29 %;  $p=0.03$ ) for heart ECs and 5 to 10 weeks (37 % and 39 % vs. 27 %;  $p=0.01$  and  $p=0.003$ ) after irradiation for lung ECs. While VEGFR-2 showed no significant difference, the percentage of prominin-1 positively stained cells was decreased (3 % and 6 % vs. 13 %;  $p=0.02$  and  $p=0.04$ ) 15 and 20 weeks for heart ECs and increased (13 % vs. 4 %;  $p=0.02$ ) 20 weeks for lung ECs after 8 Gy. VCAM-1 was increased for heart ECs (50 %, 47 % and 52 % vs. 28 %;  $p=0.02$ ,  $p=0.04$  and  $p=0.01$ ) 10, 15 and 20 weeks and for lung ECs (22 % and 29 % vs. 13 %;  $p<0.05$  and  $p=0.02$ ) 15 and 20 weeks after 8 Gy (Sievert et al. 2015).

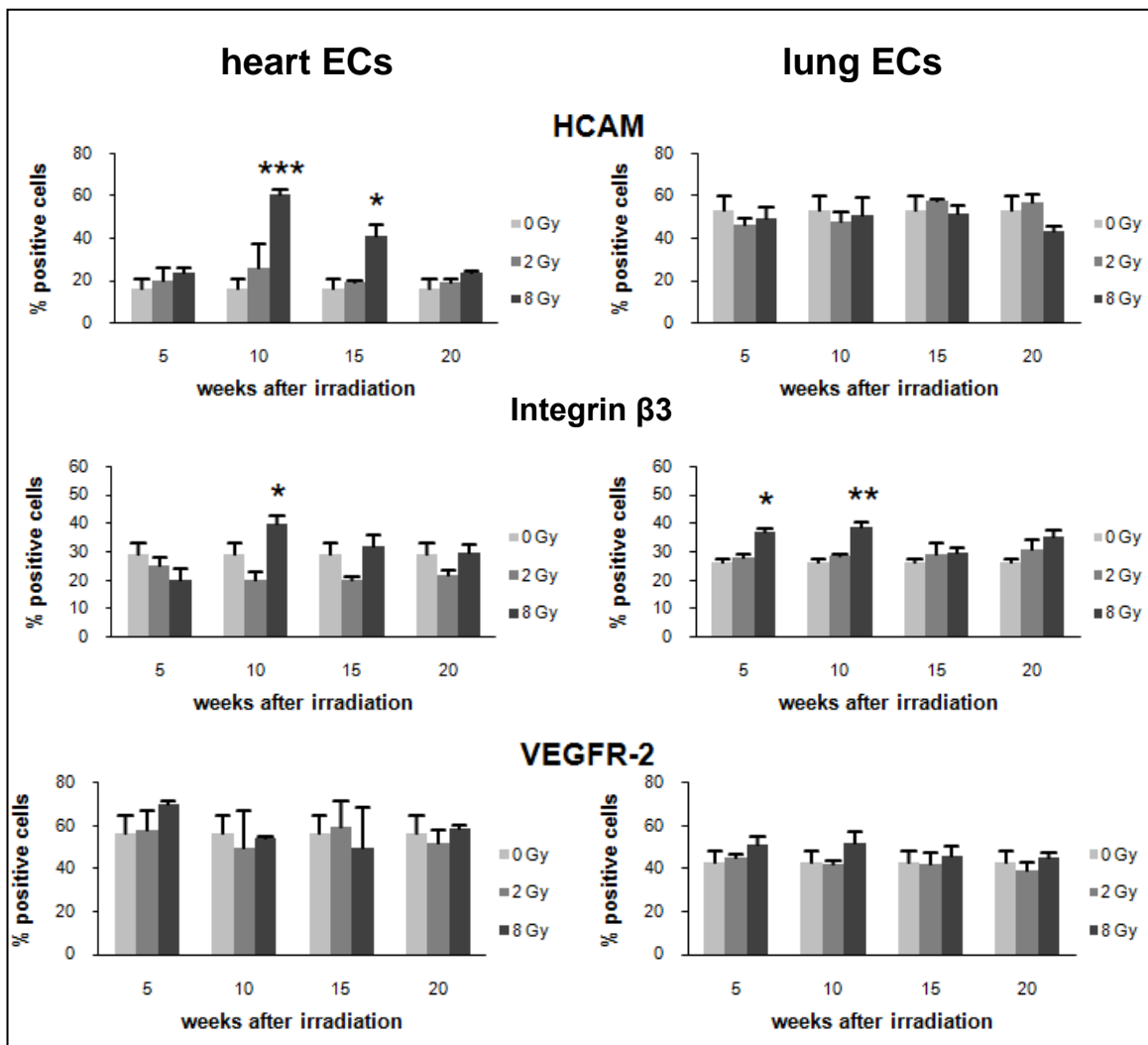
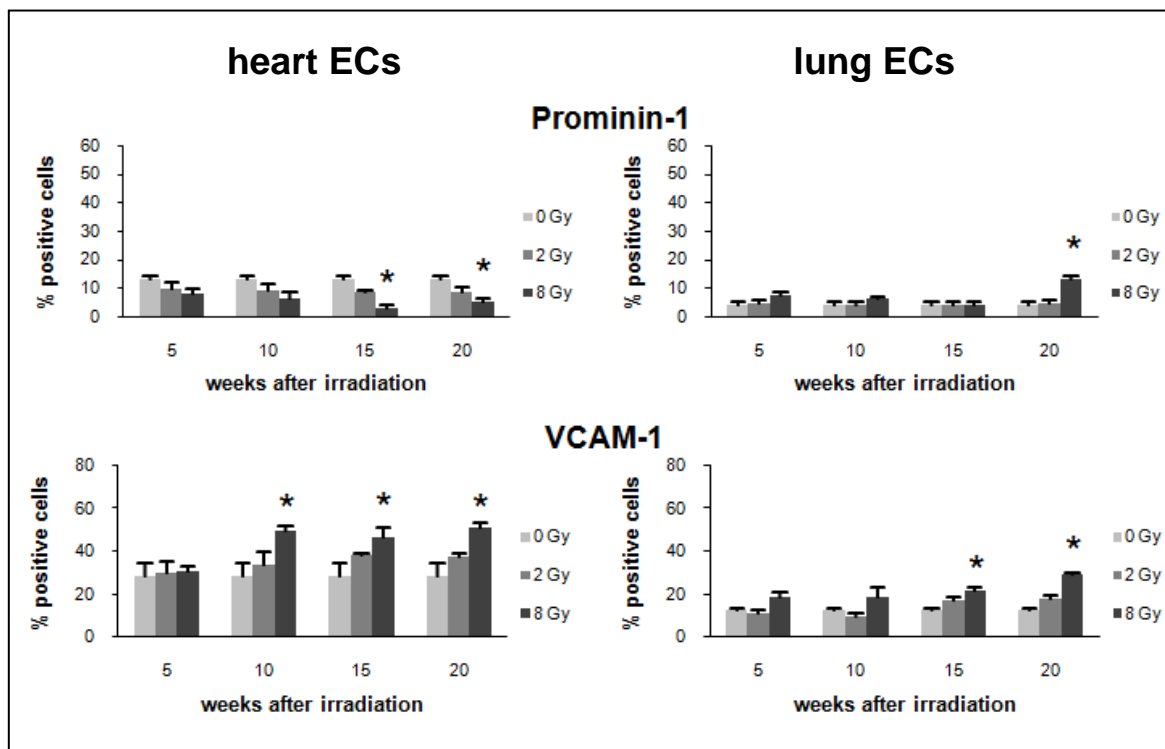


Figure 33: Legend on next page.



**Figure 33 continued:** Positively stained ECs isolated from heart (left side) and lung (right side) 5, 10, 15 and 20 weeks after irradiation with sham, 2 or 8 Gy. The proportion of cells that stained positively for HCAM, integrin  $\beta$ 3, VEGFR-2, prominin-1 and VCAM-1 are shown. The amount of heart ECs that stained positively for HCAM was significantly increased (61 % and 41 % vs. 16 %) 10 and 15 weeks after 8 Gy compared to sham-irradiated ECs. The amount of integrin  $\beta$ 3-positive cells was increased for heart ECs (40 % vs. 29 %) 10 weeks and for lung ECs (37 % and 39 % vs. 27 %) 5 to 10 weeks after 8 Gy. Prominin-1-positive cells were decreased (3 % and 6 % vs. 13 %) 15 and 20 weeks for heart ECs and increased (13 % vs. 4 %) 20 weeks for lung ECs after 8 Gy. VCAM-1-positive cells were increased for heart ECs (50 %, 47 % and 52 % vs. 28 %) 10, 15 and 20 weeks and for lung ECs (22 % and 29 % vs. 13 %) 15 and 20 weeks after 8 Gy. Three biological replicates in each group were used for the statistical analysis. Asterisk represent significantly different values ( $p^* < 0.05$ ;  $p^{**} < 0.01$ ;  $p^{***} < 0.001$ ).

### 3.5.3 Irradiation-induced alterations in the cell surface density of markers involved in endothelial cell proliferation

To investigate the proliferation of ECs after irradiation, the cell surface was analyzed using antibodies directed against surface markers which are relevant for proliferation. The expression densities of these surface markers showed a delayed but significant increase for both heart and lung ECs between 5–15 weeks after irradiation, followed by a decrease to basic levels (Figure 34). For heart ECs, the expression density of HCAM was increased (mfi: 27 vs. 8;  $p=0.02$ ) 10 weeks after 8 Gy, endoglin was elevated (mfi: 287 vs. 159;  $p=0.03$ ) 10 weeks after 8 Gy and

## Results

the expression density of VE-cadherin was enhanced (mfi: 467 and 533 vs. 337;  $p=0.03$  and  $p=0.02$ ) 10 weeks after 2 and 8 Gy. For lung ECs, the expression density of HCAM was increased (mfi: 22 and 20 vs. 9;  $p=0.03$  and  $p=0.02$ ) 10 and 15 weeks after irradiation, integrin  $\beta 3$  was elevated (mfi: 18 vs. 8;  $p=0.007$ ) 10 weeks after irradiation, endoglin was enhanced (mfi: 146, 130 and 127 vs. 72;  $p=0.02$ ,  $p<0.05$  and  $p<0.05$ ) 5, 10 and 15 weeks after irradiation and VEGFR-2 was increased (mfi: 14 and 14 vs. 6;  $p=0.002$  and  $p=0.002$ ) 5 and 10 weeks after irradiation with 8 Gy. No significant changes were observed for integrin  $\beta 3$  and VEGFR-2 for irradiated heart ECS and for VE-cadherin for irradiated lung ECs (Sievert et al. 2015).

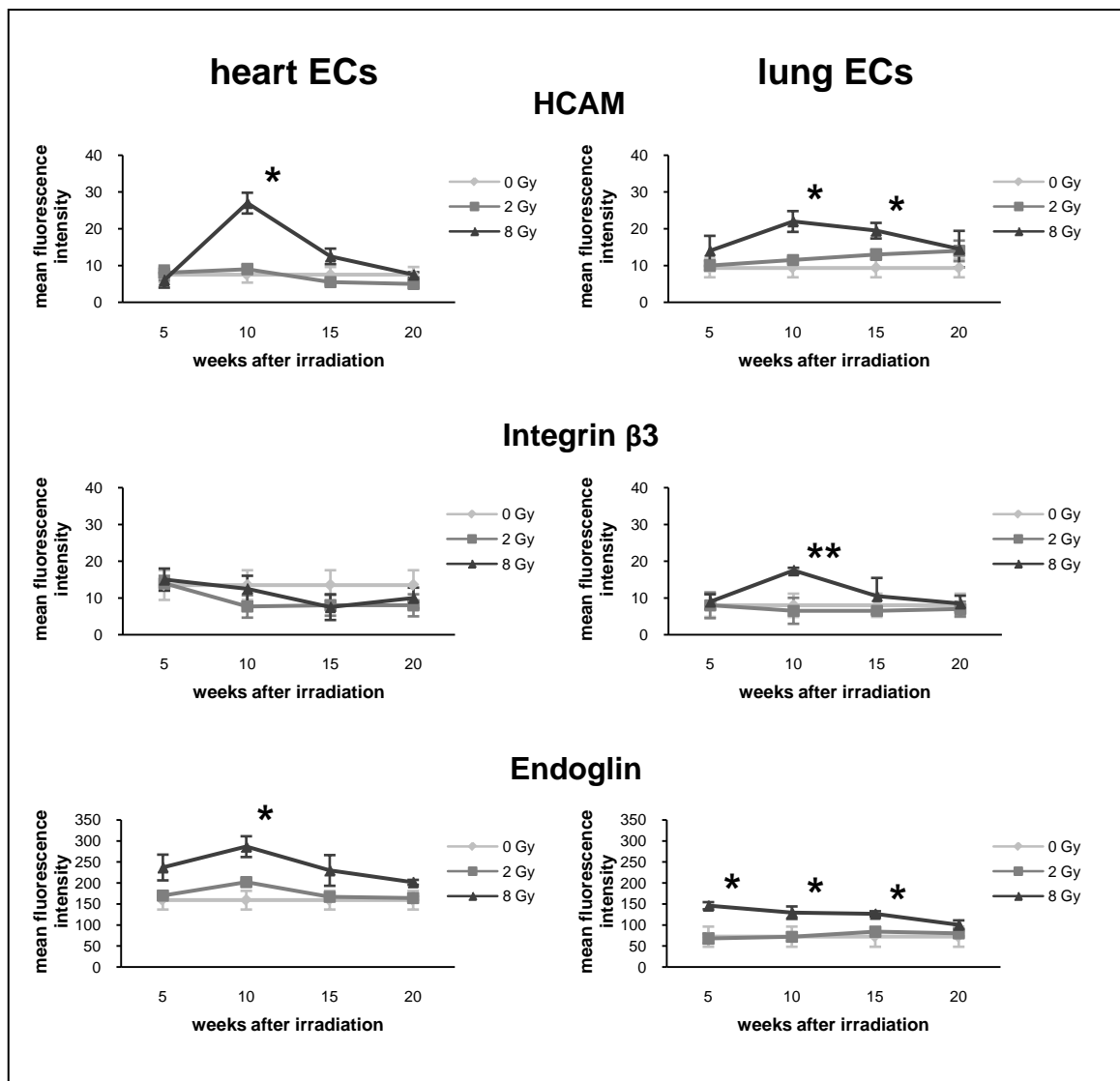


**Figure 34:** Legend on next page.

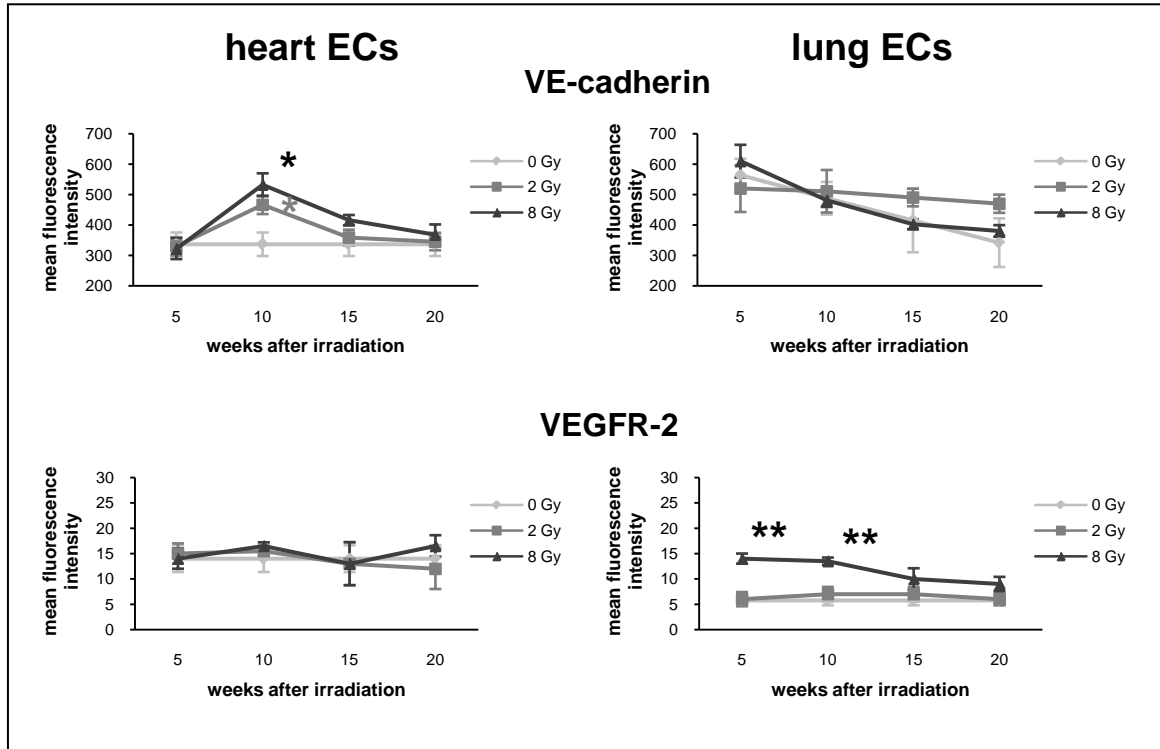


**Figure 34 continued:** Expression density (mean fluorescence intensity) of EC surface marker involved in cell proliferation isolated from heart (left side) and lung (right side) 5, 10, 15 and 20 weeks after irradiation with sham, 2 or 8 Gy. Expression density of HCAM, integrin  $\beta$ 3, endoglin, VE-cadherin and VEGFR-2 are shown. For heart ECs, the expression density of HCAM was increased (mfi: 27 vs. 8) 10 weeks after 8 Gy, endoglin was increased (mfi: 287 vs. 159) 10 weeks after 8 Gy and VE-cadherin was increased (mfi: 467 and 533 vs. 337) 10 weeks after 2 and 8 Gy. For lung EC, the expression density of HCAM was increased (mfi: 22 and 20 vs. 9) 10 and 15 weeks after 8 Gy, integrin  $\beta$ 3 was increased (mfi: 18 vs. 8) 10 weeks after 8 Gy, endoglin was increased (mfi: 146, 130 and 127 vs. 72) 5, 10 and 15 weeks after 8 Gy and VEGFR-2 was increased (mfi: 14 and 14 vs. 6) 5 and 10 weeks after irradiation with 8 Gy. Three biological replicates in each group were used for the statistical analysis. Asterisk represent significantly different values ( $p^* < 0.05$ ;  $p^{**} < 0.01$ ).

### 3.5.4 Irradiation-induced alterations of endothelial progenitor cell surface markers

To determine the role of endothelial progenitor cells, the expression density of surface markers mucosialin and prominin-1 was measured after irradiation. While the expression of prominin-1 remained unaltered low for heart and lung ECs, the mucosialin expression was increased (mfi: 40 and 54 vs. 14;  $p=0.04$  and  $p<0.05$ ) 15 and 20 weeks after irradiation for lung ECs (Figure 35) (Sievert et al. 2015).

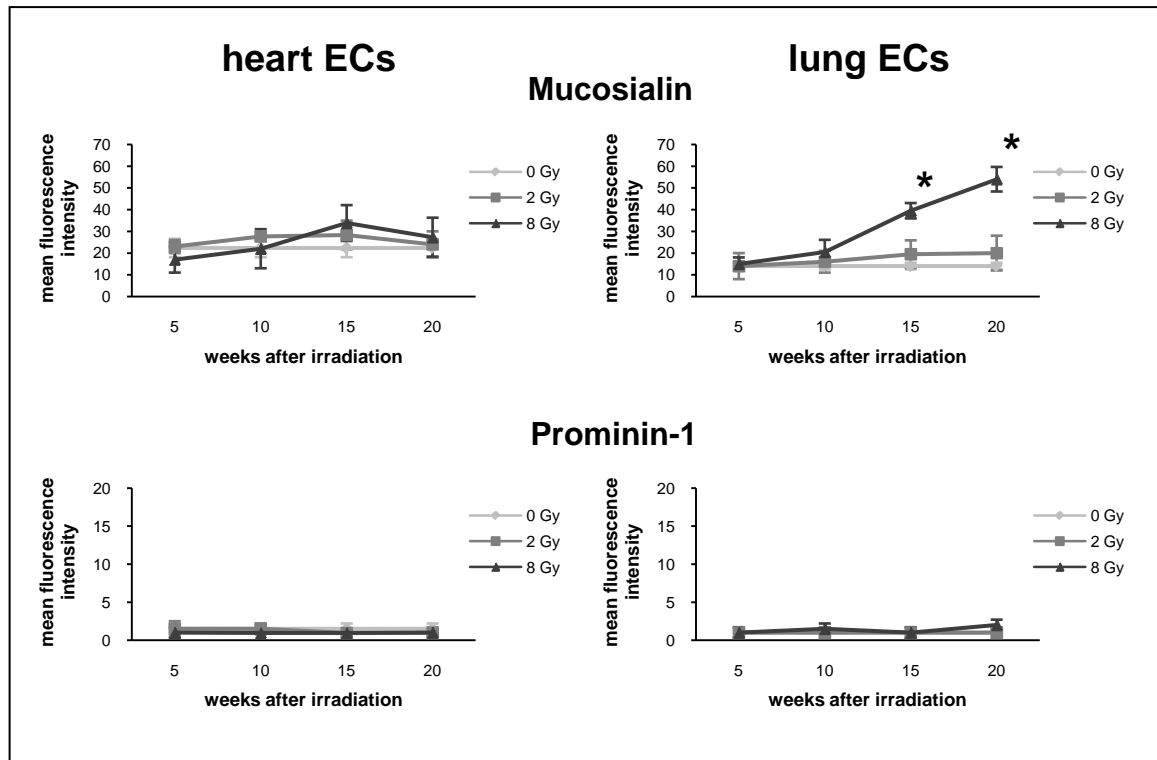


**Figure 35:** Expression density (mean fluorescence intensity) of EC surface marker involved in endothelial progenitor cells from heart (left side) and lung (right side) 5, 10, 15 and 20 weeks after irradiation with sham, 2 or 8 Gy. Expression density of mucosialin and prominin-1 are shown. For lung ECs, the expression density of mucosialin was increased (mfi: 40 and 54 vs. 14) 15 and 20 weeks after irradiation with 8 Gy. Three biological replicates in each group were used for the statistical analysis. Asterisk represent significantly different values ( $p^* < 0.05$ ).

### 3.5.5 Irradiation-induced alterations of cell surface markers involved in inflammation

To investigate the inflammatory involvement of cell adhesion molecules after irradiation, the cell surface was analyzed using antibodies directed against different adhesion molecules which are relevant for inflammation. For heart ECs, PECAM-1 was increased (mfi: 163 and 322 vs. 106;  $p=0.02$  and  $p=0.0005$ ) 10 weeks after irradiation with 2 and 8 Gy and ICAM-2 was elevated (mfi: 273 and 190 vs. 135;  $p=0.004$  and  $p=0.01$ ) 10 and 15 weeks after irradiation with 8 Gy (Figure 36). For lung ECs, PECAM-1 was increased (mfi: 160, 197, 147 and 151 vs. 79;  $p=0.01$ ,  $p<0.05$ ,  $p<0.05$  and  $p<0.05$ ) 5, 10, 15 and 20 weeks after irradiation with 8 Gy and ICAM-2 was elevated (mfi: 135, 134 and 150 vs. 91;  $p=0.006$ ,  $p=0.01$  and  $p=0.02$ ) 10, 15 and 20 weeks after irradiation with 8 Gy.

## Results

Analysis of heart and lung EC expression densities of both ICAM-1 and VCAM-1 showed a significant increase 10-20 weeks after 8 Gy compared to sham-irradiated ECs. The expression density of ICAM-1 was enhanced for heart ECs (mfi: 309, 230 and 233 vs. 110;  $p < 0.05$ ,  $p < 0.05$  and  $p = 0.04$ ) and for lung ECs (mfi: 715, 666 and 451 vs. 240;  $p = 0.0002$ ,  $p = 0.0008$  and  $p = 0.04$ ) 10, 15 and 20 weeks after 8 Gy. Furthermore, ICAM-1 was increased (mfi: 421 and 415;  $p = 0.01$  and  $p = 0.01$ ) 15 and 20 weeks after 2 Gy for lung ECs. VCAM-1 was elevated for heart ECs (mfi: 56, 43 and 49 vs. 29;  $p = 0.002$ ,  $p < 0.05$  and  $p = 0.04$ ) and for lung ECs (mfi: 25, 28 and 25 vs. 10;  $p < 0.05$ ,  $p = 0.02$  and  $p < 0.05$ ) 10, 15 and 20 weeks after 8 Gy (Sievert et al. 2015).

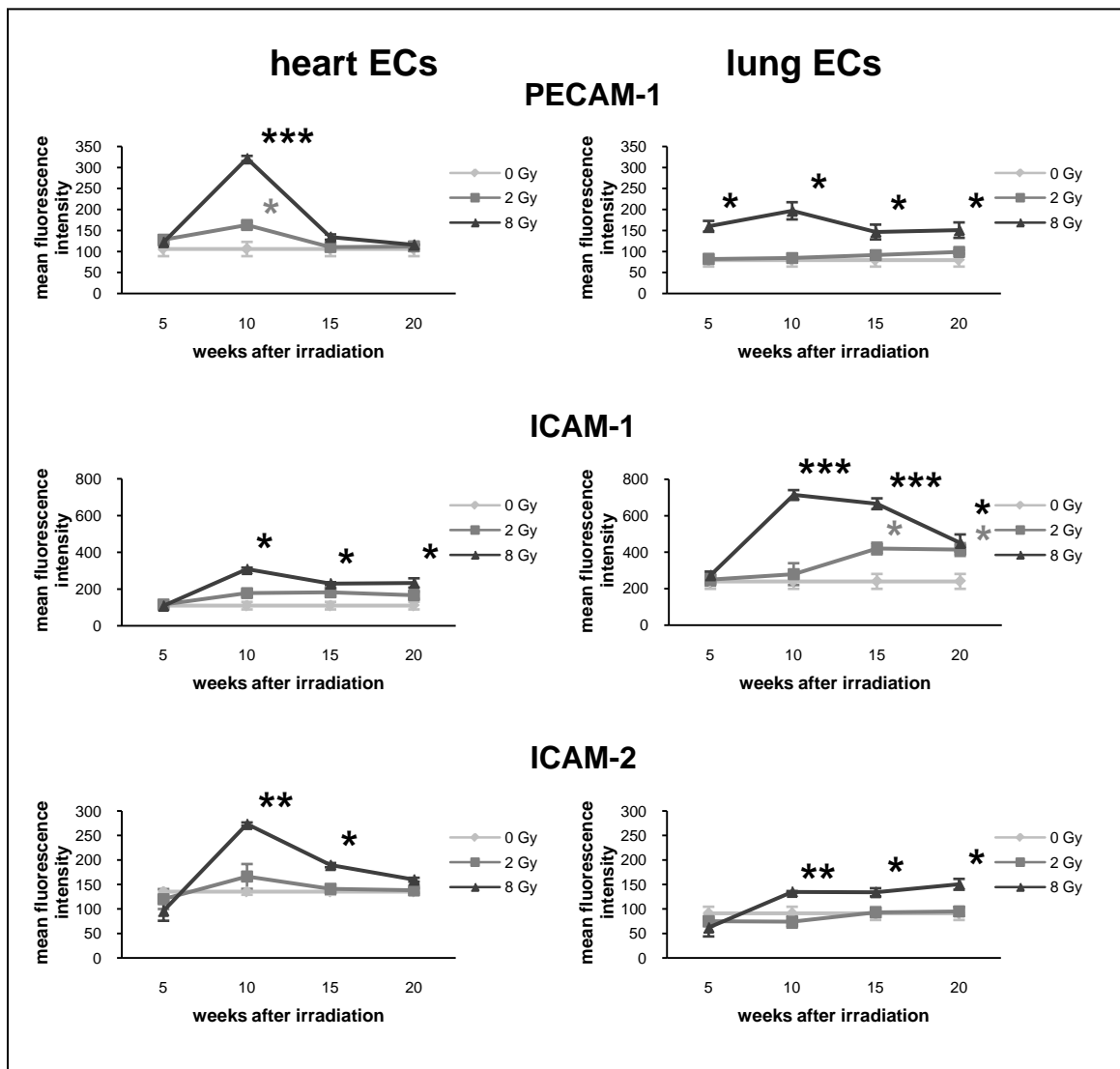
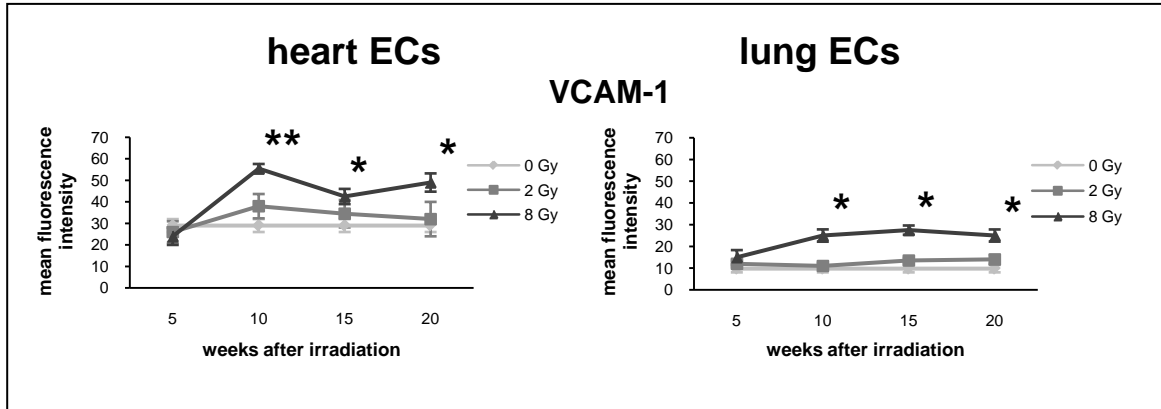


Figure 36: Legend on next page.



**Figure 36 continued:** Expression density (mean fluorescence intensity) of EC surface marker involved in cell adhesion from heart (left side) and lung (right side) 5, 10, 15 and 20 weeks after irradiation with sham, 2 or 8 Gy. Expression densities of PECAM-1, ICAM-1, ICAM-2 and VCAM-1 are shown. For heart ECs, the expression density of PECAM-1 was increased (mfi: 163 and 322 vs. 106) 10 weeks after irradiation with 2 and 8 Gy, ICAM-1 was increased (mfi: 309, 320 and 233 vs. 110) 10, 15 and 20 weeks after 8 Gy, ICAM-2 was increased (mfi: 273 and 190 vs. 135) 10 and 15 weeks after 8 Gy and VCAM-1 was increased (mfi: 56, 43 and 49 vs. 29) 10, 15 and 20 weeks after irradiation with 8 Gy. For lung ECs, the expression density of PECAM-1 was increased (mfi: 160, 197, 147 and 151 vs. 79) 5, 10, 15 and 20 weeks after 8 Gy, ICAM-1 was increased (mfi: 715, 666 and 451 vs. 240) 10, 15 and 20 weeks after 8 Gy and (mfi: 421 and 415) 15 and 20 weeks after 2 Gy, ICAM-2 was increased (mfi: 135, 134 and 150 vs. 91) 10, 15 and 20 weeks after 8 Gy and VCAM-1 was increased (mfi: 25, 28 and 25 vs. 10) 10, 15 and 20 weeks after irradiation with 8 Gy. Three biological replicates in each group were used for the statistical analysis. Asterisk represent significantly different values ( $p^* < 0.05$ ;  $p^{**} < 0.01$ ;  $p^{***} < 0.001$ ).

## 4. DISCUSSION

The goal of the thesis was the investigation of alterations in primary ECs under non- pathological and pathological conditions and following radiation therapy. For that, a new isolation method for primary ECs of tumor and normal tissue was established. Differences in the morphology, function and expression pattern of surface markers on the different ECs were analyzed. The study of tumor ECs reveals immunological interactions and functional changes in the interplay of existing and evolving ECs from benign and malignant tissue. The results of microarray gene expression analysis demonstrate that high shear stress represents an important stimulus for gene expressions of heart ECs. The analysis of heart ECs after local irradiation may provide evidences to clarify the long clinical development and progression of radiation-induced damage.

### 4.1 Reproducible method for the isolation of viable endothelial cells from different tissue

By using the newly established EC-isolation technique (Figure 11), primary ECs could be isolated from young and old mice in the absence of attached magnetic beads. Without steric effect of beads, isolated ECs can be analysed directly after isolation. Furthermore ECs are able to become adherent, survive in cell culture and allow the characterization in the stationary phase without many cell divisions *in vitro*. The long maintenance of ECs in cell culture to get rid of the attached beads with sustained cell division is no longer required. In the present study, heart and lung were used as examples of stable, non-proliferating normal tissues, the repair blastema as a rapidly proliferating normal tissue, and CT26 and B16-F0 tumors as proliferating malignant tissues. Isolated cells could be clearly identified as ECs from each individual tissue due to the expression of six different EC surface markers such as PECAM-1, endoglin, VE-cadherin, mucosialin, ICAM-1 and ICAM-2. A panel of markers needs to be used because each individual marker alone can also be found on other cell types apart from ECs (Table 2). The high proportion of positively stained cells for PECAM-1, endoglin, VE-cadherin, mucosialin, ICAM-1 and ICAM-2 proves that the isolated cells in the study are

indeed ECs. The purity was nearly 100 % ( $97\pm 2$  % for technical reason: overlapping of isotype and antibody). Further purification steps are not necessary. The time required for ECs isolation starting from sacrifice of mice to receipt of pure ECs ranged between three and a half and four hours depending on the nature of tissues.

## **4.2 Expression density of endothelial cell markers in benign and malignant tissue correlated with proliferation**

Whereas the proportion of positively stained cells for all EC-markers (PECAM-1, endoglin, VE-cadherin, mucosialin, ICAM-1 and ICAM-2) was nearly 100 %, independent from the tissue (normal, benign or malignant) from which the cells were isolated, their expression density was different. The expression density of proliferation markers such as endoglin and VE-cadherin is higher on freshly isolated ECs of proliferating tissues like tumor and repair blastema as compared to non-proliferating normal tissues such as heart and lung. The expression density of the progenitor marker mucosialin is elevated in tumor-derived ECs, but not in that of repair blastemas, whereas the adhesion molecules PECAM-1, ICAM-1 and ICAM-2 were found to be elevated in ECs of benign and malignant proliferating tissues compared to non-proliferating normal tissues.

Endoglin expression is increased in ECs during wound healing, developing embryos, inflammatory tissues and solid tumors (Burrows et al. 1995; Arthur et al. 2000). All of these processes are involved in angiogenesis and are associated with the receptor of the transforming growth factor- $\beta$  complex (TGF- $\beta$ ). A high expression of endoglin on tumor ECs correlates with a reduced survival of patients (Fonsatti and Maio 2004; Dallas et al. 2008). ECs from VE-cadherin-deficient mice form primitive vascular structures which are unstable during further development and result in embryonic death (Vittet et al. 1997; Carmeliet et al. 1999; Crosby et al. 2005). Furthermore, antibodies against VE-cadherin reduced angiogenesis and tumor growth *in vivo* (Liao et al. 2000; Corada et al. 2002; Liao et al. 2002). As might be expected the proportion and expression density of the proliferation marker integrin  $\beta 3$  were up-regulated on tumor ECs compared to normal ECs. It

was shown that depletion of integrin  $\beta 3$  transiently inhibited tumor growth and angiogenesis in mice (Brooks et al. 1994; Steri et al. 2014). Thus, the present thesis shows that high expression densities of endoglin, VE-cadherin and integrin  $\beta 3$  on freshly isolated ECs correlate with increased angiogenic capacity. Additionally, endoglin has been described as being capable of preventing apoptosis in hypoxic ECs and leading to an enhanced survival of ECs under hypoxic stress (Li et al. 2003). This may explain the fact that endoglin is expressed at higher levels on ECs isolated from tumors with hypoxic regions compared to ECs isolated from repair blastema (Sievert et al. 2014).

The expression density of the progenitor marker mucosialin in mouse embryonic blood vessels is high in pre-endothelial cells and in vessels formed by vasculogenesis and angiogenesis, but low in vessels which are involved in the process of coalescence to form larger vessels (Wood et al. 1997). In the early phase, mucosialin knockout mice with transplanted B16-F1 melanoma cells showed a decreased, and then later an increased tumor growth caused by a reduction of mucosialin knockout hematopoietic cells (Maltby et al. 2011). The fact that mucosialin is expressed at a higher level on tumor ECs could be due to circulating endothelial progenitor cells, which might be involved in the vasculogenesis of the tumor (Sievert et al. 2014).

EC adhesion molecules PECAM-1, ICAM-1 and ICAM-2 were increased in proliferating tissue (repair blastema and tumor), compared to non-proliferating tissues. Primary ECs isolated from PECAM-1 deficient mice showed a decreased cell migration and a reduced capillary morphogenesis (Park et al. 2010). Blocking of PECAM-1 inhibited the vascularization and growth of tumors in mice and inhibited the tube formation of ECs, *in vitro* (Zhou et al. 1999). However, PECAM-1 knockout mice developed a normal functional vascular system during embryonic development, but a decreased angiogenesis in inflammation (Solowiej et al. 2003). ICAM-1 is also up-regulated in various cell types by inflammatory cytokines and may increase leukocyte extravasation during inflammation (Hubbard and Rothlein 2000). ICAM-1 inhibition in mouse melanomas using ICAM-1 antisense oligonucleotides resulted in fewer metastases in the lungs (Miele et al. 1994). Antibodies against ICAM-1 also blocked the invasion of metastatic human breast cancer cells *in vitro* (Rosette et al. 2005). In contrast to ICAM-1, the expression of ICAM-2 is not elevated by inflammatory cytokines (Xu et al. 1996). Experiments in

ICAM-2-deficient mice have shown that ICAM-2 on ECs is required for angiogenesis and is involved in cell migration and survival, but not in EC proliferation (Huang et al. 2005). The present thesis demonstrates that the expression of ICAM-2 is increased on ECs from growing tumors and repair blastemas, whereas the expression of ICAM-1 is increased mainly in physiological wound healing (Sievert et al. 2014).

The higher expression of endoglin and mucosialin on ECs from the B16-F0 tumor correlates with the faster tumor growth compared to that of CT26 tumors. In contrast, the higher expression of ICAM-1 and ICAM-2 on ECs from CT26 may correlate with the higher metastatic behavior of CT26 compared to B16-F0 in lung, when cells were subcutaneously injected in syngeneic mice (Fidler 1975; Ikubo et al. 1999).

### **4.3 Alteration of morphology and migration of tumor endothelial cells**

In this thesis, it was shown that tumor ECs are larger, have a significantly higher migratory capacity and distribute in a more chaotic pattern in cell culture compared to ECs derived from normal tissue.

During angiogenesis or neovascularization, new blood vessels derived from existing vasculature. After basement membrane disruption, ECs proliferate and migrate towards an angiogenic stimulus which may be released from tumor cells or macrophages during inflammation, and finally reorganize into a three-dimensionally tubular structure (Figure 2). The rapid proliferation of tumor ECs and their persistent stimulation result in the formation of abnormal tumor vessels with increased vessel diameter and vessel length (Jain 2001; McDonald and Choyke 2003). Continual remodeling by persistent tumor growth and regression (cell apoptosis and necrosis) contribute to the instability of these networks (Jain 2003). The present thesis confirms the abnormal size of tumor ECs by microscopic pictures and FACS analysis. Not only ECs isolated from B16-F0 and CT26, but also ECs from the repair blastema were approximately twice the size of normal ECs isolated from heart and lung.

ECs migration involves three major mechanisms: chemotaxis, haptotaxis and mechanotaxis (Lamallice et al. 2007). Chemotaxis is the directional migration toward a gradient of soluble chemoattractants such as VEGF and bFGF. Haptotaxis is the directional migration towards a gradient of immobilized ligands in response to integrins. Mechanotaxis is the directional migration of ECs generated by mechanical forces based on fluid shear stress. ECs migration is the integrated result of these three mechanisms. The complex process of EC migration can be divided in several steps: sensing of the stimuli, extension and protrusion of lamellipodia, attachment of the protrusions to the extracellular matrix, contraction of the cell body to allow forward movement, rear release and recycling of adhesive and signaling components (Rousseau et al. 2000; Lamallice et al. 2007). The present thesis has analyzed the migration capacity of normal heart EC and abnormal tumor ECs in a non-proliferating state continuously for 33 hours *in vitro*. For both types of ECs, no cell divisions were detectable. Although the migration of heart ECs was significantly lower compared to that of tumor ECs, heart ECs were able to cover the area by migration to organize a complete monolayer. Tumor ECs have shown no increased covering of the area, despite their higher migration capacity. Obviously the abnormal behavior of tumor ECs is retained *in vitro*.

#### **4.4 Impairment of tube formation and flow alignment of tumor endothelial cells**

Primary ECs from non-proliferating and proliferating tissue differ in their functional properties *in vitro*. Tube formation assays showed that tumor ECs have a smaller number of branching points and loops compared to that of normal ECs. Further in contrast to normal tissue ECs, tumor-derived ECs show no tendency to align under flow conditions (Sievert et al. 2014).

Tube formation is the measurement method of the ability of ECs to form three-dimensional structures in matrigel *in vitro*. Matrigel is a solubilized tissue basement membrane matrix that was originally isolated from the Engelbreth-Holm-Swarm mouse sarcoma, composed mainly of laminin, collagen IV, heparan sulphate, proteoglycans, entactin and various growth factors such as TGF- $\beta$ , fibroblast growth factor and tissue plasminogen activator (Kleinman et al. 1986; Mullen

2004). In matrigel ECs do not make intercellular lumens or perform proliferation (Nakatsu and Hughes 2008). The number of cells plated onto matrigel and the time of the assay are critical steps and depends on the EC cell type (Arnaoutova et al. 2009). Too few cells results in incomplete cell connection, whereas too many cells results in large areas of monolayer. In both cases tube formation cannot be observed. The point of image capture should be determined for each EC type. Normally the cells attach within the first hour and migrate towards each other over the next 2-4 hours, followed by formation of capillary-like tubes, which mature within 6-16 hours. After 24 hours, cells typically undergo apoptosis and tubes detach from the matrix (Arnaoutova and Kleinman 2010). In the present thesis, primary ECs in the second passage were used. Cells in the first passage directly after isolation exhibit too many dead cells. Due to the larger size of tumor ECs compared to normal ECs, less tumor ECs (20,000 tumor ECs vs. 80,000 heart ECs per well) were seeded into the matrigel. These numbers represent the minimum number of ECs that are required to allow a tube formation within a defined area. Both types of ECs formed three-dimensional structures in matrigel. The reduced number of branching points and loops per image of tumor ECs compared to heart ECs might be the result of different amounts of seeded ECs on matrigel. On the other hand, the increased diameter or migration as well as the increased expression of surface markers could also be the reason for reduced number of branching points and loops. However, the potential to form tubes in matrigel remains intact for abnormal tumor ECs. Regardless of the results, the tube formation assay is not limited to test vascular behavior of ECs. Non-ECs, including fibroblast and tumor cells (glioblastoma cells, melanoma cells, prostata and breast carcinoma cells) also form three-dimensional structures in matrigel (Donovan et al. 2001; Francescone et al. 2011). This capability was consistent with their vasculogenic behavior of tumor cells identified in tissue samples, a process known as vasculogenic mimicry (Maniotis et al. 1999; Sharma et al. 2002; Francescone et al. 2012). Vasculogenic mimicry describes the formation of fluid-conducting channels by aggressive tumor cells. The formation of these channels does not arise from existing vessels (Folberg and Maniotis 2004).

Because of their unique location, ECs are to be exposed to pressure (created by the hydrostatic forces of blood), to stretch or tension (created by intercellular connections between ECs that exert forces on the cell during vasomotion) and to

shear stress (created by frictional forces of blood flow). Of these forces, shear stress appears to be a particularly important hemodynamic force because it stimulates the release of vasoactive substances and changes gene expression and cell metabolism (Davies 1995; Traub and Berk 1998). Steady laminar flow with high shear stress promotes the release of factors from ECs (NO, PGI<sub>2</sub>, tPA, thrombomodulin) that inhibit thrombosis, coagulation, migration of leukocytes and smooth muscle proliferation. High shear stress results in elongated and aligned morphology. The proliferation/DNA synthesis as well as the expression of adhesion molecules (ICAM-1, VCAM-1) are low. In contrast, disturbed flow with low or reciprocating shear stress changes the profile of secreted factors and expressed surface molecules (angiotensin II, endothelin-I, PDGF, increased expression of ICAM-1 and VCAM-1) in a situation that favors the opposite effect. Low shear stress results in polygonal morphology and high proliferation/DNA synthesis (Traub and Berk 1998; Reinhart-King et al. 2008; Chiu and Chien 2011). It is known that several tumors exhibit decreased blood flow (Stewart et al. 2006; Komar et al. 2009). In the present study, heart and tumor ECs were cultured under constant flow conditions, starting with 3.5 dyn/cm<sup>2</sup> for 1 day, followed with 7 dyn/cm<sup>2</sup> for four days. Whereas most heart ECs showed an alignment in the direction of the flow, tumor ECs did not align. This result is conform to the low flow rate in tumors and the increased expression of ICAM-1 and VCAM-1 on tumor ECs.

#### **4.5 Change of mRNA-expression of ECs under permanent high shear stress**

It is known that gene expression induced by shear stress is time dependent (Resnick et al. 2003). To exclude the detection of transient activated genes, heart ECs were cultured for 4 days with 20 dyn/cm<sup>2</sup>. This long-term shearing of cultured heart ECs led to the modulation of the expression of a multiplicity of novel and unknown genes. The results of the differential gene expression and subsequent pathway enrichment analysis provide 24 pathways with a FDR < 0.1, which are obviously affected by shear stress and can be assigned to different specific cell

components and functions: Extracellular organisation, cell membrane, signal molecules, hemostasis, metabolism, developmental biology and smooth muscle contraction (Table 18). The enriched cell component "extracellular organisation" includes the pathways "extracellular matrix organisation", "collagen formation", "assembly of collagen fibrils and other multimeric structures", "elastic fibre formation", "molecules associated with elastic fibres", "integrin cell surface interactions", "non-integrin membran-ECM interactions", "chondroitin sulfate/dermatan sulfate metabolism" and "laminin interactions". The impact of these pathways and candidates is supported by numerous links to ECs and angiogenesis. Collagen is the most abundant protein of the extracellular matrix and is involved in vascular elongation, stabilisation and proliferation (Bonanno et al. 2000; Di Lullo et al. 2002; Bahramsoltani et al. 2014). It was shown that aligned collagen fibrils regulate EC orientation and migration (Amyot et al. 2008; Lai et al. 2012). Elastic fibers are components of the extracellular matrix and confer resilience and flexibility (Midwood and Schwarzbauer 2002; Liu et al. 2004). Elastic fibre molecules are able to enhance EC attachment and stable monolayer formation (Williamson et al. 2007). The cell surface harbors integrin and non-integrin receptors. Integrins are membrane-associated glycoproteins with a large extracellular, a transmembrane and a short cytoplasmic domain (Evans and Calderwood 2007). The extracellular domain binds directly to extracellular matrix proteins, whereas the cytoplasmic domain interacts with cytoskeletal proteins, resulting in signal transduction, cytoskeletal organization and cell motility (Shyy and Chien 2002). Non-integrin transmembrane proteoglycans also interact with extracellular matrix proteins and influenced cell adhesion and movement (Rosso et al. 2004). It was shown that the chondroitin sulfate proteoglycan mediates EC migration on fibrinogen and invasion into a fibrin matrix (Henke et al. 1996). Laminins contribute to cell differentiation, cell shape and movement (Colognato and Yurchenco 2000).

The enriched cell component "cell membrane" is influenced by the pathway "cholesterol biosynthesis" and represents an interesting link to blood vessels. ECs maintain cholesterol homeostasis by down-regulation of cholesterol synthesis and low density lipoprotein receptors to avoid atherosclerotic plaques (Hassan et al. 2006).

The impact of "signal molecules" is reflected by the affected pathways "signaling by Rho GTPase", "axon guidance", "signaling by VEGF", "NRAGE signals death through JNK", "Nitric oxide stimulates guanylate cyclase", "Netrin-1 signaling" and "semaphorin interactions". The relevance of these pathways is reported by numerous links to ECs and their functions. Members of the Rho family GTPases are important regulators of the cytoskeleton and cell motility and polarity (Raftopoulou and Hall 2004; Villalonga and Ridley 2006; Hanna and El-Sibai 2013). So-called endothelial tip cells, which lead the sprouting and migration of ECs during angiogenesis, share many features with the axonal growth cone (Siemerink et al. 2013). Capillary tip cells and axon growth cones use common signals to regulate their guidance (Adams and Eichmann 2010). The guidance molecule netrin-1 appears to act as an angiogenic and survival factor for ECs (Castets et al. 2009; Tu et al. 2015). The guidance molecule semaphorins affects adhesion, cytoskeletal remodeling, cell motility and cell migration (Serini et al. 2008; Gelfand et al. 2009; Sakurai et al. 2012). VEGFs and their receptors (VEGFRs) play an important role in angiogenesis by regulating proliferation and migration of ECs (Bernatchez et al. 1999; Holmes et al. 2007; Wang et al. 2008b). The NRAGE, a p75 neurotrophin receptor, mediates signaling processes leading to activation of the JNK pathway and cell death in a variety of cell types (Salehi et al. 2002). NO-sensitive guanylate cyclase is an important receptor for the signal molecule NO results in the conversion of GTP to cGMP, which activates cGMP-dependent protein kinases, cGMP-regulated phosphodiesterases and cGMP-gated ion channels (Friebe and Koesling 2003). It was shown that NGF induced a significant increase in proliferation and migration of human ECs (Raychaudhuri et al. 2001; Cantarella et al. 2002; Dolle et al. 2005).

The cellular process of "hemostasis" includes the pathways "hemostasis", "platelet activation, signaling and aggregation" and "platelet homeostasis". The importance of these pathways for the endothelium has already been described. ECs play a key role in the regulation of the hemostasis balance and platelets aggregation at sites of blood vessel damage (Chen and Lopez 2005; Verhamme and Hoylaerts 2006).

The pathways "metabolism", "developmental biology" and "smooth muscle contraction" present specific additional categories and show important links to ECs. Metabolism of ECs such as glycolysis is different not only between quiescent

and angiogenic states but also between static and flow conditions (De Bock et al. 2013; Sun and Feinberg 2015). The development of ECs is being performed by stem cells and endothelial progenitor cells respectively (Balconi et al. 2000; Yamamoto et al. 2003). It was shown, that shear stress promotes differentiation of endothelial progenitor cells into mature ECs (Obi et al. 2009). Interestingly, the present study shows that shear stress not only influences the effect of endothelial progenitor cells but also of mature ECs. The vascular endothelium modulates the reactivity of vascular smooth muscle via metabolic degrades of vasoactive substances, conversions of precursors into vasoactive products and secretions of vasoactive substances (Vanhoutte et al. 1986). Thus, the present study shows, that high shear stress (20 dyn/cm<sup>2</sup>) for 4 days significantly affected the EC gene expression related to a variety of endothelial pathways.

Gene expression of *Pecam1*, *Icam1* and *Icam2* was higher on heart ECs under static conditions compared to flow conditions. This finding is consistent with the higher protein-expression on tumor ECs and confirms the hypothesis that these inflammation markers are involved in ECs dysfunction. For a functional characterization of cellular signaling and interactions, five gene-probes with an activating and five gene-probes with an inactivating expression with the measured expression of *Pecam1*, *Vcam1*, *Icam1* and *Icam2* were considered. Only genes which fulfill the level of significance for both, functional correlation and differential expression between static and flow conditions, were considered here in more detail. All gene-probes correlated with *Pecam1* and *Vcam1* expression didn't fulfill the significance for differential expression between static and flow conditions. In contrast, *Icam1* was significantly correlated with all activated gene-probes *Syt17*, *Ankrd13b*, *Fgf2*, *Basp1*, *Plxna4* and with all inactivated gene-probes *Grcc10*, *Psmb9*, *Nus1*, *Ssh3* and *Bace2*. Also, *Icam2* could be correlated with all activated gene-probes *Cda*, *Nos3*, *Galnt18*, *Sh2b3*, *Tmem44* and with two inactivated gene-probes *Rffl* and *Zswim4*.

The functions of genes correlating with *Icam1* expression range from membrane-trafficking, proliferation, migration, morphogenesis, cytoskeletal reorganization and proteolysis. *Syt17* is a member of the Synaptotagmin family responsible for membrane trafficking. Synaptotagmin contributes to endocytosis and exocytosis of synaptic vesicles (Schwarz 2004). Ankyrin repeat domain 13 (*Ankrd13*) regulates the internalization of ligand-activated EGFR in HeLa cells (Tanno et al. 2012).

Fibroblast growth factor 2 (*Fgf2*) regulates placental EC proliferation and signaling in ovine artery ECs (Wang et al. 2008a). *Basp1* promotes actin dynamics including loss of stress fibers in transfected fibroblast (Wiederkehr et al. 1997). Plexin-A4 (*Plxna4*) regulates the migration of sympathetic neurons (Waimey et al. 2008). Protein C10 (*Grcc10*) regulates ubiquitin-dependent proteolysis in keratocytes (Lee et al. 2009). The proteasome subunit beta type 9 (*Psmb9*) is a component of the ubiquitin-proteasome system and may play a role in maintaining normal cardiac function through regulation of signaling pathways and maintenance of normal sarcomere structure (Powell 2006; Nakamura et al. 2015). For HUVECs it was shown, that *Nus1/Nogo-B* receptor is essential for chemotaxis and morphogenesis (Miao et al. 2006). Slingshot homolog 3 (*Ssh3*) plays a critical role in regulating actin cytoskeletal reorganization (Ohta et al. 2003). Beta-site amyloid precursor protein cleaving enzyme 2 (*Bace2*) is a transmembrane aspartic protease (Bennett et al. 2000). Thus, the present study shows that these genes, although not always described for ECs, have a functional correlation with *Icam1* and are significantly involved in high shear stress response of heart ECs. This has an effect not only for the EC membrane (trafficking and morphogenesis) and cytoplasm (cytoskeletal reorganization and proteolysis), but also for EC functions (proliferation and migration).

The functions of genes correlating with *Icam2* expression range from cell adhesion, sensory property, atheroprotective effect, pyrimidine metabolism, protein glycosylation, proteolysis and regulation of transcription. Cytidine deaminase (*Cda*) is an enzyme involved in pyrimidine metabolism (Demontis et al. 1998). It is known that shear stress increases the transcription of endothelial nitric oxide synthase (*Nos3*) and results in atheroprotective effects (Davis et al. 2004; Fish and Marsden 2006). Polypeptide N-acetylgalactosaminyltransferase 18 (*Galnt18*) transfers N-acetyl-D-galactosamine to a serin or threonine residue on the polypeptide acceptor (Cheng et al. 2004). Sh2b adapter protein 3 (*Sh2b3*) is a regulator of integrin signaling that affects adhesion and migration of ECs (Devalliere et al. 2012). *Tmem44* might be involved in sensory receptor (Moyer et al. 2009). E3 ubiquitin-protein ligase rififylin (*Rffl*) is involved in endocytic recycling and proteolysis (Ciechanover et al. 2000; Coumailleau et al. 2004). The zinc finger swim domain-containing protein 4 (*Zswim4*) acts as regulator of transcription (Makarova et al. 2002). Overall, the present study shows that these genes,

although not always described for ECs, have a functional correlation with *Icam2* and are also involved in high shear stress response of heart ECs. This has an effect for the EC membrane (adhesion, migration and sensor), cytoplasm (protein glycosylation and proteolysis), pyrimidine metabolism and transcription.

## **4.6 Early and late radiation effects on heart endothelial cells**

The aim of this experiment was to quantify the expression and to study the time-dependent alteration of proliferation and inflammation markers on ECs isolated from heart and lung after a single *in vivo* irradiation. Radiation-induced changes on the microvasculature and the development of atherosclerotic plaques in microvessels should be investigated. Heart and lung influence each other depending on the percentage and dose of cardiac and pulmonary irradiation. Heart irradiation reduces the tolerated dose of the lung and vice versa (Ghobadi et al. 2012). This results in a significant increase in the breathing rate and a right ventricle hypertrophy. However, these documented effects do only occur at doses above 10 Gy for thorax irradiation (100 % heart and 100 % lung), and at doses above 20 Gy for local heart irradiation (100 % heart and approximately 25 % lung) (van Luijk et al. 2005; van Luijk et al. 2007; Gabriels et al. 2012). In the present thesis, the highest dose to the thorax was 8 Gy and to the heart 16 Gy. Therefore, the reciprocal influence of irradiation between heart and lung may presumably play only a minor role.

The thesis shows that irradiation of the thorax of a mouse influences the expression of endothelial surface markers which were grouped in proliferation, progenitor cells development and inflammation in a dose- and time-dependent manner. While the expression density of most EC surface markers did not significantly change after irradiation with 2 Gy (except for VE-cadherin and PECAM-1 after 10 weeks for heart ECs and for ICAM-1 after 15 and 20 weeks for lung ECs), the majority of EC surface markers which are related to proliferation and inflammation showed significant changes after 8 Gy.

New blood vessels can be developed by angiogenesis, arteriogenesis or vasculogenesis. During angiogenesis, new blood vessels are formed from

preexisting ECs which are stimulated by growth factors or hypoxia. In contrast, arteriogenesis describes the proliferation of collateral arteries from preexisting ECs which are stimulated by shear stress even in the absence of hypoxia. During vasculogenesis, new blood vessels develop from endothelial progenitor cells that differentiate into mature ECs.

The transient increase in the expression density of proliferation markers (HCAM, endoglin and VE-cadherin for heart ECs, HCAM, integrin  $\beta$ 3, endoglin and VEGFR-2 for lung ECs) suggested a stimulated proliferation of ECs in response to radiation-induced damage at earlier time points. This process occurred earlier in lung ECs than in heart ECs. These markers are normally highly expressed in proliferating ECs. The drop of these markers to normal levels after about 15 weeks reveals that radiation-induced angiogenesis is a transient response in heart and lung tissues. The increased expression density of proliferation markers correlates with an increased microvascular density 20 weeks after 8 Gy irradiation in the same animals (Seemann et al. 2012). While the formation of new blood vessels via angiogenesis is presumably finalized about 15 weeks after irradiation with 8 Gy in the heart and lung endothelium, the enhanced proportion of lung ECs that stained positively for prominin-1 20 weeks after 8 Gy and the increased expression density of mucosialin 15–20 weeks after 8 Gy irradiation suggest that a continuous formation of new blood vessels via vasculogenesis is occurring in the lung of mice. New vessel formation via vasculogenesis appears to be not relevant for heart ECs at the indicated doses and time points. Moreover, the proportion of heart ECs that stained positively for prominin-1 was decreased at 15 and 20 weeks after 8 Gy. Interestingly, it has been reported that the level of microvascular density was reduced 40 weeks after heart irradiation with 16 Gy and 60 weeks after heart irradiation with 8 Gy (Seemann et al. 2012; Patties et al. 2015). The decreased level of prominin-1 for heart ECs might confirm the observed reduced proliferation and progressive loss of microvessels (Sievert et al. 2015).

Specific adhesion molecules regulate different stages of leukocyte infiltration in inflammatory sites (Quarmby et al. 1999). Several *in vivo* studies have shown increased expression levels of inflammation markers after irradiation in Arteria saphena (Patties et al. 2014) or in the intestine (Molla et al. 2003). However, studies which analyse the alteration of inflammation markers on isolated microvascular ECs after heart or lung irradiation are missing. While the expression

density of most inflammation markers on ECs was not affected by irradiation at 2 Gy (except for PECAM-1 after 10 weeks for heart ECs and for ICAM-1 after 15 and 20 weeks for lung ECs), all inflammation markers were up-regulated by high dose irradiation at 8 Gy. Heart ECs showed a transient increase in the expression density of PECAM-1 and ICAM-2 and a persistent increase of ICAM-1 and VCAM-1 starting from 10 weeks after 8 Gy. Lung ECs demonstrated a persistently increased density of PECAM-1, ICAM-1, ICAM-2 and VCAM-1 up to 20 weeks after irradiation with 8 Gy. The expression density of ICAM-1 and VCAM-1 was increased in both heart and lung ECs at 10, 15 and 20 weeks after 8 Gy. In contrast to ICAM-1, which is ubiquitously expressed on all ECs, VCAM-1 expression is low on heart (30 %) and lung (15 %) ECs. The proportion of heart and lung ECs that stained positively for VCAM-1 was increased 10, 15 and 20 weeks after thorax irradiation with 8 Gy (Sievert et al. 2015).

In conclusion, irradiation of the thorax leads to the up-regulation of markers that may suggest a temporary proliferating and prolonged inflammatory response of heart and lung ECs. The temporary increase in proliferation is more pronounced in lung ECs compared to heart ECs. Further, the involvement of endothelial progenitor cells after irradiation might play a role in lung but not in heart ECs. Both effects confirm the late loss of microvessels in irradiated hearts. These results are shown as hypothetical model in Figure 37. The persistent increase of inflammation markers ICAM-1 and VCAM-1 up to 20 weeks after irradiation may suggest the predisposition for the development of atherosclerotic plaques in lung and heart ECs at later time points. These inflammatory markers may provide possible targets for therapeutic intervention for patients undergoing thoracic irradiation therapy (Sievert et al. 2015).

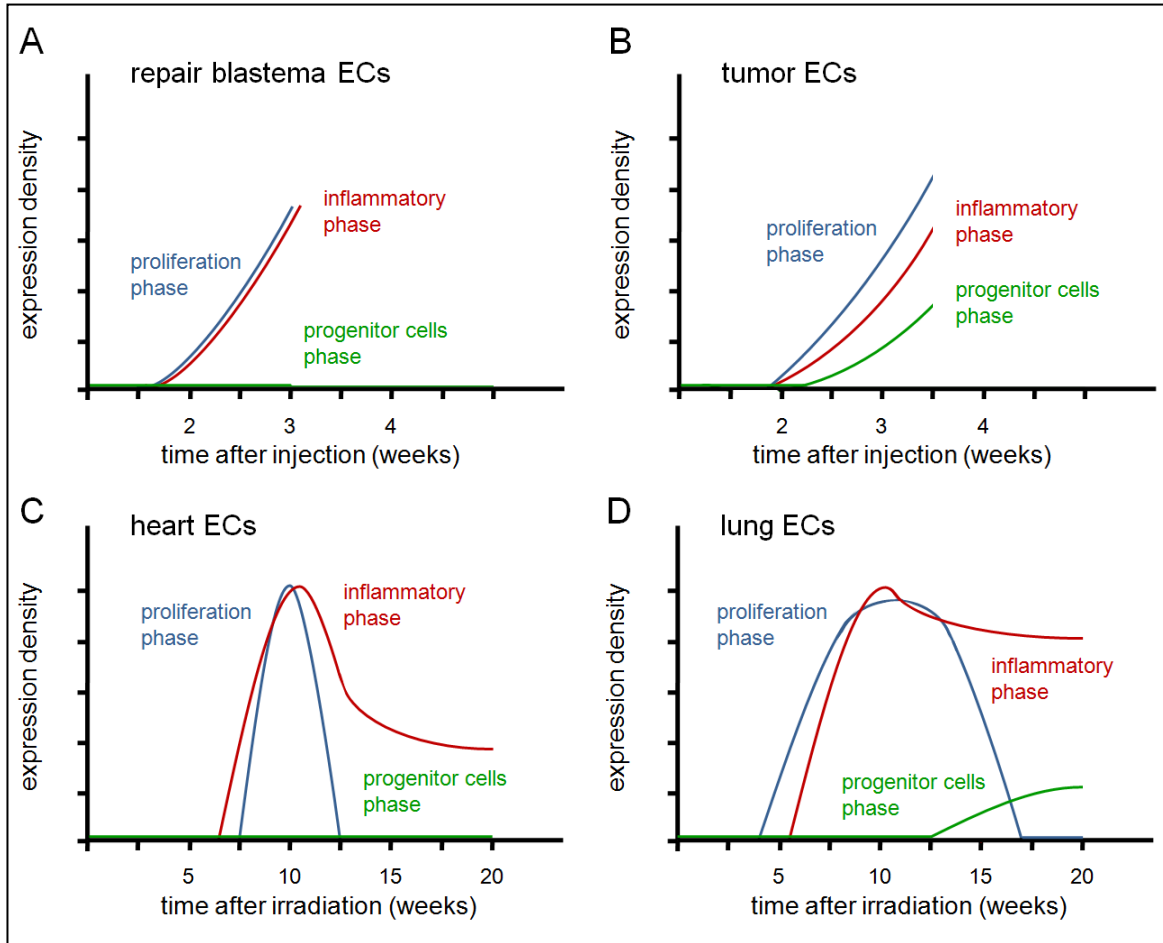


**Figure 37:** Hypothetical model of proliferation-, inflammatory- and progenitor cells- phases of ECs from different tissue. **(A, B)** Proliferation and inflammation surface markers were increased in proliferating tissue like repair blastema and tumor, compared to non-proliferating tissue. Progenitor cells may have an impact in tumors, but not in repair blastemas. **(C, D)** Local thorax irradiation with 8 Gy increased temporary the proliferation of heart and lung ECs. This process was more pronounced in lung ECs (5-15 weeks) than in heart ECs (10 weeks). Inflammation was increased in heart and lung ECs starting between 5 and 10 weeks after irradiation. This process was more pronounced in lung ECs than in heart ECs up to 20 weeks. The involvement of progenitor cells after irradiation might play a role in lung but not in heart ECs.

## 4.7 PERSPECTIVE

The novel method presented here provides a powerful tool for the purification of viable primary microvascular ECs of different origins which can be used to analyze organ-specific immunological interactions and functional changes in the interplay of existing and evolving ECs from benign and malignant tissues. The clear identification of ECs from each individual tissue due to the expression of six different EC surface markers such as PECAM-1, endoglin, VE-cadherin, mucosialin, ICAM-1 and ICAM-2 provides the basis for further research. The

analysis of surface markers on primary tumor ECs could therefore contribute to understand the effects of anti-angiogenic therapies. ICAM-1 and VCAM-1 should be tested to establish both markers as possible targets for therapeutic intervention for patients undergoing thoracic irradiation therapy.

#### **4.7.1 Effects of anti-angiogenic therapy**

The increase of different markers on tumor ECs might have an impact on the proliferation rate of ECs, the permeability for metastasis or the involvement of circulating endothelial progenitor cells. A successful approach for therapeutic treatment would be a marker, which is generally highly expressed on proliferating tumor ECs, but not on normal non-proliferating ECs. Such a molecule would be an optimal vascular target that can be used not only for tumor imaging and prognosis, but also as therapeutic drug in human tumors. The use of angiogenesis inhibitors, most of them targeting the VEGF pro-angiogenic signaling pathway, is already evaluated in different clinical studies for different disease stages (metastatic, adjuvant, neoadjuvant) (Sessa et al. 2008; Vasudev and Reynolds 2014). The pioneers of the clinical proof-of-concept for angiogenesis inhibitors are bevacizumab, a humanised monoclonal antibody that binds specifically to VEGF-A, and two tyrosine kinase inhibitors: sorafenib and sunitinib which block the activity of VEGFR1, VEGFR2 and VEGFR3. However, anti-angiogenic therapies result in transitory improvements, in the form of tumor stasis or shrinkage and in some cases increased survival. Inevitably, the tumor begins to re-grow. The improvement in progression-free survival and in overall survival is only a few months (Carmeliet and Jain 2011; Vasudev and Reynolds 2014). Moreover, several studies have shown that VEGF blockade damages healthy vessels and results in severe problems such as hemorrhagic and thrombotic events (Kubota 2012). Two general modes of resistance to angiogenesis inhibitors, in particularly those targeting the VEGF pathways, are in discussion: The evasive resistance and the intrinsic pre-existing non-responsiveness. The evasive resistance is the adaption to evade the specific angiogenic blockade. Although the specific target of the anti-angiogenic drug remains inhibited, alternative ways are activated to sustain tumor growth (Bergers and Hanahan 2008; Loges et al. 2010). The

activation or upregulation of alternative pro-angiogenic signaling pathways within the tumor is enhanced after treatment with agents targeting VEGF. The recruitment of bone marrow-derived pro-angiogenic cells confers resistance. Myeloid cells, including tumor-associated macrophages, infiltrate tumors and mediate resistance. Tumor-associated fibroblasts are activated to support tumor growth and angiogenesis. Increased pericytes coverage of tumor vasculature also enhances resistance. A further way is the activation and enhancement of invasion and metastasis to provide access to normal tissue vasculature without neovascularization. In contrast, patients with intrinsic pre-existing non-responsiveness are refractory to anti-angiogenic therapy and the disease progression continues unabated. The pre-existing multiplicity of redundant pro-angiogenic signals, the pre-existing inflammatory cell-mediated vascular protection and the hypovascularity lead to the indifference of tumors for angiogenesis inhibitors (Bergers and Hanahan 2008). A successful anti-angiogenic therapy will require a greater understanding of how tumors become vascularized and how they evade the effects of anti-angiogenic therapies. It will be important to identify the circumstances that elicit resistance, alone and in the context of standard chemotherapy and radiotherapy. The analysis of surface markers on primary tumor ECs due to the new established method could contribute to understand the effects of anti-angiogenic therapies.

### **4.7.2 Effects of radiation therapy**

The persistent increase of inflammation markers ICAM-1 and VCAM-1 up to 20 weeks after thorax irradiation with 8 Gy and the increased expression of ICAM-1 16 weeks after local heart irradiation with 8 Gy and 16 Gy may suggest the predisposition for the development of atherosclerotic plaques in lung and heart ECs of wild type mice (C57BL/6). To confirm this hypothesis, the analysis of ECs 30 and 40 weeks after local heart irradiation with 8 and 16 Gy would be useful. It is known that local heart irradiation with 16 Gy leads to sudden death between 30 and 40 weeks in 38 % of mice (Seemann et al. 2012). The reason for this was presumably the presence of amyloidosis in the hearts after irradiation with 16 Gy leading to heart failure (McCarthy and Kasper 1998). The prolonged involvement

of ICAM-1 and VCAM-1 on irradiated heart ECs would explain the late development of atherosclerotic plaques in hearts which could result in myocardial infarction. If this is the case, ICAM-1 and VCAM-1 may provide possible targets for therapeutic intervention in the future for patients undergoing thoracic irradiation therapy.

This study demonstrates that high shear stress presents an important stimulus that has a profound impact on the gene expression of ECs. In order to analyze the relevance of changes of gene expression, microarray gene expression dataset has to be extended by including characterisation of isolated heart ECs 20 weeks after 8 Gy *in vivo* irradiation.

In contrast to C57BL/6 mice, which have low plasma levels of cholesterol, Apolipoprotein E-deficient (ApoE<sup>-/-</sup>) mice have increased cholesterol levels and develop age-related atherosclerosis. Therefore, ApoE<sup>-/-</sup> mice are presumably more suitable for the analysis of irradiated heart ECs and the involvement of ICAM-1 and VCAM-1 to atherosclerotic plaques.

Previously results about the effects of local heart irradiation in a mouse model with X-ray were performed with the help of a shielding plate such as lead. The irradiation field consists of a window in the lead plate. The rest of the mouse body was shielded with the lead plate. With this setting, approximately 30-40 % of the lung volume was included in the irradiation field. Recently, a small animal radiation research platform (SARRP, X-Strahl) is available which enables a high precision CT image-guided irradiation of organs and tumors in mice in mm-range following treatment planning. Thereby heart irradiation effects based on co-irradiation of the lung can be reduced. By using this instrument the irradiation of parts from heart and lung is possible in order to study effects of a partial normal tissue irradiation.

## 5. ACKNOWLEDGEMENTS

At that point I want to say thank you to everybody who has contributed to the success of this study. Special thanks go to Prof. Gaby Multhoff and Prof. Horst Zitzelsberger, for funding and support in design of experiments and preparation of manuscripts. The work in laboratories of two leaders in two institutions was a great experience and complemented my spectrum of methods. The sustained discussions helped me to focus my topic and create new motivation. The trust placed in me and the provided freedom have greatly contributed to my scientific work. Many thanks also go to Prof. Klaus-Rüdiger Trott for great support in design of experiments and helpful tips in preparing of manuscripts. Many thanks to Dr. Soile Tapio and Omid Azimzadeh for the successful collaboration and the time spent together in meetings of the Cardiorisk project. Further I would like to thank all previous and present members of both workgroups for the pleasant working atmosphere and inspiring conversations. Thanks to Stephanie Breuninger, Janina Schwarzer and Jessica Pelzel for the practical help in the laboratory in each distress situation. Further thanks to Elke Konhäuser for the instruction in the FISH analysis. Big thanks goes to Kristian Unger, Aaron Selmeier and Laura Dajka for handling of huge RNA data sets and helping in RNA array procedure. Special thanks are due to Stefan Stangl for working together especially at mice experiments. Many thanks to Prof. Jan Wilkens and Severin Kampf for helping in dosimetry and irradiation planning. Big thanks goes to Maximilian Dobrunz for his help to solve computer problems. In addition, I would like to thank the animal keepers and veterinarians for their care of mice and their expertise for animal experiment applications. Further a lot of thanks to Jan Leichsenring and Christine Bayer for proofreading. Finally, I would thank all my friends and most important my family. Many thanks for support and pleasant diversion the whole time! The most loving support I received from my beloved Lisa. The shared time during my dissertation was a fascinating experience and very essential for me. Thank you Lisa!

## 6. REFERENCES

- AbouAlaiwi WA, Takahashi M, Mell BR, Jones TJ, Ratnam S, Kolb RJ, Nauli SM. 2009. Ciliary polycystin-2 is a mechanosensitive calcium channel involved in nitric oxide signaling cascades. *Circulation research* **104**: 860-869.
- Adams RH, Eichmann A. 2010. Axon guidance molecules in vascular patterning. *Cold Spring Harbor perspectives in biology* **2**: a001875.
- Aird WC. 2007. Phenotypic heterogeneity of the endothelium: I. Structure, function, and mechanisms. *Circulation research* **100**: 158-173.
- Alberelli MA, De Candia E. 2014. Functional role of protease activated receptors in vascular biology. *Vascular pharmacology* **62**: 72-81.
- Allport JR, Weissleder R. 2003. Murine Lewis lung carcinoma-derived endothelium expresses markers of endothelial activation and requires tumor-specific extracellular matrix in vitro. *Neoplasia* **5**: 205-217.
- Alphonsus CS, Rodseth RN. 2014. The endothelial glycocalyx: a review of the vascular barrier. *Anaesthesia* **69**: 777-784.
- Amyot F, Small A, Boukari H, Sackett D, Elliott J, McDaniel D, Plant A, Gandjbakhche A. 2008. Thin films of oriented collagen fibrils for cell motility studies. *Journal of biomedical materials research Part B, Applied biomaterials* **86**: 438-443.
- Anderson RG. 1993. Caveolae: where incoming and outgoing messengers meet. *Proceedings of the National Academy of Sciences of the United States of America* **90**: 10909-10913.
- Ando J, Yamamoto K. 2013. Flow detection and calcium signalling in vascular endothelial cells. *Cardiovascular research* **99**: 260-268.
- Andratschke N, Maurer J, Molls M, Trott KR. 2011. Late radiation-induced heart disease after radiotherapy. Clinical importance, radiobiological mechanisms and strategies of prevention. *Radiotherapy and oncology : journal of the European Society for Therapeutic Radiology and Oncology* **100**: 160-166.
- Armulik A, Genove G, Betsholtz C. 2011. Pericytes: developmental, physiological, and pathological perspectives, problems, and promises. *Developmental cell* **21**: 193-215.
- Arnaoutova I, George J, Kleinman HK, Benton G. 2009. The endothelial cell tube formation assay on basement membrane turns 20: state of the science and the art. *Angiogenesis* **12**: 267-274.
- Arnaoutova I, Kleinman HK. 2010. In vitro angiogenesis: endothelial cell tube formation on gelled basement membrane extract. *Nature protocols* **5**: 628-635.
- Arthur HM, Ure J, Smith AJ, Renforth G, Wilson DI, Torsney E, Charlton R, Parums DV, Jowett T, Marchuk DA et al. 2000. Endoglin, an ancillary TGFbeta receptor, is required for extraembryonic angiogenesis and plays a key role in heart development. *Developmental biology* **217**: 42-53.

## References

---

- Azimzadeh O, Sievert W, Sarioglu H, Merl-Pham J, Yentrapalli R, Bakshi MV, Janik D, Ueffing M, Atkinson MJ, Multhoff G et al. 2015. Integrative proteomics and targeted transcriptomics analyses in cardiac endothelial cells unravel mechanisms of long-term radiation-induced vascular dysfunction. *Journal of proteome research* **14**: 1203-1219.
- Azimzadeh O, Sievert W, Sarioglu H, Yentrapalli R, Barjaktarovic Z, Sriharshan A, Ueffing M, Janik D, Aichler M, Atkinson MJ et al. 2013. PPAR alpha: a novel radiation target in locally exposed Mus musculus heart revealed by quantitative proteomics. *Journal of proteome research* **12**: 2700-2714.
- Bahramsoltani M, Slosarek I, De Spiegelaere W, Plendl J. 2014. Angiogenesis and collagen type IV expression in different endothelial cell culture systems. *Anatomia, histologia, embryologia* **43**: 103-115.
- Balconi G, Spagnuolo R, Dejana E. 2000. Development of endothelial cell lines from embryonic stem cells: A tool for studying genetically manipulated endothelial cells in vitro. *Arteriosclerosis, thrombosis, and vascular biology* **20**: 1443-1451.
- Barakat AI, Leaver EV, Pappone PA, Davies PF. 1999. A flow-activated chloride-selective membrane current in vascular endothelial cells. *Circulation research* **85**: 820-828.
- Belloni PN, Tressler RJ. 1990. Microvascular endothelial cell heterogeneity: interactions with leukocytes and tumor cells. *Cancer metastasis reviews* **8**: 353-389.
- Bennett BD, Babu-Khan S, Loeloff R, Louis JC, Curran E, Citron M, Vassar R. 2000. Expression analysis of BACE2 in brain and peripheral tissues. *The Journal of biological chemistry* **275**: 20647-20651.
- Bergers G, Benjamin LE. 2003. Tumorigenesis and the angiogenic switch. *Nature reviews Cancer* **3**: 401-410.
- Bergers G, Hanahan D. 2008. Modes of resistance to anti-angiogenic therapy. *Nature reviews Cancer* **8**: 592-603.
- Bernatchez PN, Soker S, Sirois MG. 1999. Vascular endothelial growth factor effect on endothelial cell proliferation, migration, and platelet-activating factor synthesis is Flk-1-dependent. *The Journal of biological chemistry* **274**: 31047-31054.
- Bolender RP. 1974. Stereological analysis of the guinea pig pancreas. I. Analytical model and quantitative description of nonstimulated pancreatic exocrine cells. *The Journal of cell biology* **61**: 269-287.
- Bonanno E, Iurlaro M, Madri JA, Nicosia RF. 2000. Type IV collagen modulates angiogenesis and neovessel survival in the rat aorta model. *In vitro cellular & developmental biology Animal* **36**: 336-340.
- Brattain MG, Strobel-Stevens J, Fine D, Webb M, Sarrif AM. 1980. Establishment of mouse colonic carcinoma cell lines with different metastatic properties. *Cancer research* **40**: 2142-2146.
- Brooks PC, Clark RA, Cheresh DA. 1994. Requirement of vascular integrin alpha v beta 3 for angiogenesis. *Science* **264**: 569-571.

## References

---

- Bulla R, Villa A, Bossi F, Cassetti A, Radillo O, Spessotto P, De Seta F, Guaschino S, Tedesco F. 2005. VE-cadherin is a critical molecule for trophoblast-endothelial cell interaction in decidual spiral arteries. *Experimental cell research* **303**: 101-113.
- Burrows FJ, Derbyshire EJ, Tazzari PL, Amlot P, Gazdar AF, King SW, Letarte M, Vitetta ES, Thorpe PE. 1995. Up-regulation of endoglin on vascular endothelial cells in human solid tumors: implications for diagnosis and therapy. *Clinical cancer research : an official journal of the American Association for Cancer Research* **1**: 1623-1634.
- Buschmann I, Schaper W. 1999. Arteriogenesis Versus Angiogenesis: Two Mechanisms of Vessel Growth. *News in physiological sciences : an international journal of physiology produced jointly by the International Union of Physiological Sciences and the American Physiological Society* **14**: 121-125.
- Bussolati B, Deambrosis I, Russo S, Deregibus MC, Camussi G. 2003. Altered angiogenesis and survival in human tumor-derived endothelial cells. *FASEB journal : official publication of the Federation of American Societies for Experimental Biology* **17**: 1159-1161.
- Butler PJ, Norwich G, Weinbaum S, Chien S. 2001. Shear stress induces a time- and position-dependent increase in endothelial cell membrane fluidity. *American journal of physiology Cell physiology* **280**: C962-969.
- Cantarella G, Lempereur L, Presta M, Ribatti D, Lombardo G, Lazarovici P, Zappala G, Pafumi C, Bernardini R. 2002. Nerve growth factor-endothelial cell interaction leads to angiogenesis in vitro and in vivo. *FASEB journal : official publication of the Federation of American Societies for Experimental Biology* **16**: 1307-1309.
- Carmeliet P, Jain RK. 2011. Molecular mechanisms and clinical applications of angiogenesis. *Nature* **473**: 298-307.
- Carmeliet P, Lampugnani MG, Moons L, Breviario F, Compernelle V, Bono F, Balconi G, Spagnuolo R, Oosthuysen B, Dewerchin M et al. 1999. Targeted deficiency or cytosolic truncation of the VE-cadherin gene in mice impairs VEGF-mediated endothelial survival and angiogenesis. *Cell* **98**: 147-157.
- Castets M, Coissieux MM, Delloye-Bourgeois C, Bernard L, Delcros JG, Bernet A, Laudet V, Mehlen P. 2009. Inhibition of endothelial cell apoptosis by netrin-1 during angiogenesis. *Developmental cell* **16**: 614-620.
- Cha ST, Talavera D, Demir E, Nath AK, Sierra-Honigmann MR. 2005. A method of isolation and culture of microvascular endothelial cells from mouse skin. *Microvascular research* **70**: 198-204.
- Chen BP, Li YS, Zhao Y, Chen KD, Li S, Lao J, Yuan S, Shyy JY, Chien S. 2001. DNA microarray analysis of gene expression in endothelial cells in response to 24-h shear stress. *Physiological genomics* **7**: 55-63.
- Chen J, Lopez JA. 2005. Interactions of platelets with subendothelium and endothelium. *Microcirculation* **12**: 235-246.
- Cheng L, Tachibana K, Iwasaki H, Kameyama A, Zhang Y, Kubota T, Hiruma T, Tachibana K, Kudo T, Guo JM et al. 2004. Characterization of a novel human UDP-GalNAc transferase, pp-GalNAc-T15. *FEBS letters* **566**: 17-24.

## References

---

- Chiu JJ, Chien S. 2011. Effects of disturbed flow on vascular endothelium: pathophysiological basis and clinical perspectives. *Physiological reviews* **91**: 327-387.
- Chung-Welch N, Patton WF, Yen-Patton GP, Hechtman HB, Shepro D. 1989. Phenotypic comparison between mesothelial and microvascular endothelial cell lineages using conventional endothelial cell markers, cytoskeletal protein markers and in vitro assays of angiogenic potential. *Differentiation; research in biological diversity* **42**: 44-53.
- Ciechanover A, Orian A, Schwartz AL. 2000. Ubiquitin-mediated proteolysis: biological regulation via destruction. *BioEssays : news and reviews in molecular, cellular and developmental biology* **22**: 442-451.
- Colognato H, Yurchenco PD. 2000. Form and function: the laminin family of heterotrimers. *Developmental dynamics : an official publication of the American Association of Anatomists* **218**: 213-234.
- Corada M, Zanetta L, Orsenigo F, Breviario F, Lampugnani MG, Bernasconi S, Liao F, Hicklin DJ, Bohlen P, Dejana E. 2002. A monoclonal antibody to vascular endothelial-cadherin inhibits tumor angiogenesis without side effects on endothelial permeability. *Blood* **100**: 905-911.
- Coumailleau F, Das V, Alcover A, Raposo G, Vandormael-Pournin S, Le Bras S, Baldacci P, Dautry-Varsat A, Babinet C, Cohen-Tannoudji M. 2004. Over-expression of Rifylin, a new RING finger and FYVE-like domain-containing protein, inhibits recycling from the endocytic recycling compartment. *Molecular biology of the cell* **15**: 4444-4456.
- Creutz CE, Tomsig JL, Snyder SL, Gautier MC, Skouri F, Beisson J, Cohen J. 1998. The copines, a novel class of C2 domain-containing, calcium-dependent, phospholipid-binding proteins conserved from Paramecium to humans. *The Journal of biological chemistry* **273**: 1393-1402.
- Crosby CV, Fleming PA, Argraves WS, Corada M, Zanetta L, Dejana E, Drake CJ. 2005. VE-cadherin is not required for the formation of nascent blood vessels but acts to prevent their disassembly. *Blood* **105**: 2771-2776.
- Cunningham KS, Gotlieb AI. 2005. The role of shear stress in the pathogenesis of atherosclerosis. *Laboratory investigation; a journal of technical methods and pathology* **85**: 9-23.
- Dallas NA, Samuel S, Xia L, Fan F, Gray MJ, Lim SJ, Ellis LM. 2008. Endoglin (CD105): a marker of tumor vasculature and potential target for therapy. *Clinical cancer research : an official journal of the American Association for Cancer Research* **14**: 1931-1937.
- Darby SC, Cutter DJ, Boerma M, Constine LS, Fajardo LF, Kodama K, Mabuchi K, Marks LB, Mettler FA, Pierce LJ et al. 2010. Radiation-related heart disease: current knowledge and future prospects. *International journal of radiation oncology, biology, physics* **76**: 656-665.
- Darby SC, Ewertz M, McGale P, Bennet AM, Blom-Goldman U, Bronnum D, Correa C, Cutter D, Gagliardi G, Gigante B et al. 2013. Risk of ischemic heart disease in

## References

---

- women after radiotherapy for breast cancer. *The New England journal of medicine* **368**: 987-998.
- Davies MJ, Gordon JL, Gearing AJ, Pigott R, Woolf N, Katz D, Kyriakopoulos A. 1993. The expression of the adhesion molecules ICAM-1, VCAM-1, PECAM, and E-selectin in human atherosclerosis. *The Journal of pathology* **171**: 223-229.
- Davies P, Smith BT, Maddalo FB, Langleben D, Tobias D, Fujiwara K, Reid L. 1987. Characteristics of lung pericytes in culture including their growth inhibition by endothelial substrate. *Microvascular research* **33**: 300-314.
- Davies PF. 1995. Flow-mediated endothelial mechanotransduction. *Physiological reviews* **75**: 519-560.
- Davis ME, Grumbach IM, Fukai T, Cutchins A, Harrison DG. 2004. Shear stress regulates endothelial nitric-oxide synthase promoter activity through nuclear factor kappaB binding. *The Journal of biological chemistry* **279**: 163-168.
- De Bock K, Georgiadou M, Carmeliet P. 2013. Role of endothelial cell metabolism in vessel sprouting. *Cell metabolism* **18**: 634-647.
- de Fougères AR, Stacker SA, Schwarting R, Springer TA. 1991. Characterization of ICAM-2 and evidence for a third counter-receptor for LFA-1. *The Journal of experimental medicine* **174**: 253-267.
- DeCarlo AA, Cohen JA, Aguado A, Glenn B. 2008. Isolation and characterization of human gingival microvascular endothelial cells. *Journal of periodontal research* **43**: 246-254.
- DeLisser HM, Newman PJ, Albelda SM. 1994. Molecular and functional aspects of PECAM-1/CD31. *Immunology today* **15**: 490-495.
- Demontis S, Terao M, Brivio M, Zanotta S, Bruschi M, Garattini E. 1998. Isolation and characterization of the gene coding for human cytidine deaminase. *Biochimica et biophysica acta* **1443**: 323-333.
- Denekamp J, Hill S. 1991. Angiogenic attack as a therapeutic strategy for cancer. *Radiotherapy and oncology : journal of the European Society for Therapeutic Radiology and Oncology* **20 Suppl 1**: 103-112.
- Devalliere J, Chatelais M, Fitau J, Gerard N, Hulin P, Velazquez L, Turner CE, Charreau B. 2012. LNK (SH2B3) is a key regulator of integrin signaling in endothelial cells and targets alpha-parvin to control cell adhesion and migration. *FASEB journal : official publication of the Federation of American Societies for Experimental Biology* **26**: 2592-2606.
- Di Lullo GA, Sweeney SM, Korkko J, Ala-Kokko L, San Antonio JD. 2002. Mapping the ligand-binding sites and disease-associated mutations on the most abundant protein in the human, type I collagen. *The Journal of biological chemistry* **277**: 4223-4231.
- Dolle JP, Rezvan A, Allen FD, Lazarovici P, Lelkes PI. 2005. Nerve growth factor-induced migration of endothelial cells. *The Journal of pharmacology and experimental therapeutics* **315**: 1220-1227.

## References

---

- Dong QG, Bernasconi S, Lostaglio S, De Calmanovici RW, Martin-Padura I, Breviario F, Garlanda C, Ramponi S, Mantovani A, Vecchi A. 1997. A general strategy for isolation of endothelial cells from murine tissues. Characterization of two endothelial cell lines from the murine lung and subcutaneous sponge implants. *Arteriosclerosis, thrombosis, and vascular biology* **17**: 1599-1604.
- Donovan D, Brown NJ, Bishop ET, Lewis CE. 2001. Comparison of three in vitro human 'angiogenesis' assays with capillaries formed in vivo. *Angiogenesis* **4**: 113-121.
- Duesberg P, Rasnick D, Li R, Winters L, Rausch C, Hehlmann R. 1999. How aneuploidy may cause cancer and genetic instability. *Anticancer research* **19**: 4887-4906.
- Duff SE, Li C, Garland JM, Kumar S. 2003. CD105 is important for angiogenesis: evidence and potential applications. *FASEB journal : official publication of the Federation of American Societies for Experimental Biology* **17**: 984-992.
- Dustin ML, Rothlein R, Bhan AK, Dinarello CA, Springer TA. 1986. Induction by IL 1 and interferon-gamma: tissue distribution, biochemistry, and function of a natural adherence molecule (ICAM-1). *Journal of immunology* **137**: 245-254.
- Esmon CT. 1995. Thrombomodulin as a model of molecular mechanisms that modulate protease specificity and function at the vessel surface. *FASEB journal : official publication of the Federation of American Societies for Experimental Biology* **9**: 946-955.
- Evans EA, Calderwood DA. 2007. Forces and bond dynamics in cell adhesion. *Science* **316**: 1148-1153.
- Ewing P, Wilke A, Brockhoff G, Andreesen R, Eissner G, Holler E, Gerbitz A. 2003. Isolation and transplantation of allogeneic pulmonary endothelium derived from GFP transgenic mice. *Journal of immunological methods* **283**: 307-315.
- Fan J, Liu J, Culty M, Papadopoulos V. 2010. Acyl-coenzyme A binding domain containing 3 (ACBD3; PAP7; GCP60): an emerging signaling molecule. *Progress in lipid research* **49**: 218-234.
- Fehrenbach ML, Cao G, Williams JT, Finklestein JM, Delisser HM. 2009. Isolation of murine lung endothelial cells. *American journal of physiology Lung cellular and molecular physiology* **296**: L1096-1103.
- Feletou M. 2011. in *The Endothelium: Part 1: Multiple Functions of the Endothelial Cells-Focus on Endothelium-Derived Vasoactive Mediators*, San Rafael (CA).
- Fidler IJ. 1973. Selection of successive tumour lines for metastasis. *Nature: New biology* **242**: 148-149.
- Fidler IJ. 1975. Biological behavior of malignant melanoma cells correlated to their survival in vivo. *Cancer research* **35**: 218-224.
- Fish JE, Marsden PA. 2006. Endothelial nitric oxide synthase: insight into cell-specific gene regulation in the vascular endothelium. *Cellular and molecular life sciences : CMLS* **63**: 144-162.

## References

---

- Florian JA, Kosky JR, Ainslie K, Pang Z, Dull RO, Tarbell JM. 2003. Heparan sulfate proteoglycan is a mechanosensor on endothelial cells. *Circulation research* **93**: e136-142.
- Folberg R, Maniotis AJ. 2004. Vasculogenic mimicry. *APMIS : acta pathologica, microbiologica, et immunologica Scandinavica* **112**: 508-525.
- Fonsatti E, Maio M. 2004. Highlights on endoglin (CD105): from basic findings towards clinical applications in human cancer. *Journal of translational medicine* **2**: 18.
- Fonsatti E, Nicolay HJ, Altomonte M, Covre A, Maio M. 2010. Targeting cancer vasculature via endoglin/CD105: a novel antibody-based diagnostic and therapeutic strategy in solid tumours. *Cardiovascular research* **86**: 12-19.
- Francescone R, Scully S, Bentley B, Yan W, Taylor SL, Oh D, Moral L, Shao R. 2012. Glioblastoma-derived tumor cells induce vasculogenic mimicry through Flk-1 protein activation. *The Journal of biological chemistry* **287**: 24821-24831.
- Francescone RA, 3rd, Faibish M, Shao R. 2011. A Matrigel-based tube formation assay to assess the vasculogenic activity of tumor cells. *Journal of visualized experiments : JoVE*.
- Friebe A, Koesling D. 2003. Regulation of nitric oxide-sensitive guanylyl cyclase. *Circulation research* **93**: 96-105.
- Fu BM, Tarbell JM. 2013. Mechano-sensing and transduction by endothelial surface glycocalyx: composition, structure, and function. *Wiley interdisciplinary reviews Systems biology and medicine* **5**: 381-390.
- Fujiwara K, Masuda M, Osawa M, Kano Y, Katoh K. 2001. Is PECAM-1 a mechanoresponsive molecule? *Cell structure and function* **26**: 11-17.
- Fukata M, Watanabe T, Noritake J, Nakagawa M, Yamaga M, Kuroda S, Matsuura Y, Iwamatsu A, Perez F, Kaibuchi K. 2002. Rac1 and Cdc42 capture microtubules through IQGAP1 and CLIP-170. *Cell* **109**: 873-885.
- Gabriels K, Hoving S, Seemann I, Visser NL, Gijbels MJ, Pol JF, Daemen MJ, Stewart FA, Heeneman S. 2012. Local heart irradiation of ApoE(-/-) mice induces microvascular and endocardial damage and accelerates coronary atherosclerosis. *Radiotherapy and oncology : journal of the European Society for Therapeutic Radiology and Oncology* **105**: 358-364.
- Gajdusek CM, Schwartz SM. 1983. Technique for cloning bovine aortic endothelial cells. *In vitro* **19**: 394-402.
- Gargett CE, Bucak K, Rogers PA. 2000. Isolation, characterization and long-term culture of human myometrial microvascular endothelial cells. *Human reproduction* **15**: 293-301.
- Garlanda C, Dejana E. 1997. Heterogeneity of endothelial cells. Specific markers. *Arteriosclerosis, thrombosis, and vascular biology* **17**: 1193-1202.
- Garlanda C, Parravicini C, Sironi M, De Rossi M, Wainstok de Calmanovici R, Carozzi F, Bussolino F, Colotta F, Mantovani A, Vecchi A. 1994. Progressive growth in immunodeficient mice and host cell recruitment by mouse endothelial cells

## References

---

- transformed by polyoma middle-sized T antigen: implications for the pathogenesis of opportunistic vascular tumors. *Proceedings of the National Academy of Sciences of the United States of America* **91**: 7291-7295.
- Gaugler MH, Squiban C, van der Meeren A, Bertho JM, Vandamme M, Mouthon MA. 1997. Late and persistent up-regulation of intercellular adhesion molecule-1 (ICAM-1) expression by ionizing radiation in human endothelial cells in vitro. *International journal of radiation biology* **72**: 201-209.
- Gaugler MH, Vereycken-Holler V, Squiban C, Aigueperse J. 2004. PECAM-1 (CD31) is required for interactions of platelets with endothelial cells after irradiation. *Journal of thrombosis and haemostasis : JTH* **2**: 2020-2026.
- Gelfand MV, Hong S, Gu C. 2009. Guidance from above: common cues direct distinct signaling outcomes in vascular and neural patterning. *Trends in cell biology* **19**: 99-110.
- Ghobadi G, van der Veen S, Bartelds B, de Boer RA, Dickinson MG, de Jong JR, Faber H, Niemantsverdriet M, Brandenburg S, Berger RM et al. 2012. Physiological interaction of heart and lung in thoracic irradiation. *International journal of radiation oncology, biology, physics* **84**: e639-646.
- Gholkar AA, Senese S, Lo YC, Capri J, Deardorff WJ, Dharmarajan H, Contreras E, Hodara E, Whitelegge JP, Jackson PK et al. 2015. Tctex1d2 associates with short-rib polydactyly syndrome proteins and is required for ciliogenesis. *Cell cycle* **14**: 1116-1125.
- Gimbrone MA, Jr., Cotran RS, Folkman J. 1974. Human vascular endothelial cells in culture. Growth and DNA synthesis. *The Journal of cell biology* **60**: 673-684.
- Gougos A, Letarte M. 1988. Identification of a human endothelial cell antigen with monoclonal antibody 44G4 produced against a pre-B leukemic cell line. *Journal of immunology* **141**: 1925-1933.
- Grimwood J, Bicknell R, Rees MC. 1995. The isolation, characterization and culture of human decidual endothelium. *Human reproduction* **10**: 2142-2148.
- Gudi S, Nolan JP, Frangos JA. 1998. Modulation of GTPase activity of G proteins by fluid shear stress and phospholipid composition. *Proceedings of the National Academy of Sciences of the United States of America* **95**: 2515-2519.
- Hahn WC, Weinberg RA. 2002. Rules for making human tumor cells. *The New England journal of medicine* **347**: 1593-1603.
- Haidekker MA, L'Heureux N, Frangos JA. 2000. Fluid shear stress increases membrane fluidity in endothelial cells: a study with DCVJ fluorescence. *American journal of physiology Heart and circulatory physiology* **278**: H1401-1406.
- Hanahan D, Folkman J. 1996. Patterns and emerging mechanisms of the angiogenic switch during tumorigenesis. *Cell* **86**: 353-364.
- Hanahan D, Weinberg RA. 2011. Hallmarks of cancer: the next generation. *Cell* **144**: 646-674.

## References

---

- Hanna S, El-Sibai M. 2013. Signaling networks of Rho GTPases in cell motility. *Cellular signalling* **25**: 1955-1961.
- Hannum RS, Ojeifo JO, Zwiebel JA, McLeskey SW. 2001. Isolation of tumor-derived endothelial cells. *Microvascular research* **61**: 287-290.
- Hassan HH, Denis M, Krimbou L, Marcil M, Genest J. 2006. Cellular cholesterol homeostasis in vascular endothelial cells. *The Canadian journal of cardiology* **22 Suppl B**: 35B-40B.
- Heckmann M, Douwes K, Peter R, Degitz K. 1998. Vascular activation of adhesion molecule mRNA and cell surface expression by ionizing radiation. *Experimental cell research* **238**: 148-154.
- Heil M, Eitenmuller I, Schmitz-Rixen T, Schaper W. 2006. Arteriogenesis versus angiogenesis: similarities and differences. *Journal of cellular and molecular medicine* **10**: 45-55.
- Helmke BP, Davies PF. 2002. The cytoskeleton under external fluid mechanical forces: hemodynamic forces acting on the endothelium. *Annals of biomedical engineering* **30**: 284-296.
- Helmlinger G, Berk BC, Nerem RM. 1996. Pulsatile and steady flow-induced calcium oscillations in single cultured endothelial cells. *Journal of vascular research* **33**: 360-369.
- Henke CA, Roongta U, Mickelson DJ, Knutson JR, McCarthy JB. 1996. CD44-related chondroitin sulfate proteoglycan, a cell surface receptor implicated with tumor cell invasion, mediates endothelial cell migration on fibrinogen and invasion into a fibrin matrix. *The Journal of clinical investigation* **97**: 2541-2552.
- Herrmann H, Bar H, Kreplak L, Strelkov SV, Aebi U. 2007. Intermediate filaments: from cell architecture to nanomechanics. *Nature reviews Molecular cell biology* **8**: 562-573.
- Hida K, Hida Y, Amin DN, Flint AF, Panigrahy D, Morton CC, Klagsbrun M. 2004. Tumor-associated endothelial cells with cytogenetic abnormalities. *Cancer research* **64**: 8249-8255.
- Hobson B, Denekamp J. 1984. Endothelial proliferation in tumours and normal tissues: continuous labelling studies. *British journal of cancer* **49**: 405-413.
- Hoeben A, Landuyt B, Highley MS, Wildiers H, Van Oosterom AT, De Bruijn EA. 2004. Vascular endothelial growth factor and angiogenesis. *Pharmacological reviews* **56**: 549-580.
- Holmes K, Roberts OL, Thomas AM, Cross MJ. 2007. Vascular endothelial growth factor receptor-2: structure, function, intracellular signalling and therapeutic inhibition. *Cellular signalling* **19**: 2003-2012.
- Hoving S, Heeneman S, Gijbels MJ, Te Poele JA, Visser N, Cleutjens J, Russell NS, Daemen MJ, Stewart FA. 2012. Irradiation induces different inflammatory and thrombotic responses in carotid arteries of wildtype C57BL/6J and atherosclerosis-prone ApoE(-/-) mice. *Radiotherapy and oncology : journal of the European Society for Therapeutic Radiology and Oncology* **105**: 365-370.

## References

---

- Huang H, McIntosh J, Hoyt DG. 2003. An efficient, nonenzymatic method for isolation and culture of murine aortic endothelial cells and their response to inflammatory stimuli. *In vitro cellular & developmental biology Animal* **39**: 43-50.
- Huang MT, Mason JC, Birdsey GM, Amsellem V, Gerwin N, Haskard DO, Ridley AJ, Randi AM. 2005. Endothelial intercellular adhesion molecule (ICAM)-2 regulates angiogenesis. *Blood* **106**: 1636-1643.
- Hubbard AK, Rothlein R. 2000. Intercellular adhesion molecule-1 (ICAM-1) expression and cell signaling cascades. *Free radical biology & medicine* **28**: 1379-1386.
- Humbert MC, Weihbrecht K, Searby CC, Li Y, Pope RM, Sheffield VC, Seo S. 2012. ARL13B, PDE6D, and CEP164 form a functional network for INPP5E ciliary targeting. *Proceedings of the National Academy of Sciences of the United States of America* **109**: 19691-19696.
- Hutcheson IR, Griffith TM. 1994. Heterogeneous populations of K<sup>+</sup> channels mediate EDRF release to flow but not agonists in rabbit aorta. *The American journal of physiology* **266**: H590-596.
- Hutterer A, Berdnik D, Wirtz-Peitz F, Zigman M, Schleiffer A, Knoblich JA. 2006. Mitotic activation of the kinase Aurora-A requires its binding partner Bora. *Developmental cell* **11**: 147-157.
- Ikubo A, Aoki Y, Nagai E, Suzuki T. 1999. Highly metastatic variant of a mouse colon carcinoma cell line, LM17 and its response to GM-CSF gene therapy. *Clinical & experimental metastasis* **17**: 849-855.
- Iomini C, Tejada K, Mo W, Vaananen H, Piperno G. 2004. Primary cilia of human endothelial cells disassemble under laminar shear stress. *The Journal of cell biology* **164**: 811-817.
- Ishii K, Washio T, Uechi T, Yoshihama M, Kenmochi N, Tomita M. 2006. Characteristics and clustering of human ribosomal protein genes. *BMC genomics* **7**: 37.
- Jaffe EA, Nachman RL, Becker CG, Minick CR. 1973. Culture of human endothelial cells derived from umbilical veins. Identification by morphologic and immunologic criteria. *The Journal of clinical investigation* **52**: 2745-2756.
- Jain RK. 2001. Normalizing tumor vasculature with anti-angiogenic therapy: a new paradigm for combination therapy. *Nature medicine* **7**: 987-989.
- Jain RK. 2003. Molecular regulation of vessel maturation. *Nature medicine* **9**: 685-693.
- Jain RK. 2005. Normalization of tumor vasculature: an emerging concept in antiangiogenic therapy. *Science* **307**: 58-62.
- Jelonek K, Walaszczyk A, Gabrys D, Pietrowska M, Kanthou C, Widlak P. 2011. Cardiac endothelial cells isolated from mouse heart - a novel model for radiobiology. *Acta biochimica Polonica* **58**: 397-404.
- Jin Y, Liu Y, Antonyak M, Peng X. 2012. Isolation and characterization of vascular endothelial cells from murine heart and lung. *Methods in molecular biology* **843**: 147-154.

## References

---

- Jin ZG, Ueba H, Tanimoto T, Lungu AO, Frame MD, Berk BC. 2003. Ligand-independent activation of vascular endothelial growth factor receptor 2 by fluid shear stress regulates activation of endothelial nitric oxide synthase. *Circulation research* **93**: 354-363.
- Kajimoto K, Hossen MN, Hida K, Ohga N, Akita H, Hyodo M, Hida Y, Harashima H. 2010. Isolation and culture of microvascular endothelial cells from murine inguinal and epididymal adipose tissues. *Journal of immunological methods* **357**: 43-50.
- Kallmann BA, Wagner S, Hummel V, Buttman M, Bayas A, Tonn JC, Rieckmann P. 2002. Characteristic gene expression profile of primary human cerebral endothelial cells. *FASEB journal : official publication of the Federation of American Societies for Experimental Biology* **16**: 589-591.
- Kamiya A, Bukhari R, Togawa T. 1984. Adaptive regulation of wall shear stress optimizing vascular tree function. *Bulletin of mathematical biology* **46**: 127-137.
- Kevil CG, Bullard DC. 2001. In vitro culture and characterization of gene targeted mouse endothelium. *Acta physiologica Scandinavica* **173**: 151-157.
- King J, Hamil T, Creighton J, Wu S, Bhat P, McDonald F, Stevens T. 2004. Structural and functional characteristics of lung macro- and microvascular endothelial cell phenotypes. *Microvascular research* **67**: 139-151.
- Kleinman HK, McGarvey ML, Hassell JR, Star VL, Cannon FB, Laurie GW, Martin GR. 1986. Basement membrane complexes with biological activity. *Biochemistry* **25**: 312-318.
- Kobayashi M, Inoue K, Warabi E, Minami T, Kodama T. 2005. A simple method of isolating mouse aortic endothelial cells. *Journal of atherosclerosis and thrombosis* **12**: 138-142.
- Komar G, Kauhanen S, Liukko K, Seppanen M, Kajander S, Ovaska J, Nuutila P, Minn H. 2009. Decreased blood flow with increased metabolic activity: a novel sign of pancreatic tumor aggressiveness. *Clinical cancer research : an official journal of the American Association for Cancer Research* **15**: 5511-5517.
- Krause DS, Fackler MJ, Civin CI, May WS. 1996. CD34: structure, biology, and clinical utility. *Blood* **87**: 1-13.
- Kubota Y. 2012. Tumor angiogenesis and anti-angiogenic therapy. *The Keio journal of medicine* **61**: 47-56.
- Kuhlencordt PJ, Rosel E, Gerszten RE, Morales-Ruiz M, Dombkowski D, Atkinson WJ, Han F, Preffer F, Rosenzweig A, Sessa WC et al. 2004. Role of endothelial nitric oxide synthase in endothelial activation: insights from eNOS knockout endothelial cells. *American journal of physiology Cell physiology* **286**: C1195-1202.
- Kuzu I, Bicknell R, Harris AL, Jones M, Gatter KC, Mason DY. 1992. Heterogeneity of vascular endothelial cells with relevance to diagnosis of vascular tumours. *Journal of clinical pathology* **45**: 143-148.
- Lai ES, Huang NF, Cooke JP, Fuller GG. 2012. Aligned nanofibrillar collagen regulates endothelial organization and migration. *Regenerative medicine* **7**: 649-661.

## References

---

- Laitinen L. 1987. Griffonia simplicifolia lectins bind specifically to endothelial cells and some epithelial cells in mouse tissues. *The Histochemical journal* **19**: 225-234.
- Lamallice L, Le Boeuf F, Huot J. 2007. Endothelial cell migration during angiogenesis. *Circulation research* **100**: 782-794.
- Lampugnani MG, Resnati M, Raiteri M, Pigott R, Pisacane A, Houen G, Ruco LP, Dejana E. 1992. A novel endothelial-specific membrane protein is a marker of cell-cell contacts. *The Journal of cell biology* **118**: 1511-1522.
- Langille BL, O'Donnell F. 1986. Reductions in arterial diameter produced by chronic decreases in blood flow are endothelium-dependent. *Science* **231**: 405-407.
- Langley RR, Ramirez KM, Tsan RZ, Van Arsdall M, Nilsson MB, Fidler IJ. 2003. Tissue-specific microvascular endothelial cell lines from H-2K(b)-tsA58 mice for studies of angiogenesis and metastasis. *Cancer research* **63**: 2971-2976.
- Lauder TM, Gegen NW, Knedler A, Harbeck RJ. 1987. The isolation and characterization of enriched microvascular endothelial cells from mouse adipose tissue. The induction of class II molecules of the major histocompatibility complex (MHC) by interferon-gamma (IFN-gamma). *Journal of immunological methods* **102**: 45-52.
- Lee HJ, Koh GY. 2003. Shear stress activates Tie2 receptor tyrosine kinase in human endothelial cells. *Biochemical and biophysical research communications* **304**: 399-404.
- Lee JE, Oum BS, Choi HY, Lee SU, Lee JS. 2009. Evaluation of differentially expressed genes identified in keratoconus. *Molecular vision* **15**: 2480-2487.
- Lee MO, Song SH, Jung S, Hur S, Asahara T, Kim H, Kwon SM, Cha HJ. 2012. Effect of ionizing radiation induced damage of endothelial progenitor cells in vascular regeneration. *Arteriosclerosis, thrombosis, and vascular biology* **32**: 343-352.
- Lenaz G. 1987. Lipid fluidity and membrane protein dynamics. *Bioscience reports* **7**: 823-837.
- Li C, Issa R, Kumar P, Hampson IN, Lopez-Novoa JM, Bernabeu C, Kumar S. 2003. CD105 prevents apoptosis in hypoxic endothelial cells. *Journal of cell science* **116**: 2677-2685.
- Li JM, Mullen AM, Shah AM. 2001. Phenotypic properties and characteristics of superoxide production by mouse coronary microvascular endothelial cells. *Journal of molecular and cellular cardiology* **33**: 1119-1131.
- Liao F, Doody JF, Overholser J, Finnerty B, Bassi R, Wu Y, Dejana E, Kussie P, Bohlen P, Hicklin DJ. 2002. Selective targeting of angiogenic tumor vasculature by vascular endothelial-cadherin antibody inhibits tumor growth without affecting vascular permeability. *Cancer research* **62**: 2567-2575.
- Liao F, Li Y, O'Connor W, Zanetta L, Bassi R, Santiago A, Overholser J, Hooper A, Mignatti P, Dejana E et al. 2000. Monoclonal antibody to vascular endothelial-cadherin is a potent inhibitor of angiogenesis, tumor growth, and metastasis. *Cancer research* **60**: 6805-6810.

## References

---

- Lim YC, Garcia-Cardena G, Allport JR, Zervoglos M, Connolly AJ, Gimbrone MA, Jr., Luscinskas FW. 2003. Heterogeneity of endothelial cells from different organ sites in T-cell subset recruitment. *The American journal of pathology* **162**: 1591-1601.
- Lim YC, Luscinskas FW. 2006. Isolation and culture of murine heart and lung endothelial cells for in vitro model systems. *Methods in molecular biology* **341**: 141-154.
- Lin G, Finger E, Gutierrez-Ramos JC. 1995. Expression of CD34 in endothelial cells, hematopoietic progenitors and nervous cells in fetal and adult mouse tissues. *European journal of immunology* **25**: 1508-1516.
- Liu B, Ahmad W, Aronson NN, Jr. 1999. Structure of the human gene for lysosomal di-N-acetylchitobiase. *Glycobiology* **9**: 589-593.
- Liu X, Zhao Y, Gao J, Pawlyk B, Starcher B, Spencer JA, Yanagisawa H, Zuo J, Li T. 2004. Elastic fiber homeostasis requires lysyl oxidase-like 1 protein. *Nature genetics* **36**: 178-182.
- Liu Y, Yang FC, Okuda T, Dong X, Zylka MJ, Chen CL, Anderson DJ, Kuner R, Ma Q. 2008. Mechanisms of compartmentalized expression of Mrg class G-protein-coupled sensory receptors. *The Journal of neuroscience : the official journal of the Society for Neuroscience* **28**: 125-132.
- Loges S, Schmidt T, Carmeliet P. 2010. Mechanisms of resistance to anti-angiogenic therapy and development of third-generation anti-angiogenic drug candidates. *Genes & cancer* **1**: 12-25.
- Lou JN, Mili N, Decrind C, Donati Y, Kossodo S, Spiliopoulos A, Ricou B, Suter PM, Morel DR, Morel P et al. 1998. An improved method for isolation of microvascular endothelial cells from normal and inflamed human lung. *In vitro cellular & developmental biology Animal* **34**: 529-536.
- Mackay LS, Dodd S, Dougall IG, Tomlinson W, Lordan J, Fisher AJ, Corris PA. 2013. Isolation and characterisation of human pulmonary microvascular endothelial cells from patients with severe emphysema. *Respiratory research* **14**: 23.
- Mackman N. 2009. The role of tissue factor and factor VIIa in hemostasis. *Anesthesia and analgesia* **108**: 1447-1452.
- Makarova KS, Aravind L, Koonin EV. 2002. SWIM, a novel Zn-chelating domain present in bacteria, archaea and eukaryotes. *Trends in biochemical sciences* **27**: 384-386.
- Maltby S, Freeman S, Gold MJ, Baker JH, Minchinton AI, Gold MR, Roskelley CD, McNagny KM. 2011. Opposing roles for CD34 in B16 melanoma tumor growth alter early stage vasculature and late stage immune cell infiltration. *PloS one* **6**: e18160.
- Maniotis AJ, Folberg R, Hess A, Seftor EA, Gardner LM, Pe'er J, Trent JM, Meltzer PS, Hendrix MJ. 1999. Vascular channel formation by human melanoma cells in vivo and in vitro: vasculogenic mimicry. *The American journal of pathology* **155**: 739-752.
- Marcus JT, Gan CT, Zwanenburg JJ, Boonstra A, Allaart CP, Gotte MJ, Vonk-Noordegraaf A. 2008. Interventricular mechanical asynchrony in pulmonary arterial hypertension: left-to-right delay in peak shortening is related to right ventricular

## References

---

- overload and left ventricular underfilling. *Journal of the American College of Cardiology* **51**: 750-757.
- Marelli-Berg FM, Peek E, Lidington EA, Stauss HJ, Lechler RI. 2000. Isolation of endothelial cells from murine tissue. *Journal of immunological methods* **244**: 205-215.
- Marks RM, Czerniecki M, Penny R. 1985. Human dermal microvascular endothelial cells: an improved method for tissue culture and a description of some singular properties in culture. *In vitro cellular & developmental biology : journal of the Tissue Culture Association* **21**: 627-635.
- Martinez-Lemus LA. 2012. The dynamic structure of arterioles. *Basic & clinical pharmacology & toxicology* **110**: 5-11.
- Maruyama Y. 1963. The human endothelial cell in tissue culture. *Zeitschrift fur Zellforschung und mikroskopische Anatomie* **60**: 69-79.
- McCarthy RE, 3rd, Kasper EK. 1998. A review of the amyloidoses that infiltrate the heart. *Clinical cardiology* **21**: 547-552.
- McDonald DM, Choyke PL. 2003. Imaging of angiogenesis: from microscope to clinic. *Nature medicine* **9**: 713-725.
- McDouall RM, Yacoub M, Rose ML. 1996. Isolation, culture, and characterisation of MHC class II-positive microvascular endothelial cells from the human heart. *Microvascular research* **51**: 137-152.
- Merath K, Ronchetti A, Sidjanin DJ. 2013. Functional analysis of HSF4 mutations found in patients with autosomal recessive congenital cataracts. *Investigative ophthalmology & visual science* **54**: 6646-6654.
- Miao RQ, Gao Y, Harrison KD, Prendergast J, Acevedo LM, Yu J, Hu F, Strittmatter SM, Sessa WC. 2006. Identification of a receptor necessary for Nogo-B stimulated chemotaxis and morphogenesis of endothelial cells. *Proceedings of the National Academy of Sciences of the United States of America* **103**: 10997-11002.
- Midwood KS, Schwarzbauer JE. 2002. Elastic fibers: building bridges between cells and their matrix. *Current biology : CB* **12**: R279-281.
- Miele ME, Bennett CF, Miller BE, Welch DR. 1994. Enhanced metastatic ability of TNF-alpha-treated malignant melanoma cells is reduced by intercellular adhesion molecule-1 (ICAM-1, CD54) antisense oligonucleotides. *Experimental cell research* **214**: 231-241.
- Modzelewski RA, Davies P, Watkins SC, Auerbach R, Chang MJ, Johnson CS. 1994. Isolation and identification of fresh tumor-derived endothelial cells from a murine RIF-1 fibrosarcoma. *Cancer research* **54**: 336-339.
- Molla M, Gironella M, Miquel R, Tovar V, Engel P, Biete A, Pique JM, Panes J. 2003. Relative roles of ICAM-1 and VCAM-1 in the pathogenesis of experimental radiation-induced intestinal inflammation. *International journal of radiation oncology, biology, physics* **57**: 264-273.

## References

---

- Mosavi LK, Cammett TJ, Desrosiers DC, Peng ZY. 2004. The ankyrin repeat as molecular architecture for protein recognition. *Protein science : a publication of the Protein Society* **13**: 1435-1448.
- Moyer BD, Hevezi P, Gao N, Lu M, Kalabat D, Soto H, Echeverri F, Laita B, Yeh SA, Zoller M et al. 2009. Expression of genes encoding multi-transmembrane proteins in specific primate taste cell populations. *PLoS one* **4**: e7682.
- Mullen P. 2004. The use of Matrigel to facilitate the establishment of human cancer cell lines as xenografts. *Methods in molecular medicine* **88**: 287-292.
- Mutsaers SE. 2002. Mesothelial cells: their structure, function and role in serosal repair. *Respirology* **7**: 171-191.
- Nakamura K, Jinnin M, Kudo H, Inoue K, Nakayama W, Honda N, Kajihara I, Masuguchi S, Fukushima S, Ihn H. 2015. The role of PSMB9 up-regulated by interferon signature in the pathophysiology of cutaneous lesions of dermatomyositis and lupus erythematosus. *The British journal of dermatology*.
- Nakatsu MN, Hughes CC. 2008. An optimized three-dimensional in vitro model for the analysis of angiogenesis. *Methods in enzymology* **443**: 65-82.
- Natkunam Y, Rouse RV, Zhu S, Fisher C, van De Rijn M. 2000. Immunoblot analysis of CD34 expression in histologically diverse neoplasms. *The American journal of pathology* **156**: 21-27.
- Nauli SM, Kawanabe Y, Kaminski JJ, Pearce WJ, Ingber DE, Zhou J. 2008. Endothelial cilia are fluid shear sensors that regulate calcium signaling and nitric oxide production through polycystin-1. *Circulation* **117**: 1161-1171.
- Nilius B, Droogmans G. 2001. Ion channels and their functional role in vascular endothelium. *Physiological reviews* **81**: 1415-1459.
- Noria S, Xu F, McCue S, Jones M, Gotlieb AI, Langille BL. 2004. Assembly and reorientation of stress fibers drives morphological changes to endothelial cells exposed to shear stress. *The American journal of pathology* **164**: 1211-1223.
- Obi S, Yamamoto K, Shimizu N, Kumagaya S, Masumura T, Sokabe T, Asahara T, Ando J. 2009. Fluid shear stress induces arterial differentiation of endothelial progenitor cells. *Journal of applied physiology* **106**: 203-211.
- Ohta Y, Kousaka K, Nagata-Ohashi K, Ohashi K, Muramoto A, Shima Y, Niwa R, Uemura T, Mizuno K. 2003. Differential activities, subcellular distribution and tissue expression patterns of three members of Slingshot family phosphatases that dephosphorylate cofilin. *Genes to cells : devoted to molecular & cellular mechanisms* **8**: 811-824.
- Okaji Y, Tsuno NH, Kitayama J, Saito S, Takahashi T, Kawai K, Yazawa K, Asakage M, Tsuchiya T, Sakurai D et al. 2004. A novel method for isolation of endothelial cells and macrophages from murine tumors based on Ac-LDL uptake and CD16 expression. *Journal of immunological methods* **295**: 183-193.
- Olesen SP, Clapham DE, Davies PF. 1988. Haemodynamic shear stress activates a K<sup>+</sup> current in vascular endothelial cells. *Nature* **331**: 168-170.

## References

---

- Olson ST, Chuang YJ. 2002. Heparin activates antithrombin anticoagulant function by generating new interaction sites (exosites) for blood clotting proteinases. *Trends in cardiovascular medicine* **12**: 331-338.
- Osawa M, Masuda M, Harada N, Lopes RB, Fujiwara K. 1997. Tyrosine phosphorylation of platelet endothelial cell adhesion molecule-1 (PECAM-1, CD31) in mechanically stimulated vascular endothelial cells. *European journal of cell biology* **72**: 229-237.
- Pan S. 2009. Molecular mechanisms responsible for the atheroprotective effects of laminar shear stress. *Antioxidants & redox signaling* **11**: 1669-1682.
- Papaioannou TG, Stefanadis C. 2005. Vascular wall shear stress: basic principles and methods. *Hellenic journal of cardiology : HJC = Hellenike kardiologike epitheorese* **46**: 9-15.
- Papworth M, Kolasinska P, Minczuk M. 2006. Designer zinc-finger proteins and their applications. *Gene* **366**: 27-38.
- Park H, Go YM, Darji R, Choi JW, Lisanti MP, Maland MC, Jo H. 2000. Caveolin-1 regulates shear stress-dependent activation of extracellular signal-regulated kinase. *American journal of physiology Heart and circulatory physiology* **278**: H1285-1293.
- Park S, DiMaio TA, Scheef EA, Sorenson CM, Sheibani N. 2010. PECAM-1 regulates proangiogenic properties of endothelial cells through modulation of cell-cell and cell-matrix interactions. *American journal of physiology Cell physiology* **299**: C1468-1484.
- Patties I, Haagen J, Dorr W, Hildebrandt G, Glasow A. 2015. Late inflammatory and thrombotic changes in irradiated hearts of C57BL/6 wild-type and atherosclerosis-prone ApoE-deficient mice. *Strahlentherapie und Onkologie : Organ der Deutschen Rontgengesellschaft [et al]* **191**: 172-179.
- Patties I, Habelt B, Rosin B, Dorr W, Hildebrandt G, Glasow A. 2014. Late effects of local irradiation on the expression of inflammatory markers in the Arteria saphena of C57BL/6 wild-type and ApoE-knockout mice. *Radiation and environmental biophysics* **53**: 117-124.
- Pinheiro C, Longatto-Filho A, Azevedo-Silva J, Casal M, Schmitt FC, Baltazar F. 2012. Role of monocarboxylate transporters in human cancers: state of the art. *Journal of bioenergetics and biomembranes* **44**: 127-139.
- Postiglione L, Di Domenico G, Caraglia M, Marra M, Giuberti G, Del Vecchio L, Montagnani S, Macri M, Bruno EM, Abbruzzese A et al. 2005. Differential expression and cytoplasm/membrane distribution of endoglin (CD105) in human tumour cell lines: Implications in the modulation of cell proliferation. *International journal of oncology* **26**: 1193-1201.
- Powell SR. 2006. The ubiquitin-proteasome system in cardiac physiology and pathology. *American journal of physiology Heart and circulatory physiology* **291**: H1-H19.
- Pratumvinit B, Reesukumal K, Janebodin K, Ieronimakis N, Reyes M. 2013. Isolation, characterization, and transplantation of cardiac endothelial cells. *BioMed research international* **2013**: 359412.

## References

---

- Quarmby S, Hunter RD, Kumar S. 2000. Irradiation induced expression of CD31, ICAM-1 and VCAM-1 in human microvascular endothelial cells. *Anticancer research* **20**: 3375-3381.
- Quarmby S, Kumar P, Kumar S. 1999. Radiation-induced normal tissue injury: role of adhesion molecules in leukocyte-endothelial cell interactions. *International journal of cancer Journal international du cancer* **82**: 385-395.
- Rabausch K, Bretschneider E, Sarbia M, Meyer-Kirchrath J, Censarek P, Pape R, Fischer JW, Schror K, Weber AA. 2005. Regulation of thrombomodulin expression in human vascular smooth muscle cells by COX-2-derived prostaglandins. *Circulation research* **96**: e1-6.
- Raftopoulou M, Hall A. 2004. Cell migration: Rho GTPases lead the way. *Developmental biology* **265**: 23-32.
- Ramos-Medina R, Montes-Moreno S, Maestre L, Canamero M, Rodriguez-Pinilla M, Martinez-Torrecedrada J, Piris MA, Majid A, Dyer MJ, Pulford K et al. 2013. BCL7A protein expression in normal and malignant lymphoid tissues. *British journal of haematology* **160**: 106-109.
- Raychaudhuri SK, Raychaudhuri SP, Weltman H, Farber EM. 2001. Effect of nerve growth factor on endothelial cell biology: proliferation and adherence molecule expression on human dermal microvascular endothelial cells. *Archives of dermatological research* **293**: 291-295.
- Reinhart-King CA, Fujiwara K, Berk BC. 2008. Physiologic stress-mediated signaling in the endothelium. *Methods in enzymology* **443**: 25-44.
- Resnick N, Yahav H, Shay-Salit A, Shushy M, Schubert S, Zilberman LC, Wofovitz E. 2003. Fluid shear stress and the vascular endothelium: for better and for worse. *Progress in biophysics and molecular biology* **81**: 177-199.
- Reynolds LP, Redmer DA. 2001. Angiogenesis in the placenta. *Biology of reproduction* **64**: 1033-1040.
- Rizzo V, McIntosh DP, Oh P, Schnitzer JE. 1998. In situ flow activates endothelial nitric oxide synthase in luminal caveolae of endothelium with rapid caveolin dissociation and calmodulin association. *The Journal of biological chemistry* **273**: 34724-34729.
- Rizzo V, Morton C, DePaola N, Schnitzer JE, Davies PF. 2003. Recruitment of endothelial caveolae into mechanotransduction pathways by flow conditioning in vitro. *American journal of physiology Heart and circulatory physiology* **285**: H1720-1729.
- Rosette C, Roth RB, Oeth P, Braun A, Kammerer S, Ekblom J, Denissenko MF. 2005. Role of ICAM1 in invasion of human breast cancer cells. *Carcinogenesis* **26**: 943-950.
- Rosso F, Giordano A, Barbarisi M, Barbarisi A. 2004. From cell-ECM interactions to tissue engineering. *Journal of cellular physiology* **199**: 174-180.
- Rousseau S, Houle F, Huot J. 2000. Integrating the VEGF signals leading to actin-based motility in vascular endothelial cells. *Trends in cardiovascular medicine* **10**: 321-327.

## References

---

- Rungaldier S, Oberwagner W, Salzer U, Csaszar E, Prohaska R. 2013. Stomatin interacts with GLUT1/SLC2A1, band 3/SLC4A1, and aquaporin-1 in human erythrocyte membrane domains. *Biochimica et biophysica acta* **1828**: 956-966.
- Ryan US. 1984. Isolation and culture of pulmonary endothelial cells. *Environmental health perspectives* **56**: 103-114.
- Ryan US, Mortara M, Whitaker C. 1980. Methods for microcarrier culture of bovine pulmonary artery endothelial cells avoiding the use of enzymes. *Tissue & cell* **12**: 619-635.
- Sadler JE. 1998. Biochemistry and genetics of von Willebrand factor. *Annual review of biochemistry* **67**: 395-424.
- Sakurai A, Doci CL, Gutkind JS. 2012. Semaphorin signaling in angiogenesis, lymphangiogenesis and cancer. *Cell research* **22**: 23-32.
- Salehi AH, Xanthoudakis S, Barker PA. 2002. NRAGE, a p75 neurotrophin receptor-interacting protein, induces caspase activation and cell death through a JNK-dependent mitochondrial pathway. *The Journal of biological chemistry* **277**: 48043-48050.
- Scholz D, Schaper J. 1997. Platelet/endothelial cell adhesion molecule-1 (PECAM-1) is localized over the entire plasma membrane of endothelial cells. *Cell and tissue research* **290**: 623-631.
- Schultz-Hector S, Trott KR. 2007. Radiation-induced cardiovascular diseases: is the epidemiologic evidence compatible with the radiobiologic data? *International journal of radiation oncology, biology, physics* **67**: 10-18.
- Schwarz TL. 2004. Synaptotagmin promotes both vesicle fusion and recycling. *Proceedings of the National Academy of Sciences of the United States of America* **101**: 16401-16402.
- Scott PA, Bicknell R. 1993. The isolation and culture of microvascular endothelium. *Journal of cell science* **105 ( Pt 2)**: 269-273.
- Seemann I, Gabriels K, Visser NL, Hoving S, te Poele JA, Pol JF, Gijbels MJ, Janssen BJ, van Leeuwen FW, Daemen MJ et al. 2012. Irradiation induced modest changes in murine cardiac function despite progressive structural damage to the myocardium and microvasculature. *Radiotherapy and oncology : journal of the European Society for Therapeutic Radiology and Oncology* **103**: 143-150.
- Seemann I, Te Poele JA, Hoving S, Stewart FA. 2014. Mouse bone marrow-derived endothelial progenitor cells do not restore radiation-induced microvascular damage. *ISRN cardiology* **2014**: 506348.
- Serini G, Napione L, Arese M, Bussolino F. 2008. Besides adhesion: new perspectives of integrin functions in angiogenesis. *Cardiovascular research* **78**: 213-222.
- Sessa C, Guibal A, Del Conte G, Rugg C. 2008. Biomarkers of angiogenesis for the development of antiangiogenic therapies in oncology: tools or decorations? *Nature clinical practice Oncology* **5**: 378-391.

## References

---

- Shames SR, Croxen MA, Deng W, Finlay BB. 2011. The type III system-secreted effector EspZ localizes to host mitochondria and interacts with the translocase of inner mitochondrial membrane 17b. *Infection and immunity* **79**: 4784-4790.
- Sharma N, Seftor RE, Seftor EA, Gruman LM, Heidger PM, Jr., Cohen MB, Lubaroff DM, Hendrix MJ. 2002. Prostatic tumor cell plasticity involves cooperative interactions of distinct phenotypic subpopulations: role in vasculogenic mimicry. *The Prostate* **50**: 189-201.
- Shaul PW, Anderson RG. 1998. Role of plasmalemmal caveolae in signal transduction. *The American journal of physiology* **275**: L843-851.
- Shay-Salit A, Shushy M, Wolfvitz E, Yahav H, Breviario F, Dejana E, Resnick N. 2002. VEGF receptor 2 and the adherens junction as a mechanical transducer in vascular endothelial cells. *Proceedings of the National Academy of Sciences of the United States of America* **99**: 9462-9467.
- Shay JW, Wright WE. 2011. Role of telomeres and telomerase in cancer. *Seminars in cancer biology* **21**: 349-353.
- Shyy JY, Chien S. 2002. Role of integrins in endothelial mechanosensing of shear stress. *Circulation research* **91**: 769-775.
- Siegel G, Walter A, Kauschmann A, Malmsten M, Buddecke E. 1996. Anionic biopolymers as blood flow sensors. *Biosensors & bioelectronics* **11**: 281-294.
- Siemerink MJ, Klaassen I, Van Noorden CJ, Schlingemann RO. 2013. Endothelial tip cells in ocular angiogenesis: potential target for anti-angiogenesis therapy. *The journal of histochemistry and cytochemistry : official journal of the Histochemistry Society* **61**: 101-115.
- Sievert W, Tapio S, Breuninger S, Gaipf U, Andratschke N, Trott KR, Multhoff G. 2014. Adhesion molecule expression and function of primary endothelial cells in benign and malignant tissues correlates with proliferation. *PloS one* **9**: e91808.
- Sievert W, Trott KR, Azimzadeh O, Tapio S, Zitzelsberger H, Multhoff G. 2015. Late proliferating and inflammatory effects on murine microvascular heart and lung endothelial cells after irradiation. *Radiotherapy and oncology : journal of the European Society for Therapeutic Radiology and Oncology* **117**: 376-381.
- Smallridge RC, Gamblin GT, Eil C. 1986. Angiotensin-converting enzyme: characteristics in human skin fibroblasts. *Metabolism: clinical and experimental* **35**: 899-904.
- Sobczak M, Dargatz J, Chrzanowska-Wodnicka M. 2010. Isolation and culture of pulmonary endothelial cells from neonatal mice. *Journal of visualized experiments : JoVE*.
- Solowiej A, Biswas P, Graesser D, Madri JA. 2003. Lack of platelet endothelial cell adhesion molecule-1 attenuates foreign body inflammation because of decreased angiogenesis. *The American journal of pathology* **162**: 953-962.
- Springer TA. 1990. Adhesion receptors of the immune system. *Nature* **346**: 425-434.
- Steri V, Ellison TS, Gontarczyk AM, Weilbaecher K, Schneider JG, Edwards D, Fruttiger M, Hodivala-Dilke KM, Robinson SD. 2014. Acute depletion of endothelial beta3-

## References

---

- integrin transiently inhibits tumor growth and angiogenesis in mice. *Circulation research* **114**: 79-91.
- Stewart EE, Chen X, Hadway J, Lee TY. 2006. Correlation between hepatic tumor blood flow and glucose utilization in a rabbit liver tumor model. *Radiology* **239**: 740-750.
- Strasser A, Dickmanns A, Luhrmann R, Ficner R. 2005. Structural basis for m3G-cap-mediated nuclear import of spliceosomal UsnRNPs by snurportin1. *The EMBO journal* **24**: 2235-2243.
- Stros M, Launholt D, Grasser KD. 2007. The HMG-box: a versatile protein domain occurring in a wide variety of DNA-binding proteins. *Cellular and molecular life sciences : CMLS* **64**: 2590-2606.
- Stylli SS, Stacey TT, Verhagen AM, Xu SS, Pass I, Courtneidge SA, Lock P. 2009. Nck adaptor proteins link Tks5 to invadopodia actin regulation and ECM degradation. *Journal of cell science* **122**: 2727-2740.
- Sun X, Feinberg MW. 2015. Regulation of endothelial cell metabolism: just go with the flow. *Arteriosclerosis, thrombosis, and vascular biology* **35**: 13-15.
- Tan J, D'Agostaro AF, Bendiak B, Reck F, Sarkar M, Squire JA, Leong P, Schachter H. 1995. The human UDP-N-acetylglucosamine: alpha-6-D-mannoside-beta-1,2- N-acetylglucosaminyltransferase II gene (MGAT2). Cloning of genomic DNA, localization to chromosome 14q21, expression in insect cells and purification of the recombinant protein. *European journal of biochemistry / FEBS* **231**: 317-328.
- Tang DG, Chen YQ, Newman PJ, Shi L, Gao X, Diglio CA, Honn KV. 1993. Identification of PECAM-1 in solid tumor cells and its potential involvement in tumor cell adhesion to endothelium. *The Journal of biological chemistry* **268**: 22883-22894.
- Tanno H, Yamaguchi T, Goto E, Ishido S, Komada M. 2012. The Ankrd 13 family of UIM-bearing proteins regulates EGF receptor endocytosis from the plasma membrane. *Molecular biology of the cell* **23**: 1343-1353.
- Tarbell JM, Pahakis MY. 2006. Mechanotransduction and the glycocalyx. *Journal of internal medicine* **259**: 339-350.
- Taunk NK, Haffty BG, Kostis JB, Goyal S. 2015. Radiation-induced heart disease: pathologic abnormalities and putative mechanisms. *Frontiers in oncology* **5**: 39.
- Teng B, Ansari HR, Oldenburg PJ, Schnermann J, Mustafa SJ. 2006. Isolation and characterization of coronary endothelial and smooth muscle cells from A1 adenosine receptor-knockout mice. *American journal of physiology Heart and circulatory physiology* **290**: H1713-1720.
- Traub O, Berk BC. 1998. Laminar shear stress: mechanisms by which endothelial cells transduce an atheroprotective force. *Arteriosclerosis, thrombosis, and vascular biology* **18**: 677-685.
- Tu T, Zhang C, Yan H, Luo Y, Kong R, Wen P, Ye Z, Chen J, Feng J, Liu F et al. 2015. CD146 acts as a novel receptor for netrin-1 in promoting angiogenesis and vascular development. *Cell research* **25**: 275-287.

## References

---

- Tzima E, Irani-Tehrani M, Kiosses WB, Dejana E, Schultz DA, Engelhardt B, Cao G, DeLisser H, Schwartz MA. 2005. A mechanosensory complex that mediates the endothelial cell response to fluid shear stress. *Nature* **437**: 426-431.
- van den Berg BM, Vink H, Spaan JA. 2003. The endothelial glycocalyx protects against myocardial edema. *Circulation research* **92**: 592-594.
- van Luijk P, Faber H, Meertens H, Schippers JM, Langendijk JA, Brandenburg S, Kampinga HH, Coppes RP. 2007. The impact of heart irradiation on dose-volume effects in the rat lung. *International journal of radiation oncology, biology, physics* **69**: 552-559.
- van Luijk P, Novakova-Jiresova A, Faber H, Schippers JM, Kampinga HH, Meertens H, Coppes RP. 2005. Radiation damage to the heart enhances early radiation-induced lung function loss. *Cancer research* **65**: 6509-6511.
- Vanhoutte PM, Rubanyi GM, Miller VM, Houston DS. 1986. Modulation of vascular smooth muscle contraction by the endothelium. *Annual review of physiology* **48**: 307-320.
- Vasudev NS, Reynolds AR. 2014. Anti-angiogenic therapy for cancer: current progress, unresolved questions and future directions. *Angiogenesis* **17**: 471-494.
- Vecchi A, Garlanda C, Lampugnani MG, Resnati M, Matteucci C, Stoppacciaro A, Schnurch H, Risau W, Ruco L, Mantovani A et al. 1994. Monoclonal antibodies specific for endothelial cells of mouse blood vessels. Their application in the identification of adult and embryonic endothelium. *European journal of cell biology* **63**: 247-254.
- Verhagen HJ, Heijnen-Snyder GJ, Pronk A, Vroom TM, van Vroonhoven TJ, Eikelboom BC, Sixma JJ, de Groot PG. 1996. Thrombomodulin activity on mesothelial cells: perspectives for mesothelial cells as an alternative for endothelial cells for cell seeding on vascular grafts. *British journal of haematology* **95**: 542-549.
- Verhamme P, Hoylaerts MF. 2006. The pivotal role of the endothelium in haemostasis and thrombosis. *Acta clinica Belgica* **61**: 213-219.
- Vestweber D. 2008. VE-cadherin: the major endothelial adhesion molecule controlling cellular junctions and blood vessel formation. *Arteriosclerosis, thrombosis, and vascular biology* **28**: 223-232.
- Villalonga P, Ridley AJ. 2006. Rho GTPases and cell cycle control. *Growth factors* **24**: 159-164.
- Vittet D, Buchou T, Schweitzer A, Dejana E, Huber P. 1997. Targeted null-mutation in the vascular endothelial-cadherin gene impairs the organization of vascular-like structures in embryoid bodies. *Proceedings of the National Academy of Sciences of the United States of America* **94**: 6273-6278.
- Voyta JC, Via DP, Butterfield CE, Zetter BR. 1984. Identification and isolation of endothelial cells based on their increased uptake of acetylated-low density lipoprotein. *The Journal of cell biology* **99**: 2034-2040.

## References

---

- Waimey KE, Huang PH, Chen M, Cheng HJ. 2008. Plexin-A3 and plexin-A4 restrict the migration of sympathetic neurons but not their neural crest precursors. *Developmental biology* **315**: 448-458.
- Wang K, Song Y, Chen DB, Zheng J. 2008a. Protein phosphatase 3 differentially modulates vascular endothelial growth factor- and fibroblast growth factor 2-stimulated cell proliferation and signaling in ovine fetoplacental artery endothelial cells. *Biology of reproduction* **79**: 704-710.
- Wang M, Bronte V, Chen PW, Gritz L, Panicali D, Rosenberg SA, Restifo NP. 1995. Active immunotherapy of cancer with a nonreplicating recombinant fowlpox virus encoding a model tumor-associated antigen. *Journal of immunology* **154**: 4685-4692.
- Wang S, Li X, Parra M, Verdin E, Bassel-Duby R, Olson EN. 2008b. Control of endothelial cell proliferation and migration by VEGF signaling to histone deacetylase 7. *Proceedings of the National Academy of Sciences of the United States of America* **105**: 7738-7743.
- Weiss HJ, Turitto VT. 1979. Prostacyclin (prostaglandin I<sub>2</sub>, PGI<sub>2</sub>) inhibits platelet adhesion and thrombus formation on subendothelium. *Blood* **53**: 244-250.
- White JF, Parshley MS. 1951. Growth in vitro of blood vessels from bone marrow of adult chickens. *The American journal of anatomy* **89**: 321-345.
- Wiederkehr A, Staple J, Caroni P. 1997. The motility-associated proteins GAP-43, MARCKS, and CAP-23 share unique targeting and surface activity-inducing properties. *Experimental cell research* **236**: 103-116.
- Williamson MR, Shuttleworth A, Canfield AE, Black RA, Kielty CM. 2007. The role of endothelial cell attachment to elastic fibre molecules in the enhancement of monolayer formation and retention, and the inhibition of smooth muscle cell recruitment. *Biomaterials* **28**: 5307-5318.
- Wood HB, May G, Healy L, Enver T, Morriss-Kay GM. 1997. CD34 expression patterns during early mouse development are related to modes of blood vessel formation and reveal additional sites of hematopoiesis. *Blood* **90**: 2300-2311.
- Wu Z, Hofman FM, Zlokovic BV. 2003. A simple method for isolation and characterization of mouse brain microvascular endothelial cells. *Journal of neuroscience methods* **130**: 53-63.
- Xu H, Bickford JK, Luther E, Carpenito C, Takei F, Springer TA. 1996. Characterization of murine intercellular adhesion molecule-2. *Journal of immunology* **156**: 4909-4914.
- Yamamoto K, Ando J. 2011. New molecular mechanisms for cardiovascular disease: blood flow sensing mechanism in vascular endothelial cells. *Journal of pharmacological sciences* **116**: 323-331.
- Yamamoto K, Korenaga R, Kamiya A, Ando J. 2000. Fluid shear stress activates Ca<sup>2+</sup> influx into human endothelial cells via P2X<sub>4</sub> purinoceptors. *Circulation research* **87**: 385-391.

## References

---

- Yamamoto K, Takahashi T, Asahara T, Ohura N, Sokabe T, Kamiya A, Ando J. 2003. Proliferation, differentiation, and tube formation by endothelial progenitor cells in response to shear stress. *Journal of applied physiology* **95**: 2081-2088.
- Zhou J, Chng WJ. 2013. Roles of thioredoxin binding protein (TXNIP) in oxidative stress, apoptosis and cancer. *Mitochondrion* **13**: 163-169.
- Zhou Z, Christofidou-Solomidou M, Garlanda C, DeLisser HM. 1999. Antibody against murine PECAM-1 inhibits tumor angiogenesis in mice. *Angiogenesis* **3**: 181-188.
- Zimowska G, Shi J, Munguba G, Jackson MR, Alpatov R, Simmons MN, Shi Y, Sugrue SP. 2003. Pinin/DRS/memA interacts with SRp75, SRm300 and SRp130 in corneal epithelial cells. *Investigative ophthalmology & visual science* **44**: 4715-4723.

## 7. APPENDIX

**Table 24:** Different gene expression of heart ECs in response to high shear stress involved in extracellular matrix organisation.

Gene	Log.Fold. Change	Linear. Fold. Change	Comp. A-B	Gene	Log. Fold. Change	Linear. Fold. Change	Comp. A-B
SDC4	2.6	6.2	up	DDR1	0.8	1.7	up
ITGA1	1.4	2.7	up	COL6A3	1.4	2.7	up
BMP2	2.9	7.6	up	LAMA4	0.6	1.5	up
LEPREL2	1.2	2.3	up	COL5A1	0.7	1.6	up
COL1A2	2.7	6.6	up	ADAM17	0.5	1.4	up
LOXL2	2.4	5.2	up	COL28A1	0.5	1.5	up
MMP14	1	1.9	up	MFAP5	0.6	1.5	up
ADAMTS14	2.1	4.2	up	LAMA2	0.6	1.5	up
BMP7	2.3	4.8	up	ITGB5	0.5	1.4	up
LOXL1	1.6	3	up	FBLN2	-3.5	0.1	down
CASP3	1	2	up	CTSD	-1.2	0.4	down
LAMA3	1.2	2.3	up	LTBP4	-2.3	0.2	down
MFAP2	1.4	2.6	up	KDR	-1.5	0.4	down
ITGA11	2.4	5.2	up	PLEC	-1.9	0.3	down
MMP3	1.2	2.2	up	ACAN	-1.6	0.3	down
COL1A1	1.7	3.3	up	NID1	-0.9	0.5	down
MMP17	1.1	2.2	up	COL12A1	-1.1	0.5	down
SPP1	3.8	14.3	up	BMP1	-0.8	0.6	down
MMP11	1.2	2.3	up	COL5A2	-2.4	0.2	down
NID2	1.4	2.6	up	ITGB4	-1.2	0.4	down
TGFB3	1.7	3.3	up	TIMP2	-1.2	0.4	down
EFEMP2	0.7	1.6	up	COL4A1	-0.6	0.6	down
TGFB2	1.7	3.2	up	ADAM15	-1.3	0.4	down
COL20A1	0.9	1.8	up	CD47	-0.6	0.7	down
EFEMP1	2.4	5.1	up	ICAM4	-0.8	0.6	down
JAM3	0.6	1.6	up	COL4A2	-0.7	0.6	down
ADAMTS2	1.3	2.5	up	COL13A1	-1	0.5	down
COL3A1	1.3	2.4	up	SERPINE1	-0.8	0.6	down
ITGA8	2.2	4.7	up	ITGA6	-0.7	0.6	down
VTN	0.8	1.7	up	NCAM1	-0.7	0.6	down
LOXL3	0.8	1.8	up	HSPG2	-1.1	0.5	down
COL4A3	0.6	1.5	up	TGFB1	-0.8	0.6	down
CTSS	1.6	3	up	TLL1	-1.3	0.4	down
LUM	2	4	up	ELANE	-0.7	0.6	down
CTSL	0.7	1.6	up	ICAM2	-0.9	0.6	down
COL27A1	1	1.9	up	THBS1	-0.7	0.6	down
PCOLCE	0.7	1.6	up	ITGA3	-0.5	0.7	down
NTN4	1.3	2.5	up	VCAN	-0.6	0.7	down
COL2A1	2.1	4.4	up	JAM2	-0.8	0.6	down
LTBP2	1.9	3.9	up	ITGAM	-0.7	0.6	down
DDR2	0.9	1.9	up	ICAM1	-1.6	0.3	down
DCN	1.9	3.6	up	PECAM1	-0.5	0.7	down
PDGFB	1	2.1	up	COL5A3	-1.1	0.5	down

## Appendix

**Table 24 continued:** Different gene expression of heart ECs in response to high shear stress involved in extracellular matrix organisation.

SDC3	0.5	1.5	up	BMP4	-0.7	0.6	down
LTBP3	0.5	1.4	up	LAMA5	-0.6	0.6	down
CTSB	0.7	1.7	up				

**Table 25:** Different gene expression of heart ECs in response to high shear stress involved in assembly of collagen fibrils and other multimeric structures.

Gene	Log.Fold. Change	Linear. Fold. Change	Comp. A-B	Gene	Log.Fold. Change	Linear. Fold. Change	Comp. A-B
COL1A2	2.7	6.6	up	COL2A1	2.1	4.4	up
LOXL2	2.4	5.2	up	CTSB	0.7	1.7	up
LOXL1	1.6	3	up	COL6A3	1.4	2.7	up
LAMA3	1.2	2.3	up	COL5A1	0.7	1.6	up
MMP3	1.2	2.2	up	PLEC	-1.9	0.3	down
COL1A1	1.7	3.3	up	BMP1	-0.8	0.6	down
COL3A1	1.3	2.4	up	COL5A2	-2.4	0.2	down
LOXL3	0.8	1.8	up	ITGB4	-1.2	0.4	down
COL4A3	0.6	1.5	up	COL4A1	-0.6	0.6	down
CTSS	1.6	3	up	COL4A2	-0.7	0.6	down
CTSL	0.7	1.6	up	ITGA6	-0.7	0.6	down
COL27A1	1	1.9	up	TLL1	-1.3	0.4	down
PCOLCE	0.7	1.6	up	COL5A3	-1.1	0.5	down

**Table 26:** Different gene expression of heart ECs in response to high shear stress involved in hemostasis.

Gene	Log.Fold. Change	Linear. Fold. Change	Comp. A-B	Gene	Log.Fold. Change	Linear. Fold. Change	Comp. A-B
NOS2	3.2	9.4	up	SLC16A3	0.6	1.6	up
ANGPT2	2.4	5.4	up	RASGRP2	1.2	2.4	up
KIF3A	1.7	3.2	up	PLEK	0.6	1.5	up
GNB4	2.2	4.5	up	ZFPM1	-1.5	0.4	down
ITGA1	1.4	2.7	up	LRP8	-2	0.2	down
SLC7A7	1.1	2.1	up	VWF	-2.3	0.2	down
F2RL2	1.4	2.6	up	SLC7A11	-2.1	0.2	down
LCP2	2.5	5.7	up	ITPR3	-2.1	0.2	down
MMRN1	4.1	17.1	up	GAS6	-1.5	0.4	down
KLC3	0.8	1.8	up	DOCK8	-1.2	0.4	down
SH2B1	0.8	1.8	up	DAGLA	-1.1	0.5	down
DGKK	3.3	9.9	up	ABL1	-0.8	0.6	down
LCK	1.6	3	up	GATA3	-1.9	0.3	down
PF4	2	4.1	up	RAP1B	-0.5	0.7	down
ABCC4	1.4	2.7	up	ZFPM2	-1	0.5	down
SERPINB8	0.7	1.7	up	S100A10	-1.3	0.4	down
P2RY1	1.4	2.6	up	MGLL	-1	0.5	down
AKT3	0.8	1.8	up	PLAUR	-1.7	0.3	down
CABLES1	0.8	1.8	up	SOD1	-0.6	0.7	down
F2R	0.7	1.7	up	TFPI	-0.6	0.7	down

Appendix

**Table 26 continued:** Different gene expression of heart ECs in response to high shear stress involved in hemostasis.

TGFB3	1.7	3.3	up	GNAQ	-0.6	0.6	down
PDE3B	1.2	2.3	up	ANXA2	-0.7	0.6	down
ITPR1	0.9	1.8	up	NRAS	-0.5	0.7	down
PHF21A	0.9	1.9	up	TEK	-1.4	0.4	down
MERTK	1.6	3	up	PTK2	-0.7	0.6	down
TGFB2	1.7	3.2	up	HSPA5	-0.6	0.7	down
JAM3	0.6	1.6	up	GATA2	-0.8	0.6	down
KIF2A	0.7	1.7	up	CD47	-0.6	0.7	down
F13A1	3	8.2	up	NOS3	-1.8	0.3	down
GNG2	1.1	2.1	up	PLAT	-2.5	0.2	down
SLC8A2	0.6	1.6	up	PIK3R3	-1.8	0.3	down
KCNMB1	0.9	1.9	up	FYN	-0.8	0.6	down
SLC7A8	0.7	1.6	up	SERPINE1	-0.8	0.6	down
ARRB1	2.3	4.9	up	P2RX1	-0.6	0.6	down
DOCK10	0.7	1.7	up	ITGA6	-0.7	0.6	down
PPP2R5A	1.3	2.4	up	YWHAZ	-0.7	0.6	down
PDE10A	0.7	1.6	up	SERPINC1	-0.6	0.7	down
ITPK1	0.6	1.5	up	PRCP	-2	0.2	down
SERPING1	1.7	3.2	up	HDAC1	-0.6	0.6	down
VEGFB	0.6	1.5	up	HABP4	-0.7	0.6	down
PIK3R2	0.5	1.4	up	CD36	-2.5	0.2	down
GNAI1	0.7	1.7	up	PDE1B	-1.2	0.4	down
VEGFA	0.6	1.5	up	KRAS	-0.6	0.6	down
EHD3	0.8	1.7	up	TGFB1	-0.8	0.6	down
IGF2	0.8	1.7	up	DOCK11	-0.8	0.6	down
GNG7	0.5	1.4	up	KIF23	-0.9	0.5	down
GRB14	0.8	1.8	up	F3	-1.2	0.4	down
GNG12	0.7	1.6	up	GATA4	-0.7	0.6	down
KIF26A	0.6	1.5	up	KCNMB4	-0.6	0.7	down
GNGT2	0.8	1.7	up	THBS1	-0.7	0.6	down
PIK3CB	0.9	1.8	up	PRKAR2B	-0.5	0.7	down
WEE1	0.8	1.7	up	SH2B3	-0.7	0.6	down
PDGFB	1	2.1	up	AMICA1	-0.8	0.6	down
ANGPT4	0.7	1.6	up	INPP5D	-0.6	0.6	down
FCER1G	1.2	2.3	up	ITGA3	-0.5	0.7	down
PRKAR1B	0.9	1.9	up	JAM2	-0.8	0.6	down
RHOB	1	1.9	up	CAPZB	-0.8	0.6	down
PDE5A	0.7	1.6	up	SLC8A3	-0.6	0.6	down
GUCY1A3	1.2	2.3	up	ITGAM	-0.7	0.6	down
PDE1A	0.9	1.9	up	SELP	-0.6	0.7	down
CD84	0.5	1.5	up	KIF20A	-0.7	0.6	down
MRV11	0.8	1.8	up	PECAM1	-0.5	0.7	down
DOCK3	0.7	1.7	up	KIF22	-0.5	0.7	down
VAV1	0.7	1.6	up	ITPR2	-0.5	0.7	down
CLU	0.9	1.8	up	SLC7A6	-0.5	0.7	down
TRPC3	1.1	2.2	up	PLA2G4A	-1	0.5	down

## Appendix

**Table 27:** Different gene expression of heart ECs in response to high shear stress involved in cholesterol biosynthesis.

Gene	Log.Fold. Change	Linear. Fold. Change	Comp. A-B	Gene	Log.Fold. Change	Linear. Fold. Change	Comp. A-B
SQLE	-1.2	0.4	down	HSD17B7	-0.9	0.5	down
FDFT1	-0.9	0.5	down	FDPS	-1	0.5	down
DHCR24	-1.3	0.4	down	MVD	-0.7	0.6	down
IDI1	-1.2	0.4	down	HMGCS1	-0.9	0.5	down
NSDHL	-0.8	0.6	down	PMVK	-0.5	0.7	down
SC5D	-0.8	0.6	down	LSS	-0.8	0.6	down
DHCR7	-1.2	0.4	down	HMGCR	-0.9	0.5	down

**Table 28:** Different gene expression of heart ECs in response to high shear stress involved in molecules associated with elastic fibres.

Gene	Log.Fold. Change	Linear. Fold. Change	Comp. A-B	Gene	Log.Fold. Change	Linear. Fold. Change	Comp. A-B
BMP2	2.9	7.6	up	LTBP2	1.9	3.9	up
BMP7	2.3	4.8	up	LTBP3	0.5	1.4	up
MFAP2	1.4	2.6	up	MFAP5	0.6	1.5	up
TGFB3	1.7	3.3	up	ITGB5	0.5	1.4	up
EFEMP2	0.7	1.6	up	FBLN2	-3.5	0.1	down
TGFB2	1.7	3.2	up	LTBP4	-2.3	0.2	down
EFEMP1	2.4	5.1	up	TGFB1	-0.8	0.6	down
ITGA8	2.2	4.7	up	BMP4	-0.7	0.6	down
VTN	0.8	1.7	up				

**Table 29:** Different gene expression of heart ECs in response to high shear stress involved in axon guidance.

Gene	Log.Fold. Change	Linear. Fold. Change	Comp. A-B	Gene	Log.Fold. Change	Linear. Fold. Change	Comp. A-B
SEMA6D	1	2	up	MYH11	0.7	1.6	up
ITGA1	1.4	2.7	up	TRIO	0.9	1.8	up
EPHA5	0.9	1.9	up	CLTB	-1.2	0.4	down
SCN8A	0.9	1.9	up	EZR	-1.1	0.5	down
EPHB3	0.8	1.7	up	GIT1	-1.3	0.4	down
DPYSL5	0.8	1.8	up	EPHA4	-0.9	0.5	down
FGFR1	0.9	1.9	up	SPTBN2	-0.9	0.5	down
TRPC4	1.2	2.3	up	EPHB4	-1.4	0.4	down
MYH10	0.9	1.9	up	ABL1	-0.8	0.6	down
SCN3B	1	2.1	up	SLIT2	-0.8	0.6	down
ARHGEF28	1.1	2.1	up	KDR	-1.5	0.4	down
SRGAP2	1	2.1	up	ALCAM	-1.2	0.4	down
KALRN	0.7	1.6	up	NRP1	-1.5	0.4	down
ST8SIA4	1.6	3.1	up	ROBO3	-1.2	0.4	down
APH1B	1.3	2.5	up	EFNB2	-1.2	0.4	down
RPS6KA5	0.7	1.6	up	NRCAM	-1.6	0.3	down
SCN3A	2.1	4.4	up	PLXNA4	-1.6	0.3	down
PAK4	0.6	1.5	up	PITPNA	-0.6	0.7	down

## Appendix

**Table 29 continued:** Different gene expression of heart ECs in response to high shear stress involved in axon guidance.

ABLIM1	1.2	2.3	up	COL4A1	-0.6	0.6	down
SCN2B	0.7	1.6	up	NRAS	-0.5	0.7	down
TYROBP	2	3.9	up	SEMA3E	-0.9	0.5	down
ITSN1	0.6	1.5	up	CRMP1	-1.8	0.3	down
TRPC1	0.6	1.5	up	PTK2	-0.7	0.6	down
AGAP2	1.9	3.8	up	EFNB1	-0.7	0.6	down
TREM2	1.4	2.6	up	MSN	-0.5	0.7	down
MYL9	1.2	2.3	up	COL4A2	-0.7	0.6	down
COL4A3	0.6	1.5	up	RPS6KA3	-0.6	0.7	down
VEGFA	0.6	1.5	up	FYN	-0.8	0.6	down
NTN4	1.3	2.5	up	GSK3B	-0.6	0.7	down
CACNA1H	0.7	1.6	up	NGEF	-0.8	0.6	down
CD72	0.6	1.5	up	CDK5R1	-0.6	0.6	down
DLG1	0.5	1.4	up	SPTAN1	-0.7	0.6	down
LIMK1	0.9	1.9	up	PIP5K1C	-0.8	0.6	down
CSNK2A1	0.5	1.5	up	SHB	-0.9	0.5	down
MYO10	1	1.9	up	NCAM1	-0.7	0.6	down
RHOB	1	1.9	up	ARHGEF12	-0.5	0.7	down
RND1	1.6	3	up	KRAS	-0.6	0.6	down
COL6A3	1.4	2.7	up	RPS6KA4	-0.6	0.7	down
ARPC3	1	2	up	NEO1	-0.6	0.6	down
SRGAP3	0.7	1.6	up	SRGAP1	-0.7	0.6	down
ARHGEF7	0.5	1.4	up	EPHA7	-0.7	0.6	down
TRPC3	1.1	2.2	up	NCK1	-0.7	0.6	down
MYL12B	0.7	1.6	up	RPS6KA2	-0.7	0.6	down
PAK2	0.6	1.5	up	PAK1	-0.7	0.6	down
SLIT3	0.6	1.5	up	UNC5B	-0.7	0.6	down
SCN5A	0.9	1.8	up				

**Table 30:** Different gene expression of heart ECs in response to high shear stress involved in elastic fibre formation.

Gene	Log.Fold. Change	Linear. Fold. Change	Comp. A-B	Gene	Log.Fold. Change	Linear. Fold. Change	Comp. A-B
BMP2	2.9	7.6	up	VTN	0.8	1.7	up
LOXL2	2.4	5.2	up	LOXL3	0.8	1.8	up
BMP7	2.3	4.8	up	LTBP2	1.9	3.9	up
LOXL1	1.6	3	up	LTBP3	0.5	1.4	up
MFAP2	1.4	2.6	up	MFAP5	0.6	1.5	up
TGFB3	1.7	3.3	up	ITGB5	0.5	1.4	up
EFEMP2	0.7	1.6	up	FBLN2	-3.5	0.1	down
TGFB2	1.7	3.2	up	LTBP4	-2.3	0.2	down
EFEMP1	2.4	5.1	up	TGFB1	-0.8	0.6	down
ITGA8	2.2	4.7	up	BMP4	-0.7	0.6	down

## Appendix

**Table 31:** Different gene expression of heart ECs in response to high shear stress involved in signaling by Rho GTPase.

Gene	Log.Fold. Change	Linear. Fold. Change	Comp. A-B	Gene	Log.Fold. Change	Linear. Fold. Change	Comp. A-B
STARD13	1.5	2.8	up	ARHGAP9	0.5	1.5	up
ARHGAP18	1.7	3.3	up	ARHGEF7	0.5	1.4	up
BCR	1	2.1	up	VAV1	0.7	1.6	up
RALBP1	0.6	1.5	up	ARHGEF17	0.8	1.7	up
SRGAP2	1	2.1	up	AKAP13	0.6	1.5	up
KALRN	0.7	1.6	up	TRIO	0.9	1.8	up
PLEKHG5	0.9	1.9	up	CHN2	-1.2	0.4	down
ARHGAP26	0.9	1.9	up	RHOQ	-0.9	0.5	down
PLEKHG2	0.9	1.9	up	ARHGAP23	-0.8	0.6	down
OPHN1	0.5	1.4	up	RAC3	-0.7	0.6	down
ARHGAP29	0.9	1.8	up	MYO9A	-0.7	0.6	down
RHOJ	0.6	1.5	up	ARHGAP31	-0.5	0.7	down
ITSN1	0.6	1.5	up	NGEF	-0.8	0.6	down
SYDE1	1	2	up	ARHGAP11A	-0.5	0.7	down
PIK3R2	0.5	1.4	up	ARHGEF12	-0.5	0.7	down
ARHGEF4	0.7	1.6	up	MCF2L	-0.9	0.5	down
TAGAP	0.6	1.5	up	TIAM2	-0.6	0.7	down
ARHGAP25	0.5	1.5	up	SRGAP1	-0.7	0.6	down
ARHGAP15	0.5	1.4	up	RHOH	-0.5	0.7	down
RHOB	1	1.9	up	ARHGDIG	-0.5	0.7	down
FAM13A	0.9	1.9	up	ARHGEF18	-0.9	0.5	down
SRGAP3	0.7	1.6	up				

**Table 32:** Different gene expression of heart ECs in response to high shear stress involved in collagen formation.

Gene	Log.Fold. Change	Linear. Fold. Change	Comp. A-B	Gene	Log.Fold. Change	Linear. Fold. Change	Comp. A-B
LEPREL2	1.2	2.3	up	COL2A1	2.1	4.4	up
COL1A2	2.7	6.6	up	CTSB	0.7	1.7	up
LOXL2	2.4	5.2	up	COL6A3	1.4	2.7	up
ADAMTS14	2.1	4.2	up	COL5A1	0.7	1.6	up
LOXL1	1.6	3	up	COL28A1	0.5	1.5	up
LAMA3	1.2	2.3	up	PLEC	-1.9	0.3	down
MMP3	1.2	2.2	up	COL12A1	-1.1	0.5	down
COL1A1	1.7	3.3	up	BMP1	-0.8	0.6	down
COL20A1	0.9	1.8	up	COL5A2	-2.4	0.2	down
ADAMTS2	1.3	2.5	up	ITGB4	-1.2	0.4	down
COL3A1	1.3	2.4	up	COL4A1	-0.6	0.6	down
LOXL3	0.8	1.8	up	COL4A2	-0.7	0.6	down
COL4A3	0.6	1.5	up	COL13A1	-1	0.5	down
CTSS	1.6	3	up	ITGA6	-0.7	0.6	down
CTSL	0.7	1.6	up	TLL1	-1.3	0.4	down
COL27A1	1	1.9	up	COL5A3	-1.1	0.5	down
PCOLCE	0.7	1.6	up				

Appendix

**Table 33:** Different gene expression of heart ECs in response to high shear stress involved in developmental biology.

Gene	Log.Fold. Change	Linear. Fold. Change	Comp. A-B	Gene	Log.Fold. Change	Linear. Fold. Change	Comp. A-B
SEMA6D	1	2	up	TCF12	0.6	1.5	up
ITGA1	1.4	2.7	up	TRIO	0.9	1.8	up
FOXO1	1.1	2.2	up	KLF4	-2.4	0.2	down
EPHA5	0.9	1.9	up	CLTB	-1.2	0.4	down
NR5A2	2.6	6	up	EZR	-1.1	0.5	down
MEF2A	0.8	1.7	up	GIT1	-1.3	0.4	down
TCF4	1.4	2.7	up	NCOR2	-1	0.5	down
HIF3A	1.9	3.8	up	EPHA4	-0.9	0.5	down
SCN8A	0.9	1.9	up	SPTBN2	-0.9	0.5	down
EPHB3	0.8	1.7	up	EPHB4	-1.4	0.4	down
DPYSL5	0.8	1.8	up	ABL1	-0.8	0.6	down
FGFR1	0.9	1.9	up	SLIT2	-0.8	0.6	down
PCSK6	2	3.9	up	KDR	-1.5	0.4	down
CEBPD	2.6	6	up	ALCAM	-1.2	0.4	down
TRPC4	1.2	2.3	up	NRP1	-1.5	0.4	down
MYH10	0.9	1.9	up	ROBO3	-1.2	0.4	down
AKT3	0.8	1.8	up	EFNB2	-1.2	0.4	down
SCN3B	1	2.1	up	NRCAM	-1.6	0.3	down
ARHGEF28	1.1	2.1	up	LPL	-1.3	0.4	down
SRGAP2	1	2.1	up	CCNC	-0.7	0.6	down
NFKB1	0.8	1.7	up	PLXNA4	-1.6	0.3	down
KALRN	0.7	1.6	up	PITPNA	-0.6	0.7	down
HHEX	1	2	up	COL4A1	-0.6	0.6	down
ST8SIA4	1.6	3.1	up	NRAS	-0.5	0.7	down
APH1B	1.3	2.5	up	MAPK11	-1	0.5	down
RPS6KA5	0.7	1.6	up	SEMA3E	-0.9	0.5	down
SLC2A4	1.2	2.3	up	CRMP1	-1.8	0.3	down
SCN3A	2.1	4.4	up	PTK2	-0.7	0.6	down
PAK4	0.6	1.5	up	EFNB1	-0.7	0.6	down
CDK19	0.8	1.8	up	BNIP2	-0.6	0.7	down
ABLIM1	1.2	2.3	up	MSN	-0.5	0.7	down
SCN2B	0.7	1.6	up	COL4A2	-0.7	0.6	down
MED14	0.6	1.5	up	RPS6KA3	-0.6	0.7	down
TYROBP	2	3.9	up	FYN	-0.8	0.6	down
ITSN1	0.6	1.5	up	CDON	-0.7	0.6	down
TRPC1	0.6	1.5	up	FABP4	-0.8	0.6	down
AGAP2	1.9	3.8	up	GSK3B	-0.6	0.7	down
TREM2	1.4	2.6	up	SREBF2	-0.7	0.6	down
MYL9	1.2	2.3	up	NGEF	-0.8	0.6	down
COL4A3	0.6	1.5	up	CDK5R1	-0.6	0.6	down
VEGFA	0.6	1.5	up	SPTAN1	-0.7	0.6	down
NTN4	1.3	2.5	up	MEF2D	-0.7	0.6	down
CACNA1H	0.7	1.6	up	PIP5K1C	-0.8	0.6	down
CD72	0.6	1.5	up	SHB	-0.9	0.5	down
ACVR2B	0.9	1.9	up	NCAM1	-0.7	0.6	down
DLG1	0.5	1.4	up	MED20	-0.5	0.7	down
LIMK1	0.9	1.9	up	CTNNB1	-1	0.5	down

Appendix

**Table 33 continued:** Different gene expression of heart ECs in response to high shear stress involved in developmental biology.

CSNK2A1	0.5	1.5	up	CD36	-2.5	0.2	down
MYO10	1	1.9	up	ARHGEF12	-0.5	0.7	down
RHOB	1	1.9	up	CDK8	-0.5	0.7	down
RND1	1.6	3	up	KRAS	-0.6	0.6	down
COL6A3	1.4	2.7	up	TGFB1	-0.8	0.6	down
EGR2	0.8	1.8	up	RPS6KA4	-0.6	0.7	down
ARPC3	1	2	up	NEO1	-0.6	0.6	down
SRGAP3	0.7	1.6	up	SRGAP1	-0.7	0.6	down
ARHGEF7	0.5	1.4	up	KLF5	-1	0.5	down
TRPC3	1.1	2.2	up	EPHA7	-0.7	0.6	down
MYL12B	0.7	1.6	up	NCK1	-0.7	0.6	down
CEBPA	0.6	1.5	up	MEF2C	-0.8	0.6	down
STAT3	0.6	1.5	up	RPS6KA2	-0.7	0.6	down
PAK2	0.6	1.5	up	PAK1	-0.7	0.6	down
SLIT3	0.6	1.5	up	PPARG	-0.6	0.7	down
SCN5A	0.9	1.8	up	UNC5B	-0.7	0.6	down
MYH11	0.7	1.6	up	CCND3	-0.5	0.7	down

**Table 34:** Different gene expression of heart ECs in response to high shear stress involved in signaling by NGF.

Gene	Log.Fold. Change	Linear. Fold. Change	Comp. A-B	Gene	Log.Fold. Change	Linear. Fold. Change	Comp. A-B
BCL2L11	1.7	3.2	up	MAGED1	0.6	1.5	up
FOXO1	1.1	2.2	up	STAT3	0.6	1.5	up
SHC3	1.4	2.6	up	ADORA2A	0.9	1.9	up
MEF2A	0.8	1.7	up	AKAP13	0.6	1.5	up
ADCYAP1R1	1.3	2.5	up	HBEGF	0.8	1.8	up
TRIB3	1.9	3.8	up	TRIO	0.9	1.8	up
FGFR1	0.9	1.9	up	ITPR3	-2.1	0.2	down
PCSK6	2	3.9	up	CAMK4	-1.5	0.4	down
LCK	1.6	3	up	DUSP4	-1.6	0.3	down
CASP3	1	2	up	NGF	-0.6	0.7	down
AKT3	0.8	1.8	up	FGFR3	-1.4	0.4	down
NFKB1	0.8	1.7	up	NRAS	-0.5	0.7	down
KALRN	0.7	1.6	up	MAPK11	-1	0.5	down
KIT	3.6	12.3	up	SQSTM1	-0.9	0.5	down
PLEKHG5	0.9	1.9	up	PIK3R3	-1.8	0.3	down
APH1B	1.3	2.5	up	RPS6KA3	-0.6	0.7	down
ITPR1	0.9	1.8	up	FYN	-0.8	0.6	down
RPS6KA5	0.7	1.6	up	MDM2	-0.8	0.6	down
FGF23	2.2	4.6	up	GSK3B	-0.6	0.7	down
GAB1	0.8	1.8	up	NGEF	-0.8	0.6	down
PLEKHG2	0.9	1.9	up	HDAC1	-0.6	0.6	down
NFKBIA	0.6	1.5	up	ARHGEF1	-0.6	0.7	down
ITSN1	0.6	1.5	up	IRS1	-0.6	0.7	down
CDKN1B	0.9	1.8	up	ARHGEF12	-0.5	0.7	down
PIK3R2	0.5	1.4	up	PDE1B	-1.2	0.4	down
RALGDS	1.9	3.7	up	MCF2L	-0.9	0.5	down

Appendix

**Table 34 continued:** Different gene expression of heart ECs in response to high shear stress involved in signaling by NGF.

ARHGEF4	0.7	1.6	up	KRAS	-0.6	0.6	down
PDGFRA	0.5	1.4	up	PTEN	-0.6	0.7	down
PIK3CB	0.9	1.8	up	TIAM2	-0.6	0.7	down
ADCY2	0.5	1.5	up	MLST8	-0.6	0.7	down
PDGFB	1	2.1	up	PRKAR2B	-0.5	0.7	down
NTRK2	0.5	1.5	up	RAPGEF1	-0.5	0.7	down
PRKAR1B	0.9	1.9	up	RTN4	-0.7	0.6	down
PDE1A	0.9	1.9	up	MEF2C	-0.8	0.6	down
FGF1	1	1.9	up	RPS6KA2	-0.7	0.6	down
SHC2	0.6	1.5	up	CDKN1A	-0.6	0.7	down
ARHGEF7	0.5	1.4	up	ARHGEF18	-0.9	0.5	down
ADAM17	0.5	1.4	up	ITPR2	-0.5	0.7	down
VAV1	0.7	1.6	up	DUSP6	-0.7	0.6	down
ARHGEF17	0.8	1.7	up				

**Table 35:** Different gene expression of heart ECs in response to high shear stress involved in metabolism.

Gene	Log.Fold. Change	Linear. Fold. Change	Comp. A-B	Gene	Log.Fold. Change	Linear. Fold. Change	Comp. A-B
ETHE1	1.7	3.3	up	SQLE	-1.2	0.4	down
SDC4	2.6	6.2	up	ITPR3	-2.1	0.2	down
ITPKC	1.8	3.6	up	GGCT	-1	0.5	down
GNB4	2.2	4.5	up	NQO1	-4.2	0.1	down
GDA	3.3	10.2	up	MTM1	-1.1	0.5	down
LPIN3	1.5	2.8	up	PGD	-1.4	0.4	down
CYP4B1	2.5	5.6	up	FASN	-1	0.5	down
FMO3	4.5	22.2	up	B4GALT1	-0.8	0.6	down
B4GALT3	1.6	3.1	up	NCOR2	-1	0.5	down
DCTD	1.4	2.6	up	NT5C2	-0.7	0.6	down
PSME3	0.9	1.9	up	GPX4	-0.7	0.6	down
KCNG2	1.9	3.6	up	FDFT1	-0.9	0.5	down
ABCC3	1.7	3.3	up	KDSR	-0.7	0.6	down
GXYLT2	0.9	1.9	up	HYAL1	-1.3	0.4	down
PCBD1	1.2	2.3	up	GSTA2	-2.9	0.1	down
PYGL	2	4.1	up	B4GALT7	-1.1	0.5	down
FMO2	5.8	56.9	up	ELOVL1	-0.6	0.7	down
TRIB3	1.9	3.8	up	DHCR24	-1.3	0.4	down
PAOX	0.9	1.8	up	IDI1	-1.2	0.4	down
GLUL	1.6	3	up	LDLRAP1	-0.8	0.6	down
ARSA	0.8	1.8	up	TXNRD1	-1.1	0.5	down
IPMK	1.5	2.7	up	ENO1	-0.6	0.6	down
CTH	1.3	2.5	up	MOCS2	-0.7	0.6	down
GOS2	2.7	6.7	up	PPAP2B	-2.3	0.2	down
OAZ2	0.8	1.8	up	MGLL	-1	0.5	down
FAM213B	0.9	1.9	up	ACAN	-1.6	0.3	down
CCBL1	1.7	3.2	up	ASS1	-1.5	0.4	down
OXCT1	0.8	1.7	up	NSDHL	-0.8	0.6	down
MMAA	0.6	1.6	up	ME1	-1.3	0.4	down

Appendix

**Table 35 continued:** Different gene expression of heart ECs in response to high shear stress involved in metabolism.

NUDT16	0.6	1.6	up	HYAL2	-1.2	0.4	down
RPIA	0.9	1.8	up	ABHD5	-1.2	0.4	down
PRKAB2	0.9	1.9	up	BMP1	-0.8	0.6	down
HSD11B1	2.5	5.6	up	ARNTL	-1.2	0.4	down
CERK	1.1	2.1	up	SC5D	-0.8	0.6	down
SLC10A6	2.3	4.8	up	DHCR7	-1.2	0.4	down
GYS1	0.7	1.6	up	AOX1	-1.9	0.3	down
LDHB	1.1	2.1	up	HSD17B7	-0.9	0.5	down
ACSS1	2.4	5.1	up	FDPS	-1	0.5	down
IDH2	1.1	2.1	up	CPT1A	-1.1	0.5	down
ACP5	2.1	4.4	up	RRM1	-0.5	0.7	down
NUDT1	0.6	1.5	up	ABCC1	-1.1	0.5	down
GLS2	0.8	1.7	up	CIAPIN1	-0.6	0.7	down
PHYH	1	2	up	LPL	-1.3	0.4	down
MARCKS	0.6	1.6	up	SCO1	-0.5	0.7	down
ITPR1	0.9	1.8	up	GCLC	-1	0.5	down
BCKDHB	0.6	1.5	up	GPX1	-0.6	0.6	down
CHP1	0.7	1.7	up	LDLR	-1.3	0.4	down
GMPR	1	2	up	NUDT10	-1.1	0.5	down
VAPA	0.6	1.6	up	PSMB3	-0.6	0.6	down
HMGCL	1.3	2.4	up	DTYMK	-0.8	0.6	down
CD320	0.7	1.7	up	GNAQ	-0.6	0.6	down
NDUFA6	0.7	1.6	up	DDC	-0.6	0.7	down
MAOB	1.1	2.2	up	CCNC	-0.7	0.6	down
NUP210	2.4	5.2	up	BLVRA	-0.5	0.7	down
PAPSS2	0.9	1.8	up	BPNT1	-0.7	0.6	down
G6PC3	0.6	1.5	up	ACER3	-0.9	0.5	down
NAPRT1	1.2	2.3	up	NME1	-1	0.5	down
SLC2A4	1.2	2.3	up	NR1D1	-1.4	0.4	down
SYT5	1.9	3.7	up	ETFPA	-0.5	0.7	down
STARD6	1.1	2.1	up	MVD	-0.7	0.6	down
SHMT1	0.6	1.5	up	PDHX	-0.5	0.7	down
L2HGDH	0.6	1.5	up	ETFB	-0.6	0.6	down
MOCOS	0.9	1.9	up	NRF1	-0.5	0.7	down
GSTZ1	0.5	1.5	up	PDSS2	-0.5	0.7	down
PPIP5K1	0.6	1.5	up	ETFDH	-0.6	0.7	down
APOA2	0.8	1.7	up	RAN	-0.8	0.6	down
PANK4	0.6	1.5	up	PSMD5	-0.6	0.7	down
CDK19	0.8	1.8	up	ALOX12	-1.4	0.4	down
DPEP1	2.2	4.7	up	MTAP	-0.7	0.6	down
PNPLA2	0.8	1.8	up	GSTO2	-1	0.5	down
OPLAH	0.6	1.5	up	LPCAT3	-0.7	0.6	down
SLC44A1	0.6	1.5	up	MGST3	-0.8	0.6	down
MTMR14	0.6	1.5	up	CUBN	-0.7	0.6	down
UGCG	1.2	2.3	up	SLC25A15	-0.5	0.7	down
MED14	0.6	1.5	up	NFYC	-0.6	0.7	down
COX7A2L	0.6	1.6	up	SLC26A2	-0.6	0.7	down
GNG2	1.1	2.1	up	CAT	-0.8	0.6	down
SMS	0.5	1.5	up	SRD5A1	-0.7	0.6	down

Appendix

**Table 35 continued:** Different gene expression of heart ECs in response to high shear stress involved in metabolism.

PFKFB3	1.5	2.9	up	SLC52A3	-0.9	0.5	down
ACY3	0.9	1.9	up	DEGS2	-0.5	0.7	down
CDS2	0.6	1.6	up	NOS3	-1.8	0.3	down
PPP1R3C	1.5	2.8	up	PSMD6	-0.6	0.7	down
ARSI	0.5	1.4	up	PRPS2	-0.6	0.7	down
IDUA	0.9	1.8	up	MTMR2	-0.8	0.6	down
SUOX	0.7	1.7	up	PIK3R3	-1.8	0.3	down
PFKP	0.8	1.7	up	ABCG1	-0.8	0.6	down
MGST2	1.2	2.3	up	CHST2	-1.2	0.4	down
PLD1	0.6	1.5	up	GOT2	-0.5	0.7	down
ALDH1A1	1.6	3	up	NUP155	-0.6	0.7	down
UPP1	0.7	1.7	up	MBOAT2	-1.2	0.4	down
ENO3	0.8	1.7	up	ELOVL4	-0.8	0.6	down
LGMN	0.8	1.7	up	HMGCS1	-0.9	0.5	down
LUM	2	4	up	COX5B	-0.6	0.7	down
ITPK1	0.6	1.5	up	PITPNB	-0.6	0.7	down
ALDH6A1	0.5	1.4	up	FABP4	-0.8	0.6	down
ABCA1	2.6	6.1	up	NNMT	-1	0.5	down
CHST7	1.1	2.1	up	ADK	-1.7	0.3	down
ITPKA	0.6	1.5	up	SREBF2	-0.7	0.6	down
SLC6A12	2.5	5.8	up	PCCB	-0.6	0.7	down
HLCS	0.6	1.5	up	HMOX1	-1.3	0.4	down
PIK3R2	0.5	1.4	up	SLC25A12	-0.6	0.7	down
GNAI1	0.7	1.7	up	PMVK	-0.5	0.7	down
SGSH	0.6	1.5	up	PIP5K1C	-0.8	0.6	down
PDP1	0.7	1.6	up	MAT2A	-0.8	0.6	down
PLCE1	0.9	1.8	up	PI4KA	-0.5	0.7	down
HEXA	1	1.9	up	BDH1	-0.9	0.5	down
CHST15	0.7	1.6	up	SLC19A1	-0.7	0.6	down
CERS4	0.6	1.6	up	ASL	-0.5	0.7	down
LPCAT2	0.7	1.6	up	MED20	-0.5	0.7	down
NDUFC2	0.6	1.5	up	HSPG2	-1.1	0.5	down
CHST1	1.8	3.4	up	INPP4B	-1.2	0.4	down
PSMB8	0.9	1.9	up	CD36	-2.5	0.2	down
GNG7	0.5	1.4	up	NDUFB5	-0.5	0.7	down
GPCPD1	0.7	1.6	up	HEXB	-0.7	0.6	down
GNG12	0.7	1.6	up	ACOX1	-0.8	0.6	down
GPC3	0.7	1.6	up	CDK8	-0.5	0.7	down
GLS	0.8	1.7	up	RRM2	-1.4	0.4	down
TPI1	0.7	1.6	up	PSMC5	-0.5	0.7	down
LYVE1	1.8	3.5	up	NUPL2	-0.6	0.7	down
GNGT2	0.8	1.7	up	PSMD9	-0.6	0.7	down
PIK3CB	0.9	1.8	up	LIPE	-0.7	0.6	down
RGL1	0.9	1.8	up	HK1	-0.5	0.7	down
VAPB	0.8	1.7	up	AK1	-1.5	0.4	down
ADCY2	0.5	1.5	up	PTEN	-0.6	0.7	down
DCN	1.9	3.6	up	PDSS1	-0.6	0.7	down
SLC2A3	0.8	1.7	up	ELOVL5	-0.7	0.6	down
SGMS2	0.8	1.7	up	SLC25A32	-0.6	0.7	down

Appendix

**Table 35 continued:** Different gene expression of heart ECs in response to high shear stress involved in metabolism.

SULT1A1	2.1	4.4	up	PIP5K2	-0.7	0.6	down
PSMB9	1	1.9	up	PTGS2	-1.7	0.3	down
GPC4	0.6	1.5	up	CDA	-1.9	0.3	down
GSTT2	0.6	1.5	up	PIK3C2A	-0.7	0.6	down
ALDOC	0.9	1.8	up	COQ7	-0.6	0.7	down
SDC3	0.5	1.5	up	SLC27A1	-0.5	0.7	down
PRKAR1B	0.9	1.9	up	IDH1	-0.9	0.5	down
PLCB4	1.1	2.1	up	TIAM2	-0.6	0.7	down
SLC25A37	0.6	1.5	up	ATIC	-0.6	0.7	down
ASNS	0.8	1.8	up	NDUFAB1	-0.6	0.7	down
GPC6	0.5	1.4	up	ABCG2	-0.6	0.6	down
PLB1	0.6	1.5	up	PRKAR2B	-0.5	0.7	down
CYP7B1	0.9	1.9	up	PRKD1	-0.6	0.6	down
STARD5	0.7	1.7	up	VAC14	-0.6	0.7	down
SMPD3	1.2	2.2	up	FLAD1	-0.5	0.7	down
CSAD	0.6	1.6	up	INPP5D	-0.6	0.6	down
FBP1	0.5	1.4	up	UCP2	-2	0.2	down
PFKFB4	0.5	1.4	up	CMPK1	-0.6	0.6	down
NUDT4	0.5	1.5	up	VCAN	-0.6	0.7	down
LHB	0.6	1.5	up	SLC19A2	-0.7	0.6	down
ALOX5AP	0.8	1.7	up	SLC25A16	-0.9	0.5	down
APOE	1.7	3.1	up	ARSJ	-0.8	0.6	down
KCNB1	1	1.9	up	LSS	-0.8	0.6	down
SLC16A3	0.6	1.6	up	UCP3	-2	0.3	down
GCH1	0.6	1.5	up	AKAP5	-1.1	0.5	down
ANKRD1	1.1	2.1	up	ASAH1	-0.6	0.6	down
ITPKB	0.6	1.6	up	SNAP25	-0.7	0.6	down
CYP1A1	-7.1	0	down	PFAS	-0.6	0.7	down
APRT	-1.3	0.4	down	HMGCR	-0.9	0.5	down
GSTO1	-3.1	0.1	down	ACACB	-1	0.5	down
TEAD4	-1	0.5	down	SLC35B3	-0.6	0.7	down
ADA	-2.4	0.2	down	MINPP1	-0.5	0.7	down
GSTA4	-1.6	0.3	down	PPARG	-0.6	0.7	down
CYP1B1	-3	0.1	down	ITPR2	-0.5	0.7	down
PTGS1	-2.6	0.2	down	PPAP2A	-0.7	0.6	down
ABCC5	-1	0.5	down	PTGES	-0.6	0.6	down
GCLM	-2.1	0.2	down	BLVRB	-0.6	0.7	down
SPHK1	-1.6	0.3	down	ADSS	-0.6	0.6	down
CKB	-2.1	0.2	down	TK1	-1	0.5	down
CHPF2	-1.2	0.4	down	PLA2G4A	-1	0.5	down
CHST11	-1	0.5	down	HDC	-1	0.5	down
PLIN2	-1.8	0.3	down	CSPG4	-0.8	0.6	down
IPPK	-1	0.5	down	PFKFB2	-0.6	0.6	down

## Appendix

**Table 36:** Different gene expression of heart ECs in response to high shear stress involved in integrin cell surface interactions.

Gene	Log.Fold. Change	Linear. Fold. Change	Comp. A-B	Gene	Log.Fold. Change	Linear. Fold. Change	Comp. A-B
ITGA1	1.4	2.7	up	ICAM4	-0.8	0.6	down
ITGA11	2.4	5.2	up	COL4A2	-0.7	0.6	down
SPP1	3.8	14.3	up	COL13A1	-1	0.5	down
JAM3	0.6	1.6	up	ITGA6	-0.7	0.6	down
ITGA8	2.2	4.7	up	HSPG2	-1.1	0.5	down
VTN	0.8	1.7	up	ICAM2	-0.9	0.6	down
COL4A3	0.6	1.5	up	THBS1	-0.7	0.6	down
LUM	2	4	up	ITGA3	-0.5	0.7	down
ITGB5	0.5	1.4	up	JAM2	-0.8	0.6	down
KDR	-1.5	0.4	down	ITGAM	-0.7	0.6	down
COL4A1	-0.6	0.6	down	ICAM1	-1.6	0.3	down
CD47	-0.6	0.7	down	PECAM1	-0.5	0.7	down

**Table 37:** Different gene expression of heart ECs in response to high shear stress involved in NRAGE signals death through JNK.

Gene	Log.Fold. Change	Linear. Fold. Change	Comp. A-B	Gene	Log.Fold. Change	Linear. Fold. Change	Comp. A-B
BCL2L11	1.7	3.2	up	MAGED1	0.6	1.5	up
KALRN	0.7	1.6	up	AKAP13	0.6	1.5	up
PLEKHG5	0.9	1.9	up	TRIO	0.9	1.8	up
PLEKHG2	0.9	1.9	up	NGF	-0.6	0.7	down
ITSN1	0.6	1.5	up	NGEF	-0.8	0.6	down
ARHGEF4	0.7	1.6	up	ARHGEF12	-0.5	0.7	down
ARHGEF7	0.5	1.4	up	MCF2L	-0.9	0.5	down
VAV1	0.7	1.6	up	TIAM2	-0.6	0.7	down
ARHGEF17	0.8	1.7	up	ARHGEF18	-0.9	0.5	down

**Table 38:** Different gene expression of heart ECs in response to high shear stress involved in netrin-1 signaling.

Gene	Log.Fold. Change	Linear. Fold. Change	Comp. A-B	Gene	Log.Fold. Change	Linear. Fold. Change	Comp. A-B
TRPC4	1.2	2.3	up	EZR	-1.1	0.5	down
ABLIM1	1.2	2.3	up	SLIT2	-0.8	0.6	down
TRPC1	0.6	1.5	up	PITPNA	-0.6	0.7	down
AGAP2	1.9	3.8	up	PTK2	-0.7	0.6	down
NTN4	1.3	2.5	up	FYN	-0.8	0.6	down
MYO10	1	1.9	up	NEO1	-0.6	0.6	down
TRPC3	1.1	2.2	up	NCK1	-0.7	0.6	down
SLIT3	0.6	1.5	up	UNC5B	-0.7	0.6	down
TRIO	0.9	1.8	up				

## Appendix

**Table 39:** Different gene expression of heart ECs in response to high shear stress involved in nitric oxide stimulates guanylate cyclase.

Gene	Log.Fold. Change	Linear. Fold. Change	Comp. A-B	Gene	Log.Fold. Change	Linear. Fold. Change	Comp. A-B
NOS2	3.2	9.4	up	GUCY1A3	1.2	2.3	up
PDE3B	1.2	2.3	up	PDE1A	0.9	1.9	up
ITPR1	0.9	1.8	up	MRVI1	0.8	1.8	up
KCNMB1	0.9	1.9	up	NOS3	-1.8	0.3	down
PDE10A	0.7	1.6	up	PDE1B	-1.2	0.4	down
PDE5A	0.7	1.6	up	KCNMB4	-0.6	0.7	down

**Table 40:** Different gene expression of heart ECs in response to high shear stress involved in non-integrin membran-ECM interactions.

Gene	Log.Fold. Change	Linear. Fold. Change	Comp. A-B	Gene	Log.Fold. Change	Linear. Fold. Change	Comp. A-B
SDC4	2.6	6.2	up	LAMA2	0.6	1.5	up
LAMA3	1.2	2.3	up	ITGB5	0.5	1.4	up
VTN	0.8	1.7	up	ITGB4	-1.2	0.4	down
NTN4	1.3	2.5	up	ITGA6	-0.7	0.6	down
DDR2	0.9	1.9	up	HSPG2	-1.1	0.5	down
PDGFB	1	2.1	up	TGFB1	-0.8	0.6	down
SDC3	0.5	1.5	up	THBS1	-0.7	0.6	down
DDR1	0.8	1.7	up	LAMA5	-0.6	0.6	down
LAMA4	0.6	1.5	up				

**Table 41:** Different gene expression of heart ECs in response to high shear stress involved in platelet homeostasis.

Gene	Log.Fold. Change	Linear. Fold. Change	Comp. A-B	Gene	Log.Fold. Change	Linear. Fold. Change	Comp. A-B
NOS2	3.2	9.4	up	PDE1A	0.9	1.9	up
GNB4	2.2	4.5	up	MRVI1	0.8	1.8	up
PDE3B	1.2	2.3	up	TRPC3	1.1	2.2	up
ITPR1	0.9	1.8	up	LRP8	-2	0.2	down
GNG2	1.1	2.1	up	ITPR3	-2.1	0.2	down
SLC8A2	0.6	1.6	up	NOS3	-1.8	0.3	down
KCNMB1	0.9	1.9	up	P2RX1	-0.6	0.6	down
PPP2R5A	1.3	2.4	up	PDE1B	-1.2	0.4	down
PDE10A	0.7	1.6	up	KCNMB4	-0.6	0.7	down
GNG7	0.5	1.4	up	SLC8A3	-0.6	0.6	down
GNG12	0.7	1.6	up	PECAM1	-0.5	0.7	down
GNGT2	0.8	1.7	up	ITPR2	-0.5	0.7	down
PDE5A	0.7	1.6	up	PLA2G4A	-1	0.5	down
GUCY1A3	1.2	2.3	up				

## Appendix

**Table 42:** Different gene expression of heart ECs in response to high shear stress involved in semaphorin interactions.

Gene	Log.Fold. Change	Linear. Fold. Change	Comp. A-B	Gene	Log.Fold. Change	Linear. Fold. Change	Comp. A-B
SEMA6D	1	2	up	PAK2	0.6	1.5	up
ITGA1	1.4	2.7	up	MYH11	0.7	1.6	up
DPYSL5	0.8	1.8	up	NRP1	-1.5	0.4	down
MYH10	0.9	1.9	up	PLXNA4	-1.6	0.3	down
TYROBP	2	3.9	up	SEMA3E	-0.9	0.5	down
TREM2	1.4	2.6	up	CRMP1	-1.8	0.3	down
MYL9	1.2	2.3	up	FYN	-0.8	0.6	down
CD72	0.6	1.5	up	GSK3B	-0.6	0.7	down
LIMK1	0.9	1.9	up	CDK5R1	-0.6	0.6	down
RHOB	1	1.9	up	PIP5K1C	-0.8	0.6	down
RND1	1.6	3	up	ARHGEF12	-0.5	0.7	down
MYL12B	0.7	1.6	up	PAK1	-0.7	0.6	down

**Table 43:** Different gene expression of heart ECs in response to high shear stress involved in smooth muscle contraction.

Gene	Log.Fold. Change	Linear. Fold. Change	Comp. A-B	Gene	Log.Fold. Change	Linear. Fold. Change	Comp. A-B
ITGA1	1.4	2.7	up	ACTA2	0.9	1.8	up
TPM3	1.3	2.5	up	TPM1	0.6	1.5	up
MYLK	1.6	3.1	up	MYL12B	0.7	1.6	up
LMOD1	1.4	2.7	up	MYH11	0.7	1.6	up
ACTG2	1.9	3.8	up	ITGB5	0.5	1.4	up
MYL9	1.2	2.3	up				

**Table 44:** Different gene expression of heart ECs in response to high shear stress involved in platelet activation, signaling and aggregation.

Gene	Log.Fold. Change	Linear. Fold. Change	Comp. A-B	Gene	Log.Fold. Change	Linear. Fold. Change	Comp. A-B
GNB4	2.2	4.5	up	RHOB	1	1.9	up
F2RL2	1.4	2.6	up	VAV1	0.7	1.6	up
LCP2	2.5	5.7	up	CLU	0.9	1.8	up
MMRN1	4.1	17.1	up	TRPC3	1.1	2.2	up
DGKK	3.3	9.9	up	RASGRP2	1.2	2.4	up
LCK	1.6	3	up	PLEK	0.6	1.5	up
PF4	2	4.1	up	VWF	-2.3	0.2	down
ABCC4	1.4	2.7	up	ITPR3	-2.1	0.2	down
P2RY1	1.4	2.6	up	GAS6	-1.5	0.4	down
AKT3	0.8	1.8	up	DAGLA	-1.1	0.5	down
F2R	0.7	1.7	up	RAP1B	-0.5	0.7	down
TGFB3	1.7	3.3	up	MGLL	-1	0.5	down
ITPR1	0.9	1.8	up	SOD1	-0.6	0.7	down
TGFB2	1.7	3.2	up	GNAQ	-0.6	0.6	down
F13A1	3	8.2	up	PTK2	-0.7	0.6	down
GNG2	1.1	2.1	up	HSPA5	-0.6	0.7	down

## Appendix

**Table 44 continued:** Different gene expression of heart ECs in response to high shear stress involved in platelet activation, signaling and aggregation.

ARRB1	2.3	4.9	up	PIK3R3	-1.8	0.3	down
SERPING1	1.7	3.2	up	FYN	-0.8	0.6	down
VEGFB	0.6	1.5	up	SERPINE1	-0.8	0.6	down
PIK3R2	0.5	1.4	up	YWHAZ	-0.7	0.6	down
GNAI1	0.7	1.7	up	HABP4	-0.7	0.6	down
VEGFA	0.6	1.5	up	CD36	-2.5	0.2	down
IGF2	0.8	1.7	up	TGFB1	-0.8	0.6	down
GNG7	0.5	1.4	up	THBS1	-0.7	0.6	down
GNG12	0.7	1.6	up	SELP	-0.6	0.7	down
GNGT2	0.8	1.7	up	PECAM1	-0.5	0.7	down
PIK3CB	0.9	1.8	up	ITPR2	-0.5	0.7	down
PDGFB	1	2.1	up	PLA2G4A	-1	0.5	down
FCER1G	1.2	2.3	up				

**Table 45:** Different gene expression of heart ECs in response to high shear stress involved in chondroitin sulfate/ dermatan sulfate metabolism.

Gene	Log.Fold. Change	Linear. Fold. Change	Comp. A-B	Gene	Log.Fold. Change	Linear. Fold. Change	Comp. A-B
SDC4	2.6	6.2	up	GPC6	0.5	1.4	up
GXYLT2	0.9	1.9	up	CHPF2	-1.2	0.4	down
IDUA	0.9	1.8	up	CHST11	-1	0.5	down
CHST7	1.1	2.1	up	HYAL1	-1.3	0.4	down
HEXA	1	1.9	up	B4GALT7	-1.1	0.5	down
CHST15	0.7	1.6	up	HSPG2	-1.1	0.5	down
GPC3	0.7	1.6	up	HEXB	-0.7	0.6	down
DCN	1.9	3.6	up	VCAN	-0.6	0.7	down
GPC4	0.6	1.5	up	CSPG4	-0.8	0.6	down
SDC3	0.5	1.5	up				

**Table 46:** Different gene expression of heart ECs in response to high shear stress involved in laminin interactions.

Gene	Log.Fold. Change	Linear. Fold. Change	Comp. A-B	Gene	Log.Fold. Change	Linear. Fold. Change	Comp. A-B
ITGA1	1.4	2.7	up	ITGB4	-1.2	0.4	down
LAMA3	1.2	2.3	up	ITGA6	-0.7	0.6	down
NID2	1.4	2.6	up	HSPG2	-1.1	0.5	down
LAMA4	0.6	1.5	up	ITGA3	-0.5	0.7	down
LAMA2	0.6	1.5	up	LAMA5	-0.6	0.6	down
NID1	-0.9	0.5	down				

## Appendix

**Table 47:** Different gene expression of heart ECs in response to high shear stress involved in signaling by VEGF.

Gene	Log.Fold. Change	Linear. Fold. Change	Comp. A-B	Gene	Log.Fold. Change	Linear. Fold. Change	Comp. A-B
TRIB3	1.9	3.8	up	NRP1	-1.5	0.4	down
HSPB1	0.8	1.7	up	FLT1	-1.3	0.4	down
AKT3	0.8	1.8	up	NRAS	-0.5	0.7	down
PGF	1.8	3.6	up	MAPK11	-1	0.5	down
ITPR1	0.9	1.8	up	PTK2	-0.7	0.6	down
VEGFB	0.6	1.5	up	NOS3	-1.8	0.3	down
PIK3R2	0.5	1.4	up	FYN	-0.8	0.6	down
VEGFA	0.6	1.5	up	SHB	-0.9	0.5	down
ABI2	0.6	1.5	up	CTNNB1	-1	0.5	down
PIK3CB	0.9	1.8	up	KRAS	-0.6	0.6	down
SHC2	0.6	1.5	up	MLST8	-0.6	0.7	down
VAV1	0.7	1.6	up	NCK1	-0.7	0.6	down
PAK2	0.6	1.5	up	PAK1	-0.7	0.6	down
SPHK1	-1.6	0.3	down	ITPR2	-0.5	0.7	down
ITPR3	-2.1	0.2	down	JUP	-1.9	0.3	down
BAIAP2	-1.8	0.3	down	FLT4	-0.8	0.6	down
KDR	-1.5	0.4	down				

## Eidesstattliche Versicherung

Sievert, Wolfgang

Ich erkläre hiermit an Eides statt,

dass ich die vorliegende Dissertation mit dem Thema

Phenotypic and functional characterization of primary murine endothelial cells  
after *in vivo* irradiation

selbständig verfasst, mich außer der angegebenen keiner weiteren Hilfsmittel bedient und alle Erkenntnisse, die aus dem Schrifttum ganz oder annähernd übernommen sind, als solche kenntlich gemacht und nach ihrer Herkunft unter Bezeichnung der Fundstelle einzeln nachgewiesen habe.

Ich erkläre des Weiteren, dass die hier vorgelegte Dissertation nicht in gleicher oder in ähnlicher Form bei einer anderen Stelle zur Erlangung eines akademischen Grades eingereicht wurde.

---

Ort, Datum

---

Unterschrift Doktorand